

# Open Research Online

---

The Open University's repository of research publications and other research outputs

## Granitic Rocks of Ophiolites

### Thesis

How to cite:

Aldiss, Donald Tresham (1978). Granitic Rocks of Ophiolites. PhD thesis The Open University.

For guidance on citations see [FAQs](#).

© 1978 The Author



<https://creativecommons.org/licenses/by-nc-nd/4.0/>

Version: Version of Record

Link(s) to article on publisher's website:

<http://dx.doi.org/doi:10.21954/ou.ro.0000de69>

---

Copyright and Moral Rights for the articles on this site are retained by the individual authors and/or other copyright owners. For more information on Open Research Online's data [policy](#) on reuse of materials please consult the policies page.

---

[oro.open.ac.uk](http://oro.open.ac.uk)

31 0098946 X



Granitic rocks of ophiolites

A thesis presented for the degree of

Doctor of Philosophy

by

Donald Tresham Aldiss B.Sc. (Hons.), Birmingham

Earth Sciences, The Open University

June 1978

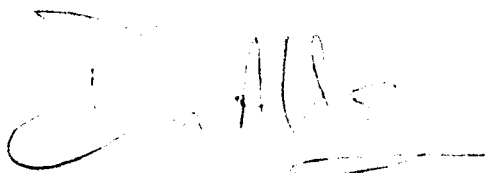
Date of submission: 12. 6. 78

Date of award: 23-8-78

Student no: HDC 6164

Statement of Availability

I am willing that this thesis, if approved and deposited in the University Library, be made available and photocopied at the discretion of the Librarian.

A handwritten signature in dark ink, appearing to read 'D.T. Aldiss', with a large, sweeping initial 'D' and a horizontal line extending from the end of the signature.

D.T.Aldiss

## Abstract

The field relationships, primary and secondary petrography and chemical composition of granitic rocks (plagiogranites) and associated formations in five ophiolites are described. In addition, the occurrence of similar rocks in other ophiolites, some island arcs and in the ocean crust is reviewed. Plagiogranites in ophiolites can be distinguished from all other granitic rocks by their almost complete lack of potassium feldspar, low alumina content, high K/Rb ratio and their LRE-depleted, flat or "dished" rare earth profiles and negative europium anomalies. The hypothesis that ophiolites represent oceanic lithosphere fragments is supported by the strong resemblance of some granitic rocks dredged from the seafloor to those in ophiolites.

Granitic rocks in ophiolites differentiate from subalkaline tholeiitic magmas at spreading axes in mid-ocean and in marginal ocean basins. These magmas evolved on a trend of iron-enrichment unless FeTioxides appeared as fractionating phases, which seems to have followed saturation of the magma by seawater. The magma then became progressively enriched in silica and sodium, evolving by the removal of plagioclase, FeTioxides, apatite and zircon. However, potassium was partitioned into the magmatic volatile phase and so entered the open hydrothermal system at the spreading axis and was thereby not enriched in the plagiogranites.



Plagiogranites in ophiolites are all deuterically altered to assemblages typical of upper greenschist or lower amphibolite facies metamorphism. Hydrothermal activity in the vicinity of each magma cell beneath the spreading axis ceased soon after the last of the silicate liquid froze and there was little repenetration of the ophiolite plutonic complex by hydrothermal fluids.

## Acknowledgments

My gratitude is due to:

My supervisor, Professor Ian Gass, for his guidance and support during the project and his criticism of the early drafts of this thesis.

All the members of the Department of Earth Sciences at the Open University, in particular Drs. Julián Pearce and John Smewing, for discussion, advice and encouragement about plagiogranites, ophiolites and other things.

The late Dr. Y. Hadjistavrinou and Drs. C. Xenophontos and A. Christodolou, of the Geological Survey Department, Cyprus, without whose help successful fieldwork on the island would not have been possible.

Dr. I.M. Elboushi, Geological Advisor to H.M. the Sultan, for invaluable logistical support during fieldwork in the Sultanate of Oman.

Dr. E.M. Moores, for his welcome to the Department of Geology, U.C. Davis, and to the staff of the U.C. Sierra Field Station, Browns Valley and especially to Koll Buer for their friendship and hospitality during fieldwork in California.

Dr. Graham Hendry, at the University of Birmingham for his assistance with XRF analysis.

Dr. Phil Potts for much practical help and guidance in RE analysis and the use of the electron microprobe.

John Holbrook and his staff for making my thin sections and to Andy Tindle for polishing those which were micro-analysed.

Dave Wright for his patience in simple computing matters.

Dr. F. Aumento and Ian Abbots for kindly providing specimens of diorite from the MAR and potassic aplite from Masirah Island.

Mrs. Sue Boggie and Mrs. Joan Harrison, who typed this thesis.

The Natural Environment Research Council for the award of a Research Studentship.

Drs. Cameron Allen and Adrian Lewis for their companionship and for prolonged and often fruitful discussion during fieldwork in Cyprus and the Oman, respectively.

## List of Contents

<u>Chapter 1 Introduction</u>	Page
1.1 Ophiolites and plagiogranites	1
1.2 History of research in ophiolites	4
1.3 Methodology and Rationale	9
1.3.1 Objectives	9
1.3.2 Background	9
1.3.3 Methodology	10
1.3.4 Nomenclature	10
1.3.5 Geochemistry	11
 <u>Chapter 2 Description</u>	
 2.1 <u>The Troodos Massif</u>	
2.1.1, Regional Geology	14
2.1.2 Field Relations of the Upper Plutonic Complex	16
2.1.2.1 Gabbros	16
2.1.2.2 Plagiogranites	17
2.1.2.3 Sheeted Intrusive Complex	19
2.1.2.4 Plagiogranites in the Axis Sequence	20
2.1.2.5 Intrusive Relations between the Plutonic Complex and the Sheeted Intrusive Complex	21
2.1.3 Petrography	22
2.1.3.1 Introduction	22
2.1.3.2 Gabbros	23
2.1.3.3 Plagiogranites	24
2.1.3.4 Intrusive Rhyolites	27

2.1.3.5	Contact Metamorphism	27
2.1.4	Geochemistry	29
2.1.4.1	Introduction	29
2.1.4.2	Metasomatism	29
2.1.4.3	Major and trace elements	31
2.1.4.4	REE Geochemistry	34

## 2.2 The Semail Nappe

2.2.1	Introduction	38
2.2.2	Field Relations and petrography of plagiogranites	40
2.2.3	Geochemistry	46
2.2.3.1	Metasomatism	46
2.2.3.2	Major and trace elements and magmatic evolution	47
2.2.3.3	Rare earth element geochemistry	48

## 2.3 The Smartville Block

2.3.1	Introduction and Regional Geology	52
2.3.2	Field Relations and Petrography	55
2.3.2.1	Introduction	55
2.3.2.2	The Volcanic Unit	56
2.3.2.2	The Dyke Complex	56
2.3.2.4	The Plutonic Unit	58
2.3.2.5	The "Nevadan" Plutons	62
2.3.3	Geochemistry	64
2.3.3.1	Introduction	64
2.3.3.2	Metasomatic variation	64
2.3.3.3	Geochemistry of the "Nevadan" Plutons	66
2.3.3.4	Primary Geochemistry	68
2.3.3.5	REE Geochemistry	72

<u>2.4</u>	<u>The Point Sal Ophiolite</u>	
2.4.1	Regional Geology	74
2.4.2	The Point Sal ophiolite	76
2.4.3.1	Plagiogranites at Point Sal	78
2.4.3.2	Other plagiogranites in the Coast Ranges	80
2.4.3.3	Plagiogranite geochemistry	82
<u>2.5</u>	<u>The Ballantrae Complex</u>	
2.5.1	Introduction and Regional Geology	84
2.5.2	Plagiogranite at Ballantrae	87
2.5.2.1	Introduction	87
2.5.2.2	Field Relations	87
2.5.2.3	Petrography	89
2.5.3	Geochemistry	91
2.5.3.1	Introduction	91
2.5.3.2	Metasomatism	91
2.5.3.3	Major and Trace element Geochemistry	92
2.5.3.4	REE Geochemistry	94
<u>2.6</u>	<u>Other plagiogranites</u>	
2.6.1	Introduction	96
2.6.2	Ophiolite plagiogranites	96
2.6.3	Island arc plagiogranites	99
2.6.4	Comparison of ophiolite and island arc plagiogranites	100
<u>2.7</u>	<u>Plagiogranites from the ocean crust</u>	
2.7.1	Introduction	102

	Page
2.7.2 Ocean-crust plagiogranites	103
2.7.3 Geochemistry of ocean-crust plagiogranites	105
2.7.4 Comparison with ophiolite plagiogranites	107

### Chapter 3 Integration

<u>3.1 Comparison of plagiogranites</u>	
3.1.1 Introduction	109
3.1.2 Ophiolite plagiogranites	110
3.1.3 Ophiolite plagiogranites and other granites	113
<u>3.2 Petrogenesis of ophiolite plagiogranites</u>	
3.2.1 Are ophiolite plagiogranites magmatic differentiates?	116
3.2.2 Constructional processes	117
3.2.3 Magmatic Differentiation	121
3.2.4 Metamorphism	128
3.2.5 The Potassium Problem	131
<u>3.3 Conclusions</u>	134

### Appendix 1 Major and Trace Element data

- 2 Rare Earth Element data
- 3 Analytical Techniques
- 4 Bibliography

## List of Figures

## Following Page

1.1	Section of the lithosphere at a slow spreading oceanic ridge	5
2.1.1	General geology of Cyprus	14
2.1.2	Geological sketch map of Troodos Massif	15
2.1.3	Schematic diagram of field relations	17
2.1.4	Chemical variation diagrams	33
2.1.5	Distribution of the rare earths relative to Zr	37
2.1.6	RE profiles - LRE depleted	37
2.1.7	RE profiles - Flat or dished	37
2.1.8	Partition coefficients	37
2.2.1	Position of Semail Nappe, Oman	38
2.2.2	Section through Semail Nappe	39
2.2.3	Chemical variation diagrams	47
2.2.4	RE profiles	48
2.2.5	Distribution of the rare earths relative to $\text{SiO}_2$ and Y	48
2.3.1	General geology of California	52
2.3.2	Geological sketch map of the Smartville Block	52
2.3.3	Section through Smartville Block	52
2.3.4	Trace element discrimination diagrams	54



<u>List of Figures (continued.)</u>	<u>Following Page</u>
2.3.5 Intrusive margins in the Dyke Complex	56
2.3.6 Major element variation diagrams	71
2.3.7 Trace element variation diagrams	71
2.3.8 Miscellaneous variation diagrams	71
2.3.9 Comparison of ophiolite and 'Nevadan' pluton geochemistry	66
2.3.10 RE profiles	72
2.4.1 Geological Map of Point Sal	76
2.4.2 Stratigraphy of Point Sal ophiolite	76
2.4.3 Major element variation diagrams	82
2.5.1 Geological map of the Ballantrae Complex	84
2.5.2 Geological map of Byne Hill	88
2.5.3 Chemical variation diagrams	93
2.5.4 RE profiles	94
2.7.1 Major element distribution	105
2.7.2 RE profiles	107
3.1 Comparitive RE profiles	114
3.2 Comparitive potassium content of granites	114
3.3 Comparitive rubidium and strontium content of granites	114
3.4 Q-Ab-An diagram	126

## List of Tables

Following  
Page

1.1	Stratigraphic Nomenclature of the Troodos Massif.	4
1.2	Lithologies of the Troodos Massif.	4
1.3	Petrographic Nomenclature.	10
1.4	Abbreviations used in text.	10
2.1.1	Flow chart of petrogenetic processes.	18
2.1.2	Summary of Petrography.	22
2.1.3	Major Element Ranges.	29
2.1.4	Trace Element Ranges.	29
2.2.1	Stratigraphy of Semail Ophiolite.	39
2.2.2	Summary of Petrography.	41
2.2.3	Garnets from ophiolites.	44
2.2.4	Major Element Ranges.	46
2.2.5	Trace Element Ranges.	46
2.3.1	Stratigraphy of the Smartville ophiolite.	55
2.3.2	Summary of petrography of Dyke Complex.	57
2.3.3	Summary of petrography of Plutonic Complex.	58
2.3.4	Comparison of "Nevadan" and ophiolite plutonic bodies.	63
2.3.5	Major Element Ranges.	64
2.3.6	Trace Element Ranges.	64
2.3.7	Potassium and Rubidium in the Smartville Block.	67
2.4.1	Summary of Point Sal Petrography.	78
2.5.1	Summary of Byne Hill Petrography.	89
2.6.1	Geochemistry of island arc plagiogranites.	99

	Following Page
2.7.1 Petrography of ocean-crust plagiogranites.	103
2.7.2 Initial Strontium isotope ratios of ocean-crust plagiogranites.	106
3.1 Comparison of ophiolite stratigraphy.	110
3.2 Comparative Thicknesses.	110
3.3 Comparison of external characteristics.	110
3.4 Distribution of plagiogranite lithologies and field types.	110
3.5 Patterns of Metasomatism.	112
3.6 Comparison of plagiogranite trace element content.	112
3.7 Comparison of Axis Sequence Geochemistry.	112

## List of Plates

Following  
Page

1.	Diffuse-margined intrusive veins.	18
2.	Sharp-margined intrusive veins.	18
3. & 4.	Mixtures of plagiogranite and dolerite.	18
5.	Liquid/liquid mixture.	20
6.	Sheeted Intrusive Complex.	20
7.	Flow banded felsite.	20
8.	Zoned plagioclase.	23
9.	Poikilitic quartz.	23
10.	Primary granophyre.	25
11.	Secondary granophyre.	25
12.	Clinozoisite replacing plagioclase.	26
13.	Epidote replacing plagioclase.	26
14.	Top of plagiogranite sheet.	41
15.	Gabbro, cross-cut by dolerite and trondhjemite.	41
16. & 17.	Epidotized trondhjemite intrudes epidote-free tonalite.	42
18.	Zoned aplite vein.	44
19.	Multiple dyking.	57
20.	Flow folded layered gabbro.	57
21.	Primary granophyre.	60
22.	Intrusive vein.	61
23.	<u>In situ</u> vein in varitextured gabbro.	61

## Chapter 1 Introduction

### 1.1 Ophiolites and plagiogranites

"Ophiolite" has suffered for want of definition since its introduction as a synonym of serpentinite in the early 19th century (Brongniart 1827). It has been used, with several other terms (roches vertes, verd antique, greenstone) to describe a variety of ultrabasic and basic rock types and associations (Green 1971, Coleman 1977 p.1). The most notable precedent was set by Steinmann (1906, 1927) who employed "ophiolite" to name the common association of serpentinite, pillow lava and radiolarite in orogenic belts (The Steinmann Trinity) and thus initiated systematic research on this suite of rocks. The currently accepted redefinition of "ophiolite", which is adopted in this work, was proposed by the participants of the 1972 GSA Penrose Conference (Geotimes, 1972).

"Ophiolite refers to a distinctive assemblage of mafic to ultramafic rocks. It should not be used as a rock name or as a lithologic unit in mapping. In a completely developed ophiolite the rock types occur in the following sequence starting from the bottom;

- (1) Ultramafic complex, consisting of variable proportions of harzburgite, lherzolite and dunite, usually with a metamorphic tectonic fabric and more or less serpentinized.
- (2) Gabbroic complex, ordinarily with cumulus textures commonly containing cumulus peridotites and pyroxenites and usually less deformed than the ultramafic complex.
- (3) Mafic sheeted dyke complex.
- (4) Mafic volcanic complex, usually pillowed.

Associated rock types include (1) an overlying sedimentary

section typically including ribbon cherts, thin shale interbeds and minor limestones. (2) Podiform bodies of chromite, generally associated with dunite (3) Sodic felsic intrusive and extrusive rocks. Faulted contacts between mappable units are common, whole sections may be missing. An ophiolite may be incomplete, dismembered or metamorphosed, in which case it should be called a partial, dismembered or metamorphosed ophiolite. Although ophiolite generally is interpreted to be oceanic crust and upper mantle the use of the term should be independent of its supposed origin".

This work is concerned with the origin of the small volumes of "sodic, felsic" rocks in five ophiolites; the Troodos Massif, Cyprus, the Semail Nappe, Oman, The Smartville Block and the Point Sal ophiolite, California, and the Ballantrae Complex, Ayrshire, Scotland. Such rock types occur in many other ophiolites (Section 2.6) but appear to be absent in some cases. A great variety of "sodic, felsic" rock types occur; diorite, quartz diorite, tonalite, trondhjemite, albite granite, albitite, keratophyre, granophyre, porphyry and rhyolite, all are characterised by the virtual absence of a potassium-rich feldspar. Coleman and Peterman (1975) proposed "oceanic plagiogranite" as a "general descriptive and collective term" to include all granitic rocks in ophiolites and this term is used hereafter but abbreviated to "plagiogranite". (Section 1.3).

Although the definition offered by the 1972 Penrose Conference specifically excludes any genetic implication, ophiolites are now generally accepted as fragments of oceanic crust emplaced on continental margins (Dewey and Bird, 1970, 1971, Moores and Vine 1971, Coleman 1971). Dietz (1963) suggested the

general equivalence of Alpine-type peridotites and the oceanic crust. The hypothesis that a complete ophiolite, The Troodos Massif, is a segment of oceanic lithosphere was first proposed by Gass and Masson-Smith (1963) and expanded by Gass (1968) and Moores and Vine (op. cit.). Subsequent multi-disciplinary studies on Troodos (Section 1.2) and other ophiolites have provided strong support for the oceanic lithosphere model although there is some conflict in this matter. (e.g. Miyashiro 1973, 1975; see also Gass et al., 1975 for discussion). The structure of the Massif bears a good resemblance to that proposed for oceanic crust on theoretical (Oxburgh and Turcotte, 1968, Cann 1970a, 1974) and geophysical grounds (Christensen, 1970 Khan et al., 1972, Moores and Jackson 1974). Lithologies found in ophiolites are common in material dredged from the ocean bottom (e.g. Aumento 1971, Cann 1971, Thompson 1973) although relatively few plagiogranites have been recovered (Section 2.7). The structure and lithology of Macquarie Island, an uplifted section of the floor of the Tasman Sea, are similar to parts of ophiolites (Varne et al., 1969, Griffiths and Varne, 1972) and its strontium isotope geochemistry resembles that of mid-ocean ridge basalt. (Williams 1977).

## 1.2 History of research in ophiolites

Although the general features of many ophiolites have been published and several areas have been studied in great detail the Troodos Massif remains the best known complete ophiolite. Many concepts have developed through research on the Massif which are applicable to the genesis of all ophiolites. Therefore, the following outline of the history of research in an ophiolite was taken largely from the literature about Troodos. In detail, the Massif has important differences from other ophiolites but they are mentioned where they become relevant. The geological setting of the Troodos Massif, which is, of course, peculiar to that ophiolite, is described in Section 2.1.1 and the relatively sparse published research on the other study areas is summarised in the separate parts of Chapter 2.

The memoirs and maps published by the Cyprus Geological Survey (e.g. Wilson 1959) form the basis of most research on the Massif and much of this work was summarised by Gass and Masson-Smith (1963) and Moores and Vine (1971). These authors described the Massif as "a pseudostratiform mass of harzburgite, dunite, pyroxenite, gabbro, quartz diorite, diabase and pillow lava arranged in a dome-like manner". Gass and Masson-Smith, who slightly modified the Survey nomenclature, divided the sequence into the Plutonic Complex, the Sheeted Intrusive Complex (SIC) and Lower and Upper Pillow Lavas (LPL and UPL) (Table 1.1). Moores and Vine (op. cit.) suggested that the Troodos parental magmas were derived by partial melting of the mantle during its upward flow beneath a mid-ocean ridge



Table 1.1 Stratigraphic Nomenclature of the Troodos Massif

				Formation Boundary
Lefkara Group <sup>2</sup> - Maestrichtian to lower Miocene				Unconformity
Perapedhi Formation <sup>1</sup> - Campanian				
Upper Pillow Lavas <sup>1</sup>				Conformity
Lower Pillow Lavas <sup>1</sup> )				Unconformity varying laterally to conformity
Axis				
Basal Group <sup>1</sup> )    Sheeted <sup>3</sup> )				Gradational
Diabase <sup>1</sup> )    Intrusive)				Gradational overall, intrusive in detail
Complex )    Sequence <sup>4</sup>				
Plutonic <sup>1</sup> Complex	( Cumulate	( Upper Plutonic <sup>6</sup>	Gradational or intrusive	
	( Sequence <sup>5</sup>	( Complex		
	( Layered Sequence <sup>6</sup>	Abrupt stratigraphic contact		
	( Mantle Sequence <sup>5</sup>		No base observed	

1. Wilson, 1959, 2. Pantazis, 1967, 3. Gass and Masson-Smith, 1963,

4. Gass and Smewing, 1973, 5. Allen, 1975, 6. Present work.

Table 1.2     Lithologies of the Troodos Massif

Lefkara Group:

Upper Cretaceous to Miocene chalks and marls.

Perapedhi Formation:

Manganiferous shales (umbers), radiolarites. Interbedded with or overlying UPL.

UPL:

Generally undersaturated olivine phyric metabasalts with limburgites and picrites. Some extrusive breccia but few dykes.

LPL:

Mainly oversaturated pyroxene and/or plagioclase phyric metabasalts and basaltic andesites. Mostly pillowed but with up to 60% massive flows, sills or dykes. Local massive sulphide mineralization.

SIC:

Subparallel dyked metabasalts. Towards the top with pillow lavas between and screens of plutonic rock towards base but without intervening host material for the main part.

Upper Plutonic Complex:

Plagiogranite, pyroxene gabbro, frequently uraltized and sometimes magnetite-rich. Cumulate layering absent, pegmatite gabbro common.

Layered Sequence:

Cumulate gabbros, olivine gabbro, anorthosite, wehrlite, pyroxenite, lherzolite, dunite with chromitite. Mineral phases appearing as intercumulus, then cumulus, usually in this order; Chromite, olivine, clinopyroxene,

Table 1.2    Lithologies of the Troodos Massif (continued)

---

Layered Sequence (continued)

Orthopyroxene, plagioclase, Cyclic, cryptic and rhythmic layering common

Mantle Sequence:

Tectonized harzburgite with gabbro dykes, minor plagioclase lherzolite, dunite pods and orthopyroxenite veins.

Sources:

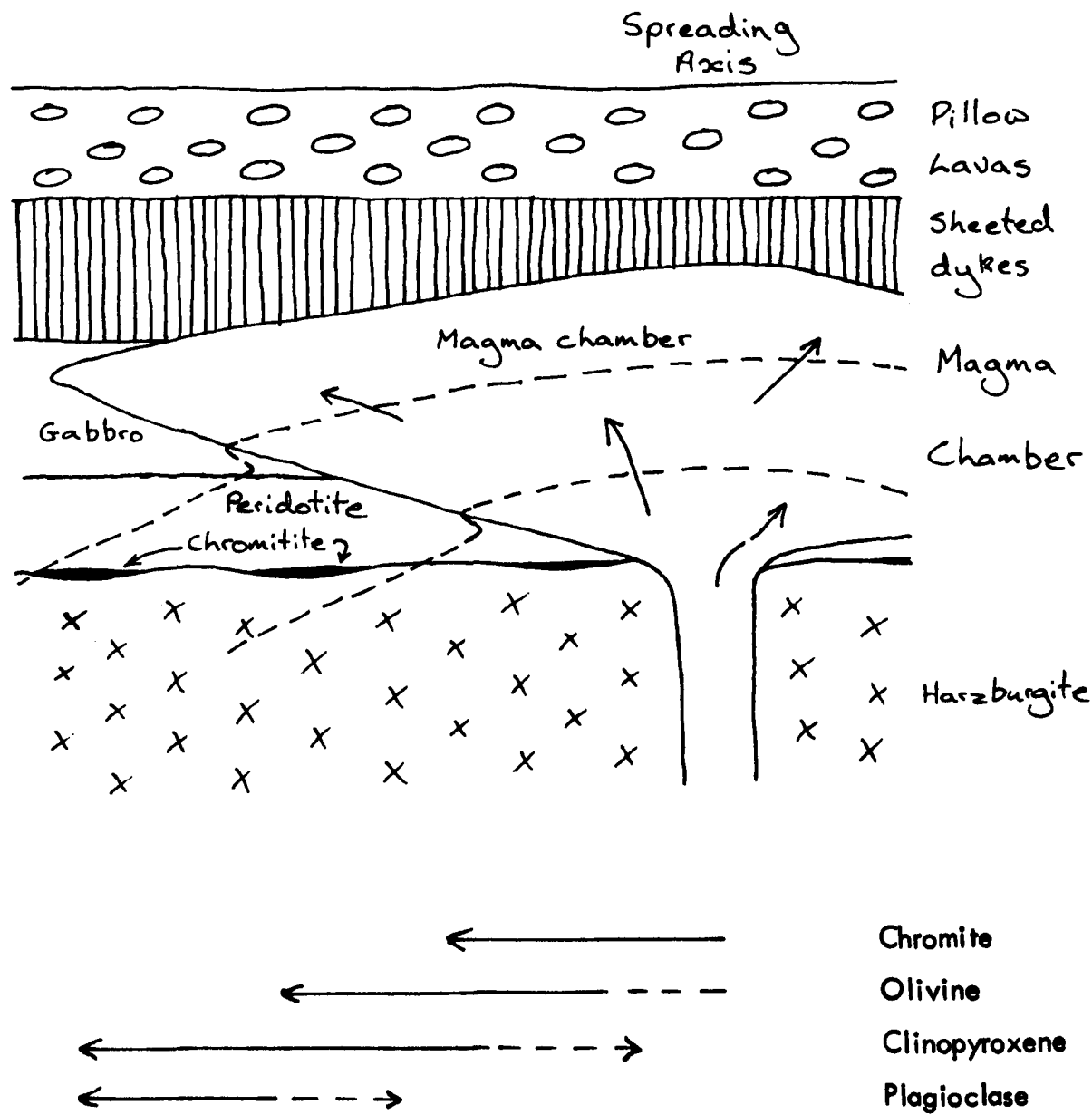
1. Wilson 1959
2. Pantazis 1967
3. Gass and Masson-Smith 1963
4. Gass and Smewing 1973
5. Allen 1975
6. Present work

and that the harzburgite and dunite represent the residual mantle which has a tectonic fabric imposed by solid state flow. The layered gabbro and pyroxenite originated by crystal accumulation in magma chambers which acted as reservoirs for the SIC and pillow lava magmas. Higher level gabbros and the quartz diorite formed by fractional crystallization of the basic melts. Wilson (1959) pointed out that the remarkable parallelism and absence of country rock in the SIC implied an origin in an extensional ensimatic environment and this has been emphasised by subsequent authors. Moores and Vine (op. cit.) interpreted the complex internal relations as the product of multiple intrusion and extrusion of small magma bodies about the spreading axis.

Their model contrasts with the alternative presented by Greenbaum (1972). He concluded from a study in the Plutonic Complex around Mount Olympus that it was formed by crystal accumulation in a single linear magma chamber beneath a mid-ocean ridge, floored by the harzburgite. Greenbaum also considered that the harzburgite is residual although he regarded the dunite as a deformed cumulate. Greenbaum suggested that the magma chamber was in a steady state in which movement of the lithosphere away from the spreading axis was approximately balanced by the influx of primitive magma from the mantle (Figure 1.1). A concentric thermal and chemical gradient was maintained towards cooler, more differentiated magma and so the four mineral phases crystallised simultaneously but in different zones of the magma chamber. Crystals accumulating on the moving floor were borne slowly outwards to where they

Figure 1.1 Hypothetical section of the lithosphere at a slow-spreading oceanic ridge

After Greenbaum 1972



- ← → indicates mineral accumulates in this zone
- ← - - - → indicates zone where mineral forms as intercumulus phase
- Flow in magma
- - - - Isotherm

were buried by a succession of lower temperature assemblages.

In a very detailed study of the Plutonic Complex, Allen (1975) preferred an intrusive model closer to that of Moores and Vine and presented evidence for numerous, discrete "magma cells" beneath spreading axes, each replenished by magmas of slightly varying composition. The evidence included intrusive contacts and zones of xenoliths within the Layered Sequence, ultrabasic sills at high levels and multiple intrusive contacts at the top of the Plutonic Complex. Allen considered that the plutonic complex differentiated from a picritic magma with low Na, K, Ti and P.

Metamorphic grade decreases steadily upwards from amphibolite facies in the Upper Plutonic Complex to cold water zeolite facies in the pillow lavas. (Gass and Smewing 1973). Metamorphic zonation is sub-concordant with lithological boundaries and late Cretaceous sediments overlying the Massif are unmetamorphosed. There is a metamorphic discontinuity within the zeolite facies at the base of the UPL which often coincides with an unconformity. It was suggested by Gass and Smewing that the LPL and SIC were metamorphosed together at an oceanic spreading axis in a thermal gradient of not less than  $150^{\circ}\text{C km}^{-1}$  and should be combined as the "Axis Sequence" (Table 1.1). The UPL were considered to have erupted "off-axis", away from the Axis Sequence metamorphic regime and to have been metamorphosed in their own "perched" thermal gradient.

Similar hydrothermal metamorphism is seen in the ophiolites of East Liguria, Italy (Spooner and Fyfe, 1973) and southern Chile. (Stern et al., 1976). Spooner and Fyfe (op. cit.) postulated that a circulating hydrothermal system was the

prime agent of metamorphism and heat and mass transfer at the then active constructive margin. Seawater was envisaged as percolating down through the crust, being heated and returning up narrow zones to discharge into the ocean. They attributed the formation of cherts and massive sulphide deposits associated with ophiolites to this hydrothermal activity. Ferromanganese sediments (umbers) in the Troodos pillow lavas are thought to have been precipitated from thermal springs which discharged seawater enriched in heavy metals leached from the Axis Sequence. (Robertson and Fleet 1976). Analogous heavy metal enriched hot brines occur in the basal waters of the Red Sea (Degens and Ross 1969) and metalliferous sediments on modern ocean ridges (Robertson and Hudson 1973).

Stable isotope geochemistry provides confirmatory evidence for both the origin of these metamorphic fluids and of the parent magmas of the Troodos Massif. Early  $^{87}\text{Sr}/^{86}\text{Sr}$  determinations for the gabbros, plagiogranites and Axis Sequence fall in the range 0.7038 to 0.7056 (Peterman, Coleman and Hildreth 1971, Greenbaum 1972) Peterman et al., pointed out that these values are outside the range of tholeiites from ocean ridges. However, Spooner et al., (1977) found that  $^{87}\text{Sr}/^{86}\text{Sr}$  in the gabbros and plagiogranites increased even with slight metamorphism and so high values could be the result of contamination by isotopically heavier material such as seawater. Analysis of pristine gabbros established that Troodos Sr isotope ratios did overlap the higher values of fresh modern ocean floor basalts. This indicates that the Massif formed from mantle which had a similar depletion history to that which underlies some modern ocean ridges. Determinations of  $\delta^{18}\text{O}$  in low grade metabasites

from Troodos, East Liguria and Pindos, Greece, are consistent with the hypothesis that seawater, rather than meteoric water, was the hydrothermal fluid. (Spooner et al., 1974). The magnitude of change in isotope composition indicates very large water: rock ratios. A progressive decrease in  $\delta^{18}\text{O}$  was correlated with increasing metamorphic temperatures at greater stratigraphic depth. (Heaton et al., 1977).

Many elements are labile during hydrothermal metamorphism (Section 1.3) so several interpretations of primary geochemistry on Troodos have depended on the immobile trace elements. Pearce and Cann (1973) considered that the Ti, Zr, Y and Nb content of the basalts was diagnostic of ocean floor tholeiites. Pearce (1975) combined several lines of geochemical evidence and concluded that the Axis Sequence shared many chemical features with ocean floor basalts (although there were significant differences) but the Upper Pillow Lavas were more like low potassium (immature island-arc) tholeiites. He suggested the ophiolite originated in a behind-arc basin above a south-dipping subduction zone.

Smewing et al., (1975) reached a similar conclusion. They also pointed out that the range in abundance of incompatible elements in the lavas suggests extensive pre-eruption crystal fractionation. However, they found the range in composition is too great to be explained by this mechanism alone, requiring, in addition, variation in the composition of the parental magma. A general upward decrease of the incompatible traces in the lava pile suggests a succession of magma batches, each more depleted in traces, arising by incremental partial melting of the mantle. The distribution of the REE supports this model. (Smewing and Potts 1976).



### 1.3 Methodology and Rationale

#### 1.3.1 Objectives

The objectives of this project were (i) to identify the types of plagiogranite occurring in five ophiolites of differing age and tectonic setting and to determine and compare their detailed field relations, primary and secondary petrography and geochemistry. (ii) To determine by what magmatic and metamorphic processes the plagiogranites were formed, from what parent material and at what stage in the evolution of the ophiolite. (iii) To compare plagiogranites from ophiolites with similar dredged rocks from the present day oceanic crust and thereby to test the hypothesis that ophiolites represent oceanic lithosphere fragments.

#### 1.3.2 Background

The Troodos Massif (Section 2.1) was chosen as the first field area for several practical and scientific reasons. It is arguably the most thoroughly documented and best understood ophiolite in the world. All parts of the ophiolite sequence are moderately well exposed and accessible. No later metamorphism has obscured spreading axis processes. The second area, the Semail Nappe, (Section 2.2) is a huge, undeformed, complete ophiolite and, although less intensively studied, has many features in common with the Troodos Massif, including Tethyan origin and Upper Cretaceous age. Excellent exposures of plagiogranite abound. The general similarities corroborate observations on Cyprus, the differences exemplify spatial

petrogenetic variations in the Tethyan belt. The third and fourth areas, The Smartville Block (Section 2.3) and the Point Sal ophiolite (Section 2.4) are Jurassic ophiolites preserved in contrasting tectonic situations in the western American Cordillera. The Smartville Block was only recognized as an ophiolite very recently and is sparsely documented. The last area, the Ballantrae Complex (Section 2.5), is a dismembered Lower Palaeozoic ophiolite in the southern Caledonides.

### 1.3.3 Methodology

Instead of conventional field mapping, the adopted strategy was to visit several areas within each ophiolite where plagiogranites crop out and to determine and collect from the various types and their host rocks and to analyse the details of their field relationships. The areas were chosen by reference to existing maps. Although field work concentrated on the Upper Plutonic Complex and the lower part of the sheeted intrusive complex, representative sections of the rest of each ophiolite were also studied. Petrographic study was mostly by optical microscopy with a limited contribution from electron probe microanalysis. Geochemical analyses were by X-ray fluorescence, neutron activation and wet chemical methods (Appendix 3).

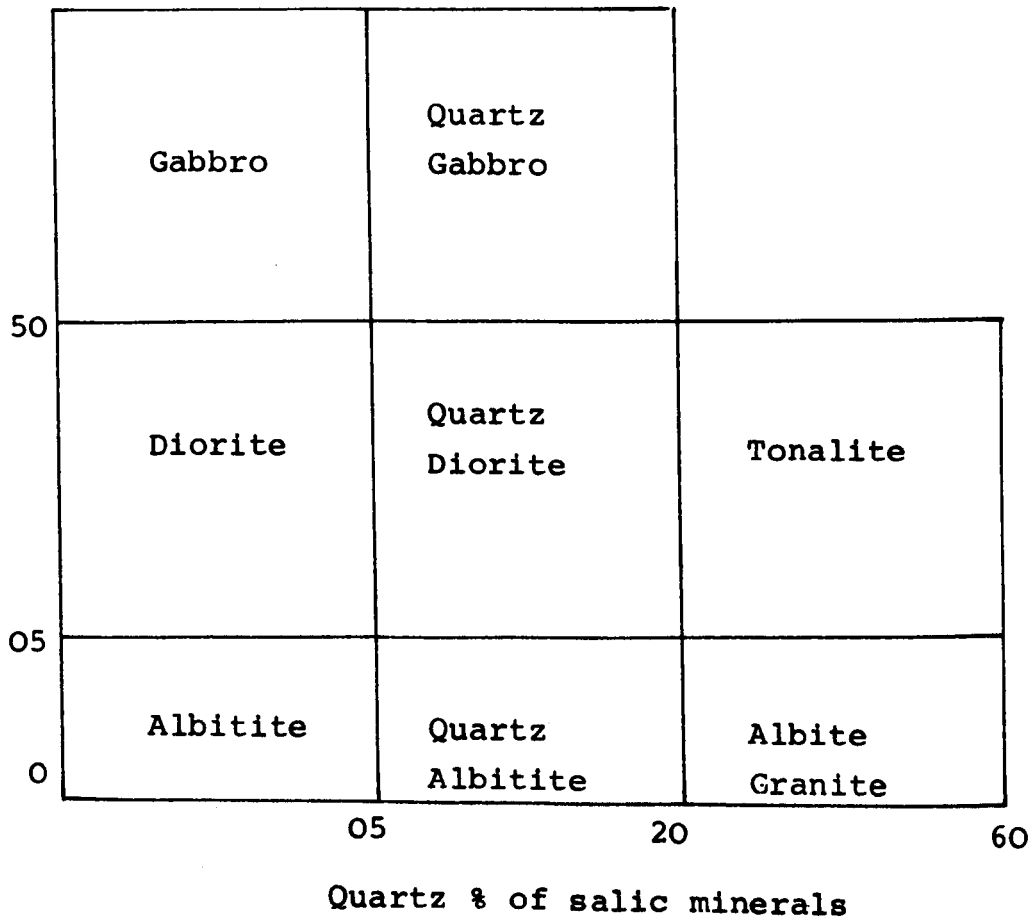
### 1.3.4 Nomenclature

The petrographic nomenclature adopted is based on a modal classification proposed by an IUGS commission (Streckeisen, 1976) (Table 1.3). However, "albite" and "quartz albitite" are

Table 1.3     Petrographic Nomenclature

Classification of coarse to medium grained plagioclase-rich igneous rocks by mode

Average Anorthite %  
in plagioclase



K-feldspar is less than 5% total feldspar.

When mafic minerals are less than 10% of the mode the prefix 'leuco' is added. Trondhjemite is equivalent to leucotonalite.

After Streckeisen 1976.

Table 1.4    Abbreviations used in text

---

Conventional symbols are used for S.I units,  
Chemical elements, oxides and ions.

Fe <sub>2</sub> O <sub>3</sub> *	Total iron as Fe <sub>2</sub> O <sub>3</sub>
F.Z	Fracture Zone
G.V.S	Great Valley Sequence
H.R.E	Heavy rare earths
L.I.L	Large ion lithophile
L.P.L	Lower pillow lavas
L.R.E	Light rare earths
L.V.U	Lower volcanic unit
M.A.R	Mid-Atlantic Ridge
M.O.R	Mid-ocean ridge
my	million years
RE(E)	Rare earth (elements)
ΣRE	Sum of chondrite normalised abundances of Ce, Nd, Sm, Eu, Gd, Tb, Tm, Yb, Lu
S.I.C	Sheeted Intrusive Complex
U.P.L	Upper Pillow Lavas
U.V.U	Upper Volcanic Unit

Mineral abbreviations

Ab	Albite	Ha	Haematite
Acc	Accessory	Hnd	Hornblende
Act	Actinolite	Ol	Olivine
Amph	Amphibole	Op	Opagues
Ap	Apatite	Opx	Orthopyroxene
Biot	Biotite	Or	Orthoclase
Cal	Calcite	Pl	Plagioclase

Table 1.4    Abbreviations used in text (continued.)

---

Chl	Chlorite	Preh	Prehnite
Cpx	Clinopyroxene	Py	Pyrite
Cr	Chromite	Qz	Quartz
Cum	Cummingtonite	Saus	Saussurite
Cz	Clinozoisite	Sph	Sphene
Ep	Epidote	Zrc	Zircon

retained in preference to the recommended albite syenite and quartz albite syenite to avoid implication of alkalic association. Although "plagiogranite" is used in the collective sense proposed by Coleman and Peterman (1975), their cumbersome adjective "oceanic" is dropped to avoid genetic connotations. However, in order to distinguish plagiogranites found in ophiolites from those of island arcs (Section 2.6) and the ocean crust (Section 2.7) prefixes are used where appropriate. Several difficulties preclude the precise classification of individual plagiogranites. They are frequently heterogeneous on a small scale and this is often due to variable development of secondary minerals which obscure the primary assemblage. Average anorthite content is usually impossible to determine because of complex zoning of plagioclase. However, as the plagiogranites generally occur in a continuous monogenetic series these difficulties are not of critical importance.

As all plagiogranites have been at least slightly altered, the prefix "meta" is employed herein only when it is important to distinguish fresh and metamorphosed specimens. "Epidosite" describes metamorphites composed essentially of epidote and quartz. First identified on Troodos by Wilson (1959), and termed a quartz granulite, epidosite can be derived from either a plagiogranite or a dolerite by extensive hydrothermal metasomatism.

#### 1.3.5 Geochemistry

In the interpretation of geochemical variation among the plagiogranites, the following factors were taken into account.

- (i) Composition of parent magmas; both primary mantle melt and

the evolved basic melt from which the first plagiogranite liquid was derived. (ii) Composition and proportion of fractionating and accumulating mineral phases. (iii) The efficiency of melt separation from precipitated crystals and so whether a particular specimen represents a liquid composition, a cumulate or a crystal mush. (iv) Chemical mobility due to post-solidification hydrothermal activity (metasomatism) (v) chemical mobility in late stage magmatic aqueous phases (vi) assimilation of xenoliths.

The internal consistency of the geochemical data and their overall correlation with petrography suggests geochemical variation due to analytical error is small relative to that caused by petrogenetic factors. It is assumed that where analytical error does occur it is random and causes divergence from primary trends rather than convergence to a false trend.

Several authors have commented on the mobility of elements such as Si, Fe, the alkali and alkaline earth elements in zeolite and greenschist facies metabasites (e.g. Hart 1974, Smewing 1975). Other elements; Ti, Zr, Y, Nb, Cr and the heavy REE, are considered to be immobile during hydrothermal alteration (Frey 1968, Cann 1970, Pearce and Cann 1973, Bloxham and Lewis 1973, Wood 1977) although doubt has been expressed about the universal immobility of the REE. (Frey 1974, Hellman and Henderson 1977). The immobility of these elements usually has been demonstrated empirically (e.g. Cann op. cit., Wood op. cit.) but, as Pearce (1973) has pointed out, the relative likelihood of an element being retained in

a crystal lattice or taken into aqueous solution during metamorphism can be predicted from thermodynamic considerations.

The secondary mobility of labile elements in plagiogranites was investigated by identifying groups of fresh and altered specimens with the same primary mineralogy and immobile trace element content and then seeking consistent variation of labile element content with degree and type of alteration. The percentage and variety of secondary minerals was assessed microscopically. It was assumed that the more radical the change from primary mineralogy the more likely was metasomatism to have occurred. The converse, that metasomatism necessarily accompanies recrystallization was found not to be the case.

The iron oxidation ratio,  $\text{FeO}/\text{FeO} + \text{Fe}_2\text{O}_3$ , and  $\text{H}_2\text{O}^+$  have both been employed as indices of alteration in basaltic rocks (e.g. Miyashiro 1969). In the Troodos Upper Plutonic Complex, the iron oxidation ratio is not sufficiently predictable for this purpose. Some altered rocks are heavily oxidised but some are reduced with the formation of pyrite. There is also magmatic variation, later differentiates being more oxidised. (Section 2.1.3). The variable development of primary hydrous phases in the Upper Plutonic Complex suggests magmatic water content also varied and volatiles were not analysed. In the Troodos pillow lavas,  $\delta^{18}\text{O}$  does not vary systematically with  $\text{H}_2\text{O}^+$ . (Heaton et al., 1977).



## Chapter 2 Description

### 2.1 The Troodos Massif

#### 2.1.1 Regional Geology

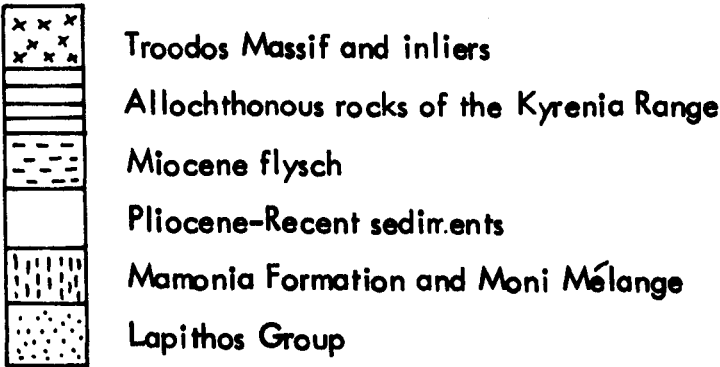
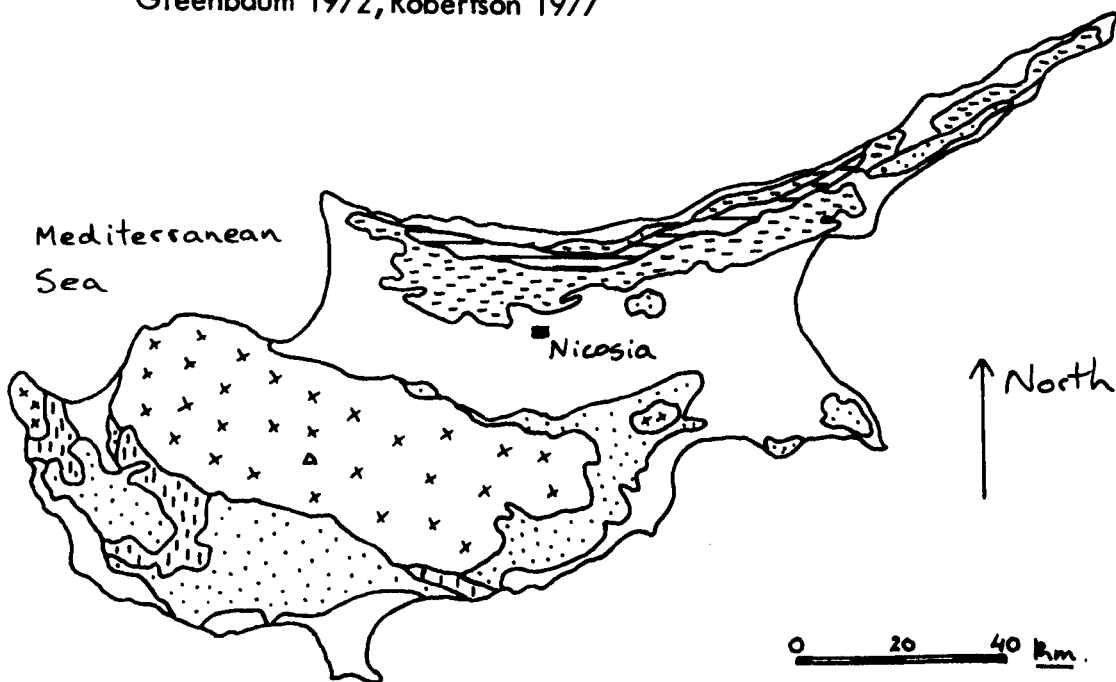
The Troodos Massif is the main mountain range on the island of Cyprus which is situated in the Eastern Mediterranean 70 km. south of Turkey and 100 km. west of Syria. The island is small, only 230 km. E-W by 100 km. N-S and occupying a total of 9200 sq. km..

The geological structure of the island controls the topography which can be conveniently divided into five regions (Gass and Masson-Smith 1963) Figure 2.1.1. The northernmost unit comprises the allochthonous Upper Paleozoic to Cretaceous limestones, radiolarites and volcanics of the Kyrenia range. These are flanked by structurally related but less deformed autochthonous Miocene Flysch. The central plain of Cyprus, the Mesaoria, is underlain by thick, undisturbed, mainly marine sediments of Pliocene to Recent age. These rest unconformably on the deformed flysch to the north and on gently dipping calcareous sediments to the south. These autochthonous sediments, of Maestrichtian to upper Miocene age, overlie the Troodos Massif to its north and south. To the south they are more deformed and include pelitic and detrital lithologies. To the west and south of the Massif they overlie the allochthonous Mammonia Formation and the Moni Mélange. The former is a series of nappes of Late Triassic to Jurassic sandstones, limestones, pillowed alkaline basalts and serpentinite (e.g. Lapierre 1972). The

Figure 2.1.1 Geological sketch map of Cyprus

After Gass and Masson-Smith 1963,

Greenbaum 1972, Robertson 1977



Moni Mélangé is a chaotic mass of rocks similar to those of the Mammonia Formation in a matrix of deep water clays (Robertson 1977).

The Troodos Massif, rising to nearly 2,000 m, is a complete ophiolite complex, according to the 1972 Penrose Ophiolite Conference definition. It's main outcrop is continuous over an area measuring 90 km. by 30 km. with two small inliers to east and west. Boreholes have proved its northerly extension under the Mesaoria (Vine, Poster and Gass 1973). Extreme uplift of the ophiolite complex has exposed its lowest member, the tectonized harzburgite, in the middle of the Massif and this is surrounded by annular outcrops of progressively higher members. In the south, this simple pattern is disturbed by the Arakapas Fault Belt, a palaeotransform fault, (Simonian, 1976) and the Limassol Forest Serpentinite. Palaeontological evidence suggests extrusion of the pillow lavas, now outcropping on the periphery of the Massif, during Upper Cretaceous but pre-Campanian times (Mantis 1971). The sparse radiometric data available support this hypothesis (Vine et al., 1973),

Although most authors agree that the Massif was formed at an oceanic spreading axis, the exact nature of its original tectonic setting and mode of emplacement remain uncertain. It lies in the southern most structural belt of the Taurides and related ophiolite terrain lies to the northwest (Antalya, Turkey) and northeast (Ba<sup>II</sup>er-Bassit/Hatay, Syria/Turkey) (Ricou 1971). Palaeomagnetic data show the Massif has rotated 90° anticlockwise since the Cretaceous. (Moores and Vine 1971).

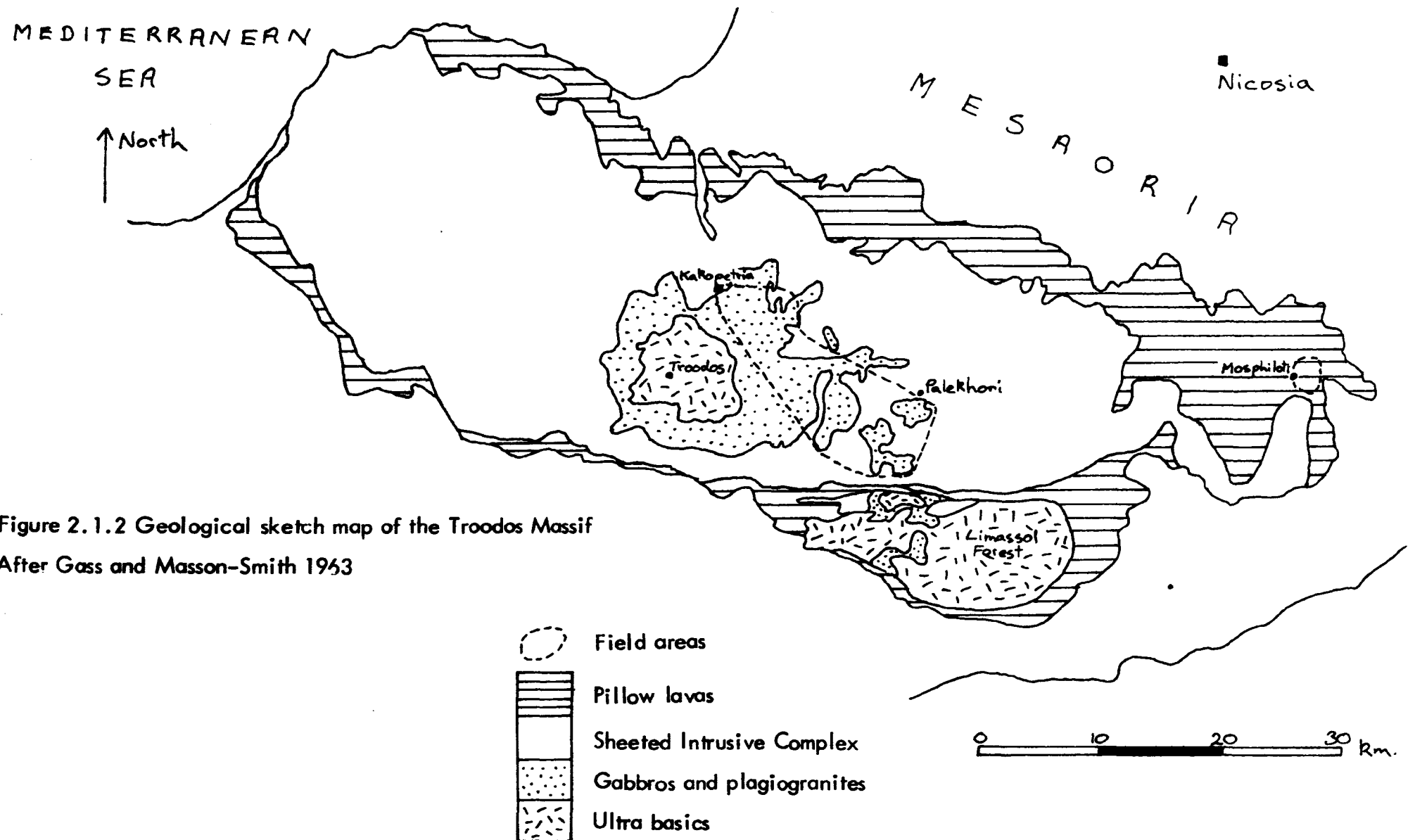


Figure 2.1.2 Geological sketch map of the Troodos Massif  
After Gass and Masson-Smith 1963

Gass (1977) suggested the Massif was underthrust by the African plate in the late Mesozoic, during the convergence of Africa and Eurasia. Subsequent uplift of the ophiolite was centred on a 10 km. diameter serpentinite diapir, mantle material hydrated by water released from the underthrust slab. Pre-emplacement uplift by serpentinite has been suggested for other ophiolites (Smith and Woodcock, 1976). Pearce (1975), Smewing et al., (1975) concluded from geochemical affinities that the Massif originated in a marginal basin, above a south-dipping subduction zone. However, Robertson (1977) contends that both the Mammonia Formation and the Moni Mélange were emplaced from a continental margin to the southwest (northwest before palaeorotation). He postulated northwesterly subduction of Mesozoic ocean crust beneath the Eurasian continental margin. When subduction ceased in the late Cretaceous, a section of the ocean crust was preserved on the edge of the trench, which was filled with sediments slipping from the continental margin.

## 2.1.2 Field Relations of the Upper Plutonic Complex

### 2.1.2.1 Gabbros

The relationships within the Layered Sequence of the Plutonic Complex have been described by Wilson (1959) and Allen (1975). The criteria which distinguish gabbros in the Layered Sequence from those in the Upper Plutonic Complex do not permit a sharp division to be drawn. There is a transition zone beneath which the gabbros are unaltered medium to fine grained pyroxene gabbros with compositional layering. The overlying gabbros are massive coarse to medium grained, frequently

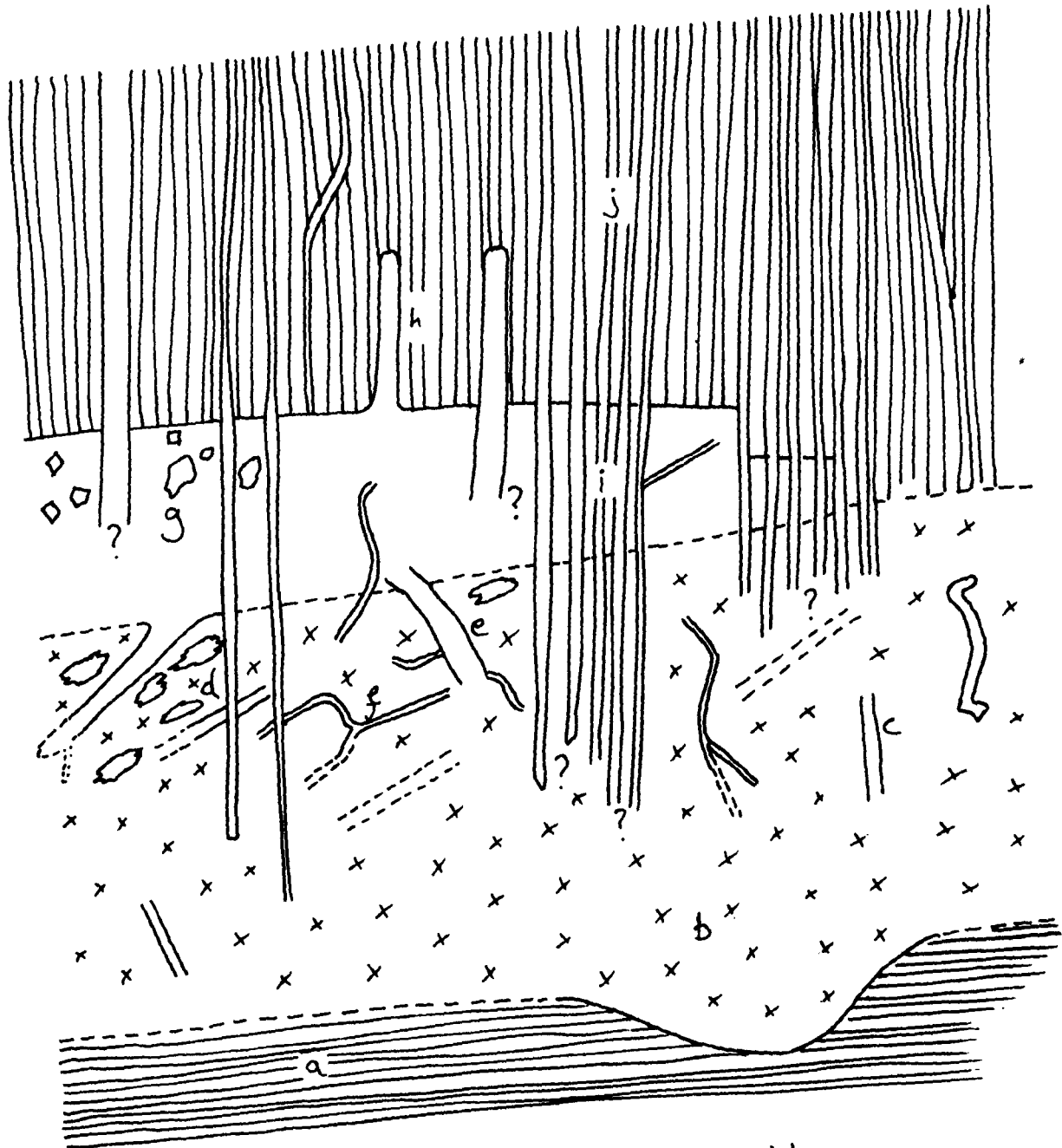
amphibolitized and most readily distinguished in the field by the absence of cumulate layering. These gabbros can be uniform at outcrop level but are more usually compositionally and/or texturally heterogeneous. They have been referred to as either "high level gabbros", by virtue of their stratigraphic position, or "varitextured gabbros". The latter term was adopted because it is based solely on textural criteria.

Random or en echelon pegmatite veins, pods and dykes are common in the varitextured gabbro. Segregation gabbro is a type of varitextured gabbro which is particularly significant in the study of the granitic rocks. It has leucocratic, often quartz bearing, patches veins or pods up to one metre across which have gradational contacts with the gabbro host. The veins are commonly associated with coarse, acicular amphiboles and gabbro pegmatities. As they appear to have no feeder vein they seem to have originated in situ by segregation from the gabbro. The veins in segregation gabbro are the "stratigraphically lowest" occurrence of plagiogranite. The presence of segregation textures does not imply the formation of two immiscible liquids. It is thought that the segregations are a residual liquid separating from a crystal mush.

#### 2.1.2.2 Plagiogranites

The leucocratic segregations are not invariably isolated and at a few localities they pass directly into sharp margined veins that range in width from a few centimetres to over a metre. The absence of chilled margins and the frequently observed variation from quite sharp to rapidly gradational margins suggests that the host was sometimes plastic and in

Figure 2.1.3 Schematic summary of field relations at the top of the Plutonic Complex  
Not to scale



- Gradational margin
- Intrusive margin
- a Layered gabbro
- b Varitextured gabbro
- c Pegmatite gabbro dyke
- d Segregation gabbro  
with in situ veins
- e Plagiogranite dyke
- f Sharp-margined acid vein
- g Tonalite / Trondhjemite, with xenoliths
- h Trondhjemite / Rhyolite dykes
- i Dolerites cross-cutting plutonics
- j Sheeted Intrusive Complex

other instances was sufficiently cool to be brittle. Although the in situ veins are confined to segregation gabbro, the sharp margined plagiogranitic veins intrude both layered gabbro and other plagiogranite.

The apparent mobilization and coalescence of tonalitic material into larger intrusive bodies culminates in the formation of sheets of acidic rock up to kilometric horizontal dimensions and a hundred metres thickness. These bodies are the highest stratigraphic horizon in the Plutonic Complex. They are laterally discontinuous and pass gradationally sideways and downwards into varitextured gabbro. This may occur within a few metres or over several tens of metres. At one locality, near Phterikoudhi, a variety of heterogeneous intermediate types are seen between a segregation gabbro and a metatonalite. The absence of intrusive margins in this outcrop suggests the heterogeneity is due to incomplete segregation rather than mixing of two types. Diorites are apparently less abundant than the quartz-rich plagiogranites. On Troodos this diorite gap seems to be the product of the gabbro/platiogranite segregation process.

The acidic differentiates range from quartz diorites and tonalites to mafic-free trondhjemites. They are often texturally and mineralogically inhomogeneous. This is attributed to variation in the many processes involved in their formation. (Table 2.1.1). (Plate 3 and 4). Columnar jointing occurs in the thickest bodies, implying the existence of a single sizeable body of stagnant liquid.



Table 2.1.1 Flow chart of petrogenetic processes

---

Variation in these processes would produce heterogeneity amongst the plagiogranites

Fractional crystallization in basic melt



Segregation of interstitial acidic residuum from gabbroic crystal/liquid mush



Mixing of many small acidic segregations



Mixing of acid and basic liquids



Incorporation of xenoliths

(Dolerite, diorite, tonalite, gabbro)



Retention/Incorporation of xenocrysts

(Plagioclase, Pyroxene)



Assimilation



Crystallization of acidic liquid

Crystal growth, settling, accumulation

Separation of interstitial liquid



Metamorphism

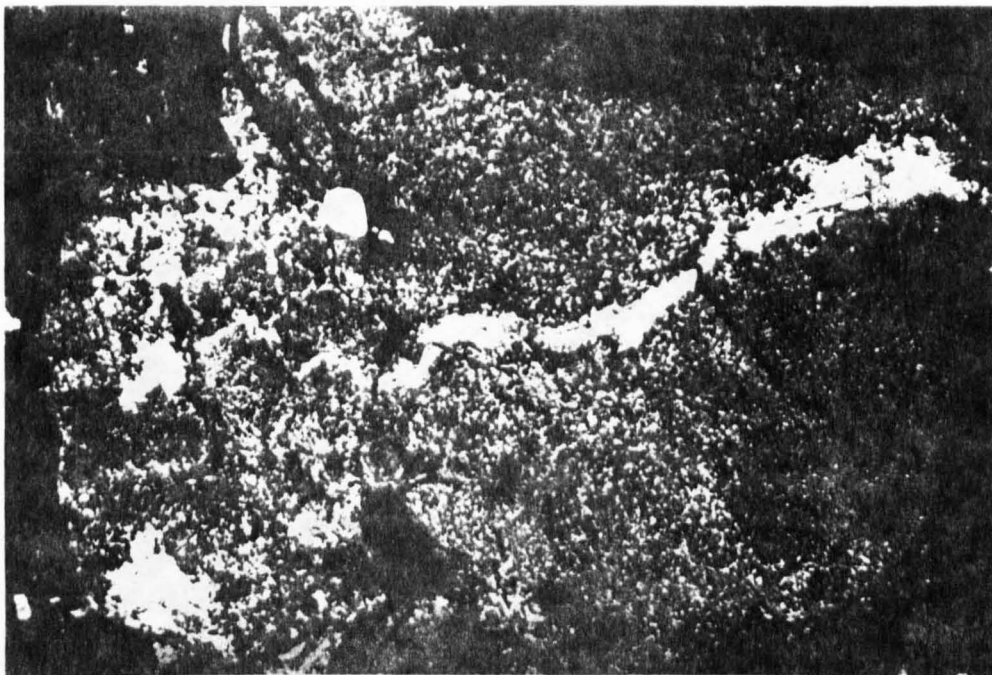


Plate 1 Diffuse - margined microtrondhjemite veins  
in varitextured gabbro, Pelendria, Cyprus.

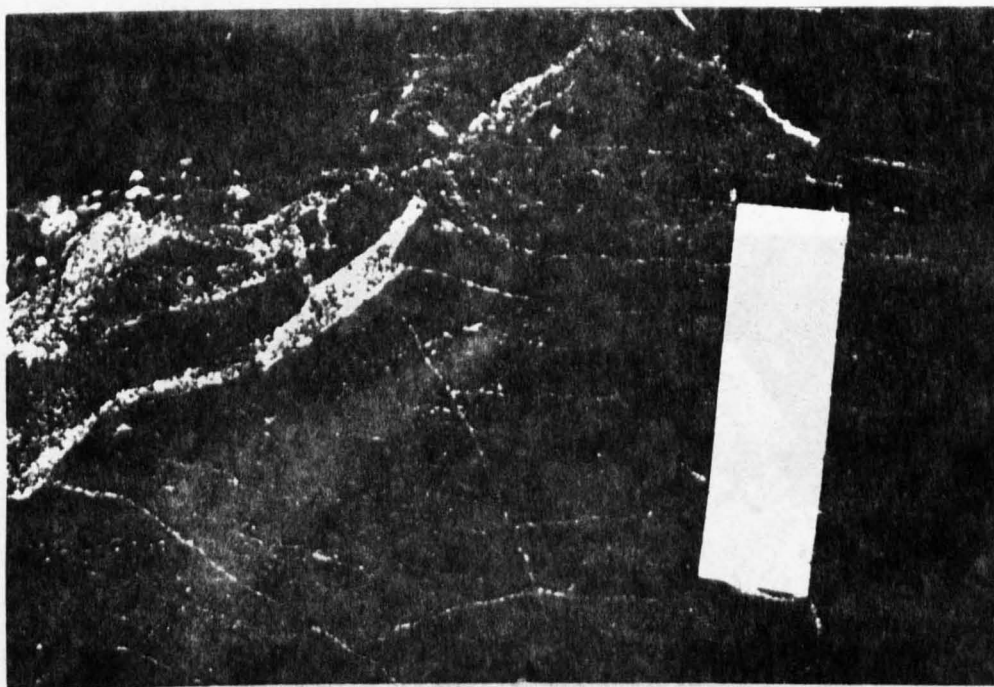
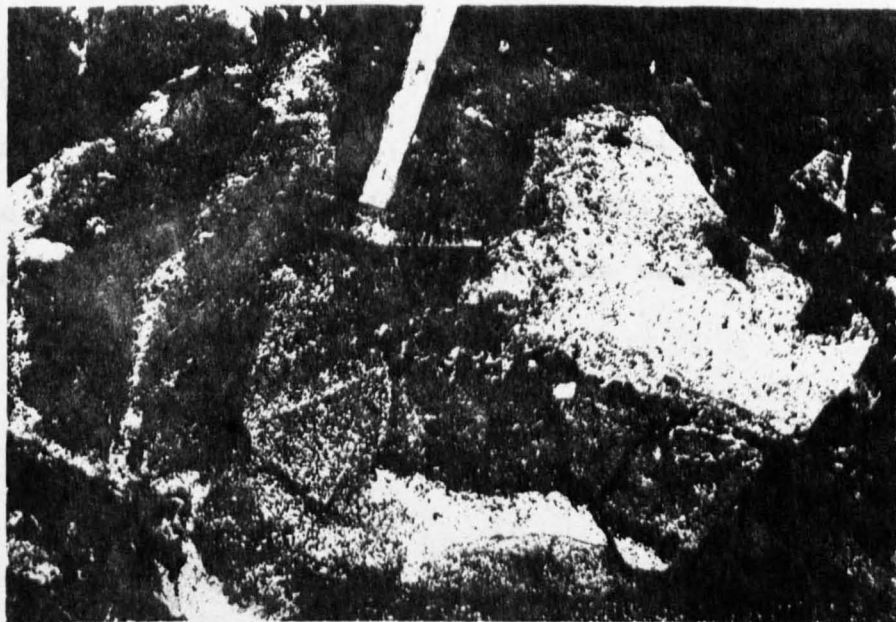


Plate 2 Sharp - margined microtonalite veins in  
two - pyroxene gabbro, Moutillas, Cyprus.



Plate 3 and 4 Mixtures of microtrondhjemite,  
microtonalite and dolerite, Palekori, Cyprus. The  
textures in these boulders are typical of  
heterogeneous plagiogranite outcrops.  
Hammer head is 17cm. long.



Xenoliths, although common, are not ubiquitous. They are normally doleritic or basaltic, sometimes dioritic or tonalitic, rarely gabbroic. In many cases they have undergone assimilation and thereby lost coherence. Although unaltered examples are almost always sharp-edged and angular, rounded basaltic inclusions occur at Palekhor. (Plate 5). These are up to one metre across, with irregular, generally rounded, crenulated, convex margins which maybe sharp or diffuse on any one xenolith. Similar textures have been described by Walker and Skelhorn (1966) who attribute them to be mixing of acid and basic magmas and this is thought to have occurred here. The phenomenon has only been observed at one locality. There are two possible reasons for its rarity on Troodos; either such a mixture is unstable and homogenisation is rapid or mixing is uncommon. Since partly homogenised hybrids are not seen it is thought that the injection of a basic into an acidic liquid rarely occurs.

The plagiogranite sheets are often cut by veins of more differentiated acidic material, including aplite, and dykes of dolerite, porphyritic rhyolite or gabbro. Dolerite dykes also intrude varitextured gabbro. In some sections, the proportion of dykes exceeds 50%

#### 2.1.2.3 The Sheeted Intrusive Complex

In its central section, the SIC is composed entirely of subvertical basic dykes with regional north-south orientation. Local low angles of dip are attributed to faulting. Dykes vary from filaments a few centimetres thick which are often of irregular shape to planar sheets several metres wide.

Thin basaltic types often occur as apparently highly fluid late stage emplacements.

The dykes are normally parallel, with little transgression, (Plate 6) and this has given rise to the striking sheeted aspect which has named this part of the ophiolite complex. Multiple dyking is the rule, later formed dykes being emplaced up the centre of previous ones, with a fine grained chilled margin forming against the coarser interior of the older dyke. Multiple splitting up the same axis can isolate one dyke margin from its original pair. Kidd et al., (1974) has suggested that the preponderance of west chilling dyke margins on Troodos indicates the original spreading axis lay to the present day geographic east.

The regional parallelism of the dyke swarm suggests that the same pattern of regional extensional stress was maintained for a long period of time relative to the time scale of individual dyke emplacement. However, the parallelism is enhanced on a local scale by the constraint imposed upon later dykes by the fabric of the swarm. Dykes cutting the pillow lavas are not so constrained and tend to be sinuous. (Wilson 1959).

#### 2.1.2.4 Plagiogranites in the Axis Sequence

Microtonalite, porphyritic and aphyric rhyolite dykes intrude tonalite and dolerites at the top of the Plutonic Sequence and in the SIC.

At Mosphiloti, in the extreme east of the Massif, a cluster of rhyolite bosses intruding the Axis Sequence forms prominent

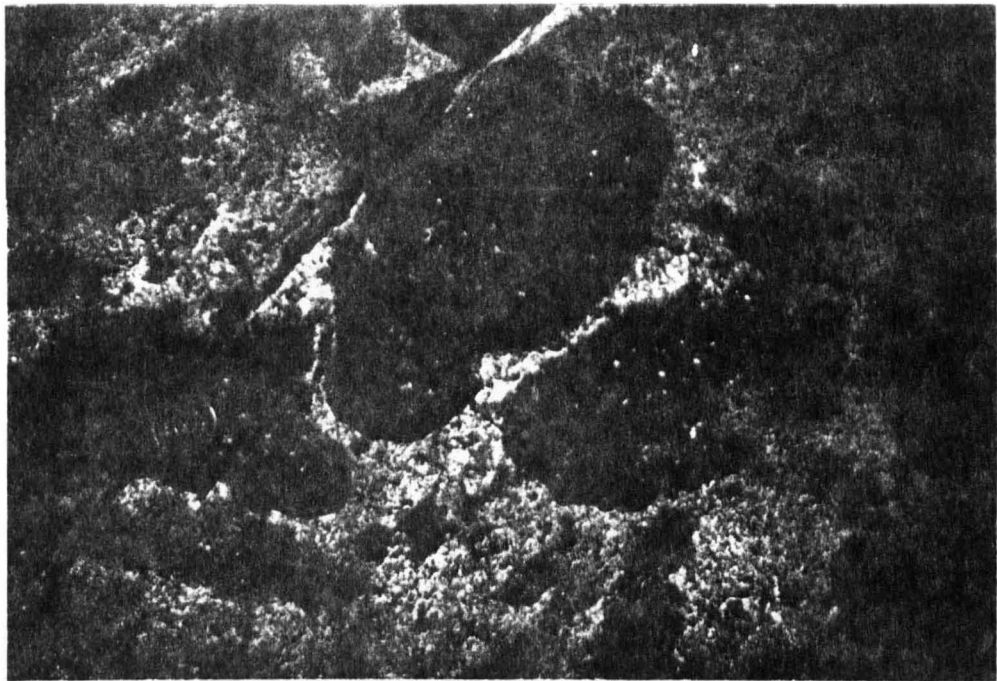


Plate 5 Liquid / liquid mixture of tonalite and basalt. Note lobate and crenulate margins and quartz-feldspar ocelli within dolerite. Palekori, Cyprus. Coin is 2cm. diameter.

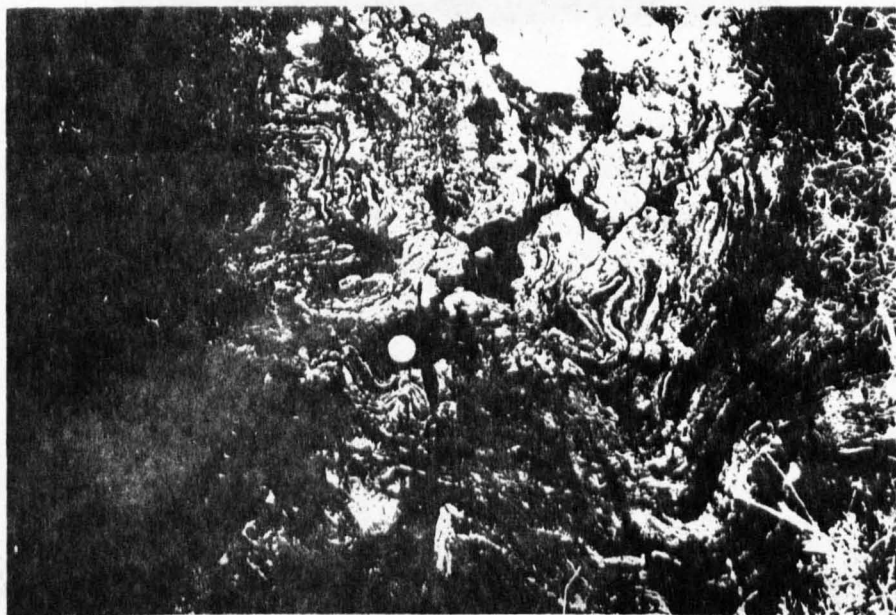


Plate 7 Flow-banded felsite, Mosphiloti, Cyprus. Coin is 2cm. diameter.





Plate 6 Sheeted Intrusive Complex, dipping away  
and to the right of the hammer. There is a single  
transgression, just to the left of the hammer.  
Hammer-head is 17cm. long.

hills up to 100 m. above the general level. The intrusions are of a variety of sizes up to about 4-5 km<sup>2</sup> outcrop and of irregular shape. The poor exposure in the area does not permit unequivocal interpretation of dolerite outcrops within the rhyolites. These could be xenoliths, roof pendants, screens or dykes. The geographical remoteness of Mosphiloti from the main outcrop of the Plutonic Complex suggests these bodies have intruded a high level of the Axis Sequence. The frequent presence of vesicles, flow banding and autobrecciation testifies to a high volatile content which could be responsible for their unusually high level of emplacement. (Plate 7).

#### 2.1.2.5 Intrusive relations between the Plutonic Complex and the Sheeted Intrusive Complex

Dolerite dykes cut the Upper Plutonic Complex and screens of plutonic rock appear in the SIC and so there is no clear definition of the base of the SIC. There is a regional upward increase in the proportion of hypabyssal to plutonic rock but on the local scale this ratio changes abruptly either upwards or sideways. This is shown in stylized form in Figure 2.1.3. Where it is well exposed the top of the "acid cap" (or gabbro where this is absent) intrudes the SIC, cross-cutting and terminating the dykes. The later liquids stopped off the base of dykes which themselves were probably formed from earlier liquids within the same magma chamber. However, later dykes of the same trend frequently cross-cut the Upper Plutonics.



### 2.1.3 Petrography

#### 2.1.3.1 Introduction

The rocks of the Upper Plutonic Complex contain relatively few mineral species but these occur in a range of abundances, textures and compositions. Potassium-rich phases are absent. Only a few specimens are entirely free of secondary crystallization that partly or totally obscures the primary mineralogy and texture.

The petrography of the varitextured gabbros and plagiogranites is summarised in Table 2.1.2. The secondary mineral assemblages are identical to those found in basaltic rocks at lower amphibolite and greenschist facies regional metamorphism. The hydrothermal metamorphism of the Axis Sequence has been described by Gass and Smewing (1973). As there is no identifiable metamorphic discontinuity at the base of the SIC, it appears that the Upper Plutonic Complex was metamorphosed by the same agency. The Layered Sequence rarely displays any significant metamorphic modification (Allen op. cit) and obviously lay spatially below the limits of the metamorphic field.

Three other generalizations can be made. Very commonly metamorphic assemblages are in disequilibrium; shown by inhomogeneous, partial replacement textures on small (single grain) to large (outcrop) scales. In addition, mineral reactions are usually retrograde, that is, they appear to have taken place in a regime of falling rather than rising temperature. Stress oriented fabrics are absent (except close to faults).

Table 2.1.2 Summary of Petrography

Rock Type	Primary Minerals and Macroscopic textures	Microscopic Textures
Gabbro	Pl, An 90 to An 40, cpx, opx. <u>Acc</u> Op hnd qz. Coarse to medium grained. Uniform or varitextured (heterogeneous, pegmatitic) No cumulate layering.	Pl, euhedral to subhedral, elongate or equant grains $\pm$ complex zonation. Pyx, subhedral, elongate often poikilitic. Op, anhedral to subhedral, often enclosed in secondary amph. Qz, interstitial, occasional graphic texture
Magnetite gabbro	As gabbro with 5% - 10% modal op.	Strongly zoned pl. common
Pegmatite gabbro	As gabbro, with abundant hnd. In veins and dykes crosscutting gabbro. Coarse grained.	Strongly zoned pl. Interstitial granophyre
Segregation gabbro	As varitextured gabbro with <u>insitu</u> veins of leucocratic, often qz-rich, material	

Table 2.1.2 (continued)

Rock Type	Primary Minerals and Macroscopic textures	Microscopic Textures
Tonalite	Pl, An 60-An 10, Qz, Hnd (green, browngreen or rarely bluegreen) $\pm$ cpx. <u>Acc</u> sph, ap, zrc. Medium to fine grained. Rarely pl - phyr. Usually heterogeneous. Medium to pale grey/green, to white or pink to rustyred. pl, Anhedral to euhedral, complex zonation. Hnd, Interstitial or poikilitic anhedral, rarely subhedral acicular. Qz, Anhedral, equant or interstitial or poikilitically encloses plag. Fine to coarse irregularly developed granophyre. Sph, Anhedral, rare rhombs. Ap, Rods and needles usu. enclosed in plag or qz. Zrc, sparse anhedral	
Trondhjemite	As tonalite, richer in Qz and very poor in mafics. No cpx. Pale grey/green or white. Granophyre very common	
Qz Diorite	As tonalite, poorer in Qz and often richer in mafics Medium to pale grey/green	
Rhyolite or Quartz Porphyry	Qz, pl. <u>Acc</u> op, sph + irresolvable groundmass Pale grey to rustyred Porphyritic or finegrained aphyric with flowbanding, vesiculation and autobrecciation often glomeroporphyritic. Usu qz and pl - phyr. Resorbed qz phenocrysts up to 3mm diameter, can have fluid inclusions. Groundmass usu recrystallized/devitrified? Pl rarely zoned.	

Table 2.1.2 (continued)

Summary of Secondary Petrography

<u>Rock Type</u>	<u>Secondary Minerals and Textures</u>
Gabbros	Hnd $\pm$ Act (Uralite) $\pm$ cum $\pm$ saus $\pm$ Qz $\pm$ some cz, chl, sph. Amph, fibrous to columnar, wholly or partly pseudomorphs pyx or hnd or forms fibrous aggregates or mats. Qz, replaces pl or interstitial. Cz, small amounts replace pl or interstitial. Chl, usu. fibrous in parallel growth with amph. or interstitial mats or within pl.
Tonalite	$\pm$ Hnd $\pm$ Act $\pm$ chl $\pm$ Ab $\pm$ saus $\pm$ Qz $\pm$ cz
Trondhjemite	$\pm$ ep $\pm$ sph $\pm$ ha $\pm$ cal. Rare allanite, py.
Qz Diorite	Amph and chl, as gabbro. Saus in pl cores or whole grain. Qz, replaces pl, often forms granophyres. Cz. intergranular, ep, interstitial, both replace pl. Fine or medium; coarse grains or aggregates or radiating. Some weak zonation. Hm replaces mag. Sph fringes or totally replaces ilm. Cal in matrix and in veins.

Table 2.1.2      (continued)

Summary of Secondary Petrography

<u>Rock Type</u>	<u>Secondary Minerals and Textures</u>
Epidosite	Ep + Qz <u>±</u> sph.      Remnant minerals from host. Complete replacement of host (tonalite or dolerite) by coarse irregular grains.      Often grades into less altered rock
Rhyolite	Qz + ab <u>±</u> Act <u>±</u> chl <u>±</u> ep + sph + ha. Rare geotite, some cal. Pl phenocrysts sassuritized and epidotized.      Ha and goetite replace py.

Regionally, the lower parts of the Upper Plutonic Complex have mineral assemblages typical of lower amphibolite facies passing upwards into greenschist facies assemblages. Amongst the rock types in the Plutonic Complex, the trondhjemites regularly have the highest proportion of secondary minerals.

#### 2.1.3.2 Gabbro

Although zoned plagioclase is rarely found in the Layered Sequence, it is very common in the Upper Plutonic Complex. A zoned crystal typically has a euhedral core of optically uniform composition with a zoned inner rim and more uniform outer rim. (Plate 8). The zonation is often on a very fine scale and can be continuously or discontinuously normal or oscillatory. Individual zones may be sharply defined or indistinct. Resorption often occurs during rim formation. Core compositions are highly calcic, between  $An_{90}$  and  $An_{80}$ . This is very little less calcic than either cumulate or poikilitic feldspar in the Layered Sequence. (Allen op. cit.). However, rim compositions show very great variation, to  $An_{40}$ . Beyond these generalizations zonation is highly inconsistent within a single thin section, unzoned and zoned crystals of a range of complexity can coexist. Preliminary microprobe analysis indicates that unzoned plagioclase has a similar composition to the cores of zoned feldspar.

Clinopyroxene dominates orthopyroxene in the varitextured gabbros. Both varieties are usually partly or wholly replaced by amphibole. Replacement commences along the margins and cleavage planes and so pyroxene most frequently

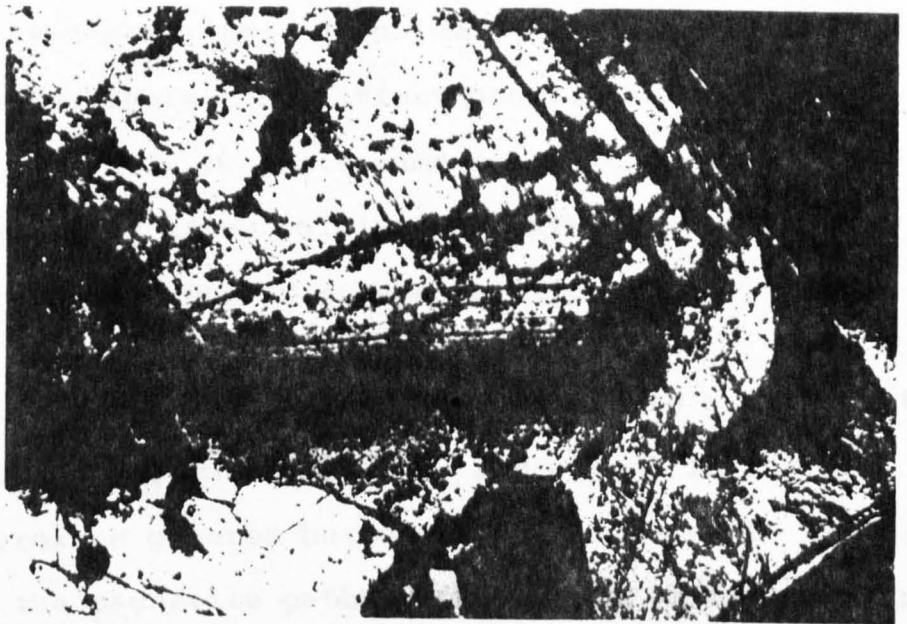


Plate 8 Zoned plagioclase in magnetite gabbro. Unzoned core at top, complex inner rim with resorption feature centre and weakly zoned outer rim below. (x-pols)

0 0.5mm

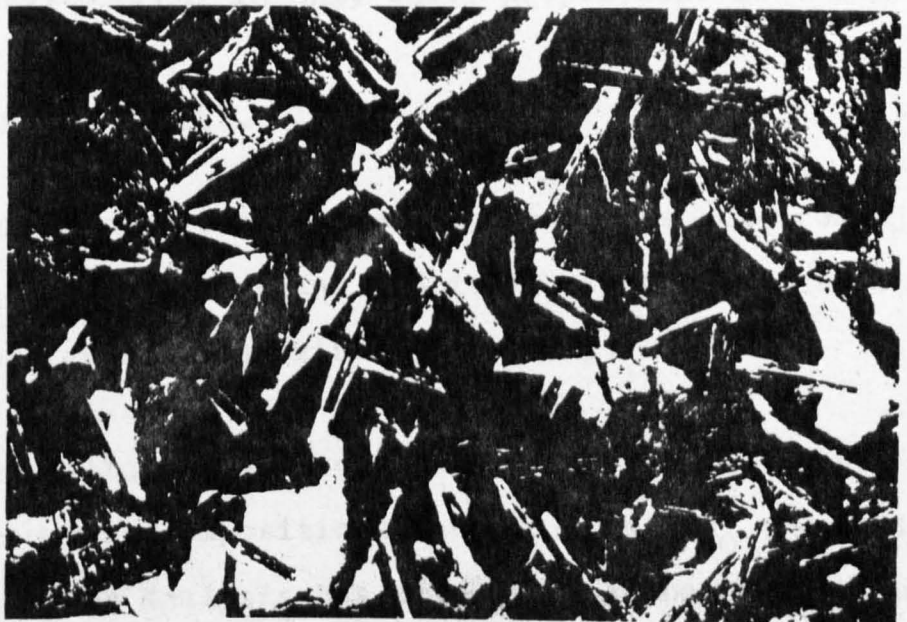


Plate 9 Trondhjemite. Zoned plagioclase laths with saussuritised cores, poikilitically enclosed and slightly resorbed by quartz. Extinct background is a single quartz. (x-pols)

0 1mm

occurs as netted remnants. Hornblende, actinolite and intermediate amphibole compositions occur. Rare multiple twinning in amphibole suggests cummingtonite is also present, presumably after calcium-poor pyroxene. Little primary hornblende occurs in non-pegmatitic gabbros.

The abundance of the opaque minerals, magnetite and ilmenite, varies widely in the gabbros. They are absent in the unaltered pyroxene gabbros but occur in grains up to 1 mm. diameter in the magnetite gabbros indicating that they only appear late in the differentiation series. Ilmenite can often be distinguished by its angular habit and local alteration to leucoxene and sphere. Preferential alteration of ilmenite reveals delicate exsolution textures within magnetite. Secondary minerals typical of the greenschist facies generally occur in only small proportions in the gabbros.

#### 2.1.3.3 Plagiogranites

The plagiogranites are predominantly tonalites and trondhjemites with some quartz diorites and diorites. They rhyolites are a distinct type and are described separately.

Plagioclase, ubiquitously zoned in similar style to the gabbros, occurs in compositions ranging from  $An_{60}$  (core) to  $An_{10}$ . Microprobe analysis has determined a composition range of almost 50% anorthite in a single zoned crystal. In some rocks larger feldspars have a uniform core and zoned rim whereas smaller ones exhibit continuous zoning. Microprobe data suggest that potassium is accommodated in plagioclase and coexisting hornblende in comparable amounts.



The acidic differentiates display a complete range in degree of alteration, from 1% to 100% secondary mineralogy. Plagioclase is the best indicator of alteration. Zoned feldspar often has a saussuritized core and pellucid rim. Some examples of continuous zoning in pellucid feldspar may be secondary, caused by differential albitization but there are insufficient microprobe data to verify this. Discontinuous zoning is considered too delicate to have arisen by secondary processes. In otherwise little altered rocks, secondary quartz may still replace plagioclase, indicating not all secondary silica is a product of the breakdown of anorthite to epidote, albite and quartz.

Quartz occurs in a wide variety of textures which are frequently inhomogeneously developed. Often there is no clear distinction between primary and secondary quartz as partial replacement of plagioclase by quartz in optical continuity with interstitial quartz is usual. Although feldspar is always more abundant than primary quartz, primary and secondary quartz together can comprise up to 70% of the mode. Quartz and feldspar commonly appear in a variety of granophyric textures (Plate 10 and 11). The most leucocratic and late formed rocks have the most extensive development of skeletal quartz but plumose intergrowth also occurs in in situ veins in quartz-free gabbro. The presence of both quartz and plagioclase phenocrysts in the rhyolites indicates that cotectic crystallization is attained in some liquids. It is probable that many examples of quartz feldspar intergrowth originate by the simultaneous crystallization of the two phases. The association of granophyric texture with late formed rocks suggests it may also arise through the interaction of late-stage silica-enriched fluids.

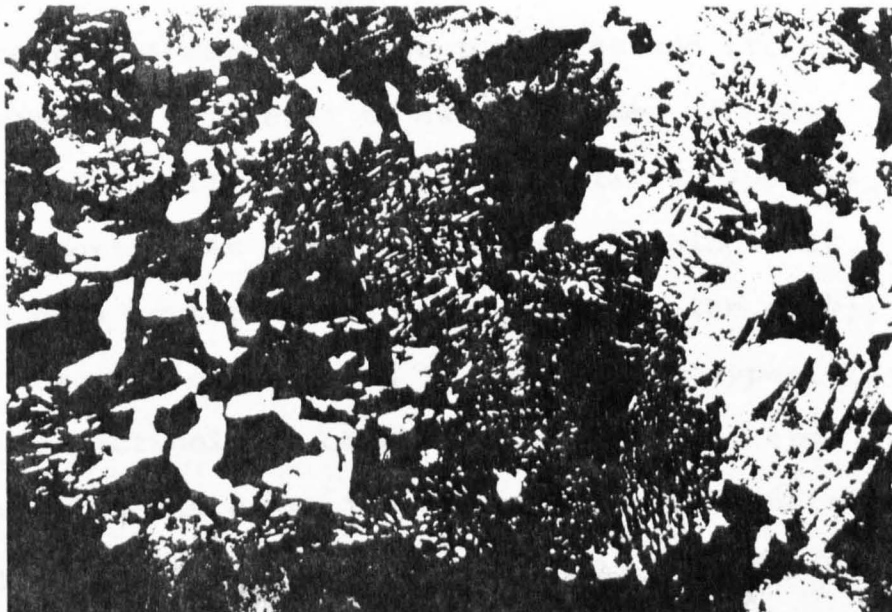


Plate 10 Trondhjemite. Primary granophyre; quartz and oligoclase. Note small euhedral plagioclase, right of centre. (x-pols)

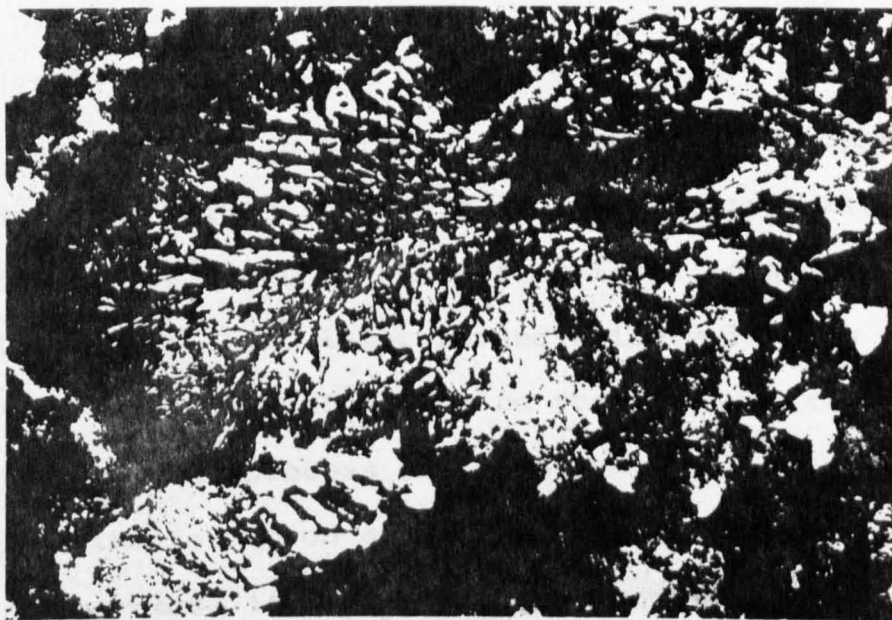
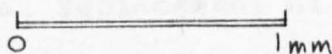
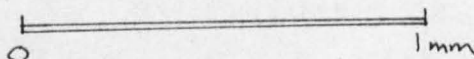


Plate 11 Trondhjemite. Secondary granophyre. Plumose secondary quartz replacing turbid (extinct) feldspar and also enclosing a single acicular hornblende. (x-pols)



Pyroxene occurs but rarely in the tonalites and its original extent is difficult to assess because of widespread amphibolitization. Hornblende certainly appears to be more important as a primary phase. Amphibole is variable in both texture and volume (0-25% of the mode). A range of compositions between the two common types, hornblende and actinolite, occurs (Allen op. cit. and present work) but there are too few analyses to confirm a miscibility gap such as found by Grapes (1975) and Hietanen (1974). However, as pointed out by these authors, the coexistence of two amphiboles cannot by itself be taken to indicate disequilibrium. Chlorite is most common in heavily altered tonalites but it may also coexist with unaltered plagioclase. The partial replacement of amphibole by chlorite is taken to indicate disequilibrium.

Epidote minerals of a range of compositions occur, almost invariably associated with turbid plagioclase and secondary quartz. The early formed type is clinozoisite, typically replacing the calcic cores or, exceptionally, individual zones of plagioclase. The later formed epidote is more pistacitic and develops without regard for pre-existing grain boundaries. The process of epidotization is progressive, culminating in the formation of an epidosite. Epidote frequently forms close to joints or along joints and also in narrow cross-cutting veinlets. The importance of a fluid phase as the agent of epidotization is affirmed by the occurrence of late veins of apple-green epidote and quartz in both the Upper Plutonic Complex and the SIC.



Plate 12 Tonalite. Saussuritised, euhedral, zoned plagioclase in centre. Inner zones are partly replaced by clinozoisite. (ppl)

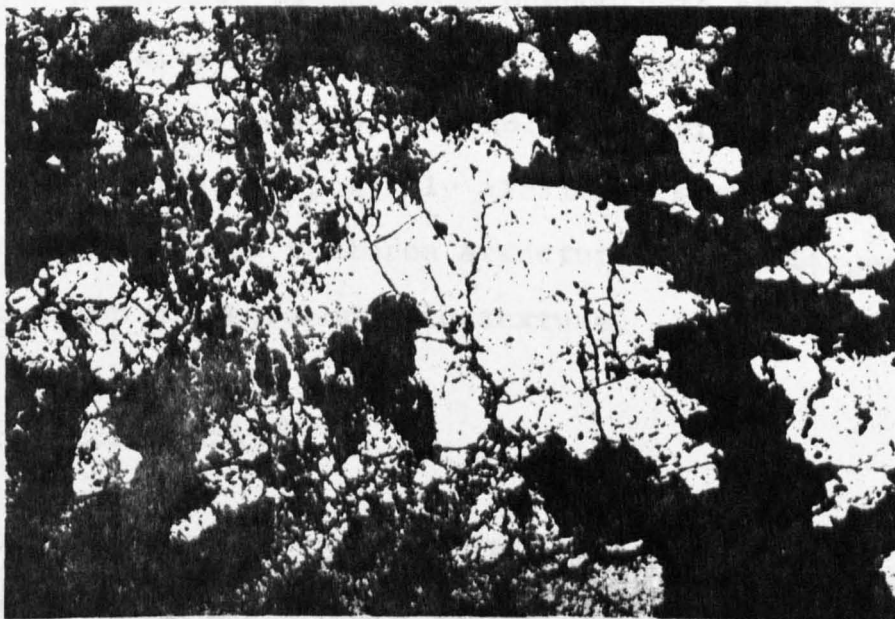
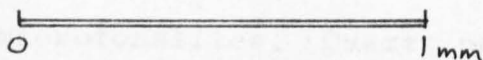
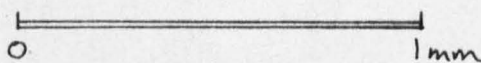


Plate 13 Epidosite. Right side is epidote and quartz, Left side is quartz and turbid plagioclase with remnant opaque. Note partial development of secondary assemblages in both plates. (ppl)



Opaque phases are the most abundant accessory in the acidic rocks but are nowhere as common as in the magnetite gabbros. Two modes of opaque occur in some specimens; as finely disseminated grains within and around secondary amphibole and as isolated primary grains 10 to 100 times their diameter, throughout the rock.

#### 2.1.3.4 Intrusive Rhyolites

Rhyolites, or quartz feldspar porphyrys, are found in dykes and bosses intruding the acid plutonics and the SIC. Aphyric types with flow banding, vesiculation and auto-brecciation also occur. The presence of corroded quartz phenocrysts distinguishes the rhyolites from the rare plagioclase phyric microtonalites. Quartz phenocrysts never occur in the absence of plagioclase phenocrysts and their volumes are approximately equal. The groundmass is everywhere fine grained but never glassy, probably devitrified. Recrystallized quartz and possibly albite form spherules with radial, concentric and/or sectorial structures. The larger spherules develop microgranophyric texture.

#### 2.1.3.5 Contact Metamorphism

The effects of contact metamorphism are widespread but insignificant in the development of the Upper Plutonic Complex. They may be observed in two situations, the second rather unusual. The first situation is the intrusion of the sheeted dolerites by a large body of tonalite or gabbro.

Recrystallization to a hard dark grey hornfels containing clinopyroxene and plagioclase in fresh equant grains takes place in xenoliths and in a narrow zone around the intrusion. Once hornfelsed, dolerites generally resist further metamorphism. At a few localities a massive tonalite has been intruded by gabbro. The most notable effects are recrystallization of quartz into sutured grains and the formation of andradite garnet and diopside. (Allen op. cit.). The assemblages and textures found in prograde contact metamorphosed rocks contrast strongly with the effects of the pervasive retrograde metamorphism.

## 2.1.4 Geochemistry

### 2.1.4.1 Introduction

Certain features of the overall geochemical distribution are significant. In general, the abundances of oxides and elements vary with petrography in a continuous and predictable way. The intrusive rhyolites overlap the trondhjemites to a great extent. The tonalites and Axis Sequence dolerites have similar ranges of potassium and the incompatible trace elements and both are more enriched in these elements than the gabbros. No dolerites are as iron-enriched as the magnetite gabbros.

### 2.1.4.2 Metasomatism

Although the correlation with primary petrology indicates the main variation trends are magmatic, secondary petrology shows that the more differentiated types have also suffered the most alteration. If metasomatism is quantitatively related to the intensity of alteration (proportion of secondary minerals) then it is likely to have had a differential effect on the chemistry of the various rock types. Some of the scatter on the variation diagrams is probably due to secondary processes but metasomatism may not just widen, it may modify or extend the original distribution. Therefore, it is necessary to consider possible alteration of each element before its magnetic variation. The techniques employed to do this and the assumptions involved were discussed in Section 1.3.

Table 2.1.3 Major Element Ranges (wt%)

Rock Type No. Specimens	Gabbro 9	Magnetite Gabbro 3	Pegmatite Gabbro 2	Dioritic <u>insitu vein</u> 1
SiO <sub>2</sub>	48.2-54.5	48.1-52.1	49.9-53.3	61.7
TiO <sub>2</sub>	0.20-0.39	0.89-1.88	0.45-0.29	0.79
Al <sub>2</sub> O <sub>3</sub>	13.4-18.2	12.4-16.2	14.7-15.61	14.3
Fe <sub>2</sub> O <sub>3</sub> *	8.1-9.1	13.5-15.5	10.7-7.7	3.9
MnO	0.11-0.16	0.19-0.24	0.19-0.10	0.08
MgO	8.6-14.4	4.6-8.6	11.7-9.5	3.2
CaO	9.6-14.7	6.6-11.6	12.4-13.4	10.2
Na <sub>2</sub> O	0.4-3.1	1.1-2.4	1.00-1.2	2.5
K <sub>2</sub> O	0.02-0.42	0.13-0.80	0.07-0.14	0.26
P <sub>2</sub> O <sub>5</sub>	<0.01-0.04	0.02-0.03	0.01-0.02	0.09

Rock Type No. Specimens	Tonalite 15	Trondhjemite 10	Rhyolite 5
SiO <sub>2</sub>	62.0-73.1	71.0-77.0	75.6-80.9
TiO <sub>2</sub>	0.23-0.96	0.09-0.39	0.16-0.20
Al <sub>2</sub> O <sub>3</sub>	12.0-15.3	11.6-13.7	9.8-13.1
Fe <sub>2</sub> O <sub>3</sub> *	3.6-10.6	1.1-7.4	1.4-3.1
MnO	0.03-0.17	0.01-0.09	0.01-0.04
MgO	0.5-1.9	0.15-2.2	0.3-0.6
CaO	2.6-5.8	1.6-6.6	0.5-3.0
Na <sub>2</sub> O	2.7-5.6	1.9-6.4	3.5-7.7
K <sub>2</sub> O	0.06-0.68	0.08-0.68	0.02-0.37
P <sub>2</sub> O <sub>5</sub>	0.06-0.24	0.01-0.09	0.02-0.04



Table 2.1.4 Trace Element Ranges (ppm)

Rock Type No. Specimens	Gabbro 9	Magnetite Gabbro 3	Pegmatite Gabbro 2	Dioritic <u>insitu vein</u> 1	-
Zr	6-24	8-18	11-16	38	
Y	<1-12	4-12	5-9	84	
Nb	<1-3	<1-3	<1-2	<1	
Cr	52-351	8-71	59-113	7	
Ni	33-80	5-48	121-51	19	
Zn	13-51	71-99	64-29	20	
Ba	15-50	53-67	24-27	53	
Sr	26-108	61-84	67-77	157	
Rb	<1-2	<1-4	<1	<1	

Rock Type No. Specimens	Tonalite 15	Trondhjemite 10	Rhyolite 5	Dolerite 5	Dolerite* 25
Zr	32-120	36-189	81-122	21-70	9-94
Y	17-55	3-80	19-47	9-29	9-46
Nb	<1-8	<1-9	<1-3	<1-3	-
Cr	<1-5	<1-9	<1-7	12-256	54-173
Ni	<1-6	<1-4	<1-3	13-66	16-76
Zn	13-63	6-30	9-13	37-67	-
Ba	32-88	<4-137	<4-135	33-77	-
Sr	69-152	50-160	34-157	72-150	-
Rb	<1-2	<1-2	<1-4	<1-4	-

\*From Smewing 1975

The frequent occurrence of secondary quartz suggests many plagiogranites have suffered secondary enrichment in silica and high values around and above 75%  $\text{SiO}_2$  support this. There has been some loss of calcium in the plagiogranites, especially in the trondhjemites. The majority of rocks with less than 4% CaO are also stained pink by haematite. The redistribution of CaO and of  $\text{Na}_2\text{O}$  are closely related and the loss of one is often matched by a gain in the other. However, some specimens have lost both. The usual case, a loss of CaO with gain of  $\text{Na}_2\text{O}$ , mimics the magmatic trend but can be distinguished by change of CaO/ $\text{Na}_2\text{O}$  ratio or by differing relative positions of analyses on, for instance, CaO v.  $\text{Na}_2\text{O}$  and Zr v. Y binary diagrams. The scatter of potassium analyses and the very low values, particularly at high levels of  $\text{SiO}_2$ , seems to indicate widespread potassium metasomatism. However, even specimens with pellucid plagioclase, which would be most likely to retain their primary abundance, have low  $\text{K}_2\text{O}$  content, lower, in some cases, than more altered specimens. This suggests that potassium is not enriched with differentiation indeed, it may be depleted in the plagiogranites. This is discussed in Section 3.2.5. Rb only occurs in detectable amounts in a few of the more potassic specimens. Ba can be enriched or depleted by metasomatism and its primary distribution is obscured. Sr is generally depleted and the greatest loss occurs in those rocks which also have low CaO. Depletion of iron during hydrothermal metamorphism is closely related to the instability of the FeTioxides in greenschist facies conditions and their replacement by sphene. MnO and Zn are also depleted. Variations in the iron oxidation ratio,  $\text{FeO}/(\text{FeO}+\text{Fe}_2\text{O}_3)$ , indicate there is a primary decrease with differentiation but that in

addition altered rocks are more oxidised. However, two abnormally high values are related to the sporadic appearance of pyrite. There is much less variation in this ratio amongst the gabbros than the plagiogranites. There is no variation in the distribution of the other elements which is obviously related to secondary alteration. Except for Ba, variation due to metasomatic processes is generally less than primary variation.

Although silica is secondarily enriched in some specimens, it is considered that its use as a differentiation index in this Section is justified because (i), except in epidiosites and a few other highly silicic rocks, the silica content of the plagiogranites and gabbros correlates with other major oxides in a way which is consistent with primary petrography and (ii) essentially the same variation trends are obtained using immobile or compatible trace elements (Zr, Y, REE) as independent variables, bearing in mind their partition into minor phases.

#### 2.1.4.3 Major and Trace Elements

Most aspects of the primary geochemical distribution can be accounted for by crystal fractionation of a basic magma. The very low Zr and Y in the gabbros indicates they are composed of accumulated crystals with only a small proportion of interstitial liquid. The range of Zr and Y in the aphyric dolerites overlaps that in the tonalites. This indicates that either some tonalites are also crystal cumulates or mushes or that the plagiogranites evolved from a less differentiated liquid than the most evolved dolerites. There is some evidence to suggest that most plagiogranites are not

dominated by cumulus crystals in the same way as the gabbros. The one plagiogranite specimen from the Troodos Massif which is unequivocally a fairly pure plagioclase cumulate has very high  $\text{Al}_2\text{O}_3$ , CaO and Sr, which is admitted to Ca sites in plagioclase and very low Y, which is not. (Taylor 1966, Lambert et al., 1974). Thus Sr, when compared to Y, is a sensitive indicator of plagioclase accumulation in unaltered rocks. Variations in Sr,  $\text{Al}_2\text{O}_3$  and CaO in the gabbros do correlate with variations in modal plagioclase. However, as only a few plagiogranites have the combination of mild enrichment in Sr and  $\text{Al}_2\text{O}_3$  and depletion in Y, the remainder are believed to approximate liquid compositions.

$\text{Fe}_2\text{O}_3^*$  and  $\text{TiO}_2$  are progressively enriched in the dolerites but are depleted in the plagiogranites as a result of FeTi oxide fractionation. Although there is some scatter about this trend, presumably due to variations in accumulation of Ti-rich phases, it appears that the least evolved plagiogranites have lower  $\text{TiO}_2$  content than the more evolved dolerites (Figure 2.1.4). Therefore the plagiogranites did not arise as the final stage in the evolution of the dolerites but developed from a similar parental magma along a completely different trend. The magnetite gabbros are enriched in  $\text{Fe}_2\text{O}_3^*$  and  $\text{TiO}_2$  as a result of concentration in opaque phases.  $\text{Mn}^{2+}$  is theoretically admitted to  $\text{Fe}^{2+}$  sites and in practice MnO follows FeO very closely. However, the magnetite gabbros are poor in MnO, which suggests little is accommodated by the FeTi oxides. Zn shows a positive correlation with MnO.

The distribution of CaO has an inflexion superimposed on the general decrease from the gabbros to plagiogranites which coincides with the cessation of clinopyroxene crystallization while fractionation of the other main Ca-bearing phase, plagioclase, continues to deplete the melt in Ca. Na undergoes continuous depletion. The inflexion in the same position on the MgO trend is more acute as all the plagiogranites have very low MgO. The plagiogranites are generally leucocratic as a result of depletion in MgO and  $\text{Fe}_2\text{O}_3^*$  and hornblende is constrained to a subordinate role as a fractionating phase, relative to plagioclase.  $\text{P}_2\text{O}_5$  has an arched distribution, the maximum marking the onset of apatite fractionation in the plagiogranites.

Zr increases with silica in the plagiogranites but the distribution is scattered. Comparison of  $\text{TiO}_2/\text{Zr}$ ,  $\text{TiO}_2/\text{SiO}_2$  and  $\text{Zr}/\text{SiO}_2$  diagrams indicates it is the Zr values which are most scattered, probably due to variable weak zircon fractionation. Similar scatter in Y is attributed to partition into apatite or sphene. Whereas the gabbros are rather poor in Zr and Y, with moderate to large Cr and Ni, the reverse is true of the plagiogranites. However, the dolerites show a gradation between high Cr and high Zr. The low abundance of Cr and Ni in the plagiogranites implies that they evolved from a parent which had already been depleted in these elements, by removal of olivine and the pyroxenes, cumulus phases in the gabbros. Hf, Nb, Ta and Th are present as a few ppm. or less and appear to behave incompatibly. Sc has a positive correlation with FeO, a result of capture in place of  $\text{Fe}^{2+}$  in pyroxene. (Wager and Mitchel, 1951).

wt%  
2

Figure 2.1.4 Variation diagrams : Troudos Massif

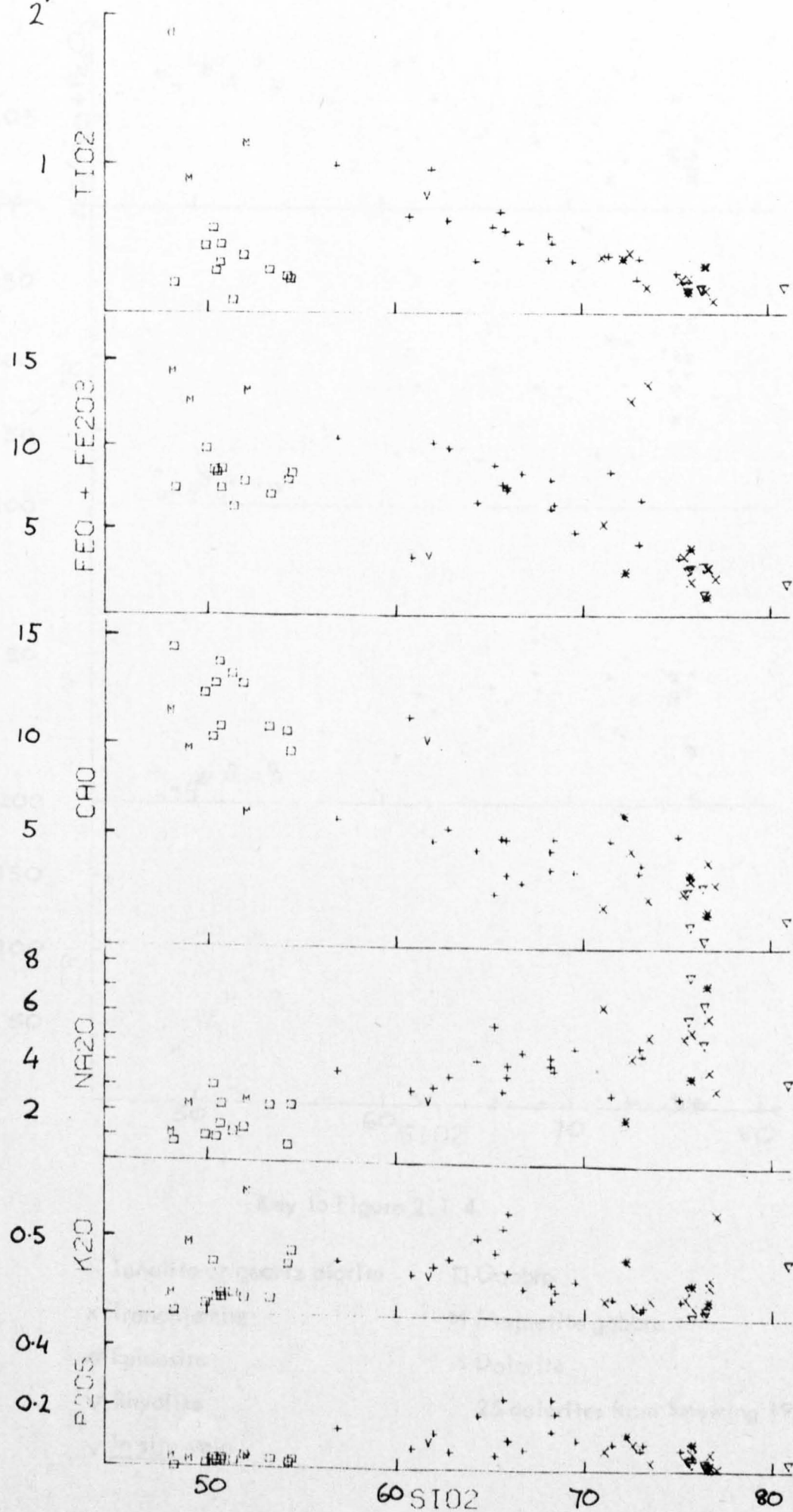
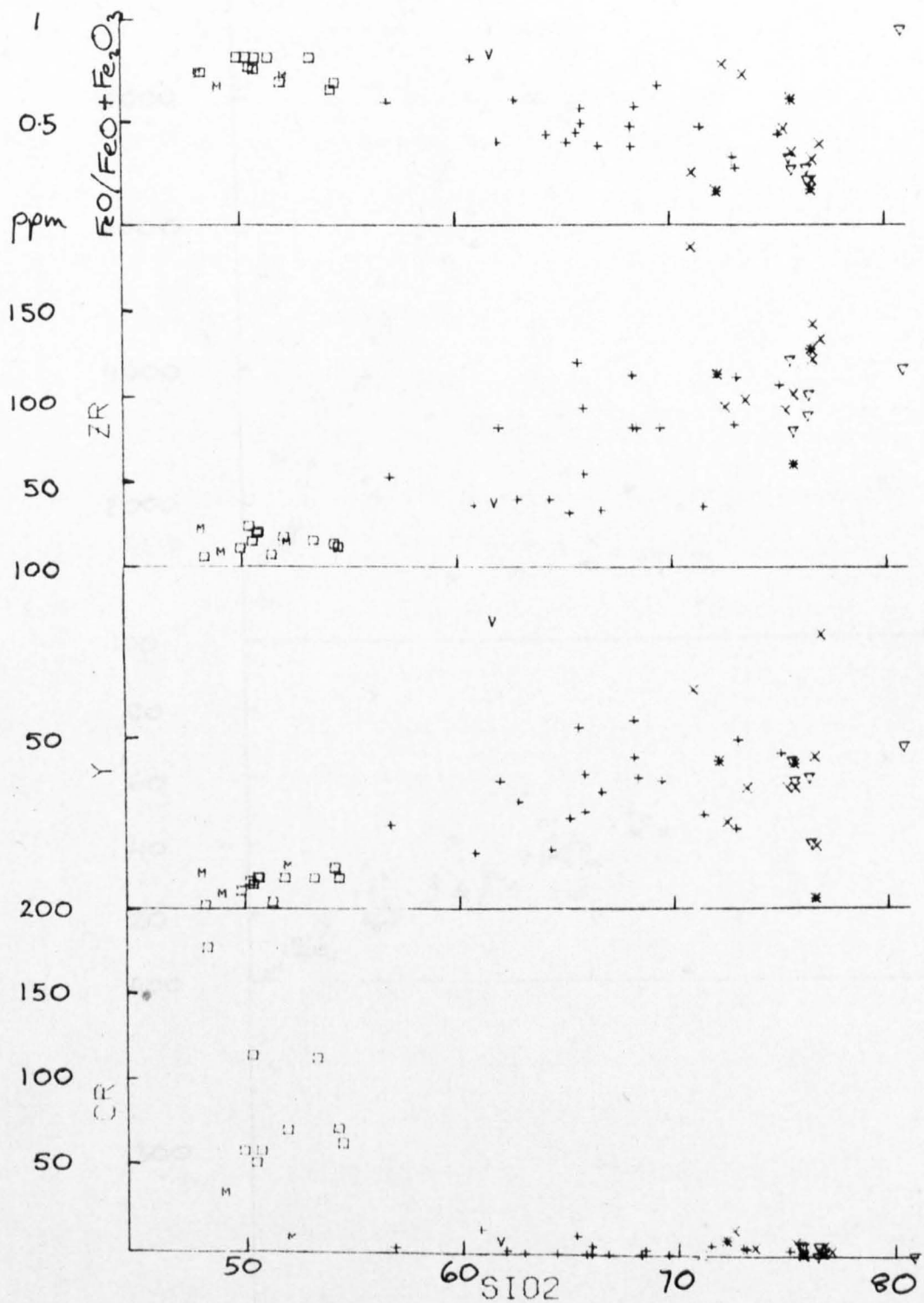


Figure 2.1.4 Variation diagrams: Troodos Massif, continued



Key to Figure 2.1.4

+ Tonalite or quartz diorite

x Trondhjemite

\* Epidosite

▽ Rhyolite

∇ In situ vein

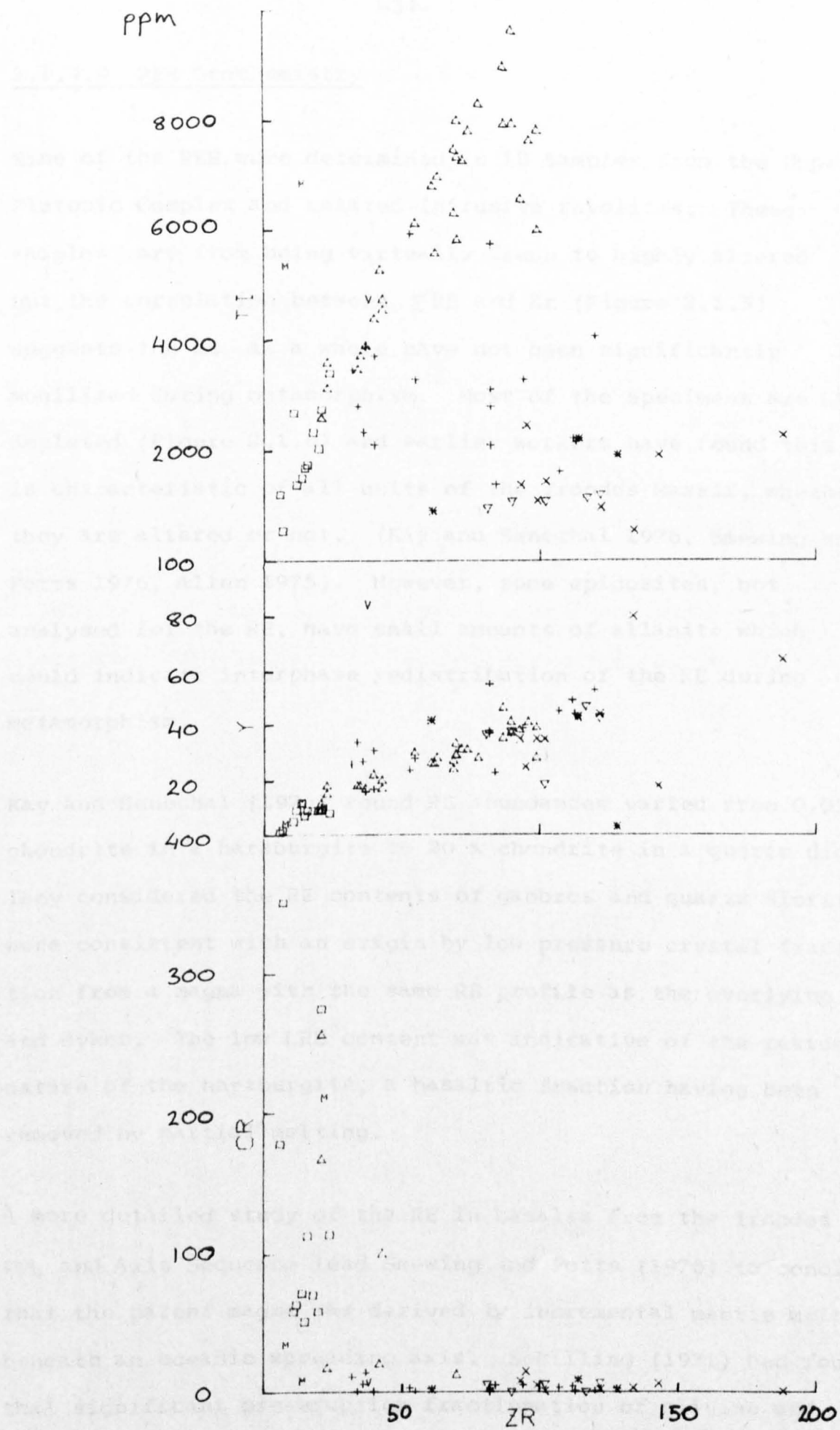
□ Gabbro

M Magnetite gabbro

△ Dolerite

25 dolerites from Smewing 1975

Figure 2.1.4 Variation diagrams: Troodos Massif, continued





#### 2.1.4.4 REE Geochemistry

Nine of the REE were determined in 18 samples from the Upper Plutonic Complex and related intrusive rhyolites. These samples vary from being virtually fresh to highly altered but the correlation between  $\Sigma$ RE and Zr (Figure 2.1.5) suggests the RE as a whole have not been significantly mobilized during metamorphism. Most of the specimens are LRE depleted (Figure 2.1.6) and earlier workers have found this is characteristic of all units of the Troodos Massif, whether they are altered or not. (Kay and Senechal 1976, Smewing and Potts 1976, Allen 1975). However, some epidiosites, not analysed for the RE, have small amounts of allanite which could indicate interphase redistribution of the RE during metamorphism.

Kay and Senechal (1976) found RE abundances varied from 0.05 x chondrite in a harzburgite to 20 x chondrite in a quartz diorite. They considered the RE contents of gabbros and quartz diorites were consistent with an origin by low pressure crystal fractionation from a magma with the same RE profile as the overlying lavas and dykes. The low LRE content was indicative of the residual nature of the harzburgite, a basaltic fraction having been removed by partial melting.

A more detailed study of the RE in basalts from the Troodos UPL and Axis Sequence lead Smewing and Potts (1976) to conclude that the parent magma was derived by incremental mantle melting beneath an oceanic spreading axis. Schilling (1971) had found that significant pre-eruption fractionation of olivine and orthopyroxene could take place without changing profile shape.

Ultimately, removal of large amounts of plagioclase should cause a negative Eu anomaly and of clinopyroxene an increase in La/Sm. The existence on Troodos of basalts with a range of depletion in Sm+Eu+Tb relative to Tm+Yb+Lu was therefore taken to indicate variations at source rather than in the magma chamber.

Various authors have published phenocryst/liquid partition coefficients for most of the RE (Figure 2.1.8). (Schnetzer et al., 1968, 1970, Nagasawa et al., 1971, Arth, 1976, Arth and Barker 1976). Their findings suggest that in general a particular coefficient is critical upon liquid and crystal composition and may vary considerably. In addition, minor phases such as apatite and zircon may exert a disproportionate influence on RE content. The Axis Sequence rocks have no significant Eu anomaly whereas the plagiogranites usually have negative Eu anomalies. The gabbros may either have a slight positive or no Eu anomaly. The similar chemical behaviour of the RE arises because their ions are of very similar size and are all normally trivalent. However, Eu can also exist as a divalent ion and is thus partitioned into crystal phases in a more variable way. Of the common primary phases found in the Upper Plutonic Complex, plagioclase is the most significant in this respect. It accommodates Eu in preference to the other REE, the effect being enhanced in more acidic liquids (Arth, 1976). The anomalous entry of Eu into plagioclase is greatest in more sodic plagioclase (Schnetzer and Philpotts 1970). The Troodos magma precipitated highly calcic plagioclase until the appearance of plagiogranites and so the Axis Sequence dolerites have only small (or absent)

negative Eu anomalies. Small positive Eu anomalies in some gabbros are attributed to plagioclase accumulation.

Hornblende fractionation in the gabbros could have a similar effect but hornblende is not a common primary phase in non-pegmatitic gabbros.

The  $\Sigma$ RE content increases from the gabbros into the dolerites and metabasalts and also from gabbros to plagiogranites. There is considerable compositional overlap of the dolerites and plagiogranites. The least enriched of the plagiogranites, a tonalitic segregation enclosed in gabbro, (TM139 and TM140) has a slight negative Eu anomaly which corresponds to a possible slight positive anomaly in its host. By analogy with TM139, it appears that the plagiogranite magma has the same RE profile as its immediate parent but with a superimposed negative Eu anomaly. This is increased by fractionation of sodic plagioclase in the plagiogranites. Five of the specimens, trondhjemites and rhyolites, are LRE enriched and thus do not conform to the type. (Figure 2.1.7). Moreover, GA11 and GA14 have "dished" profiles. i.e. both LRE and HRE are enriched relative to Sm, Gd and Tb. GK2 and GA8 also have Ce values which are anomalously high relative to the type. However, both values approach the practical detection limit and so the anomaly is attributed to analytical error. In the group of five, however, Nd is enriched consistently with Ce. The LRE are mobile in some hydrothermal regimes (Wood 1977) but Ce anomalies attributed to alteration of sea floor basalts are negative (Frey et al., 1974). Moreover, the five rocks are the most leucocratic of the specimens analysed for the RE and therefore it is considered that the flattened and dished profiles are due not to alteration or analytical error but are the result of fractional crystallization.

Removal of either hornblende or apatite from a LRE depleted liquid would deplete it in  $\Sigma$ RE but also, because the partition coefficients are generally higher for the middle range of lanthanides (Figure 2.1.8), the profile would progressively flatten and then become dishd. However, it should also develop a positive Eu anomaly. In practice, of the five, only GA17 has a slight positive anomaly and QAP, GA16 and GA11 all have marked negative anomalies. This is attributed to the superimposed effect of plagioclase fractionation. Plagioclase dominates the other primary phases volumetrically and thus it is able to offset the fractionating effect of hornblende and/or apatite on Eu. However, quantitative analysis would be required to determine the relative proportions of these three phases which would produce such an effect.

Figure 2.1.5 Variation of RE with Zr

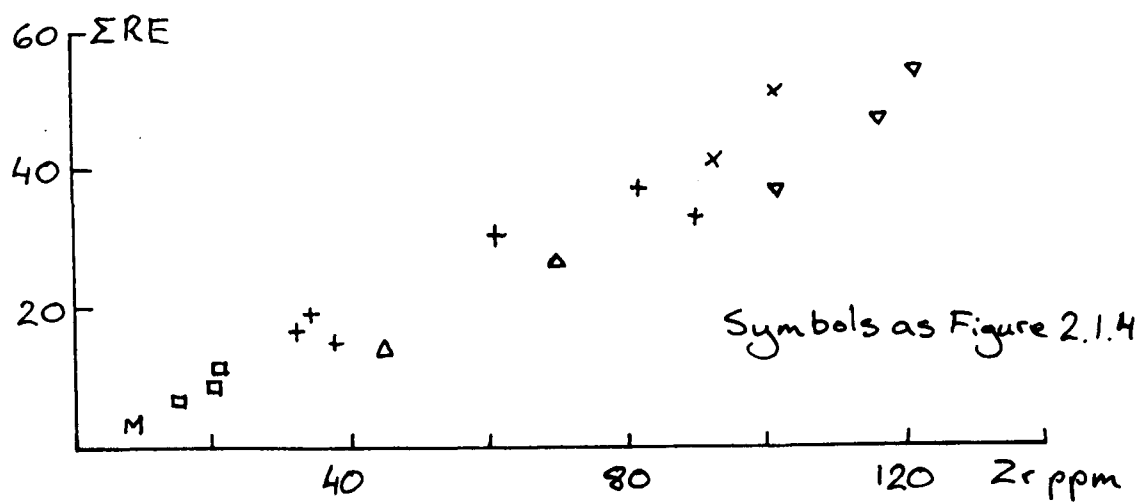


Figure 2.1.6 Troodos RE profiles: LRE depleted

- × TM13 Trondhjemite
- TM158 Tonalite
- ◻ TM101 "
- ◻ TM142 Dolerite
- ◻ TM143 "
- TM140 Gabbro
- ◉ TM139 Segregation from 140
- + TM116 Gabbro
- ◻ TM102 Magnetite gabbro

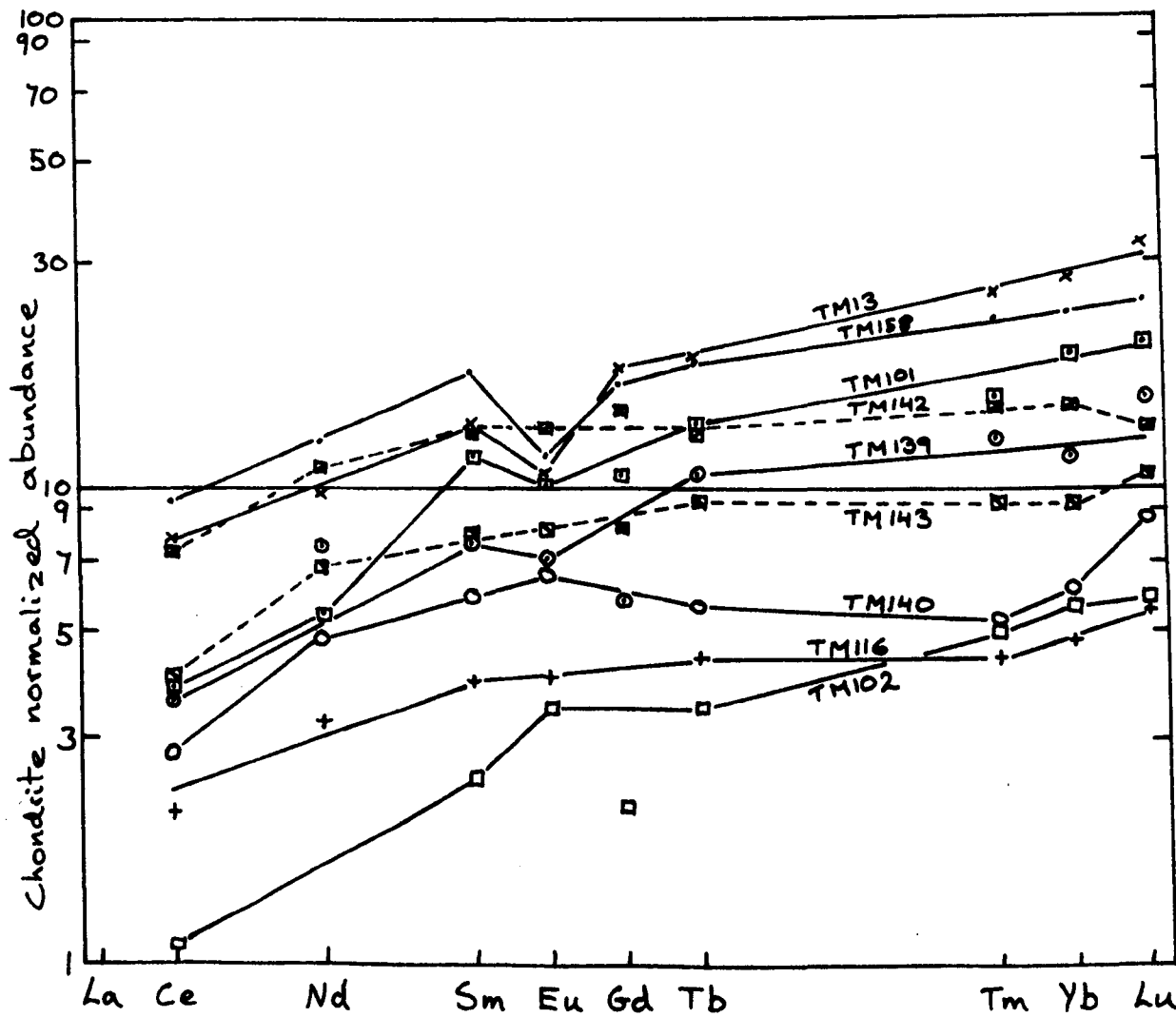


Figure 2.1.7 Troodos RE profiles: flat or dished

- GA16 Rhyolite
- GA11 "
- QAP "
- × GA 14 Trondhjemite
- GA17 "
- GA2 Tonalite
- + GK2 "
- ▣ GA8 Gabbro

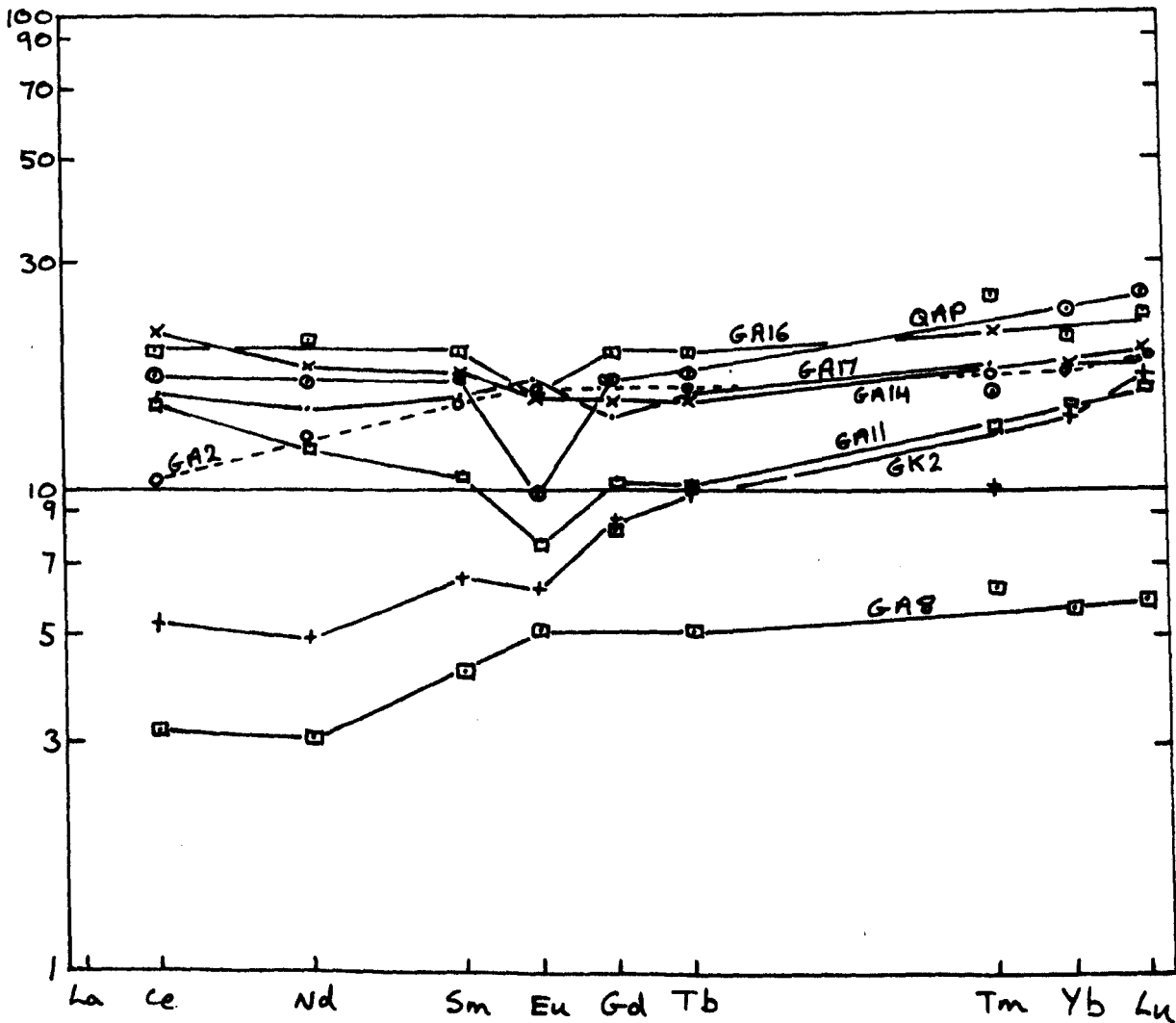
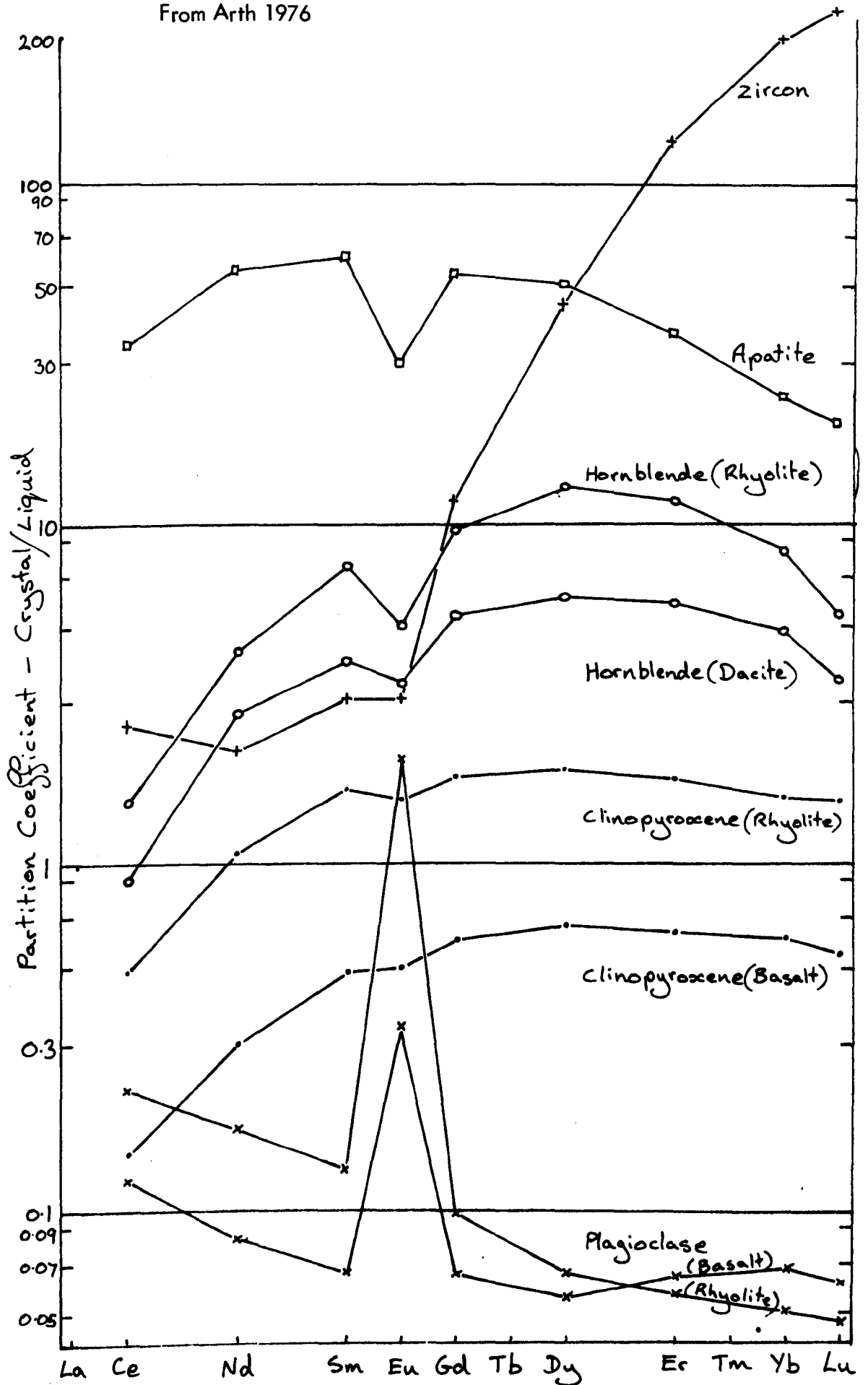


Figure 2.1.8 Crystal / liquid partition coefficients  
From Arth 1976



## 2.2 The Semail Nappe

### 2.2.1 Introduction

The Sultanate of Oman lies on the eastern side of the Arabian Peninsula. In the north, its topography is dominated by the narrow, arcuate chain of the Oman Mountains which runs the length of the Gulf of Oman, rising to 2980 m. on Jebel Akhdar (Figure 2.2.1). It is widely and currently accepted that the Oman Mountains are a series of olistotromes and similar deposits emplaced in a trough on the Arabian continental margin during the last half of the Cretaceous. The uppermost major unit of this allochthon, the Semail Nappe, is a complete ophiolite, probably the world's largest, with an estimated volume of 30,000 km.<sup>3</sup>, an outcrop length of 450 km. and width of 50 to 70 km. (Glennie et al., 1974, Coleman 1977).

Geological research in the area has a long but spasmodic history. The earliest mention of "The Basic Igneous Series of Oman" is by Pilgrim (1908) and that of "The Semail Nappe" by Lees (1928). Research was continued after the Second World War, particularly by geologists of the Iraq Petroleum Co. and Petroleum Development (Oman) Ltd., (e.g. Hudson et al., 1954, Tschopp 1967, Wilson 1969, Reinhardt 1969). This work culminated with the publication of reports in 1973 and 1974, including a geological map of the Mountains (1:500,000), by Glennie et al.. The first description of the Semail ophiolite was by Reinhardt (1969), this was considerably expanded by Glennie et al., (1974) and it has recently been studied in detail by research teams from the Open University and the U.S.G.S./University of California. This summary of the



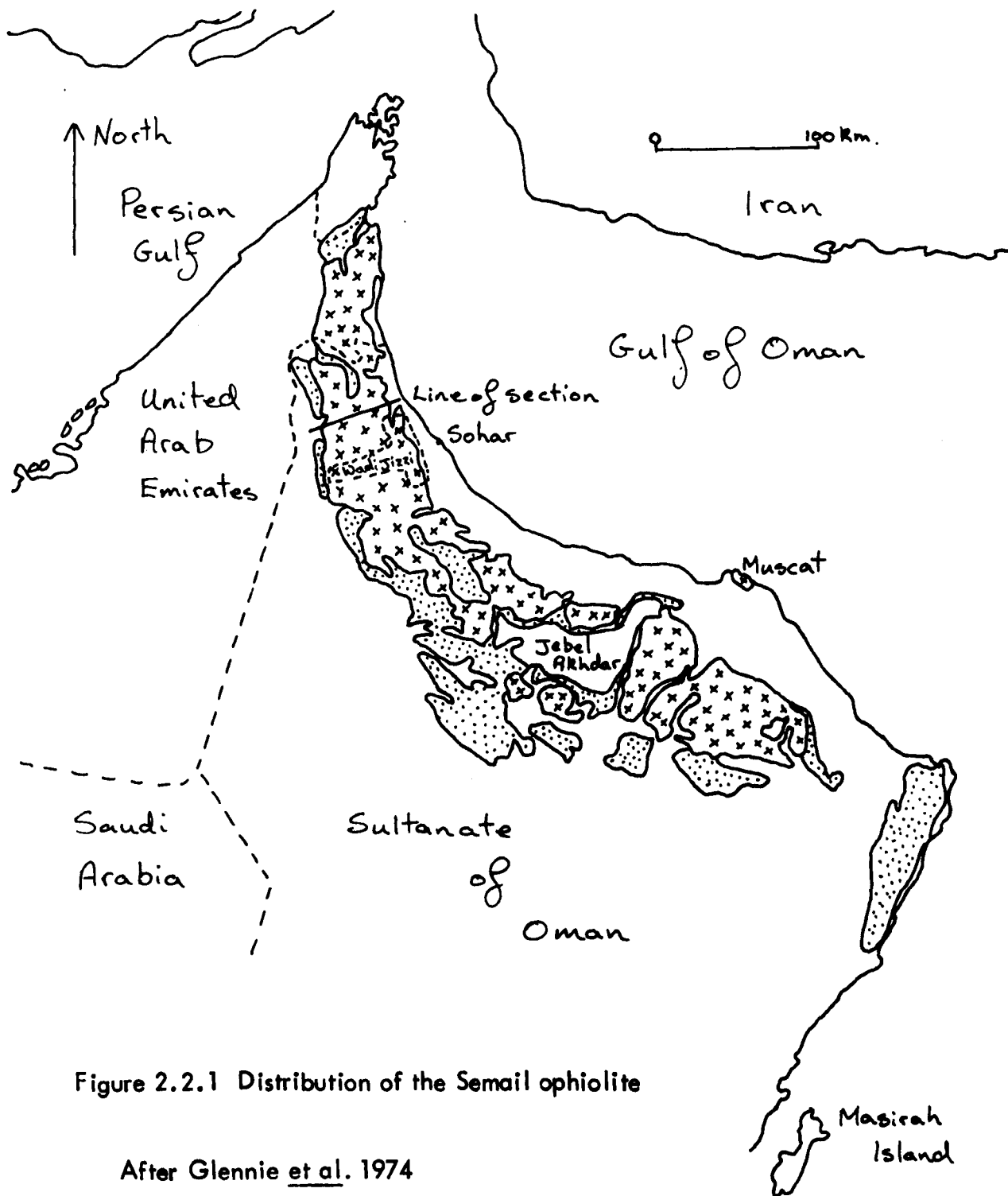
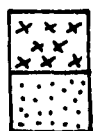


Figure 2.2.1 Distribution of the Semail ophiolite

After Glennie et al. 1974



Semail ophiolite

Hawasina formation

Approximate international boundaries

Field area

structure and regional setting of the ophiolite is based on Glennie et al., (op. cit.) but takes account of the largely unpublished findings of recent studies. (e.g. Coleman 1977, Smewing et al., 1977).

The allochthonous formations of the Oman Mountains were emplaced on top of a thick sedimentary autochthon. This is mainly a shelf carbonate sequence, The Hajar Super-Group, with continental edge and slope deposits, The Sumeini Group, both deposited on the pre-Permian crystalline basement during mid-Permian to Cenomanian times. This autochthon is overlain by the Hawasina Formation, olistostromes of unmetamorphosed deep water marine sediments; turbidites and radiolarites, with pillow basalt, of the same age span as the autochthon. The Semail Nappe, which was emplaced over the Hawasina, is interpreted as a relatively undeformed slice of the oceanic lithosphere more than 15 km. thick derived with the sediments from the northeast. After emplacement of the Semail, shallow-water limestone sedimentation was re-established during the upper Maestrichtian and early Tertiary. Irregular but spectacular uplift of the Arabian continental margin started in the mid-Tertiary and appears to have continued to the present. A calculated 3 to 5 km. of vertical uplift occurred during the last 20 my. In the northern Mountains, which is the structurally simplest area, the originally horizontally disposed units of the ophiolite are now inclined at between  $10^{\circ}$  and  $30^{\circ}$  to the east so that the structurally lowest units crop out to the west and are progressively replaced eastwards by higher units. (Table 2.2.1 and Figure 2.2.2).

The metamorphic sheet which now occurs in thin thrust slices

Table 2.2.1 Stratigraphy of Semail Ophiolite

Nomenclature after Smewing et.al. 1977

Lithology after Glennie et.al. 1974

Upper Pillow Lavas	Dominantly metabasalts, pillowed, massive or brecciated. Rare rhyolites. Interbedded pelagic sediments. Massive sulphide deposits.
Axis Sequence	Sheeted dolerite dykes, some quartz porphyrys. Lavas and dykes metamorphosed at zeolite or greenschist grade.
Upper Plutonic Complex	Varitextured gabbros, plagiogranites Metamorphosed at greenschist and lower amphibolite grade.
Cumulate Sequence	Varied cumulate gabbros passing down into cumulate peridotites. Complex intrusive relations and agmatites. Chromitite pods towards base. Unmetamorphosed
Mantle Sequence	Massive harzburgite, with minor dunite, chromitite, plagioclase hercynite. More or less serpentinitized, especially towards base. Local tectonic fabrics. Intruded by occasional pyroxenite, gabbro and plagiogranite dykes.

Table 2.2.1 Stratigraphy of Semail Ophiolite (continued.)

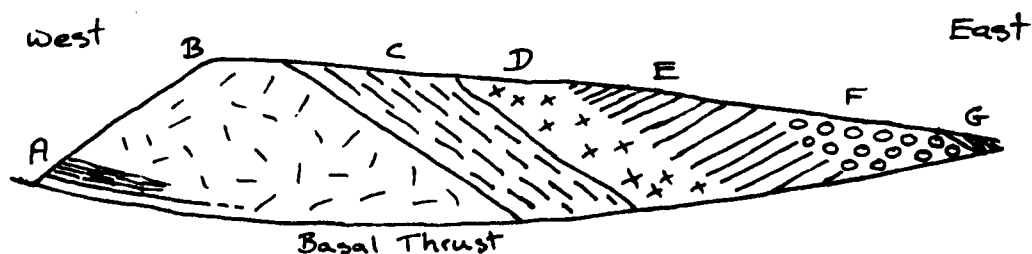
---

Metamorphic Sheet	Sediments of the Hawasina Formation, metamorphosed to greenschist and garnet amphibolite grade, in slices up to 50m thick.
----------------------	---

---

Figure 2.2.2 Diagrammatic cross-section through the Semail ophiolite  
After Glennie et al. 1974, Smewing et al. 1977

Not to scale



- A Metamorphic sheet and mylonitized serpentinite
- B Harzburgite and dunite
- C Layered peridotite and gabbro
- D Varitextured gabbro and plagiogranite
- E Sheeted Intrusive Complex
- F Pillow lavas
- G Thin shales and mudstones (above and within lavas)

beneath the ophiolite is believed to have been formed when the hot ophiolite was first emplaced on the Hawasina sediments. This sheet is cut by irregular veins of aplite, K-feldspar and mineralized quartz (Alleman and Peters, 1972) which are probably related to partial melting of the metamorphites. However, the small volume of these veins and their localization at the sole of the nappe beneath upto 12 km. of massive harzburgite implies that the metamorphic products and processes could not have contributed to the formation of the plagiogranites within the nappe.

#### 2.2.2 Field Relations and Petrography of Plagiogranites

Plagiogranites are found in several different parts of the Semail ophiolite sequence. They occur as (i) large sub-horizontal sheets, at the top of the plutonic sequence, (ii) their intrusive equivalents in the Axis Sequence, (iii) diffuse pods within varitextured gabbro, (iv) intrusive bodies in the plutonic complex, (v) extrusives and (vi) large, steep-sided stocks.

The sub-horizontal sheets are the most important volumetrically, except for the stocks, and occur at the boundary between the dyke swarm and the gabbros. Several well exposed examples indicate these sheets are up to about 1 km. across but laterally discontinuous and less than 100 m thick. The upper margin of the sheet intrudes the base of the sheeted dykes, which are hornfelsed over a short distance, although the plagiogranite is not chilled. Dolerite xenoliths occur in the granite and acid veins penetrate the dolerite. In detail, the intrusion has vertical sides and a stepped roof, controlled by the planar

structure and orthogonal jointing of the dyke swarm. Locally, plagiogranite and gabbro melts have been intruded along major faults to higher levels in the dyke swarm, (Smewing et al., 1977). The intrusive relationships within the dyke swarm and between the swarm and the plutonics are essentially the same as on Troodos. (Section 2.1.2.5). The plagiogranite sheets pass sideways and downwards into varitextured gabbro. The complex boundary zone, composed of diorite and leuco gabbro, is thinner than the plagiogranite and is sometimes cross-cut by acidic and basic veins and dykes. Crenulated basic inclusions chilled on the granite, but backveined by it were found at one locality. These are comparable to the structures found at Palekhor, on Troodos (Section 2.1.2.2) and are likewise interpreted as basic liquid injected into a fluid plagiogranite. Rarely, intrusive veins are composed of a similar mixture of two liquids.

Oman plagiogranite is petrographically inhomogeneous, probably for the same reasons proposed in Section 2.1.2.2. (Table 2.1.1). In the best exposed large sheet at the intersection of Wadi Fizh with the base of the dyke swarm, there is an overall gradation from diorite at the base upwards into trondhjemite, which forms the bulk of the intrusion. Generally, the primary mineralogy of the plagiogranites and gabbros is very similar to that on Troodos (Table 2.2.2). Hornblende, the primary mafic phase in the large plagiogranite bodies, is of variable composition, judging by its colour. Pyroxene is not seen in quartz-rich rocks. Indeed, primary hornblende appears to be more widespread than on Troodos, frequently appearing in gabbros.

At the Wadi Fizh locality foliated quartz diorite occurs towards

Table 2.2.2 Summary of petrography

Rock Type	Primary Petrography	Alteration
Varitextured gabbro	Pl, cpx $\pm$ hnd $\pm$ opx <u>Acc</u> Op, Qz. Med to v coarse grained, very variable. Pl is euhedral to anhedral, weak or strong zoning. Hnd, after op. $\pm$ chl. green and/or brown, interstitial, subhedral or rims cpx.	Some saus. Fibrous pale green amph replaces cpx and hnd. Minor sph.
Plagio-granite (in large sheets, intrusive or <u>insitu</u> veins.)	Pl, qz, hnd. <u>Acc</u> Op, sph, zrc, ap. All in variable proportions. (Diorite to trondhjemite). Leucocratic, med. to fine grained. Pl is euhedral to subhedral, zoned or unzoned, rarely aligned, Qz, interstitial, granophyre common, often continuous with zoned pl. Hnd interstitial.	Pl is turbid and patchily albitized. Ab in zoned rims and granophyre. Minor secondary qz. Mats of fibrous amph. after hnd, often with assoc. fine op + chl + ep $\pm$ cz $\pm$ prh + sph $\pm$ ha $\pm$ cal.

Table 2.2.2 (continued)

<u>Rock Type</u>	<u>Primary Petrography</u>	<u>Alteration</u>
Feldspathic veins	Pl, hnd. <u>Acc</u> Qz, sph, ap, op. Med. grained, unzoned subhedral pl. Very leucocratic	Saus, prehn, common. + fibrous amph + cz + cal + <u>chl</u> + ep. Often cataclastized.
Aplite veins	Pl, qz. <u>Acc</u> Biot, zrc, ap. Rare garnet. Very leucocratic, med. to fine grained, usu. with granophyre. Rarely zoned.	Saus. Chl, after biot. Rare zoisite. Ep.
Rhyolite	Pale brown glass. Small amount of pl, qz + op. microphenocrysts. Perlitic fracture. Weakly vesicular. Felsites mostly irresolvable.	Minor alteration of glass along fractures. Zeolite in vesicles.



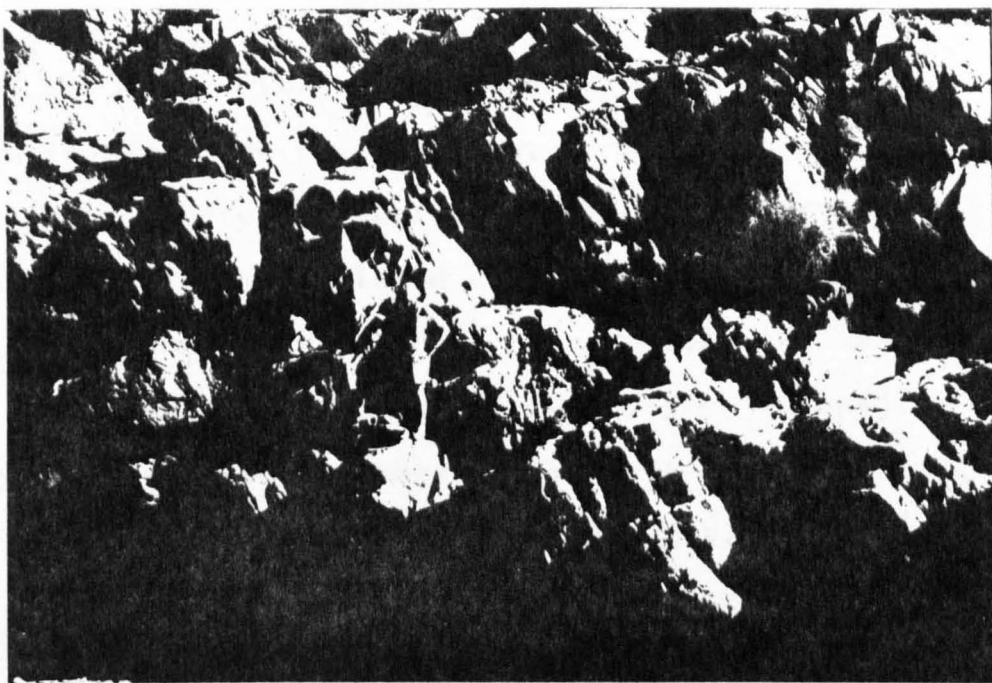


Plate 14 Top of sub-horizontal plagiogranite sheet, Wadi Fizh, Oman. Trondhjemite intrudes and is intruded by dolerite dykes. Dark grey hornfels on left contrasts with medium grey dolerite in centre.

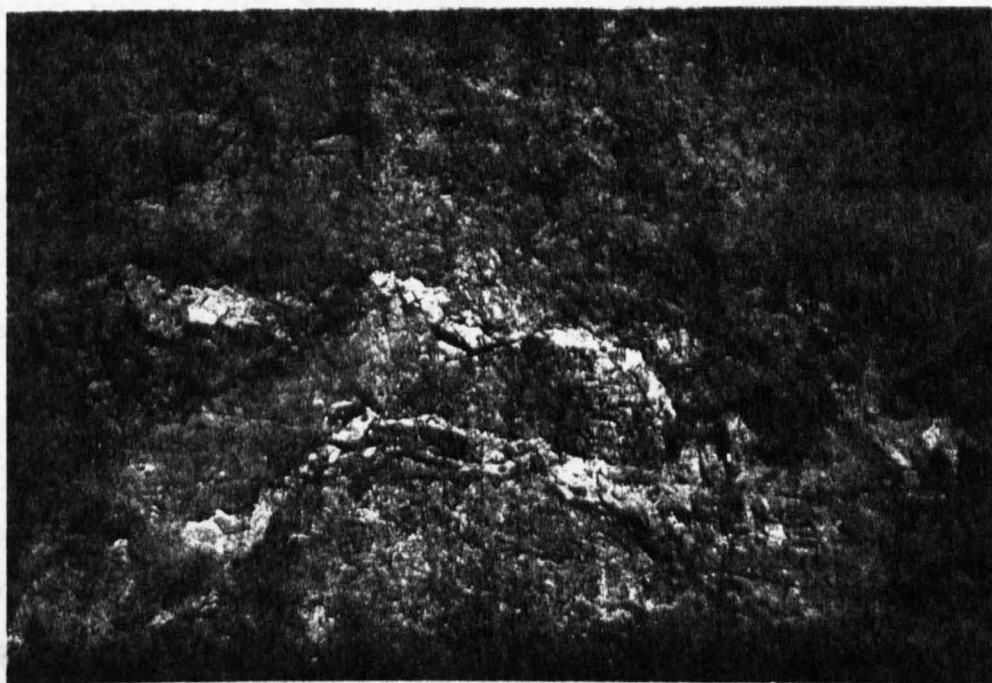


Plate 15 Pale grey gabbro (centre) is intruded by several buff-coloured dolerite dykes. Gabbro and dolerite are cross-cut by thick trondhjemite veins. Wadi Jizzi, Oman. Hammer head is 12cm. long.

bottom of the very well exposed plagiogranite sheet. The foliation is caused by the alignment of euhedral plagioclase, apparently during crystal settling on the floor of the small magma chamber. The accumulated crystals developed intercumulus zoned rims and some of the widest rims enclose the smaller cumulus crystals. Quartz, hornblende, apatite and opaques are also intercumulus phases. These rocks pass downwards into varitextured gabbros without cumulus textures. This agrees with the model suggested by field relations; that the plagiogranites crystallized from a pool of residual liquid lying on essentially solid gabbro, below a solid dyke swarm roof.

The metamorphism of the plagiogranites and gabbros is of a similar style to that of Troodos. As on Cyprus, the more leucocratic rocks have the greater percentage and variety of secondary minerals. At Wadi Fizh, epidote is very irregularly distributed through the intrusion. It does not occur in the basal diorites and tonalites and only appears in quantity in the trondhjemites. In one place epidote-rich trondhjemite intrudes epidote-free tonalite (Plate 16). Dyke margins and joints are frequently loci for epidotization, indeed, it rarely occurs in the absence of late dolerite dykes. As on Troodos, the strong localization of epidote suggests its formation depends on chemical variation, especially volatile concentration, rather than PT conditions. In situ veins are usually seen in outcrops of varitextured gabbro close to the top of the plutonic sequence but also occur within gabbro pegmatite dykes intruding layered gabbro. They are randomly oriented or en echelon leucocratic pods or veins, often several metres long but less than 50 cm. wide. The leucocratic material can be feldspar-rich or quartz-rich and is typically

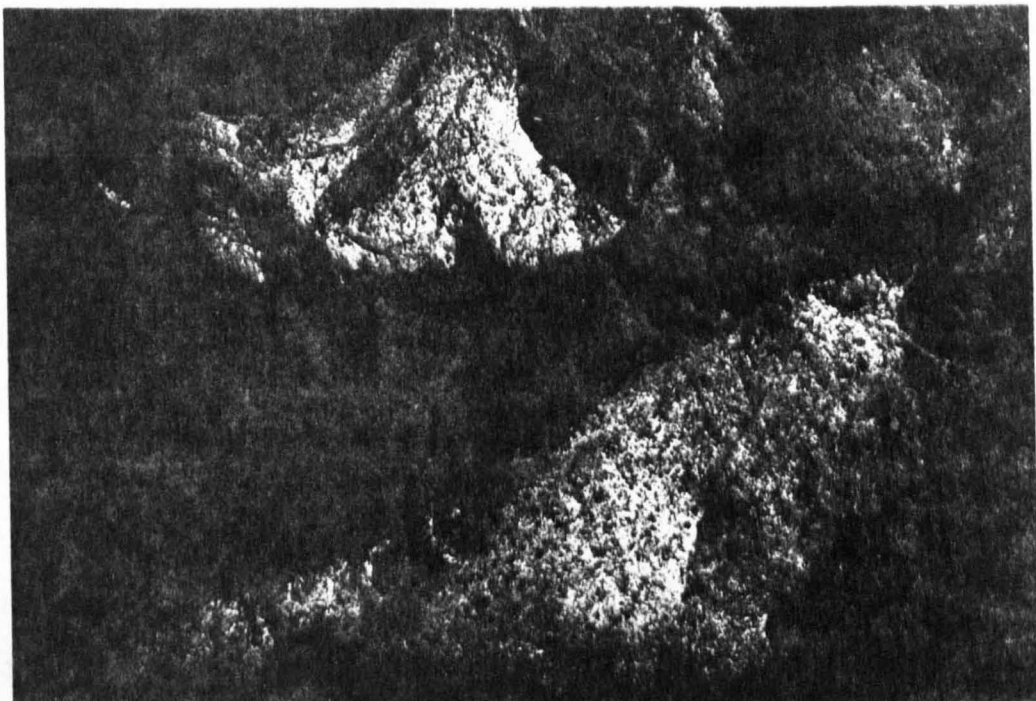


Plate 16 Trondhjemite with epidote blotches intrudes epidote-free tonalite. (Tonalite is at top-centre and bottom of plate.) Both are intruded by dolerite dykes. Note late epidote growth along lower dyke margin. Lenscap (5cm. diam.) lies on intrusive margin.

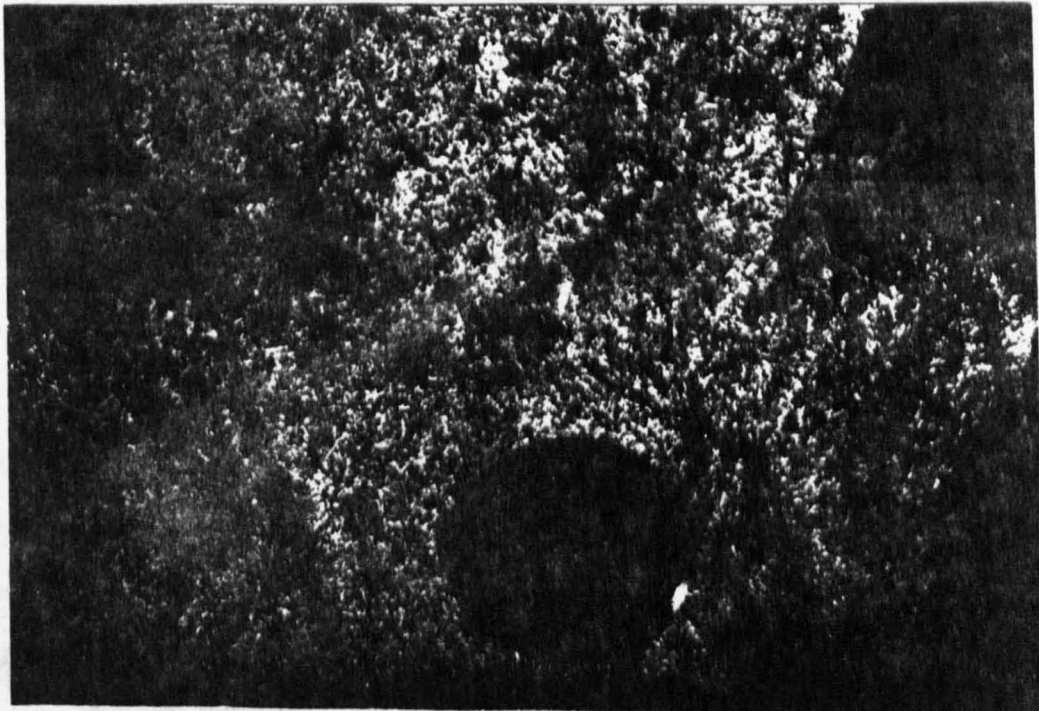


Plate 17 Detail of intrusive margin at bottom centre of Plate 16. Late epidote along minor joints. Wadi Fizh, Oman.

heterogeneous. The veins, which do not enclose gabbro xenoliths, grade rapidly into the gabbro via a diffuse margin which is often coarse grained. The field appearance of these veins suggests they are in situ segregations of residual liquid. They are composed of saussuritized plagioclase laths, with interstitial quartz and hornblende and a variety of secondary greenschist facies minerals. However, in the gabbro host, the feldspar often remains fresh and only small amounts of epidote and chlorite appear.

Leucocratic intrusive bodies in the plutonic complex, veins and dykes, are usually characterized by well-defined, angular margins but there is a gradation to diffuse margined types. There is also a range in shapes and sizes from simple narrow fracture infillings to wide complex zones of netveining or agmatite with numerous, partly assimilated xenoliths. Veins and dykes are commonly found in varitextured or layered gabbro, predating any dolerite dykes. They have no consistent regional orientation. Three distinct petrographic types; microgranitic, feldspathic and aplitic (Table 2.2.2) are found in the intrusive plagiogranite veins. The aplite veins are occasionally zoned but have no marginal chilling. Cataclastic textures frequently appear feldspathic veins and less commonly in microgranitic ones, indicating they were emplaced in a tectonically active regime. Xenoliths of gabbro are common and some have been plastically deformed. Biotite appears in the aplites.

Garnetiferous granitic veins are described from the upper peridotite by Alleman and Peters (1972). Garnet was found

at one locality during the present study, in a concentrically zoned aplite vein intruding pyroxene gabbro. The margins of this 30 cm. thick vein are fine equant quartz and albite with acicular amphibole, chlorite and biotite, grading inwards to graphically intergrown quartz and feldspar; the texture is elongate radially. Discontinuous quartz pods in the centre of the vein are associated with euhedral red garnet, mats of chlorite and radiating acicular epidote with minor zircon and sphere. The garnet which is partly replaced along fractures by chlorite and quartz, has a composition close to 60% spessartine, 40% almandine (Table 2.2.3). Garnets are widespread but rare in pegmatites and aplites (Hsu 1968) but have not been described from other ophiolites. The field occurrence and chemical composition of the garnet leave no doubt that it is primary and was formed in situ. Metamorphic garnets from ophiolites are manganese poor. (Table 2.2.3) Hsu (op. cit.) noted that there is no physical constraint which would inhibit spessartine crystallization from magmas, chemical composition being the decisive factor. The presence of garnet can therefore be attributed to a local concentration of manganese (and iron) during the ordinary development of a residual fluid.

The field relationships within the Semail dyke swarm are the same as in the S.I.C. on Troodos (Section 2.1.2.3). Metadolerites are the most common rock type and many of these have secondary silica enrichment but silicic porphyry dykes and stocks also occur (Glennie et al., 1974). Other acidic dykes, usually intruding low levels of the dyke swarm, are fine grained

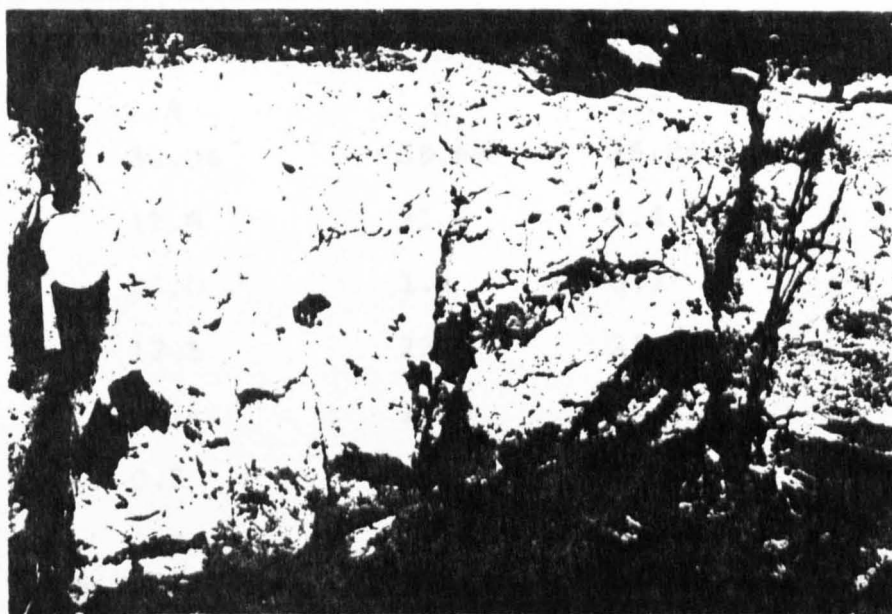


Plate 18 Zoned aplite vein. Equigranular margins, granophyric interior and quartz pod with single euhedral garnet in centre. Vein is 10 to 20cm. thick. Specimen OM 3090, Wadi Fizh, Oman.

Table 2.2.3 Garnets from ophiolites

	A	B	C
SiO <sub>2</sub>	36.0%	38.6%	36.8%
Al <sub>2</sub> O <sub>3</sub>	19.8	21.6	4.4
MnO	26.0	1.2	0.3
FeO	17.5	23.6	24.0
CaO	0.1	11.3	32.2
MgO	0.5	4.8	-
TiO <sub>2</sub>	0.4	0.1	0.3
Total	<u>100.3*</u>	<u>101.2*</u>	<u>98.0</u>
Spessartine	60.5		
Almandine	40.7		
Pyrope	<u>0.2</u>		
	<u>101.4</u>		

A-OM3090 - Aplite vein - Semail Nappe

Average of nine analyses

B-OM902 - Metasediment from metamorphic sheet  
beneath Semail Nappe

C-T371 - Trondhjemite, contact metamorphosed  
by gabbro intrusion - Troodos Massif, Cyprus.  
Average of two analyses, from Allen (1975)

\* oxygen by difference



equivalents of the massive sheets at its base.

The Semail extrusives are nearly all basaltic or metabasaltic pillowed or massive lavas and breccias, often crosscut by dykes and sills of similar composition. Acidic intrusives and lavas were found in one area towards the top of the mapped lava outcrop a few km. south of Wadi Jizzi (Figure 2.2.1) and others in a similar structural position have been located north of that Wadi. They are hard pale yellow to red brown felsites intimately mixed with a small proportion of dark grey glass. Typically, the felsites have narrow (10-20 cm.) columnar joints but some are autobrecciated.

Preliminary field studies suggest that these rocks are related at depth to the larger plagiogranite bodies. Their spatial coincidence with a known zone of sulphide mineralization is probably chance, although the same fracture system could have acted as channels for both the silicic melt and the mineralizing fluids. Recent fieldwork (winter 1977/1978) by the Open University Oman research team suggests, as yet inconclusively that the acidic extrusives postdate the mineralization. Members of the team have also found large trondhjemitic stocks invading the gabbros and dyke swarm at depth beneath the same zone of mineralization. Plagiogranite in stocks, rather than in subhorizontal sheets, appears to be typical of island arcs. (Section 2.6).but no geochemical analyses of the stocks are available to test their affinity.



### 2.2.3 Geochemistry

#### 2.2.3.1 Metasomatism

With the exception of two pyroxene gabbros and one of the glassy rhyolites none of the analysed specimens were fresh, i.e. had less than 5% secondary minerals. As in the previous section on the geochemistry of Troodos plagiogranites (2.1.3), metasomatic alteration is considered before the primary variation trends.

Similar reasoning to that outlined in Section 1.3 suggests that there is minor enrichment in silica among some of the trondhjemites and dolerites which is, however, insufficient to affect the overall primary distribution. A few plagiogranites are mildly depleted in iron. The wide range in  $\text{Na}_2\text{O}$  values suggests that enrichment generally accompanies albitization but a few individuals have abnormally low values. Sr and Ba are also generally enriched. The uniform low levels of  $\text{K}_2\text{O}$  and some very low levels (0.01 or less) suggest this element is thoroughly depleted during metamorphism and that the primary distribution has been obscured. However, although the aplites, the most differentiated liquids, are saussuritized, they cross-cut gabbro which is itself unaltered. Therefore they are presumed to have been "insulated" from circulating hydrothermal fluids. In spite of this, the aplites all have very low  $\text{K}_2\text{O}$ , which is therefore taken to be the primary content. More extreme metasomatism takes place during epidotization when there appears to be a slight gain in  $\text{SiO}_2$  and loss of  $\text{Fe}_2\text{O}_3^*$ , MnO, Zn,  $\text{K}_2\text{O}$  and Ba. It is interesting to note that Ba seemingly behaves in an opposite way during greenschist style

Table 2.2.4 Major Element Ranges (wt%)

Rock Type	Gabbro	Dolerite	<u>Insitu</u> vein*	Tonalite
No. Specimens	7	17	3	4
SiO <sub>2</sub>	48.5-55.0	48.3-57.7	57.6-73.0	58.7-65.6
TiO <sub>2</sub>	0.14-1.59	0.35-1.89	0.31-0.48	0.44-1.30
Al <sub>2</sub> O <sub>3</sub>	10.3-15.3	11.6-17.6	13.7-17.4	13.3-14.8
Fe <sub>2</sub> O <sub>3</sub> *	7.3-12.5	6.3-13.8	1.5-5.3	5.9-10.1
MnO	0.12-0.16	0.07-6.25	0.03-0.07	0.06-0.23
MgO	5.9-15.5	4.4-9.2	0.6-1.9	1.2-3.9
CaO	7.3-16.2	4.4-15.3	1.4-8.8	3.0-5.8
Na <sub>2</sub> O	0.4-4.6	2.2-5.0	5.6-7.9	4.7-6.9
K <sub>2</sub> O	0.02-0.21	0.04-0.50	0.01-0.2	0.15-0.40
P <sub>2</sub> O <sub>5</sub>	<0.01-0.12	0.01-0.25	0.05-0.13	0.15-0.49

Rock Type	Trondhjemite	Epidosite	Rhyolite	Aplite
No. Specimens	2	4	2	4
SiO <sub>2</sub>	71.5-75.6	67.0-71.8	79.1-70.4	73.0-77.4
TiO <sub>2</sub>	0.27-0.38	0.40-0.87	0.22-0.26	0.08-0.31
Al <sub>2</sub> O <sub>3</sub>	12.8-15.2	11.6-13.9	9.7-10.9	13.0-13.3
Fe <sub>2</sub> O <sub>3</sub> *	1.5-3.2	1.9-3.5	3.7-4.9	0.5-2.4
MnO	0.01-0.03	0.03-0.06	0.14-0.11	0.01-0.03
MgO	0.3-1.1	0.8-1.7	0.5-0.3	0.1-1.3
CaO	1.9-3.9	3.7-5.5	1.3-4.7	0.7-3.0
Na <sub>2</sub> O	5.6-6.7	4.4-8.3	3.6-1.7	4.9-8.3
K <sub>2</sub> O	0.06-0.31	0.01-0.07	0.83-0.75	0.02-0.16
P <sub>2</sub> O <sub>5</sub>	0.03-0.08	0.09-0.26	0.03-0.02	0.01-0.04

\*Range from Quartz dioritic to trondhjemitic

Table 2.2.5 Trace Element Ranges (ppm)

Rock Type	Gabbro	Dolerite	<u>Insitu</u> Vein	Tonalite
No. Specimens	7	17	3	4
Zr	2-95	16-153	114-401	122-243
Y	3-34	11-46	10-40	41-68
Nb	<1-5	<1-5	2-3	4
Cr	2-1063	3-186	4-8	2-30
Ni	<1-144	<1-90	<1-4	<1-12
Sr	61-213	44-567	54-152	109-190
Ba	8-63	28-82	15-77	46-93
Rb	<1	<1-2	<1	<1-1
Zn	7-50	3-108	<1-5	3-36
Rock Type	Trondhjemite	Epidosite	Rhyolite	Aplite
No. Specimens	2	4	2	4
Zr	313-497	180-270	107-138	40-140
Y	46-76	51-63	32-40	5-35
Nb	3-5	2-6	3	1-3
Cr	4-9	4-7	3-6	7-35
Ni	<1	<1-2	<1	<1-4
Sr	77-104	66-128	67-321	18-111
Ba	65-102	18-49	148-107	20-75
Rb	<1-1	<1	12-20	<1
Zn	<1	<1-5	37-60	<1-7

metamorphism and epidotization. Other metasomatic variation, if present, cannot be distinguished from primary variations such as minor differences in mode.

#### 2.2.3.2 Major and trace elements and magmatic evolution

The elements behave in a very similar manner as in the Troodos suite and their distribution can be accounted for by a similar scheme of crystal fractionation from a basic magma. Accumulation of two pyroxenes, calcic plagioclase and olivine (the cumulate phases in the gabbros) gives rise to incompatible-impoverished gabbros which are enriched in MgO, CaO, Cr, Ni and, where plagioclase dominates the mafic phases,  $Al_2O_3$ . The evolving liquid, which fractionates these phases, represented by the (aphyric)dolerites, has progressively increasing  $SiO_2$ ,  $TiO_2$ ,  $Fe_2O_3^*$ ,  $Na_2O$ , Zr, Y,  $P_2O_5$  and Sr. The more differentiated dolerites are also strongly depleted in Cr and Ni. Dolerites which crosscut plagiogranites can be either primitive or evolved types. The iron-enrichment of the dolerites contrasts with the silica-alkali enrichment in the plagiogranites. These seem to evolve from moderately differentiated basic magmas by FeTi-oxide fractionation, indeed a few of the dolerites are depleted in  $TiO_2$  and iron relative to other differentiated dolerites.

The aplites and rhyolites represent the extreme of silica-alkali enrichment. They are depleted in Zr and Y relative to the trondhjemites. The depletion is presumed to occur when zircon (Zr), apatite (Y) and perhaps sphene (Y) appear as fractionating phases. The rocks have, as a group, the characteristics expected of ultimate residua; the aplites occur in complex networks and

Figure 2.2.3 Variation diagrams : Semail Nappe

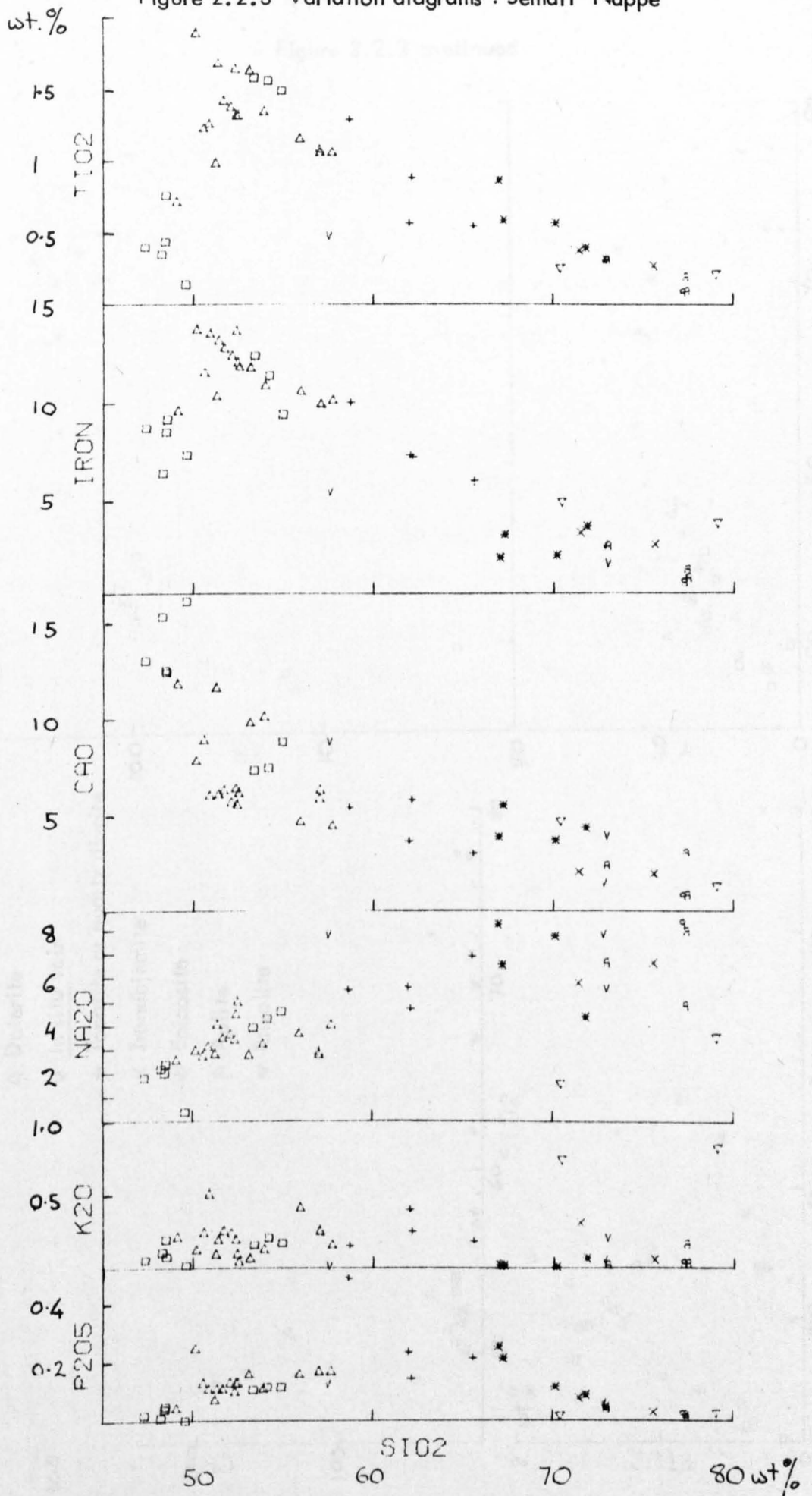
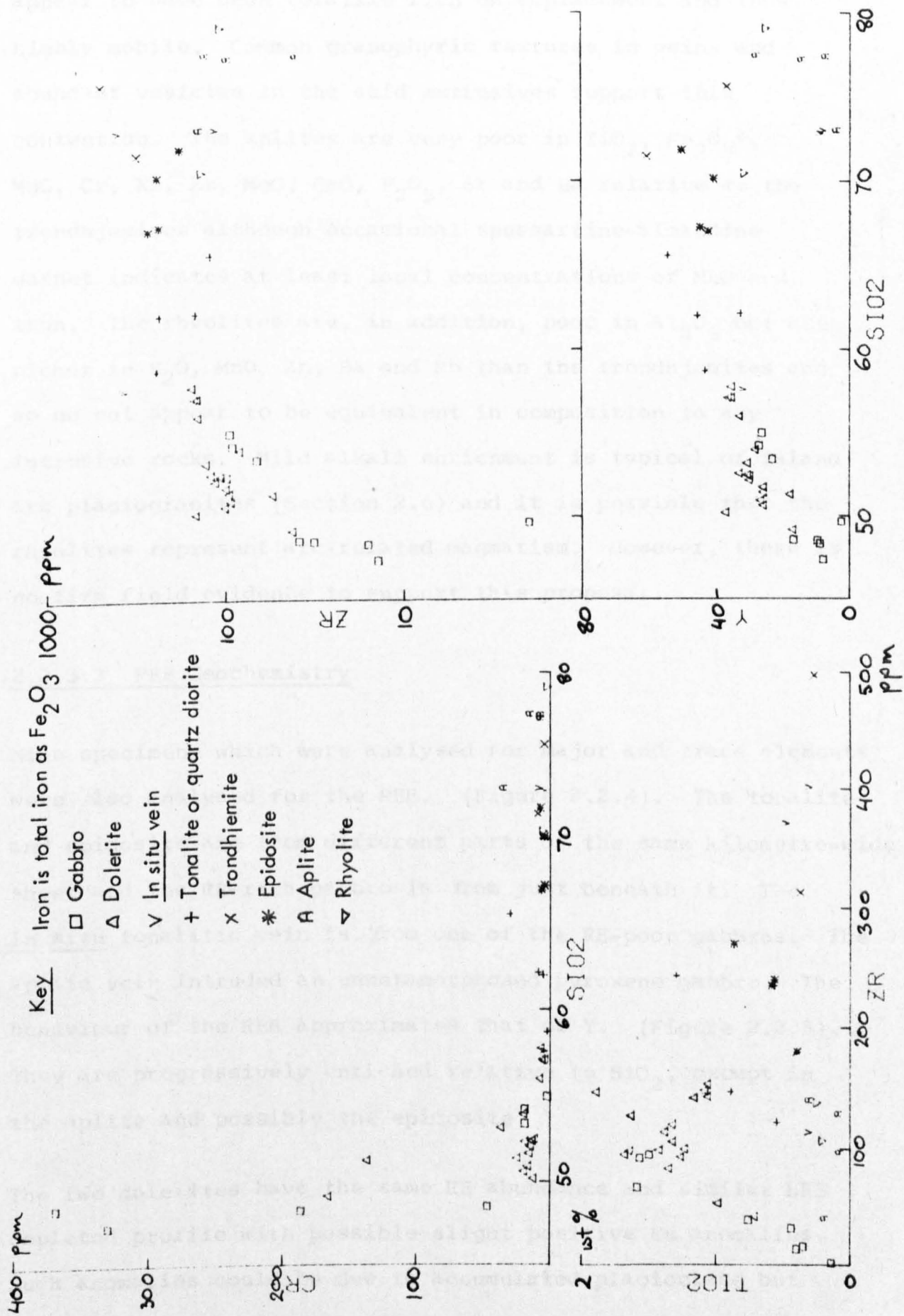


Figure 2.2.3 continued



appear to have been volatile rich on emplacement and thus highly mobile. Common granophyric textures in veins and abundant vesicles in the acid extrusives support this contention. The aplites are very poor in  $\text{TiO}_2$ ,  $\text{Fe}_2\text{O}_3^*$ ,  $\text{MnO}$ ,  $\text{Cr}$ ,  $\text{Ni}$ ,  $\text{Zn}$ ,  $\text{MgO}$ ,  $\text{CaO}$ ,  $\text{P}_2\text{O}_5$ ,  $\text{Sr}$  and  $\text{Ba}$  relative to the trondhjemites although occasional spessartine-almandine garnet indicates at least local concentrations of  $\text{MnO}$  and iron. The rhyolites are, in addition, poor in  $\text{Al}_2\text{O}_3$  but are richer in  $\text{K}_2\text{O}$ ,  $\text{MnO}$ ,  $\text{Zn}$ ,  $\text{Ba}$  and  $\text{Rb}$  than the trondhjemites and so do not appear to be equivalent in composition to any intrusive rocks. Mild alkali enrichment is typical of island arc plagiogranites (Section 2.6) and it is possible that the rhyolites represent arc-related magmatism. However, there is no firm field evidence to support this proposal.

#### 2.2.3.3 REE Geochemistry

Nine specimens which were analysed for major and trace elements were also analysed for the REE. (Figure 2.2.4). The tonalite and epidosite are from different parts of the same kilometre-wide sheet and the RE-rich gabbro is from just beneath it. The in situ tonalitic vein is from one of the RE-poor gabbros. The aplite vein intruded an unmetamorphosed pyroxene gabbro. The behaviour of the REE approximates that of Y. (Figure 2.2.5). They are progressively enriched relative to  $\text{SiO}_2$ , except in the aplite and possibly the epidosite.

The two dolerites have the same RE abundance and similar LRE depleted profile with possible slight positive Eu anomalies. Such anomalies could be due to accumulated plagioclase but

Figure 2.2.5 Variation of RE with silica

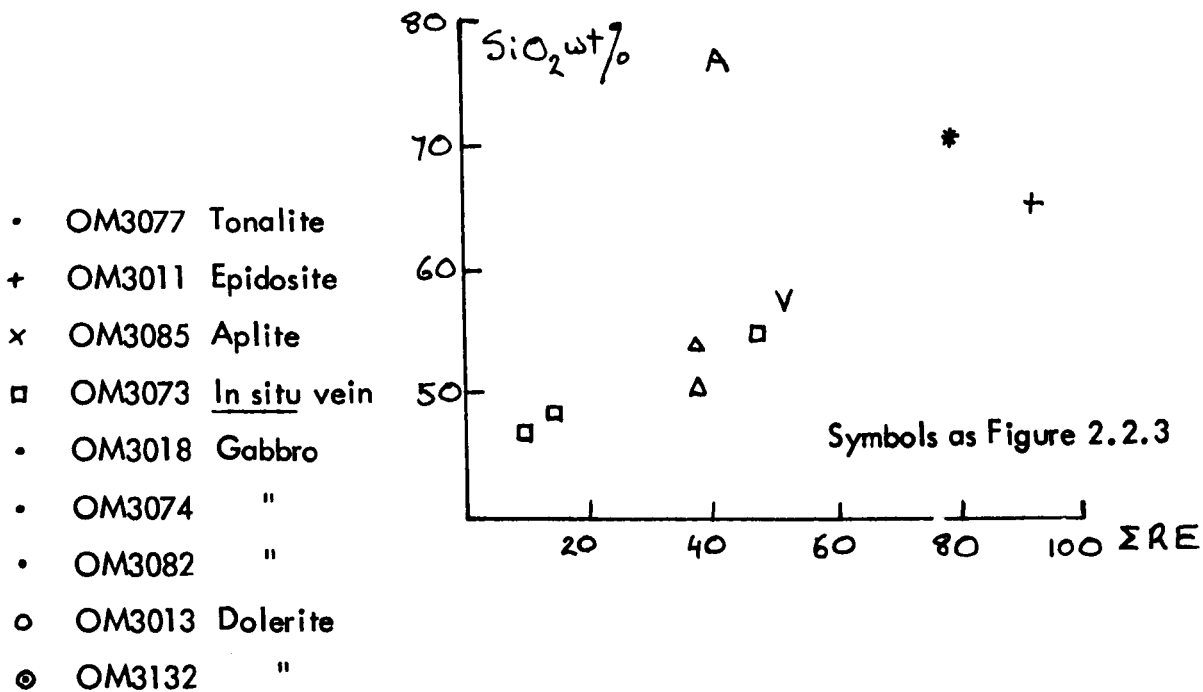
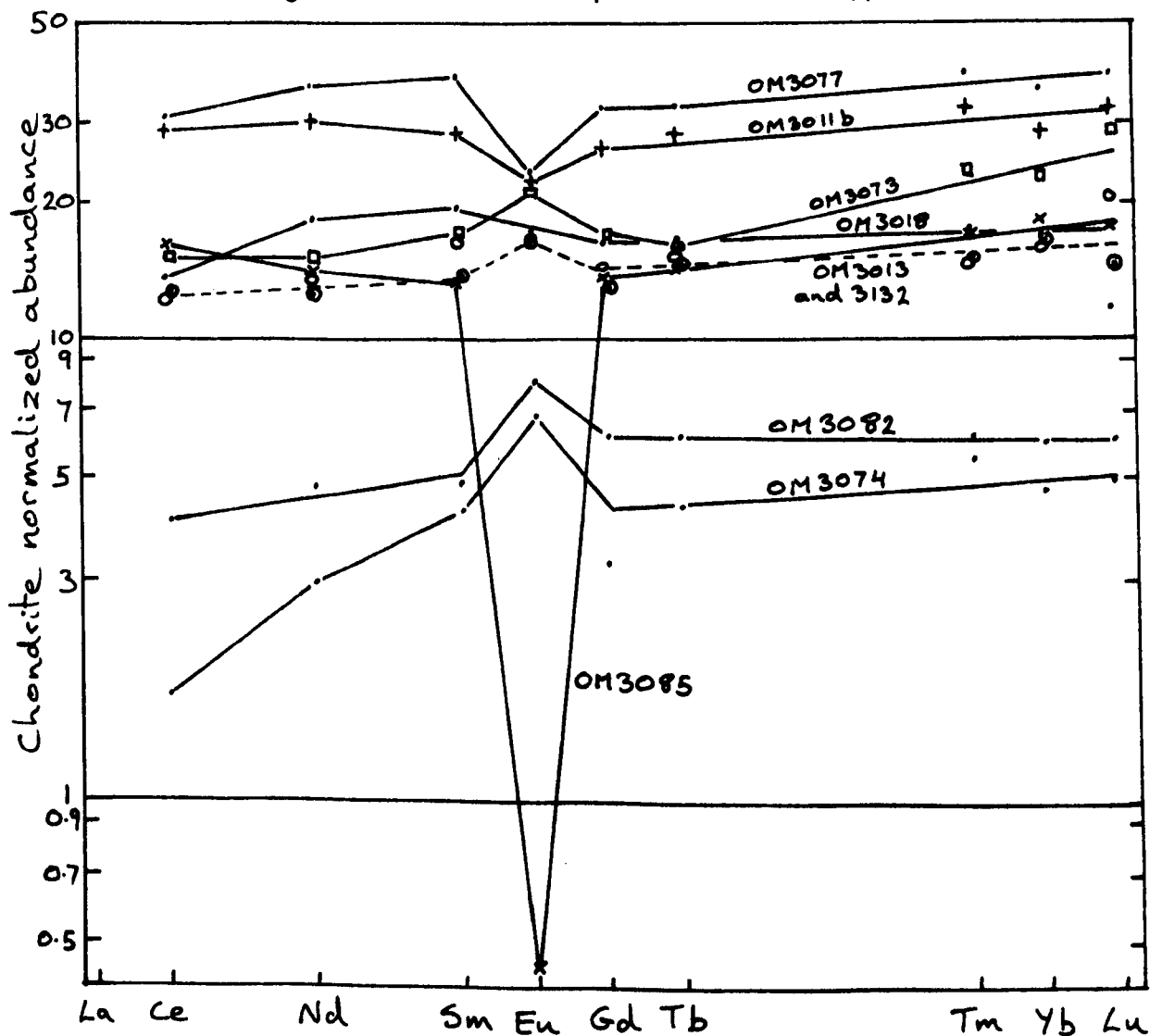


Figure 2.2.4 Rare earth profiles: Semail Nappe





both dolerites are uniformly fine grained with, in one specimen, sparse small clinopyroxene phenocrysts. However, clinopyroxene/melt partition coefficients for Eu are anomalously low (Figure 2.1.8) and so the removal of pyroxene would leave a melt richer in Eu than Sm or Gd. Clinopyroxene fractionation should also increase the Ce/Sm ratio in the melt. (Schilling 1971). Although the RE-rich gabbro has  $\Sigma$ RE slightly greater than the two dolerites it has a lower Ce/Sm ratio and no Eu anomaly suggesting that clinopyroxene fractionation was less extreme in the gabbro. Other immobile trace element data suggest that these three samples represent differentiated basic liquids. Therefore these RE data only provide general indications of the likely RE content of the primitive basic magma. The most undifferentiated profile type, in fact the only one without an Eu anomaly, is that of the RE-rich gabbro and this is taken as the closest approximation to the profile shape of the primitive magma. Extrapolation of RE abundances to levels expected in the least evolved of the analysed dolerites (based on Zr, Y and Cr content) suggests the primitive magma had not more than 8x chondritic RE abundance. However, it probably had greater  $\Sigma$ RE than the RE-poor gabbros.

It was suggested earlier that the low abundance of Y, Zr and  $\text{TiO}_2$  in the gabbros was a result of being largely composed of cumulate crystals. Their RE content is consistent with this interpretation. As well as having a smaller  $\Sigma$ RE than the dolerites, they both have larger positive Eu anomalies and one is more LRE depleted. These features can be explained if the

RE content of the intercumulus liquid is overwhelmed by the prescence of RE poor, Eu-rich cumulus plagioclase and RE poor, LRE depleted cumulus pyroxene dominating the RE content of the rock. The in situ vein also has a positive Eu anomaly and so is probably a plagioclase crystal mush.

The tonalite and epidosite have flat profiles, like the dolerites but with distinct negative Eu anomalies which are diagnostic of feldspar fractionation (Section 2.1.4.5). The epidosite has half the phosphorous content of the tonalite and the slight change in profile shape from one to the other could be attributed to apatite fractionation, this phase having large partition coefficients (Figure 2.1.8). However, there is a possibility that  $P_2O_5$  depletion and the differences in RE profile in the epidosite are metasomatic but quantitative analysis would be required to clarify this point.

The influence of apatite fractionation can be seen in the difference in RE profiles of the tonalite and aplite. Ignoring Eu, it is apparent that both LRE and HRE in the aplite are somewhat enriched relative to Sm, Gd and Tb. This dishd profile and the  $\Sigma$ RE depletion relative to tonalite can be attributed to apatite (or possibly, hornblende) fractionation because both minerals take up the "middle range" lanthanides in preference to others. Extreme plagioclase fractionation is suggested as the cause of the huge negative Eu anomaly in the aplite. The lack of Eu could possibly be due to metasomatism but because the rock has no Ce anomaly and it is enclosed in unaltered gabbro, this is considered unlikely.

The REE distribution in the nine analysed specimens appears to be consistent with the previous interpretations of field, petrographic and geochemical data although requiring quantitative analysis for a more rigorous application.

## 2.3 Smartville Block

### 2.3.1 Introduction and Regional Geology

The geology of the Sierra Nevada, in the western U.S. Cordillera, is dominated by a huge late Mesozoic calc-alkaline granitic batholith. The Mesozoic and Palaeozoic metasedimentary and metavolcanic country rocks are exposed only on the fringes of the mountain chain. In California, the Sierra Nevada is overlain to the west by the undeformed Upper Cretaceous to Recent sediments of the Great Valley and to the north by the Tertiary volcanics of the Cascades (Figure 2.3.1).

The Smartville Block, which is up to 30 km. wide and 80 km. long, lies along the northwestern foothills of the Sierra Nevada, about 75 km. northeast of Sacramento. It was delineated on geophysical evidence and named after a township on the Yuba River by Cady (1975). The Smartville area was originally mapped by Lingren and Turner (1895; Geologic Map of California, Chico and Sacramento Sheets, 1965) who recorded basic metavolcanic rocks of Triassic to Jurassic age, intruded by large granite and gabbro plutons. Recent reappraisal suggests the "metavolcanic rocks" are an ophiolite deformed in a gentle antiform with a north-south axis. (Figure 2.3.2) (Schweickert and Cowan 1975). Volcanic rocks are exposed on each flank and plagiogranites and gabbros along the centre of the structure. A dyke complex separates the volcanics and plutonics. In contrast to the extensive plutonic sequences of complete ophiolites (Section 1.2) there are very few exposures of cumulate gabbro or peridotite (Menzies et al. 1975). The

Figure 2.3.1 Geological map of California

After Bailey et al. 1970, Schweickert and Cowan 1975

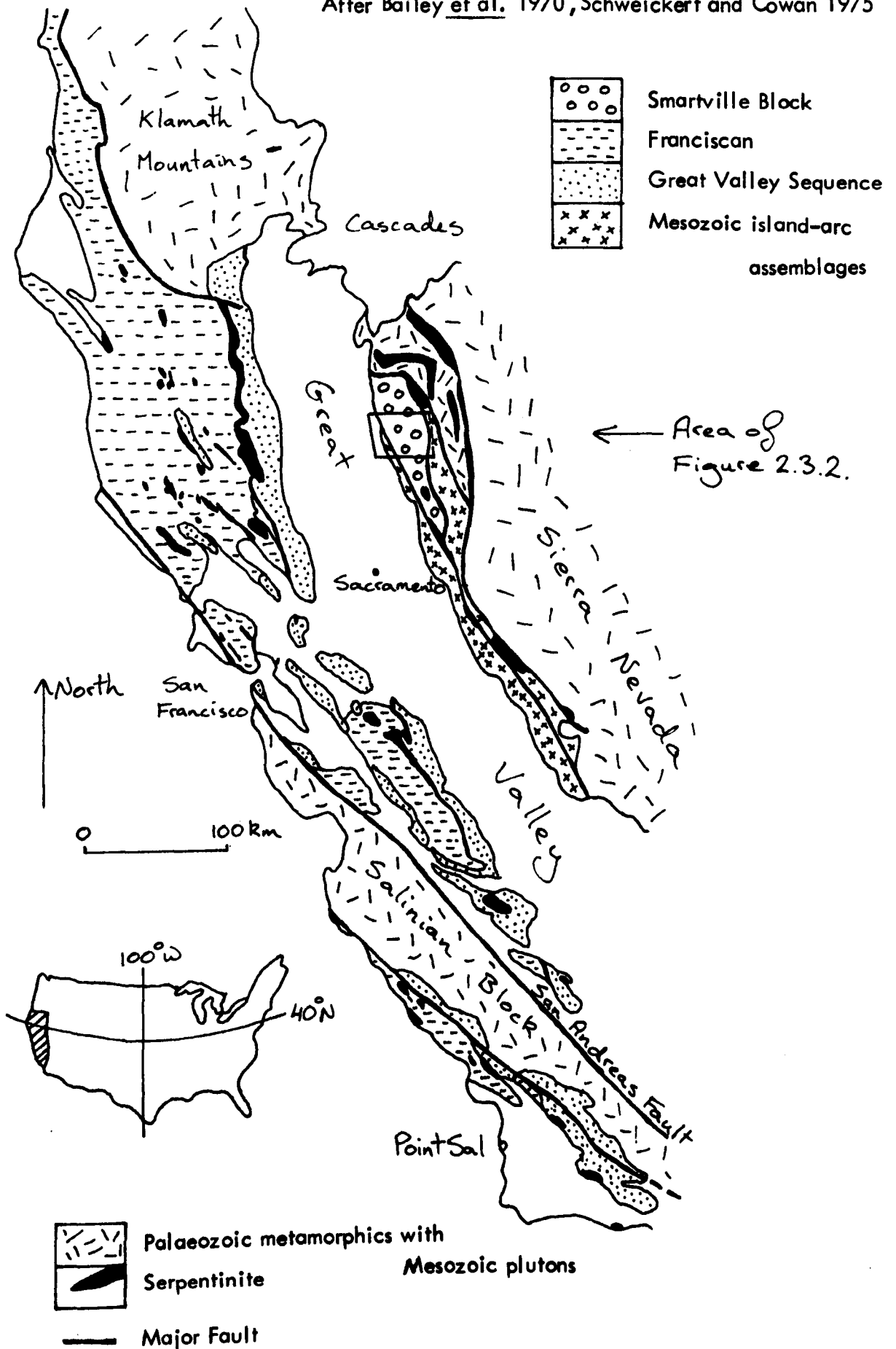
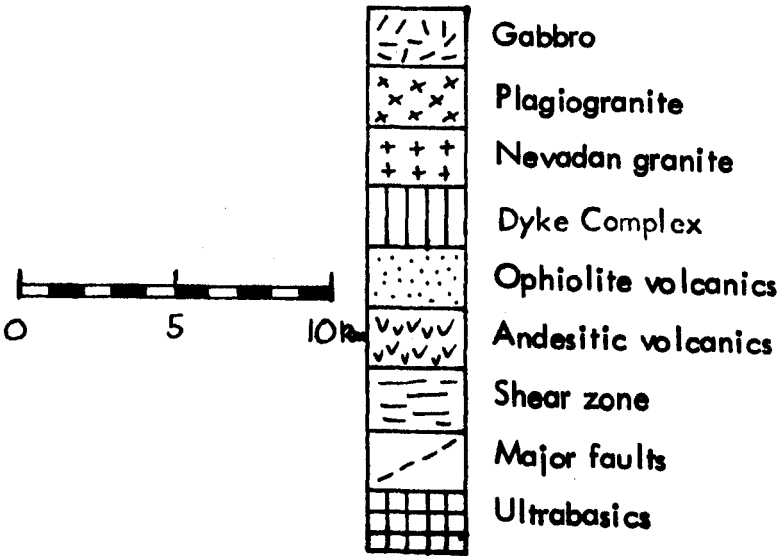
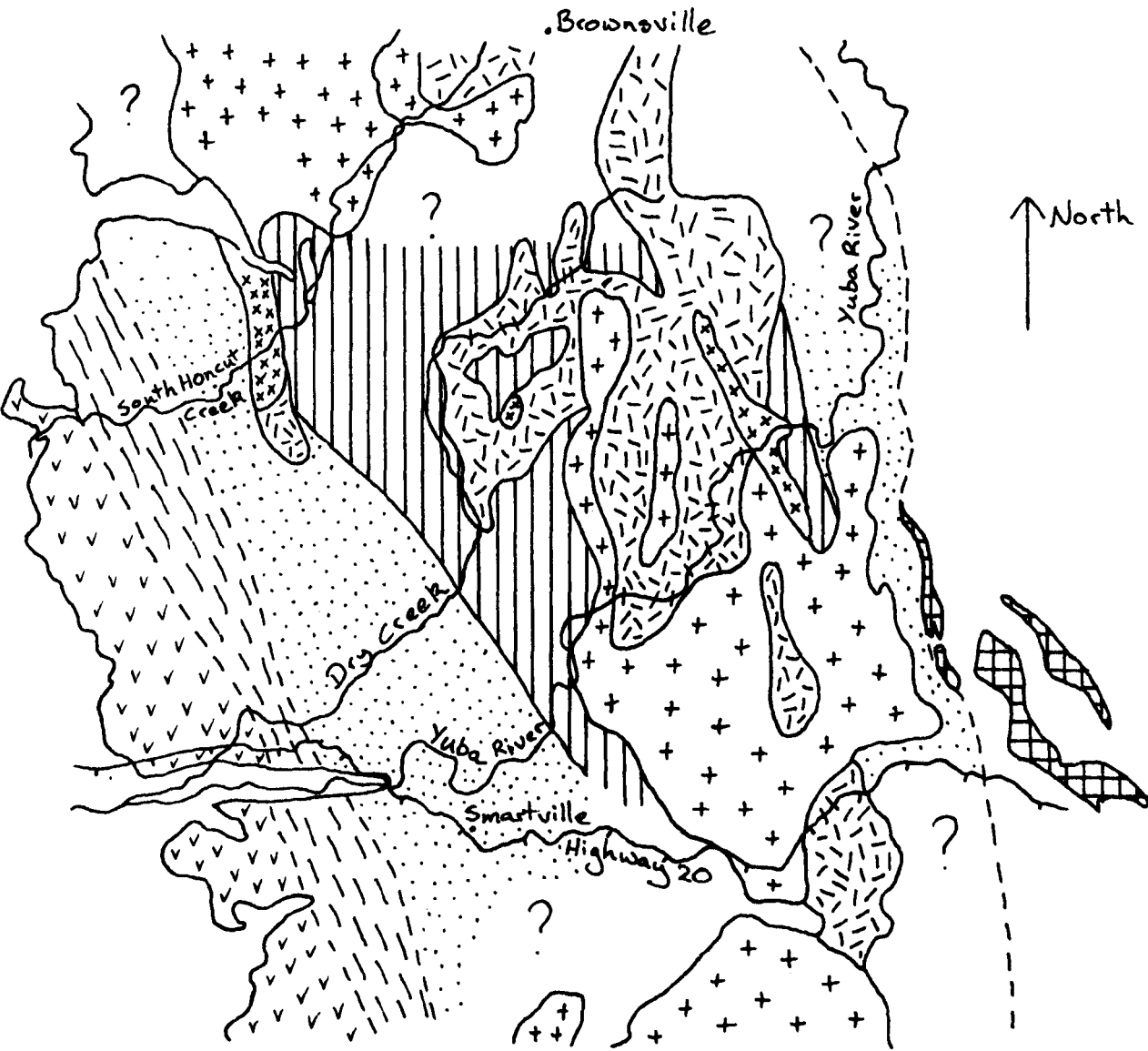
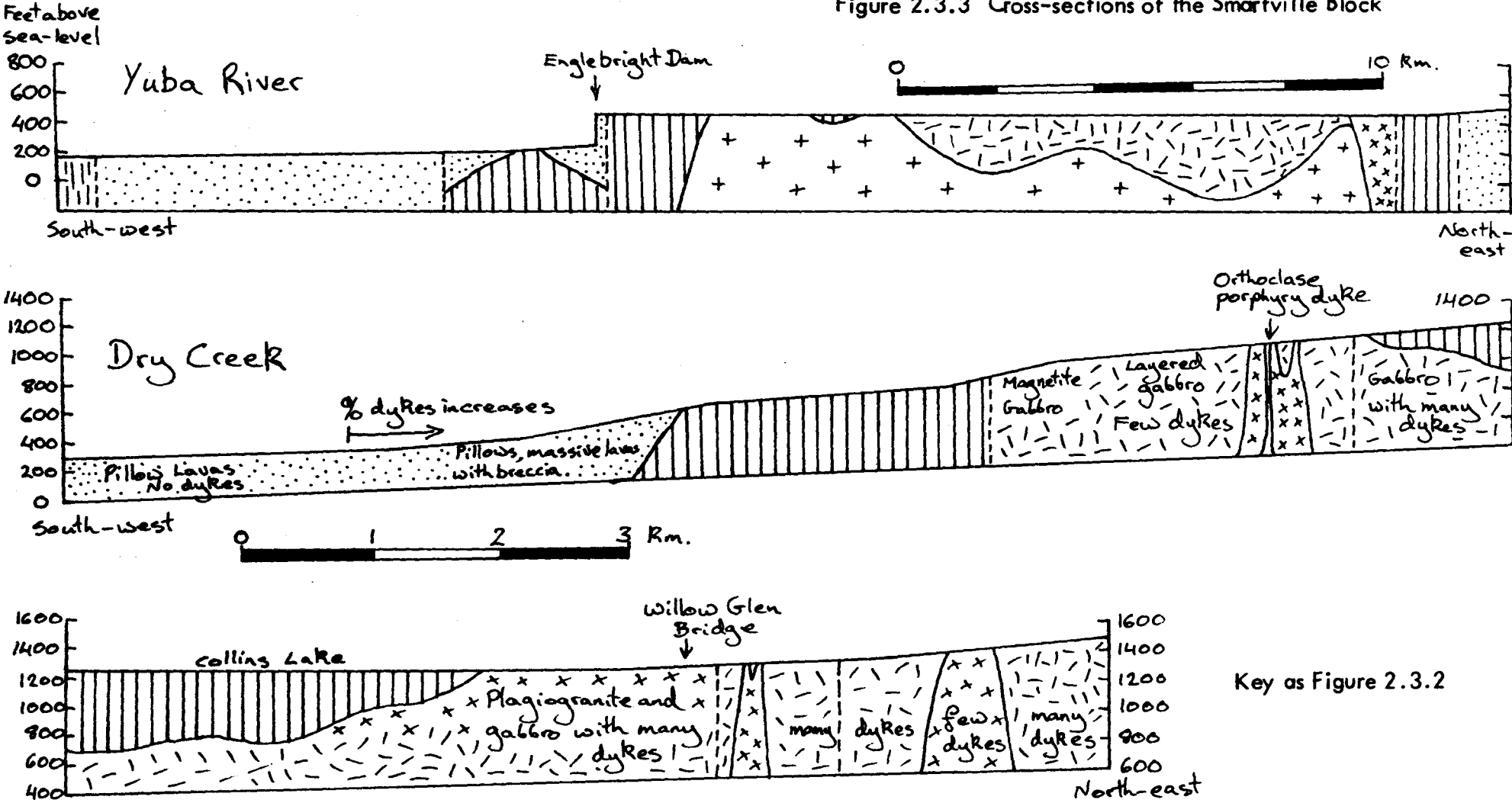


Figure 2.3.2 Geological sketch map of the Smartville Block



After Menzies et al., 1975, Geol. map of California, Sacramento Sheet  
and present work

Figure 2.3.3 Cross-sections of the Smartville Block



only large outcrops of ultramafic rock associated with the ophiolite are in lenses of serpentinite which lie along the boundary fault zones. Small scale deformation of the ophiolite occurs adjacent to these faults. Minor, parallel, fractures cut the Block.

The lack of ultramafic rocks, combined with poor exposure, was probably the reason for the late recognition of this ophiolite. However, recent road cutting and reservoir construction created some excellent exposures, particularly of a dyke complex, and it was realised that this was very similar to, for example, the Sheeted Intrusive Complex of the Troodos Massif. (Section 2.1.2.3). Most of the terrain is covered by forest, woodland, scrub or pasture and exposure is sparse. Fieldwork was largely confined to road and river sections. However, the main rivers run across strike and so provide excellent representative sections (Figure 2.3.3), most of which occur between Brownsville in the north and State Highway 20 in the south.

Sediments within the volcanics are unfossiliferous and there are no radiometric age determinations available. The ophiolite is assumed to be of similar age to the Jurassic sediments which flank it to east and west and it is known that the area was structurally defined as a fault block before the intrusion of a group of Late Jurassic plutons (Hietanen 1973).

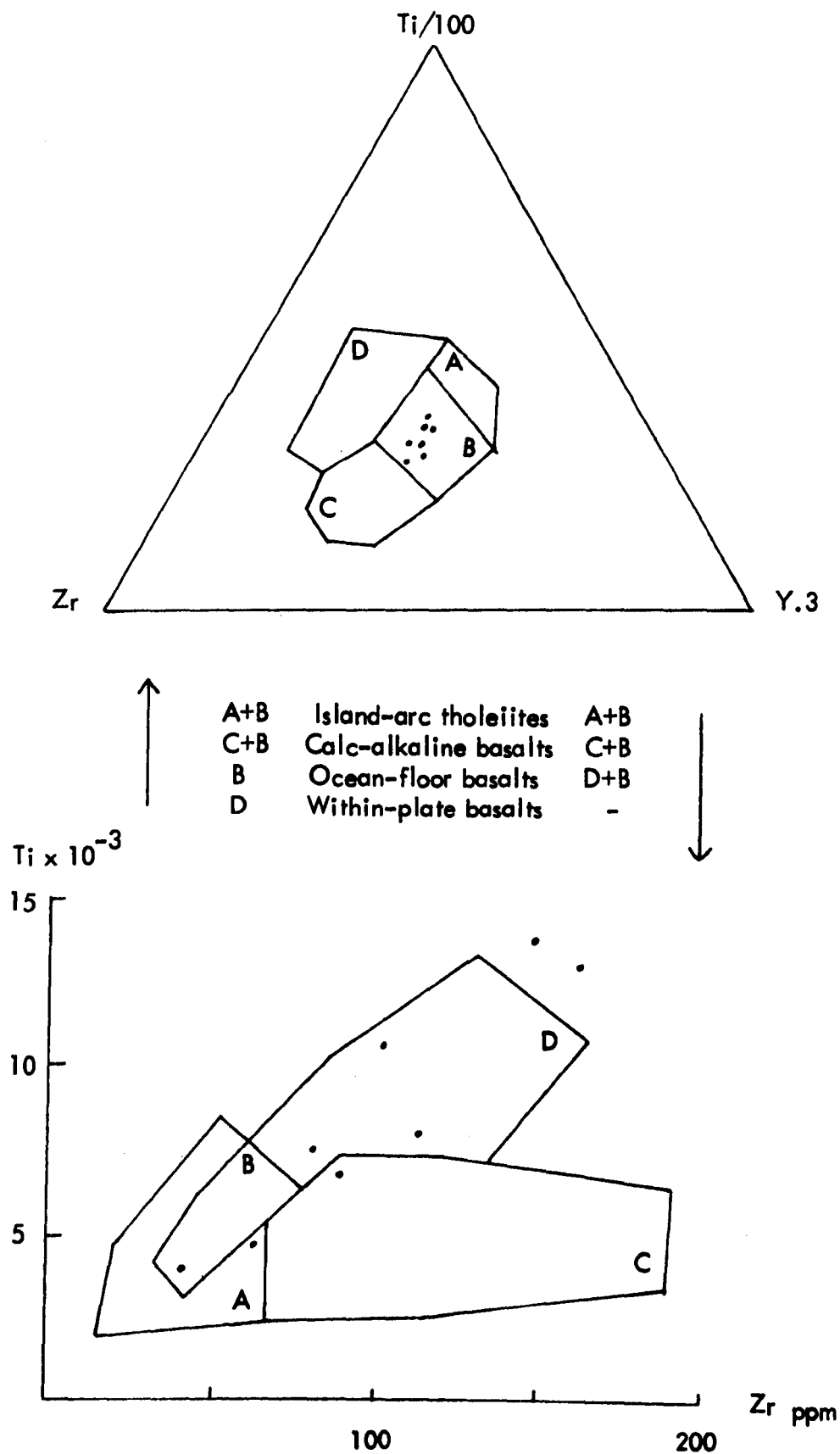
Palaeogeographic reconstruction of the western U.S. Cordillera indicates that the Palaeozoic - Mesozoic American continental margin was underthrust from the west by an oceanic plate and dominated by destructive margin magmatism now represented by



the plutons and volcanic sequences of the Sierra Nevada and the Klamath Mountains. (Burchfiel and Davis 1972, Hietanen 1973). Two major zones of thrusting related to this eastward subduction can be recognised in California; a pre-uppermost Jurassic zone in the western Sierra Nevada (Davis, 1969) and a younger zone in the coast ranges (Section 2.4). In the north-western Sierra Nevada, these Jurassic thrusts separate four westward younging belts of metamorphosed Palaeozoic volcano - sedimentary formations and, on the west, a relatively unmetamorphosed Jurassic belt, which includes the Smartville Block (Figure 2.3.1). All these belts are intruded by the post-kinematic Nevadan plutons. Schweickert and Cowan (1975) suggest that the Smartville Block is sandwiched, with thrust contacts, between two Jurassic island arc assemblages, one each to the east and west, and suggested that the Smartville ophiolite represents oceanic crust formed in an interarc basin. They postulated a west dipping subduction zone as well as the main east-dipping zone beneath the continental margin. At about 150 my. the subduction locus shifted westwards, initiating the underthrusting of the Coast Range ophiolite by the Franciscan (Section 2.4) and shortly thereafter the Sierra Nevadan plutonism.

It has been suggested by Menzies and Blanchard (1977), on the basis of RE geochemistry and lithology, that the lower part of the Smartville volcanic unit is composed of island arc tholeiites or, possibly, ocean-floor tholeiites, and is intruded and overlain by a calc-alkaline upper volcanic unit. The Ti-Zr-Y content of seven dolerites from the smartville dyke complex, which fed the volcanic unit, is more similar to that of ocean-floor tholeiites (Figure 2.3.4). In summary, the Smartville ophiolite probably

Figure 2.3.4 Trace element discrimination diagrams: Smartville ophiolite  
Dolerites from the dyke complex



Diagrams after Pearce and Cann 1973

represents ocean crust that was formed either at a spreading centre in a Jurassic interarc basin or possibly at a somewhat older, but still Mesozoic, mid-oceanic ridge and that subsequently became the basement to island arc volcanism. The Smartville Block was structurally defined during the Nevadan Orogeny and was then intruded by Nevadan plutons related to the Coast Ranges subduction zone. Therefore igneous rocks in the Smartville Block are the products of three phases of magmatism; at a spreading centre, in Early/Mid Jurassic island arcs and above a late-Jurassic/Cretaceous subduction zone. The plutonic products of each phase may be chemically well defined or have intermediate variation which makes identification difficult.

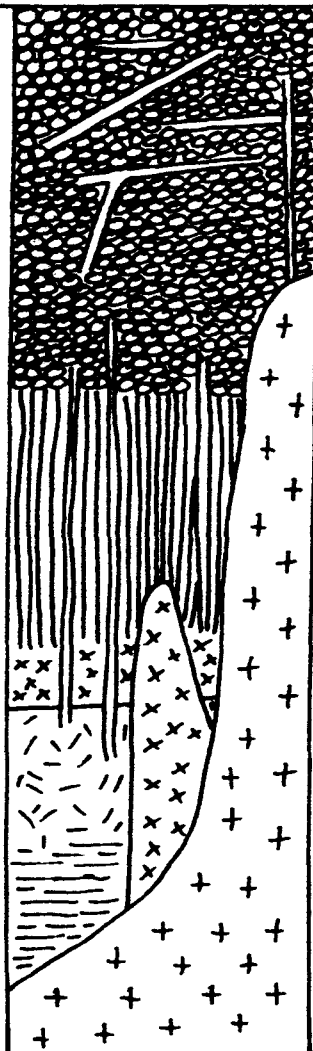
### 2.3.2 Field Relations and Petrography

#### 2.3.2.1 Introduction

For ease of description the Smartville ophiolite is divided into three units (Table 2.3.1). By analogy with complete ophiolites, it is assumed that these units formed a near-horizontal sequence before the Nevadan plutonism. The structure of the Smartville Block and geopotential indicators in the pillow lavas and cumulate gabbros are consistent with this interpretation. The maximum observed outcrop width in Dry Creek (Figure 2.3.3) of the volcanic unit is 5.6 km., the dyke complex 1.7 km. and the plutonic unit 4.4 km. There are three uncertainties in the calculation of their thickness; (i) the attitude of the units is imperfectly known (ii) most sections could be abbreviated or lengthened by faulting and

Table 2.3.1 Stratigraphy of the Smartville ophiolite

Unit	Thickness	
Volcanic Unit	4-5 km	UVU Waterlain tuff, breccia, lava sills and dykes
		LVU Pillow lava, tuffaceous sediment, interpillow chert and limestone. Volcanic breccia is more frequent at base. Sills and dykes
Dyke Complex	1-1.5 km	Dolerite with up to 10% microtonalite, felsite episodite and 1% orthoclase porphyry. Small epidote-quartz veins along dyke margins and joint planes.
Plutonic Unit	3-3.5 km	Hornblende gabbro with minor magnetite gabbro (2-3%) and layered pyroxene gabbro (10-15%) plagiogranite; Diorite and qz.diorite (10%), tonalite (60%) trondhjemite (30%)
'Nevadan' plutons		Calc-alkaline granodiorite, trondhjemite, tonalite, diorite and gabbro.



(iii) the upper boundary of the volcanic unit and the base of the plutonics are not seen. Field data suggest the volcanic unit dips southwest at about  $50^{\circ}$  and is therefore at least 4-5 km. thick. Assuming the same regional dip there is 1-1.5 km. of dyke complex which has less than 10% screens of extrusive or plutonic rock and on the same criteria 3-3.5 km. of plutonic rocks are exposed.

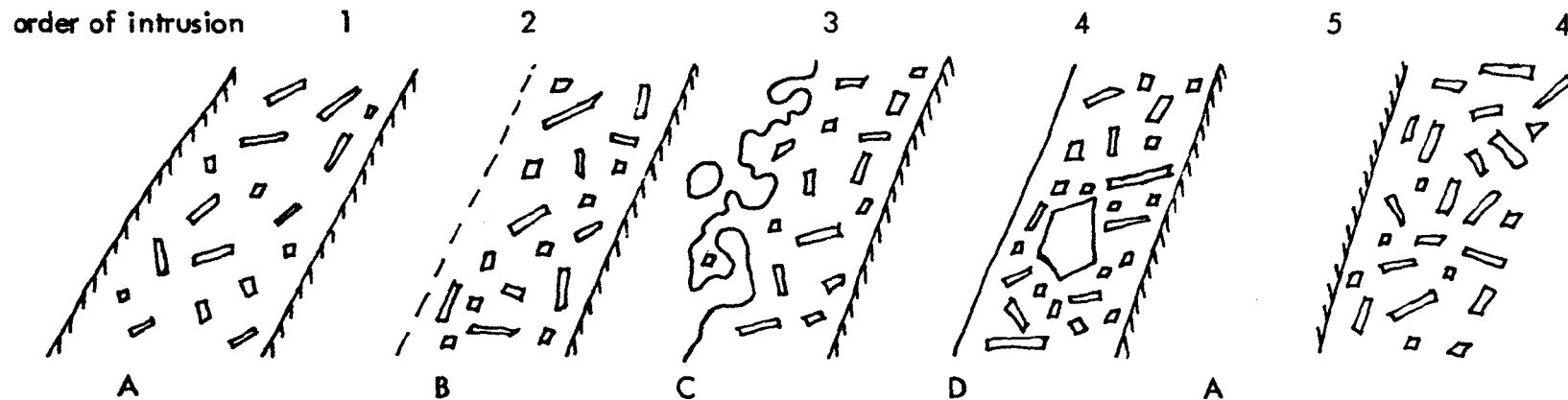
#### 2.3.2.2 The Volcanic Unit

The volcanic unit was divided into an upper (U.V.U) and a lower (L.V.U ) division on the basis of lithology (Table 2.3.1) and RE geochemistry (Section 2.3) by Menzies and Blanchard (1977). These divisions are not strictly analogous to the UPL and LPL of the Troodos Massif. Petrographic examination shows the lavas to be mainly basaltic (no analyses are available) and can be vesicular, aphyric or pyroxene and/or plagioclase phyrlic. They were metamorphosed under zeolite or green schist facies conditions, the metamorphic grade increasing down the sequence (Menzies et al., 1975). There is some stratabound copper-zinc sulphide mineralization in the western volcanic zone but, according to Menzies et al., (1975), this is associated with the calc-alkaline suite beyond the bounding fault zone.

#### 2.3.2.3 The Dyke Complex




The dyke complex is composed of dykes which either intrude other dykes or invade massive (structureless) dolerite. It's top and bottom boundaries are gradational, having screens of volcanic rock at the top and of plutonic rock at the base.

Figure 2.3.5 Schematic of dyke complex - Variation in intrusive phenomena in multiple dykes in Smartville ophiolite



- A - Brittle fracture with chilling
- B - No fracture, compositional gradation
- C - No fracture, liquid / liquid mixing
- D - Brittle fracture, no chilling

Not to scale

 Chilled margin  
 Non-chilled margin  
 Gradational margin



 Aphyric dolerite or felsite  
 Porphyritic dolerite or felsite

Table 2.3.2 Summary of petrography of the dyke complex

Rock Type	Primary Petrography	Alteration
Plagio-granite	Pl, qz, hnd. <u>Acc</u> Op. Med. to fine ground mass with complexly zoned enhedral pl phenocrysts, up to 2mm. Rare Qz phenocrysts. Some aphyric felsites with flow banding and orbicular texture.	Ab, ep, cz, sph, act and/or hnd, chl, some cal. Pl phenocrysts are turbid and replaced by cz. Ep is interstitial in clusters or veins.
Orthoclase Porphyry	Pl, Or, qz, hnd. <u>Acc</u> Op, biot. Pl and Or phenocrysts in med. to fine ground mass strongly zoned in some specimens, unzoned in others.	As plagiogranites but generally less intense.
Dolerite	Pl, cpx, hnd. <u>Acc</u> Op, qz, opx, sph. Med. to aphanitic. Usually pl + cpx or pl phyrlic, some aphyric. Weak flow structures.	As above but with some ha or py. Late fractures infilled with ep, qz, py. Epidosite also occurs.

Occasional dykes are found throughout the rest of the ophiolite. However, the features described in the following paragraphs are the same whether the dykes intrude volcanic, plutonic or hypabyssal material.

The strike of the dykes varies between  $310^{\circ}$  and  $040^{\circ}$  and most dip at moderate to steep angles to the east. Later intrusives frequently crosscut early ones at a high angle, indicating variable regional stress during magmatism. (This contrasts with the occasional weak transgressions in the S.I.C.s of the Troodos Massif and the Semail Nappe). The dykes are usually planar, up to 3m thick, but late narrow sinuous dolerites also occur.

The splitting of early dykes by later ones is commonplace, subsequent dykes forming chilled margins against the usually coarser interiors of their host. The various petrographic types in the dyke complex are described in Table 2.3.2. Acidic dykes are mostly confined to the Dyke Complex and also crosscut plagiogranite. They are typically plagioclase phyrlic and a few also have quartz phenocrysts. The rarer orthoclase porphyrys (two feldspar porphyrys) form dykes up to 10 metres thick, intrude plagiogranite, the dyke complex or the volcanic unit. They have strongly chilled, often aphyric, margins. This type of dyke is usually the last in the intrusive sequence although one example is crosscut by a late dolerite. Although the orthoclase porphyrys are altered in the same manner as the plagioclase porphyrys, their primary petrography and field character set the group apart.



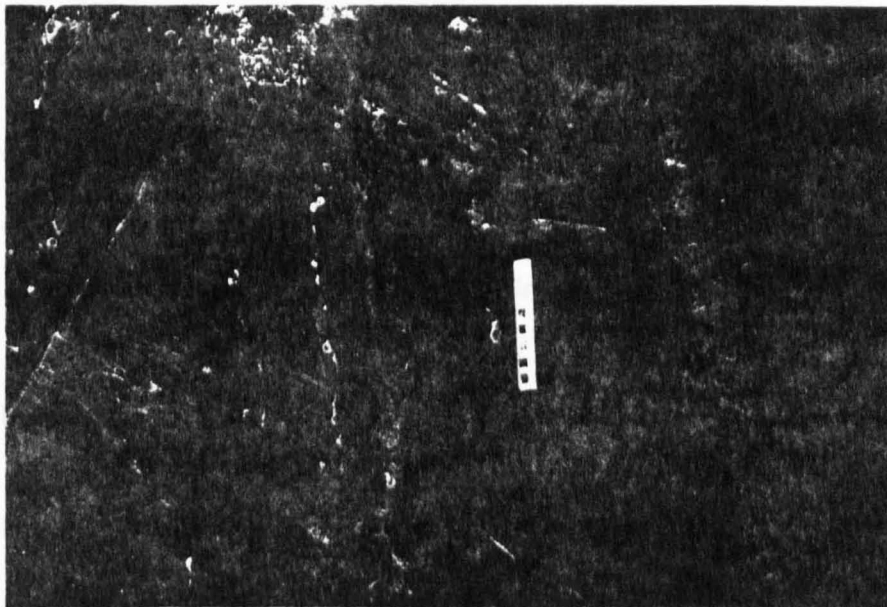


Plate 19 Single and multiple dykes in microgabbro, Dry Creek, Smartville Block. Liquid /liquid contact to left of hammer. Scale is 10cm. long.

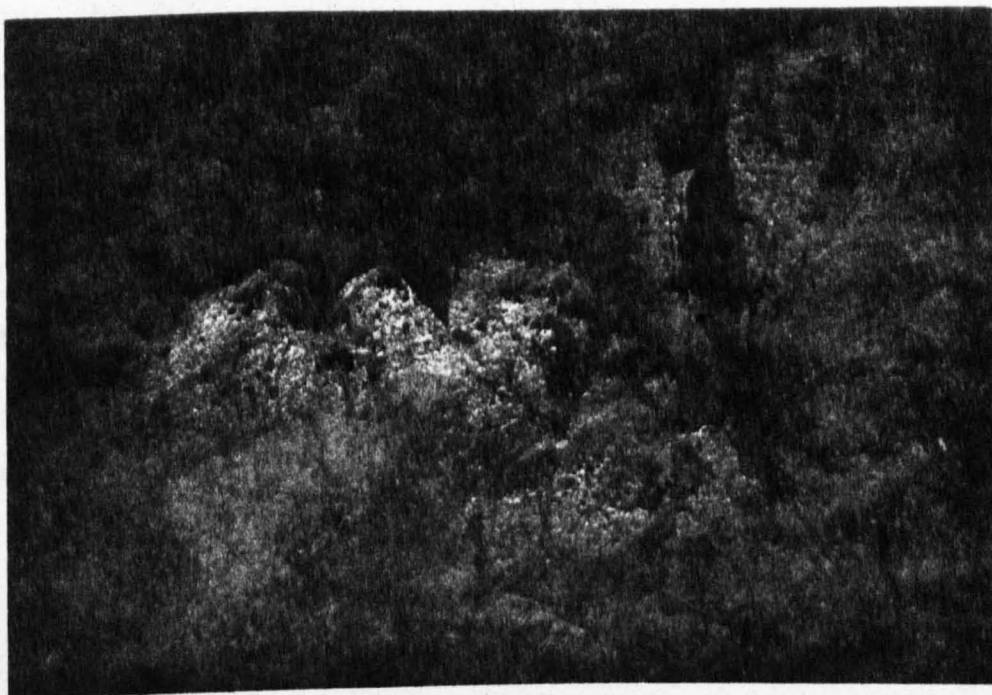


Plate 20 Flow-folded layered pyroxene gabbro, Dry Creek, Smartville Block. Scale on hammer is 10cm. long.

#### 2.3.2.4 The Plutonic Unit

The plutonic rocks within the Smartville Block fall into two groups; those which were formed before the Nevadan orogeny (the ophiolite Plutonic Unit) and the post-kinematic "Nevadan" plutons. The latter will only be described briefly.

The ophiolite Plutonic Unit consists of gabbro and plagiogranite, the latter in relatively small bodies, up to about 1 km. across. Screens of plagiogranite and gabbro make up a small fraction of some outcrops of the dyke complex and the proportion of plutonic rock generally increases downwards until the dykes are very widely spaced. Thus the boundary between the dyke complex and the plutonic unit appears to be gradational but some sections are fault-shortened and critical parts of others are unexposed. The available evidence suggests that the plutonics intrude the dyke complex upwards and sideways and then are often themselves intruded by later dykes. (Section 2.1.2.5). Only mild contact metamorphism is seen but dolerite xenoliths in all stages of assimilation are numerous. Fine grained plagiogranites are common but it is not clear whether some of these are the chill facies of larger bodies or if they are all small intrusions. Gabbro is definitely observed chilling on dolerite. In some instances, plagiogranite passes laterally into varitextured gabbro over a few metres, in others plagiogranite intrudes gabbro. It is not possible to determine the size and shape of these small plutons with any certainty because exposure is so poor away from stream and road sections.

Table 2.3.3 Summary of petrography of the plutonic complex

Rock Type	Primary Petrography	Alteration
Pyroxene gabbro	Cpx, opx, pl. <u>Acc</u> Op, Hnd. Med. grained, homogeneous or, rarely, with aligned pl or compositional layering. All phases euhedral to anhedral.	Pyx and hnd rimmed or replaced by fibrous amph, which is pale green, blue green or browngreen and often encloses op. Sph replaces op, often along exsolution lamellae.
Hornblende gabbro	Hnd, pl. <u>Acc</u> cpx, op, qz. Coarse to fine. Homogeneous or Varitextured with pegmatite veins, leucocratic and quartz-rich patches. Hnd is green or brown. Occ. pl phenocrysts. Pl is frequently zoned.	Saus. and cz after pl, often in cores only. Some chl.
Magnetite gabbro	Hnd, pl, op. <u>Acc</u> qz, cpx. Coarse to medium grained. Op can be euhedral or anhedral with or without inclusions of pl. and amph.	

Table 2.3.3 continued

Rock Type	Primary Petrography	Alteration
Diorite, Qz diorite, tonalite trond- hjemite	Variable proportions of pl, qz, hnd. <u>Acc</u> Op, ap, sph, zrc. Rare Or, biot. Can be homogeneous or not. Euhedral or subhedral zoned pl. Interstitial granophyre common. Hnd. subhedral. Qz anhedral.	Ab, cz, ep, act, sph. Ab and saus after pl, which is also partly replaced by cz. Ep in aggregates or single grains. Aggregates of fibrous act. after hnd, pale green, green brown, blue green, often encloses op. Sph after primary op.
Leuco- diorite	Pl. <u>Acc</u> Qz, cpx, hnd, sph. Very leucocratic veins. Straight and sharp-margined up to 20 cm. thick	Chl after amph. Some cal. Occassional brittle deformation
<u>In situ</u> veins	Pl, hnd, qz. <u>Acc</u> Op, cpx, sph, ap, zrc. Euhedral, strongly zoned pl. Accessories can be med. grained and plentiful. Veins up to 2m. long, 30cm thick.	
Epidosite	Remnant primary minerals (Plagio granite or dolerite)  Intensity of epidotization varies but can completely replace primary assemblage.	Ep, qz, sph, some cz, hnd, chl.

There are three mineralogical and three textural varieties of gabbro. The dominant mafic mineral can be hornblende or pyroxene (although both are normally present) and the hornblende gabbros can also have a large proportion (up to 10%) of opaque minerals. The gabbros are usually fairly homogeneous but can also be varitextured or, rarely, layered. The varitextured gabbros are remarkably similar to those described from Cyprus and the Oman. They are only found close to outcrops of the dyke complex and have variable grain size, leucocratic or melanocratic patches and are crosscut by some gabbro pegmatite veins. The varitextured gabbros also have in situ leucocratic, quartz-bearing veins with diffuse, pegmatitic margins and are crosscut by sharp-margined feldspathic or plagiogranite veins.

Layered gabbro crops out at few localities. The best examples occur in isolated roadside exposures to the east of Dobbins and their relationship to the remainder of the ophiolite is unknown. These are medium grained cumulate pyroxene gabbros with very strong compositional layering. Cumulate ultramafic material crops out nearby (Menzies et al., 1975). Weak layering, probably also of cumulate origin, occurs in Dry Creek, south of Collins Lake. Thin, widely spaced mafic layers persist over many metres and are locally deformed, presumably by flow. (Plate 20). They are crosscut by pegmatite gabbro veins. However, these rocks contain intercumulus primary amphibole and magnetite, unlike the cumulates at Dobbins and those of the Troodos Massif.

Completely unmetamorphosed gabbros are rare but gabbros that outcrop furthest from the dyke complex are generally the least altered, consistent with the depth control on metamorphism observed in the volcanics. Both pyroxene and primary hornblende

are usually rimmed or completely pseudomorphed by fibrous secondary amphibole which often encloses fine grained opaques.

Plagiogranite occurs as (i) screens in the Dyke Complex or in massive intrusions, (ii) dykes in both plutonic and hypabyssal formations, (iii) thin sharp margined veins crosscutting the plutonic unit and (iv) diffuse-margined in situ veins in varitextured gabbro. There are two types of massive plagiogranite intrusions - early and late formed. The early ones crop out between the dyke swarm and the gabbro and are crosscut by numerous dykes. The later ones are stocks intruding gabbro or the volcanic unit and are crosscut by only a few dykes. One example is invaded by an irregular body of orthoclase porphyry.

The same rock types (diorite, quartz diorite, tonalite, trondhjemite, quartz albitite and epidosite) appear in both early and late intrusions. However, those types with the rare accessory orthoclase only occur in late-formed bodies. Hornblende is the most common primary mafic mineral and biotite occurs only very rarely. Many plagiogranites have a particular type of granophyric texture. Zoned, euhedral plagioclase is set in a halo of radial plagioclase/quartz intergrowth. The intergrown plagioclase is in optical continuity with the sodic outer zones of the euhedral grain and the intergrown quartz frequently passes into an anhedral quartz grain. The same texture is found in medium and fine grained rocks. As the quartz is never seen to overlap the euhedral outline of the plagioclase grain it can be inferred that this texture is primary and represents crystallization on the plagioclase/quartz cotectic. Indeed, secondary quartz is not common in the plagiogranites. Granophyric textures are not found in sharp-marginal veins, the "Nevadan" plutons,

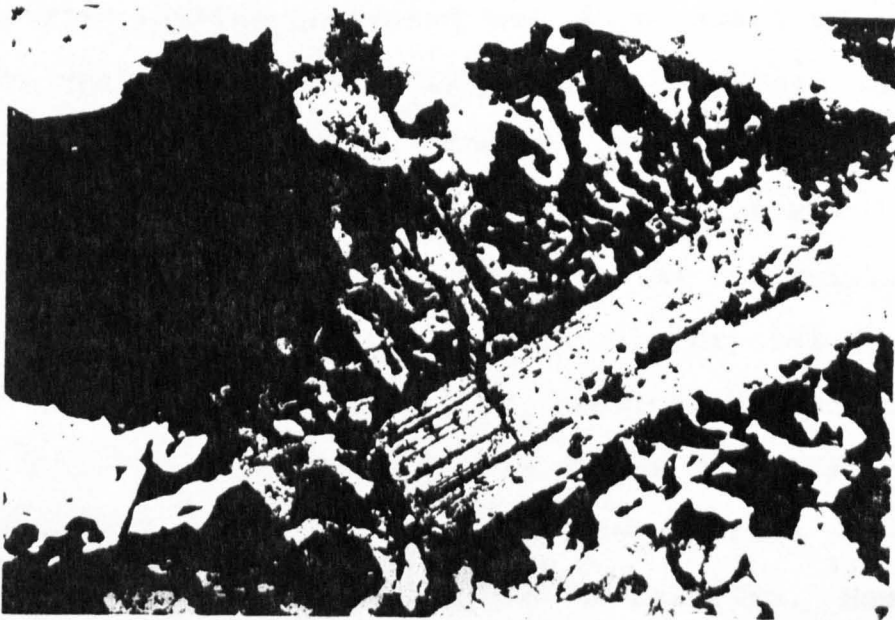
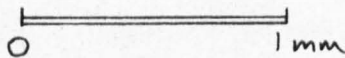


Plate 21 Primary granophyre in trondhjemite.  
Intergrown feldspar is continuous with euhedral  
grain and intergrown quartz(extinct)is continuous  
with grain to left. (x-pols)



orthoclase porphyrys or plagiogranites with accessory orthoclase.

No plagiogranite remains unaltered and, in contrast to the gabbros, feldspars are never wholly pellucid. Epidote and chlorite are much more plentiful than in the gabbros but, as usual in plagiogranites, secondary mineralogies are imperfectly developed. Some plagiogranites at Smartville have limited brittle deformation, manifest by crystal fracture and recrystallisation, mortar texture, undulose extinction in quartz and deformed cleavages and twin planes in feldspar. The primary mafic mineral has been fractured, strung out and synkinematically replaced by actinolite or chlorite. However, post kinematic epidote grains and epidote veins parallel to the deformation fabric are also found.

Massive (undyked) epidosite crops out in South Honcut Creek, close to the western edge of the Block, where it is faulted against the volcanic unit. Remnant primary mineralogy, trace element geochemistry and field relations show that the epidosite formed from a plagiogranite which intruded or possibly passed gradationally into the epidote free varitextured gabbro upstream. The epidosite is very inhomogeneous, epidote is often patchily developed and the rock encloses swarms of rounded and angular basic xenoliths. The growth of epidote was preceded by the replacement of plagioclase by secondary quartz which often nucleates upon granophyric intergrowth.

The diffuse margined veins (leucocratic quartz diorites or trondhjemites) are not common and nowhere achieve the density found in the segregation gabbros of the Troodos Massif. They have irregular margins which grade rapidly into a pegmatitic fringe and then into the gabbro host and they have no feeder



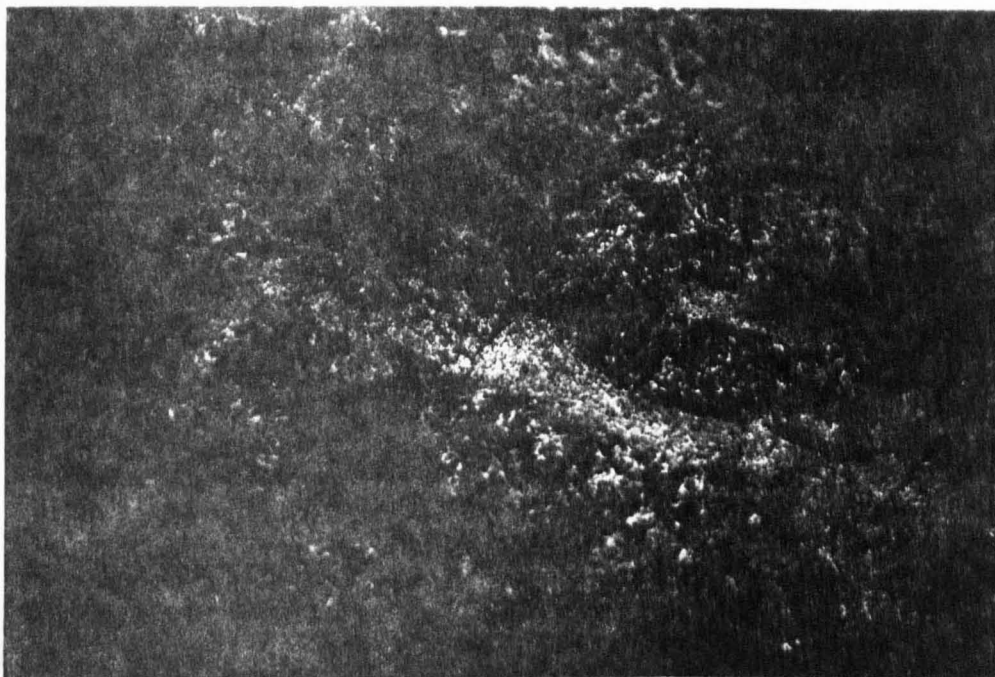


Plate 22 Intrusive trondhjemite vein in varitextured gabbro, Dry Creek, Smartville Block. Note epidote on joint plane, only. Lenscap is 5cm. diameter.

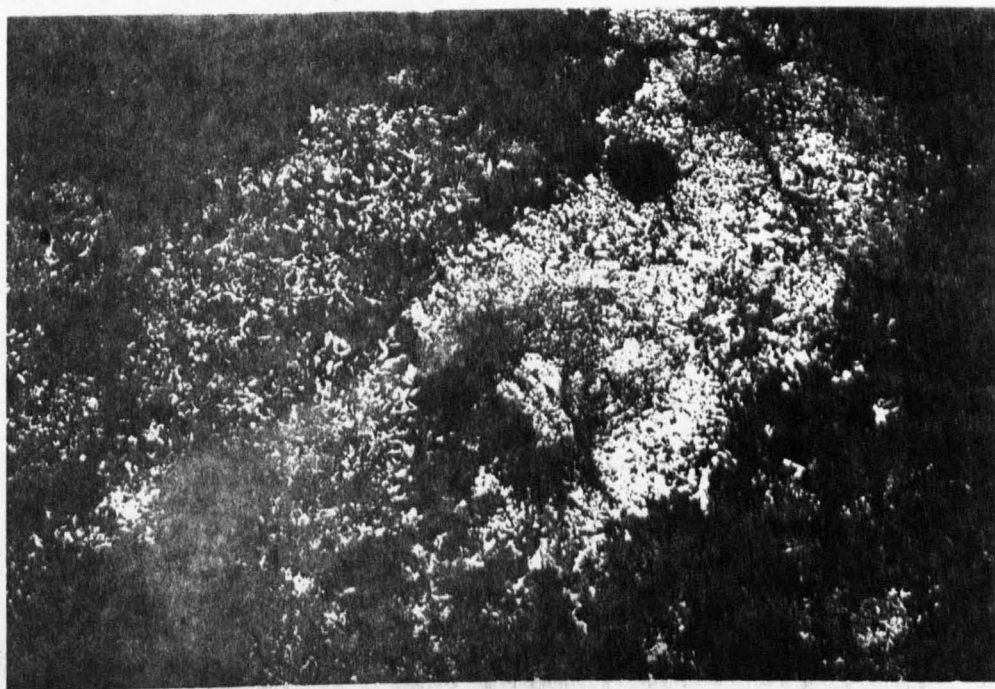


Plate 23 In situ tonalite vein in varitextured gabbro, Dry Creek, Smartville Block. Lens cap is 5cm. diameter.

or vent, which suggests they were formed in situ. In contrast to their host, they have euhedral feldspar, quartz and, often, plentiful sphene or other accessories. They also tend to be more intensely altered and to develop clinozoisite where this mineral is absent from the host. One feldspathic specimen has an abnormally high content of  $Al_2O_3$  and CaO, representing an accumulation of plagioclase.

The sharp-margined veins fall into two groups. The first are microgranite or felsite and are clearly fine grained equivalents of the plagiogranites in the larger intrusions. The second are leucocratic diorites which are sparse and mostly intrude gabbro. The sharp margined veins have all undergone brittle deformation. Some examples have a macroscopic planar fabric parallel to the vein margins but the deformation is invariably confined to the vein.

#### 2.3.2.5 The 'Nevadan' Plutons

These large intrusions represent the final phase of magmatism in the area. They belong to a group of late Jurassic plutons of calc-alkaline affinity which intrude the metamorphosed palaeozoic rocks to the north and east of the Block. (Hietanen 1973) This group lies about 40 km. west of the northern part of the main Sierra Nevada batholith.

The plutons are typically several kilometres across and are mesoscopically homogeneous. They cut right across the ophiolite sequence and have wide metamorphic aureoles (Menzies et al., 1975). Complex net veining, with swarms of xenoliths, occurs at the margins. Although a few microgranites and aplites

crosscut the plutons no dolerites or orthoclase porphyrys do so. The rock types range from gabbro to trondhjemite and granodiorite but differ from the plutonic unit of the ophiolite in many ways (Table 2.3.4). However, it must be noted that a single criterion is usually insufficient to make the distinction.

Table 2.3.4 Comparison of 'Nevadan' and Ophiolite

plutonic bodies

	<u>Property</u>	<u>Ophiolite</u>	<u>'Nevadan'</u>
1.	Size	Up to 1 km across	several km across
2.	Homogeneity	Inhomogeneous	Usually Homogeneous on outcrop scale
3.	Intruded by dolerite dykes	Often	Never
4.	Rock Types	Gabbro, Quartz- Diorite, Tonalite, Trondhjemite, orthoclase porphyry	Granodiorite, tonalite, trond- hjemite, quartz- diorite, gabbro
5.	Grainsize	Fine — Medium	Medium — Coarse
6.	Primary Mafic	Hornblende with very rare biotite	Biotite with hornblende
7.	Granophyric intergrowth	Common	Absent
8.	K-feldspar	Rarely present, in small amounts	Usually present in small amounts
9.	Alteration	Always	Occasionally
10.	Chemistry (Section 2.3.3)	Low $\text{Al}_2\text{O}_3$ and very low $\text{K}_2\text{O}$ High K/Rb	High $\text{Al}_2\text{O}_3$ and moderate $\text{K}_2\text{O}$ Moderate K/Rb

### 2.3.3 Geochemistry

#### 2.3.3.1 Introduction

The range in abundance of the major and minor oxides is summarised in Table 2.3.5 and their distribution relative to  $\text{SiO}_2$  in Figure 2.3.6. The trace elements are likewise represented in Table 2.3.6 and Figure 2.3.7. With two exceptions, discussed below, the 29 whole rock analyses indicate the suite is geochemically compatible.

#### 2.3.3.2 Metasomatic variation

As described in the previous section, all the igneous rocks in the Smartville Block, except the "Nevadan" Plutons, have been metamorphosed to hydrous assemblages. By analogy with the effects of hydrothermal metamorphism on similar suites (Sections 2.1.4.2; 1.2.), it seems possible that metasomatic alteration accompanied that metamorphism. The chemical distributions were examined for the effects of metasomatism on the entire suite and on individual specimens before the magmatic trends were considered. Unfortunately, very few fresh specimens were found and so it is not possible to compare fresh and altered specimens of similar original chemistry. However, there is a range in the degree of mineralogical alteration among the altered specimens and so metasomatism also varies in intensity. There is a positive correlation of  $\text{SiO}_2$  and immobile incompatible traces (Zr, Y) and only one specimen, an epidosite, is clearly secondarily enriched in silica. The background scatter of values about the trend could be primary or secondary, or both. The strong correlation

Table 2.3.5 Ranges of abundance of major elements,

by rock type

	Magnetite Gabbro	Gabbro	Dolerite	Quartz Dioritic <u>Insitu</u> vein
No.Specimens	1	4	10	2
SiO <sub>2</sub> Wt%	44.9	47.6-54.8	46.3-56.6	64.1-61.6
TiO <sub>2</sub>	3.2	0.3-1.4	0.7-2.3	0.9-0.7
Al <sub>2</sub> O <sub>3</sub>	9.7	12.5-20.8	13.1-15.2	14.9-17.3
Fe <sub>2</sub> O <sub>3</sub> *	17.1	5.8-10.8	9.8-12.7	2.2-5.9
MnO	0.21	0.07-0.15	0.16-0.3	0.06-0.08
MgO	8.7	6.4-12.1	4.6-10.6	2.8-0.9
CaO	12.2	8.3-16.7	4.4-12.3	8.4-4.5
Na <sub>2</sub> O	1.9	1.0-3.9	1.7-5.8	4.6-7.4
K <sub>2</sub> O	0.14	0.05-0.19	0.06-0.38	0.48-0.08
P <sub>2</sub> O <sub>5</sub>	0.09	0.01-0.18	0.08-0.44	0.02-0.18
	Tonalite	Trondhjemite	Epidosite	Orthoclase 'Nevadan' Porphyry Gabbro
	3	4	1	2 2
SiO <sub>2</sub>	59.7-69.1	65.8-74.2	76.4	71.1-71.5 50.4-50.3
TiO <sub>2</sub>	0.6-1.0	0.2-0.7	0.4	0.2-0.3 0.9-1.0
Al <sub>2</sub> O <sub>3</sub>	13.9-15.6	13.4-14.4	10.5	14.4-14.1 17.4-17.4
Fe <sub>2</sub> O <sub>3</sub> *	4.6-8.7	3.3-6.9	4.1	3.0-3.8 10.1-10.4
MnO	0.1-0.19	0.03-0.14	0.06	0.08-0.15 0.17-0.19
MgO	0.3-3.9	0.1-1.2	1.0	0.3-0.2 6.1-5.48
CaO	1.8-5.2	2.1-3.4	6.3	0.9-1.6 11.5-11.03
Na <sub>2</sub> O	5.6-7.1	5.6-8.0	2.6	4.4-6.6 2.2-2.7
K <sub>2</sub> O	0.12-0.71	0.04-0.13	0.11	5.3-1.33 0.51-0.59
P <sub>2</sub> O <sub>5</sub>	0.06-0.31	0.01-0.16	0.06	0.03-0.04 0.23-0.42

Table 2.3.6    Ranges of abundance of trace elements,  
by rock type

No. Specimens	Magnetite		Dolerite 10	Insitu vein	
	Gabbro 1	Gabbro 4		2	
Zr, ppm	30	19-174	41-288	237	728
Y	17	5-41	14-63	49	48
Nb	2	<1-4	1-9	15	<1
Cr	31	12-295	6-534	9	3
Ni	<1	11-107	<1-157	242	195
Ba	87	12-76	53-142	151	157
Rb	2	<1-2	<1-5	6	<1
Sr	142	167-173	159-311	7	4
Zn	82	15-56	23-207	5	14

No. Specimens	Tonalite	Trondhjemite	Epidosite	Orthoclase Porphyry	'Nevadan' Gabbro
	3	4	1	2	2
Zr	148-322	345-628	281	456 367	62 46
Y	43-61	69-95	34	78 66	17 25
Nb	4-13	9-17	6	13 9	2
Cr	4-7	<1-9	7	2 5	67
Ni	<1	<1	1	<1	18
Ba	155-461	55-148	56	543 333	168 218
Rb	<1-8	<1	2	42 11	10 11
Sr	89-236	74-207	189	81 78	284 295
Zn	13-43	7-28	13	22 45	63 69

between  $\text{TiO}_2$  and  $\text{SiO}_2$  in the intermediate and acid specimens confirms that there has been little secondary change in silica content in these rocks (Figure 2.3.6). The epidosite also has a very low aluminium content. In the two specimens which have lost iron, the opaque phases are extensively replaced by sphene. MnO varies in proportion to total iron and is depleted in the same two specimens. Two other dolerites are possibly enriched in MnO, relative to iron. The range in sodium content increases with differentiation, enhanced  $\text{Na}_2\text{O}$  values accompanying albitisation of the plagiogranites and the epidosite being strongly depleted in  $\text{Na}_2\text{O}$ . The distribution of potassium is problematic. The very low level of potassium in the majority of specimens could be explained by extensive leaching during metamorphism. However, no remnants or pseudomorphs of K-rich phases are observed in thin section in the K-poor plagiogranites. Indeed, the orthoclase prophyrys have much larger  $\text{K}_2\text{O}$  values although they, too, have been saussuritised, albeit mildly. Therefore, it seems most probable that the abnormally small abundance of  $\text{K}_2\text{O}$  in the tonalites and trondhjemites is primary, with only minor secondary modification. This interpretation is supported by the Ba data. Only four of the analysed plagiogranites are seriously depleted in Ba; one of those is the epidosite and two others are enriched in  $\text{Na}_2\text{O}$ . Although the remaining plagiogranites also have very low  $\text{K}_2\text{O}$  values they have not suffered major secondary LIL depletion. (Figure 2.3.6) Sr values are scattered but there is no consistent "alteration trend". The distribution of MgO, CaO,  $\text{P}_2\text{O}_5$ , Ni, Cr and Zn shows no variation that can be attributed to metasomatism. In summary, the epidosite is the only single



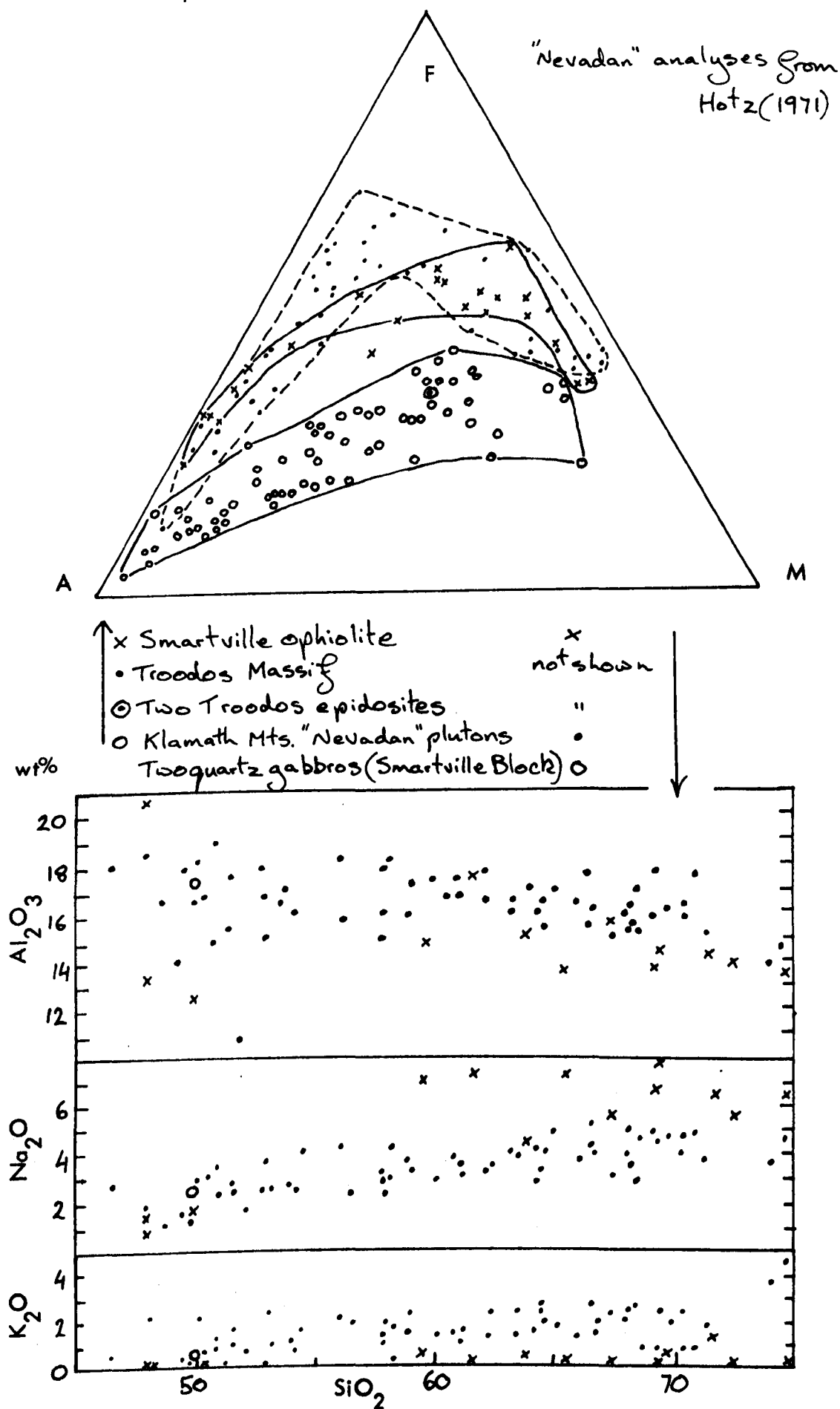
specimen which has suffered sufficient metasomatism to alter its primary geochemistry in an unequivocal way. It has lost Al, Fe, Mn, Na, K and Ba and gained Si, Ca and Sr. Other samples, with greenschist or amphibolite assemblages, have been enriched in  $\text{Na}_2\text{O}$  but with the exception of Sr, metasomatic alteration does not obscure the primary geochemical distribution.

#### 2.3.3.3 The geochemistry of the Nevadan plutons

It was noted previously that the Smartville Block has been intruded by several late Jurassic plutons, which contrast with the other formations in the Block. Geochemically, there are three possibilities; (i) the Nevadan plutons may be chemically distinct from the ophiolite, they may have (ii) partial or (iii) complete compositional overlap.

According to Hotz (1971) the plutonic rocks of the Klamath Mountains in northern California are similar in composition and age to those in the western Sierra Nevada (including those in the Smartville Block) and are considered by him to be related. Both groups are more sodic than the younger intrusives in the east and central Sierra. Of course, many major element variation trends and abundances are similar in any suite ranging from gabbroic to granitic compositions but some differences were found. The most obvious is shown on the AFM diagram (Figure 2.3.9). The Klamath Plutons follow a typical calcalkaline trend whereas the Smartville analyses fall on a trend of initial iron enrichment which is characteristic of tholeiitic suites (Carmichael et al., 1974 p. 568 and p. 478). These trends are mimicked by the distribution of  $\text{TiO}_2$ . The two

Figure 2.3.9 Comparison of major oxide content of ophiolite and 'Nevadan' plutonic rocks



suites also have different abundances of  $\text{Al}_2\text{O}_3$ . Nearly all the Klamath suite have greater than 15%  $\text{Al}_2\text{O}_3$  whereas the majority of the Smartville analyses fall between 15.5% and 13%  $\text{Al}_2\text{O}_3$ , (Figure 2.3.9). Also, most of the Klamath rocks are more potassic, for a given silica content, than most of the Smartville suite, although the distinction is not so marked as with  $\text{Al}_2\text{O}_3$ . The Smartville plagiogranites are more sodic than the calcalkaline granitic rocks.

Only two specimens were analysed which were obviously from one of the Nevadan plutons, both quartz gabbros. Although insufficient to define a trend on any variation diagram their content of  $\text{Al}_2\text{O}_3$  and  $\text{K}_2\text{O}$  is closer to that of the Klamath suite. They also have distinctly lower  $\text{MgO}$  than the other gabbros. No other specimens have high  $\text{Al}_2\text{O}_3$  and high  $\text{K}_2\text{O}$ , suggesting that none of those assigned to the ophiolite suite on petrographic grounds has a "Nevadan" chemistry.

Unfortunately, no trace element data are available from the northwest Sierra or the Klamaths but a comparison of Rb, Ba and Sr values reveals that the two "Nevadan" quartz gabbros are strongly enriched in these elements relative to most of the ophiolite including most of the plagiogranites and have lower K/Rb ratios (Table 2.3.7). These elements are very sensitive to alteration and although the two quartz gabbros are very fresh, the others have slightly or moderately saussuritised feldspars and these few data must be treated with caution.

Table 2.3.7 Potassium and Rubidium

Rock Type

(Alteration)

<u>'Nevadan'</u>	<u>K<sub>2</sub>O%</u>	<u>Rb ppm</u>	<u>K/Rb</u>
Quartz Gabbro SM23 (Fresh)	0.51	10	423
Quartz Gabbro SM91 (Fresh)	0.59	11	445
<u>Ophiolite</u>			
Orthoclase Porphyry SM15 (Mild alteration)	5.32	42	1051
Orthoclase Porphyry SM57 (Moderate)	1.33	11	1004
Tonalite SM56 (Moderate)	0.85	6	1176
Tonalite SM48 (Moderate)	0.71	8	737

N.B. (1) All other analysed specimens have less than 0.5% K<sub>2</sub>O and less than 6 ppm Rb (2) SM57 intrudes SM56

#### 2.3.3.4 Primary Geochemistry

The distribution of  $\text{TiO}_2$  is highly significant in the geochemical evolution of the ophiolite. There are two quite different trends;  $\text{TiO}_2$  increases strongly in the dolerites but then decreases with further differentiation in the plagiogranites (Figure 2.3.6). Among the basic rocks, the gabbros (with one exception) have the lowest abundance of  $\text{TiO}_2$ , followed by the porphyritic dolerites than the aphyric ones. This indicates that most of the gabbros represent a cumulate or, at least, a non-liquid composition. Similarly, the liquid composition of the porphyritic dolerites groundmass has been somewhat diluted by their (non-titaniferous) phenocrysts. Steadily increasing  $\text{TiO}_2$  (and total iron) amongst the dolerites shows that the basic magma was not fractionating Fe Ti oxide. However, the magnetite gabbro, SM63, is dramatically enriched in  $\text{TiO}_2$  (and total iron) although it's content of  $\text{SiO}_2$  and incompatibles resembles that of other gabbros. The high proportion of opaque minerals in the rock leaves no doubt it has accumulated Fe Ti oxide. The evolution of the intermediate and acidic rocks starts with the onset of Fe Ti oxide fractionation.

Amongst the other major element variation trends the following points are significant. Total iron follows the same pattern as titanium. Like iron, phosphorous increases amongst the basic rocks and then reverses trend amongst the plagiogranites (Figure 2.3.6) indicating fractionation by apatite.  $\text{Mn}^{2+}$  substitutes for  $\text{Fe}^{2+}$  and so is distributed in a similar way to total iron. However, the magnetite gabbro, strongly enriched in iron and titanium, has the same MnO content as the other

gabbros. Moreover, MnO undergoes continuous depletion with differentiation. It can be inferred that  $Mn^{2+}$  does not enter Fe Ti oxides to a significant extent, compared to pyroxene and, perhaps, amphibole. Zn, which follows total iron and MnO reasonably closely, is moderately enriched in the magnetite gabbro and so appears to be accepted by both the oxide and inosilicate lattices. MgO decreases with differentiation but there is a large range in MgO values at low levels of  $SiO_2$  and vice versa. The distribution patterns of Cr and Ni are similar to that of MgO but their form is exaggerated.

Judging by these data, the plagiogranites evolved from a magma which had already been strongly depleted in MgO, Cr and Ni, presumably by removal of olivine and pyroxene. The low abundance of Cr and Ni in the magnetite gabbro and the overall Cr-Ti distribution suggests very limited entry of Cr and Ni into Fe Ti oxide. The range to high values of MgO and Cr is due to variable accumulation of pyroxene. Thus the gabbros, which have the composition of crystal mushes, and two clinopyroxene - phyric dolerites are strongly enriched in Cr relative to their presumed parent magma. However, the evolving magma is rapidly depleted in this element and even basic rocks with moderate MgO contain very little Cr or Ni.

The common occurrence of clinopyroxene and plagioclase as phenocrysts in the dolerites affirms that they are fractionating phases in the basic magmas. A fresh pyroxene gabbro, SM74, has very high  $Al_2O_3$ , high CaO and a very low content of incompatible elements and so appears to have accumulated plagioclase. The other trace element - impoverished gabbros are also rich in CaO but are magnesian rather than aluminous,

indicating their composition is dominated by cumulus clinopyroxene instead.

Only broad generalisations can be made about the primary distribution of strontium. Predictably, it decreases with differentiation. Relative to CaO, its distribution pattern has an inflexion. (Figure 2.3.8)  $\text{Sr}^{2+}$  enters  $\text{Ca}^{2+}$  sites in plagioclase but not in pyroxene (Taylor 1966) and so the sharp downward trend amongst the plagiogranites is consistent with a strong increase in the proportion of plagioclase crystallizing.

Zr increases steadily in abundance from the gabbros to dolerites to tonalites and finally to trondhjemites and orthoclase porphyrys. It correlates closely with Y and Nb but Zr/Y increases somewhat with differentiation and a few points deviate from the main Zr-Y distribution trend. Cross-reference to Nb-Zr and Nb-Y diagrams reveals both Zr and Y values which do not conform to the trend, probably due to Y entering Ca sites in apatite or possibly hornblende and sphene (Lambert 1974) and Zr entering zircon. For instance, two dolerites which have slightly high Y/Zr (Figure 2.3.8) also have a relatively high phosphorous content. It is likely that they contain cumulus apatite which nucleated early and fractionated both elements.

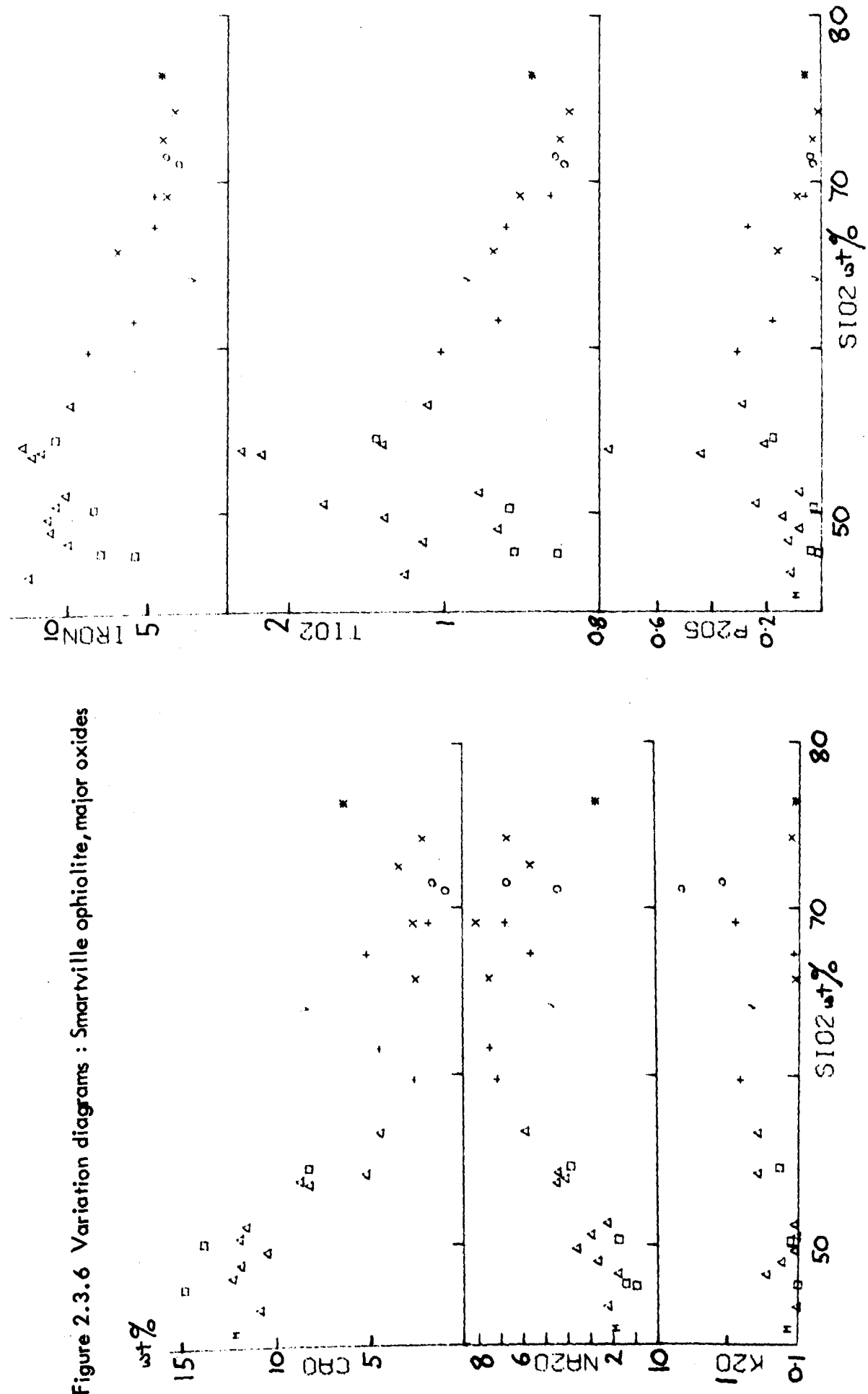
The granitic rocks that contain significant amounts (greater than 0.5%) of  $\text{K}_2\text{O}$  are all late formed plagiogranites and orthoclase porphyrys. Rb closely follows potassium and is generally present at very low levels (but up to 42 ppm in one orthoclase porphyry). Ba is theoretically captured by K-rich

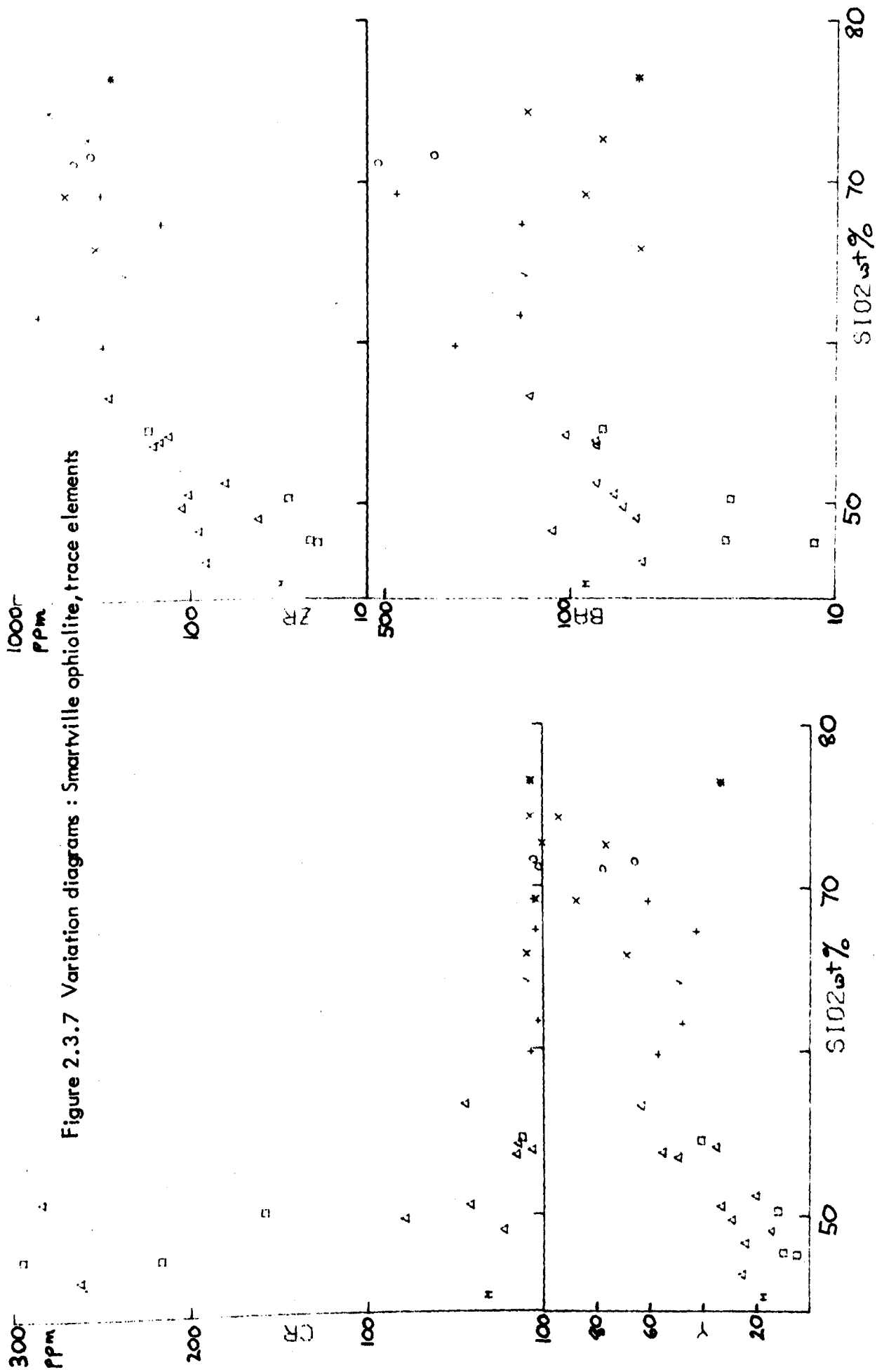
minerals and so should correlate with  $K_2O$ . The few rocks with modal orthoclase are rich in Ba but in the rest Ba is roughly in proportion with  $Na_2O$  instead and only present in moderate amounts. (Figure 2.3.8). In the absence of orthoclase, Ba is accommodated by albite.

It is now possible to consider if the plutonic rocks of the Smartville Block represent three phases of magmatism, as suggested at the end of Section 2.3.1, or only two. The "Nevadan" plutons can be unequivocally distinguished as the final episode, on field, petrographic and chemical criteria. (Table 2.3.4) Of the remainder, the orthoclase porphyrys have high K/Rb ratios, field relations and a style of mineralogical alteration which separate them from the Nevadan plutons. Their alkali element content is higher than any of the plagiogranites although porphyrys and plagiogranites cannot be distinguished by any other chemical criteria. Similarly, the late plagiogranites tend to be richer in alkalis than the early ones. At the one locality where orthoclase porphyry invades a late plagiogranite, the relationship is not strongly intrusive (the porphyry has a rather irregular indefinite margin and is not chilled) suggesting the two are not widely separated in time. Therefore, on the basis of field evidence and alkali element content, it seems possible that, whereas the earlier plagiogranites represent the first magmatic phase (Lower Volcanic Unit, spreading ridge), the later plagiogranites and the orthoclase porphyrys represent the second magmatic phase. (Upper Volcanic Unit, island arc). The mode of occurrence and chemistry of plagiogranites in modern island arcs supports this conclusion (Section 2.6.4).



Figure 2.3.6 Variation diagrams : Smartville ophiolite, major oxides



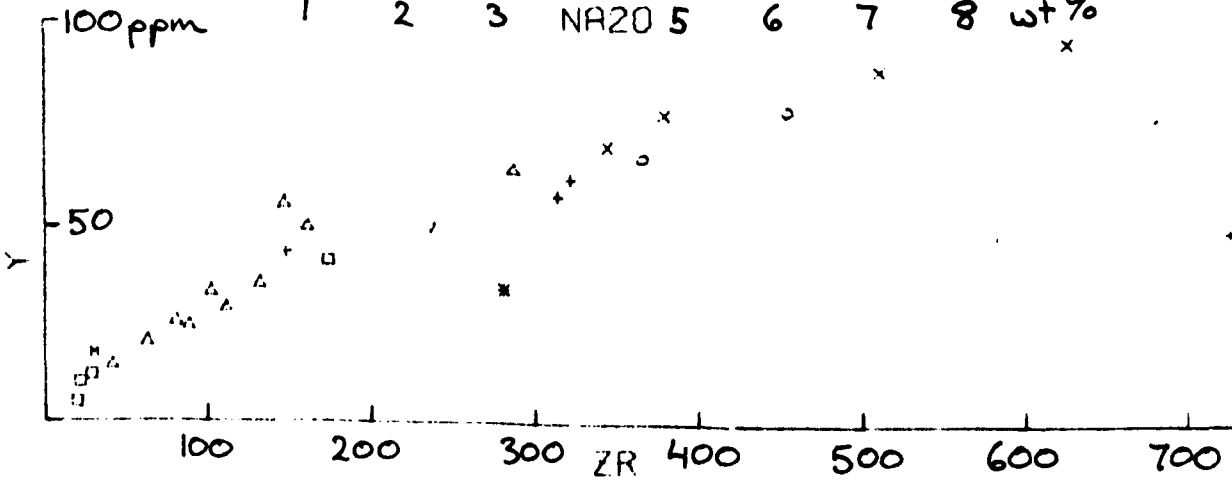
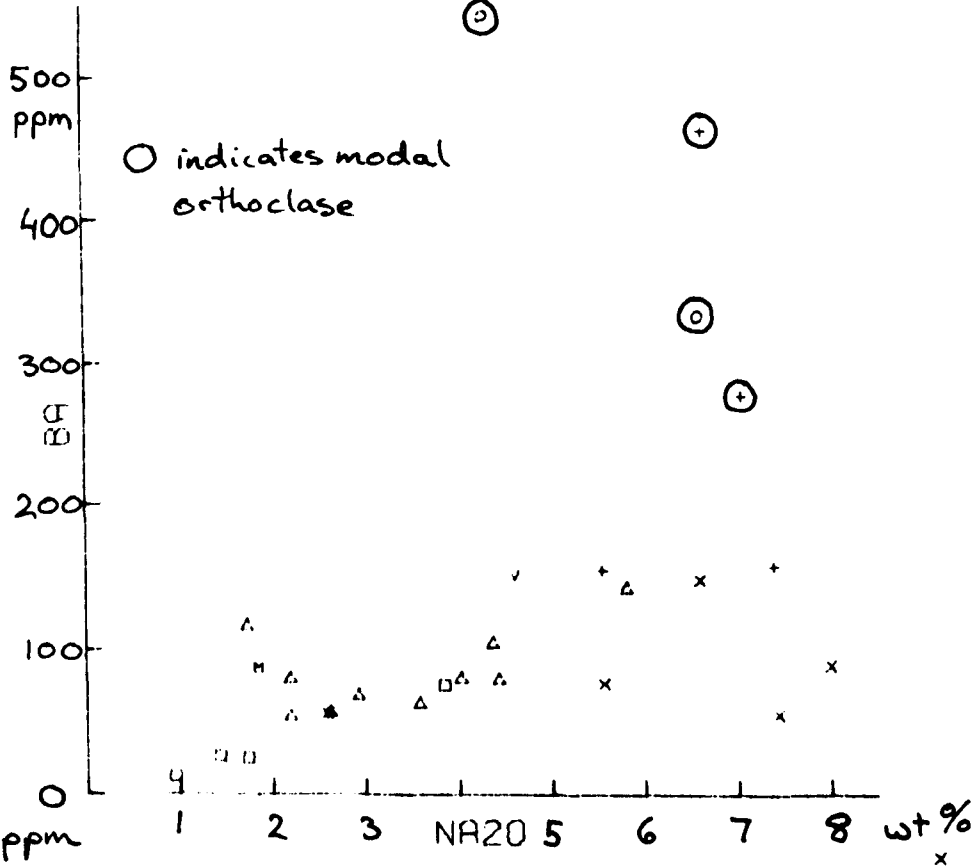
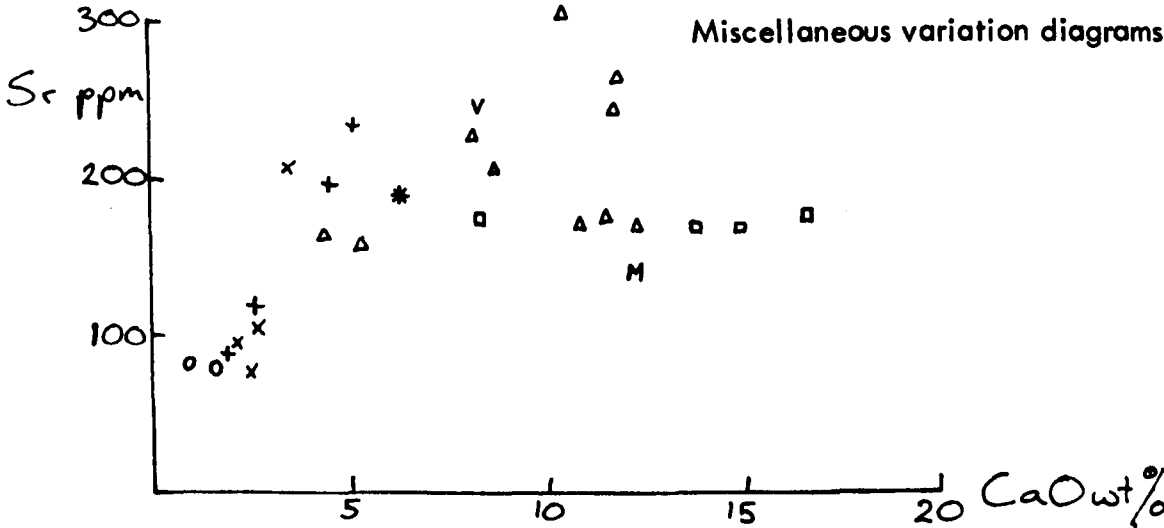


Key to Figure 2.3.6, 2.3.7, 2.3.8.

- Gabbro
- M Magnetite gabbro
- Δ Dolerite
- + Tonalite
- x Trondhjemite
- o Orthoclase porphyry
- \* Epidosite
- v Insitu vein

Figure 2.3.8

Miscellaneous variation diagrams



### 2.3.3.5 REE Geochemistry

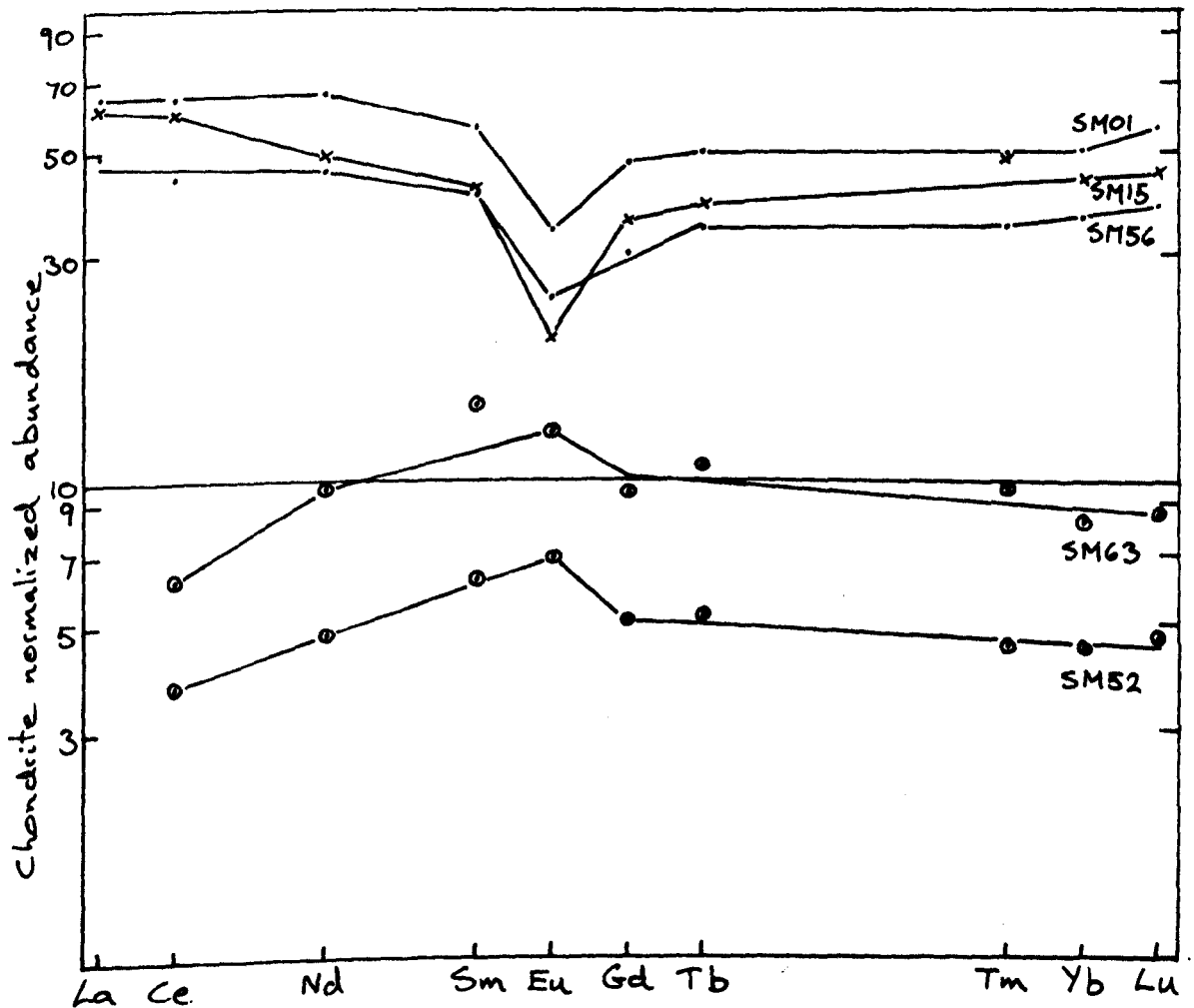
Menzies and Blanchard (1977) found that the Upper Volcanic Unit was LRE enriched and they suggested a different (calc-alkaline) source to the lower volcanic unit which is typically LRE depleted. The dyke complex has both LRE enriched and depleted types which can be mutually intrusive. According to Menzies (op. cit.) the plutonic unit is composed of LRE depleted rocks,  $\Sigma$ RE ranging from chondritic levels in a gabbro-pyroxenite to 60X chondrite in some plagiogranites.

Five specimens from Smartville were analysed for the REE, two gabbros, an early and a late tonalite and an orthoclase porphyry. (Figure 2.3.10). There are insufficient data to assess the mobility of the REE in the Smartville suite but by analogy with other studies (Sections 1.2, 2.1.4, 2.2) they are taken to be immobile.

The two gabbros have LRE depleted profiles which are assumed to be similar to those of the Lower Volcanic Unit (Menzies et al. have not, at the time of writing, published their data) but with superimposed positive Eu anomalies attributed to cumulus plagioclase. The three granitic rocks have LRE enriched profiles with large negative Eu anomalies. These data can be interpreted in three ways. (i) The LRE depleted plagiogranites recorded by Menzies et al. are cogenetic with the Lower Volcanic Unit. Data presented in previous sections show that LRE depleted plagiogranite liquids can evolve to residua with flat or LRE enriched profiles, probably by the combined fractionation of plagioclase, hornblende and/or apatite. The three analysed rocks could be examples of such residua. (ii) Some of the

Figure 2.3.10 Smartville RE profiles

- SM01 Early tonalite
- × SM15 Orthoclase porphyry dyke
- SM56 Late tonalite
- ⊙ SM63 Magnetite gabbro
- ⊙ SM52 Varitextured gabbro



Smartville plagiogranites are cogenetic with the Upper Volcanic Unit, as suggested at the end of the previous section. In this case they would be expected to have similar profiles to the lavas but to be enriched overall, with negative Eu anomalies as the result of plagioclase removal. The three analysed rocks could be cogenetic with the upper lavas. (iii) Two of the analysed rocks are cogenetic with one volcanic unit and the third with the other.

According to their field relations and alkali content, the more  $\Sigma$ RE enriched of the tonalites is an early type, the others belong to a later episode. These RE data are compatible with this, the third possible interpretation, although it is acknowledged that the data are too few to be dogmatic about this proposal.

### 2.4.1 Regional Geology

The California Coast Ranges, which extend 900 km. down the Pacific coast of North America, are dominated geologically by the Franciscan formation. (Figure 2.3.1). This is an assemblage of Upper Jurassic to Upper Cretaceous greywackes, siltstones and shales with altered mafic and rarer felsic lavas, serpentinites, some cherts and rare limestone (Bailey et al., 1964). Although some coherent structures are recognisable within the formation, it is largely a chaotic *mélange* (Hsu 1968). For most of their length, the Coast Ranges are flanked on the east by The Great Valley, underlain by the Great Valley Sequence (G.V.S.). This covers the same time span as the Franciscan sediments but it is a little deformed sequence of siltstone and mudstone with some arkosic sandstones. Conglomerates and mafic lavas with cherts occur in the lower parts of the Sequence (Bailey op cit., Pessagno 1973) which in the west rests depositionally upon an ophiolite assemblage which Bailey, Blake and Jones (1970) considered to be oceanic crust. Indeed, recent geophysical studies indicate much of the Great Valley basement has the characteristics of oceanic crust, except for unusual thickness (about 30 km.) (Cady 1975). However, the G.V.S. overlaps the Sierran basement in the east. Ernst (1965) concluded the Franciscan was deposited entirely on oceanic crust, perhaps partly or wholly within a trench but certainly in a more distal environment than the G.V.S. .

The coeval assemblages of the Franciscan and Great Valley Sequence are everywhere separated by reverse faults. (Irwin, 1964). Ernst (1970) interpreted these boundary faults as the expression of a Late Mesozoic Benioff zone in which the Franciscan, a prism

of sediment which accumulated in the trench, was subducted and metamorphosed beneath the Great Valley Sequence. Bailey et al. (1970) also recognised the regional equivalence of the boundary faults and proposed that they all be renamed "The Coast Ranges Thrust". In their interpretation, the Coast Range Thrust is subhorizontal (albeit folded) over most of the Coast Ranges, steepening dip to disappear beneath the Great Valley. Thus, the present outcrop of the Franciscan is viewed through wide tectonic windows whose margins are delineated by serpentinite and pillow basalt, the dismembered remnants of the Mesozoic ocean crust on which the Great Valley Sequence was deposited. (Bailey et al., 1970). The "Coast Range ophiolite" does not occur in the north, where the Franciscan is thrust beneath the continental basement of the Klamath mountains. Mid-late Jurassic radiometric ages have been determined for several of the ophiolite fragments. (Lanphere 1971, Maxwell 1974, Hopson et al., 1975). Bailey et al., did not suggest a specific emplacement age for the Coast Range ophiolite and their model implies a progressive underthrusting of the Franciscan. Detailed mapping of the northern Coast Ranges has revealed several distinct tectonic units within the Franciscan. The oldest was thrust against the Great Valley Sequence in the Tithonian or before and the youngest, on the coast, in the Eocene. (Maxwell, 1974).

Two of the best known fragments of the Coast Ranges ophiolite occur at Point Sal and San Luis Obispo (Hopson et al., 1975 Page 1972), both to the south of the Salinian Block (Figure 2.3.1). Detailed descriptions of these areas made since



1970 support Bailey et al.'s hypothesis that the Coast Range ophiolite represents Jurassic ocean crust.

#### 2.4.2 The Point Sal ophiolite

In the sense of the 1972 GSA conference definition, the Point Sal ophiolite is complete but dismembered. It's 10 km<sup>2</sup> outcrop is less than one thousandth the area of the Semail Nappe. It was first described by Fairbanks (1896), subsequently by Woodring and Bramlette (1950) and has been re-examined only very recently (Hopson et al., 1973).

The following description of the ophiolite is largely taken from Hopson et al., 1975. This is followed by the present writers observations on the plagiogranites (Section 2.4.3). The upper part of the Point Sal sequence (sediments, extrusives, dyke and sill complex, plagiogranites and hornblende gabbro) is completely separated from the lower part (ol- cpx- pl cumulate gabbros and peridotites) in surface outcrop.

The whole ophiolite is about 3 km. thick. The two main outcrops are separated by at least one major fault and the northern outcrop is further fault-dissected (Figure 2.4.1, 2.4.2). A high angle fault at the base of the sequence juxtaposes Miocene sediments and ultrabasic cumulates. Slivers of serpentized harzburgite occur along the basal fault.

According to Hopson (op cit.,) the gabbro and diorite in the northern outcrop lack cumulus textures, and primary hornblende appears in place of pyroxene and olivine. There are numerous flow-aligned miarolytic cavities partly filled with fibrous

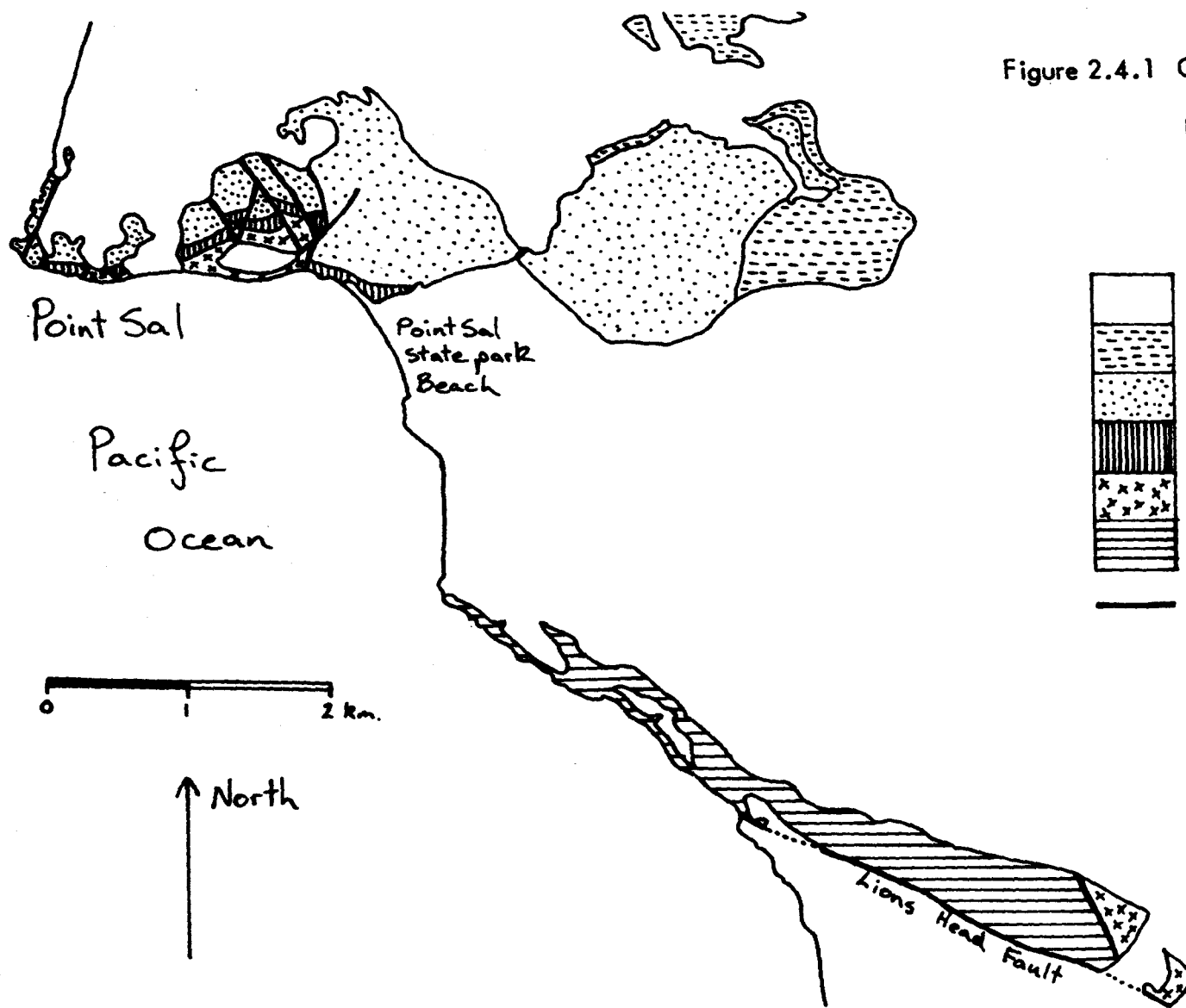


Figure 2.4.1 Geological map of the Point Sal area

From Hopson et al. 1975

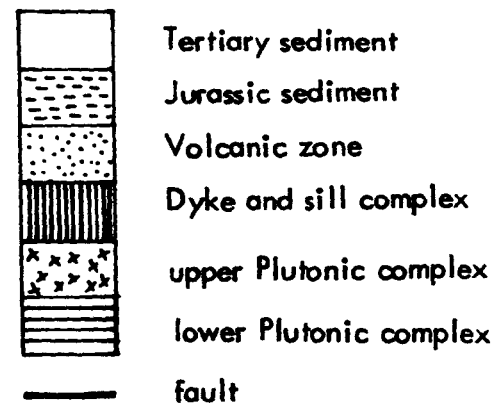
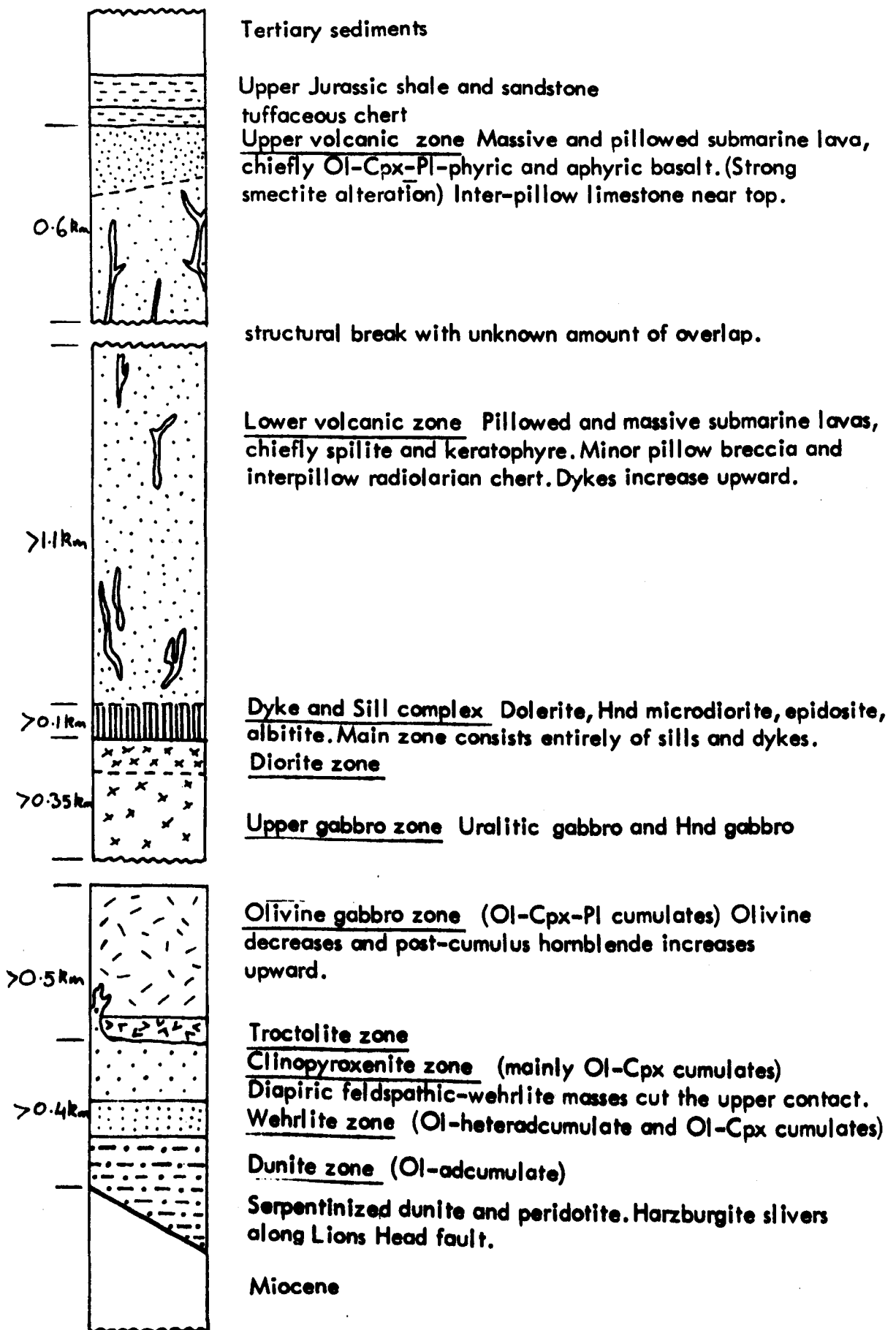


Figure 2.4.2 Section through the Point Sal ophiolite

From Hopson et al. 1975



amphibole.

The dykes and sills are classified in two groups; an upper and lower dyke series. The upper series is an intrusive complex between the volcanic and plutonic sequences (Figure 2.4.2) which are also crosscut by dykes. The upper series is mostly albitized, spilitized, uralitized and epidotized dolerite and hornblende microdiorite with some thin dykes and veins of albitite in the top of the plutonic sequence. The intrusive complex is similar to S.I.C.s (Section 2.1.2.3) in several ways; in some sections no intervening wall rock remains and multiple dyking is common, but Hopson et al., considered that it was originally a sill complex. They suggested that the sheets were intruded subhorizontally beneath a passive roof of volcanic rock, contrasting this situation with active tensional rifting which permitted intrusion along vertical fissures elsewhere. Such a sill complex could have formed beneath an ocean rise at which spreading rate was very low, relative to magma production. However, there is a possibility that hydrothermal alteration and tectonic disturbance have merely disguised what was a dyke complex.

The lower dyke series intrudes the olivine-bearing plutonics. They are mostly olivine and orthopyroxene bearing microgabbros, these two minerals being absent in the upper dyke series. There are also minor siliceous members. The dykes are rodingitized where they crosscut serpentinitized ultramafics but are otherwise unaltered.

The volcanic zone is largely composed of pillowed and massive tholeiitic andesite and pyroxene basalt, now altered to

"Keratophyre" and "spilite". Hopson et al., distinguished an upper zone with zeolitized olivine basalt and a lower zone metamorphosed at prehnite - pumpellyite facies and, lower down, greenschist facies.

Red radiolarian chert occurs in the lower volcanic zone and grey limestone in the topmost 30 m of the volcanic section. Tuff is absent from the volcanic sequence but tuffaceous bedded chert rests depositionally upon it. The composition of sparse euhedra and microlites suggests a calc-alkaline source for the tephra. No other terrigenous material is found. The age of the chert, based on radiolaria, is Late Jurassic. A U-Pb isotopic age of 160 my was determined from a zircon in a dyke intruding olivine gabbro. This date, which agrees with other radiometric age determinations from two other fragments of the Coast Range ophiolite (Lanphere 1971), suggests an appreciable time-lapse between the formation of the ophiolite at a mid-oceanic spreading centre and onset of sedimentation. The chert is overlain by distal turbidites in the lower G.V.S..

#### 2.4.3.1. Plagiogranites at Point Sal

Three types of plagiogranite are found in the Point Sal ophiolite; (i) the quartz diorite at the top of the plutonic sequence (ii) sparse sharp margined "albitite" veins in the plutonic sequence and (iii) occasional leucocratic in situ veins in the hornblende gabbro. None of these types transgress the margins of the ophiolite, indeed, they are concentrated towards the top of the plutonic sequence. Their petrography is summarised in Table 2.4.1.

Table 2.4.1 Summary of petrography of Point Sal upper  
plutonic complex

Rock Type	Primary Petrography	Alteration
Quartz Diorite (Minor tonalite)	Pl, hnd, qz. <u>Acc</u> Op, sph, zrc. Med to fine grained. Euhedral to subhedral pl. with unzoned core and narrow, zoned, albitic rim which is continuous with radial granophyre. Also interstitial qz. anhedral. Green brown hnd subhedra are interstitial or subophitic. Proportion of qz. variable.	Pl all saussuritized except rims and intergrowth. Some cz after pl. Interstitial ep. and minor 2 ndy qz. Fibrous pale green amph encloses fine grained op. Minor chl, cal. sph rims op and picks out exsolved ilm.
"Albitite"	Pl. <u>Acc</u> Hnd?, sph, op. Variable grain size. Mostly euhedral pl. Other phases anhedral. Brittle deformation.	Pl all turbid. Fibrous amph. Preh infills early fractures. Ep infills later fracture. Sph.
Hornblende gabbro	Pl, hnd, $\pm$ cpx, <u>Acc</u> op, qz. Same textures as qz diorite but more variable grain size. Some e.g.s. are op - rich.	Pl partly turbid. Amph after cpx and hnd, also infills miarolytic cavities. Cal veins. Greenschist phases are absent.
Pyroxene gabbro (norite)	Pl, cpx, opx. <u>Acc</u> Op, qz. Med. grained, Unzoned pl subhedra, poikilitic pyx. Very few accs.	Fibrous amph. after cpx.

The maximum observed thickness of quartz diorite is 60 m, in a fault bounded wedge but it changes thickness and disappears laterally. The quartz diorite passes up into finer diorite which intrudes the base of the dyke complex and passes downwards into hornblende gabbro. The most quartz-rich "quartz diorite" would be most accurately described as a tonalite. Both gabbro and quartz diorite are intruded by dolerite and microdiorite dykes. The quartz diorite includes resistant 10 cm wide pods which are enriched in secondary quartz and epidote.

Sporadic leucocratic veins of the same appearance as the in situ veins found in varitextured gabbros in other ophiolites (Section 2.1.2.1) are associated with coarser facies of the hornblende gabbro. The veins are now almost wholly replaced by prehnite but inclusions and remnants indicate they were originally composed of subhedral plagioclase and quartz with minor amphibole. It should be noted that the host gabbro is not prehnitised suggesting the alteration was caused by reaction with volatiles confined to the vein.

The so-called "albitites" (Hopson et al., 1975) occur in straight, sharp-margined veins up to 10 cm. thick, crosscutting hornblende gabbro. An albite granite (which was radiometrically dated) also intrudes olivine gabbro (Hopson et al., 1975). The primary composition of the feldspar in these veins is obscured by alteration but the analysis of one such vein shows it is rich in calcium as well as sodium and so was probably a leuodiorite originally.

One gabbro specimen, collected insitu near the waterline in the hornblende gabbro outcrop is a patchily amphibolitised norite with cumulus plagioclase and intercumulus orthopyroxene, clinopyroxene and rare olivine pseudomorphs. No cumulus textures are apparent in hand specimen but the chemical analysis supports the microscopic evidence. Previously, none of the cumulate gabbros and no orthopyroxene have been recognised in the northern outcrop. This finding supports the inferred original continuity of the two outcrops and suggests the thickness of the hornblende gabbro is not greatly curtailed.

#### 2.4.3.2 Other plagiogranites in the Coast Range ophiolite

Descriptions of many of the ophiolite localities at the base of the Great Valley Sequence were summarised by Bailey et al., 1970 and their chemistry described by Bailey and Blake (1974). Plagiogranites occur at six of the ten localities, including those at Point Sal. Most of these are extrusive or intrusive "quartz keratophyre" but diorite fragments appear in one volcanic breccia and, at another locality, prehnitised trondhjemitic aplite veins cross-cut hornblende gabbro. Bailey and Blake noted that the plagiogranites' field relations make it clear that they should be regarded as an integral part of the Coast Range ophiolite. The quartz keratophyres are commonly plagioclase and quartz phyrlic and, as in the Troodos porphyrys (Section 2.1), the quartz phenocrysts are much corroded. The primary mafic phase is hornblende, with minor biotite but the rocks are ubiquitously altered and little of either survives (Bailey et al., 1974). Another fragment of the Coast Range



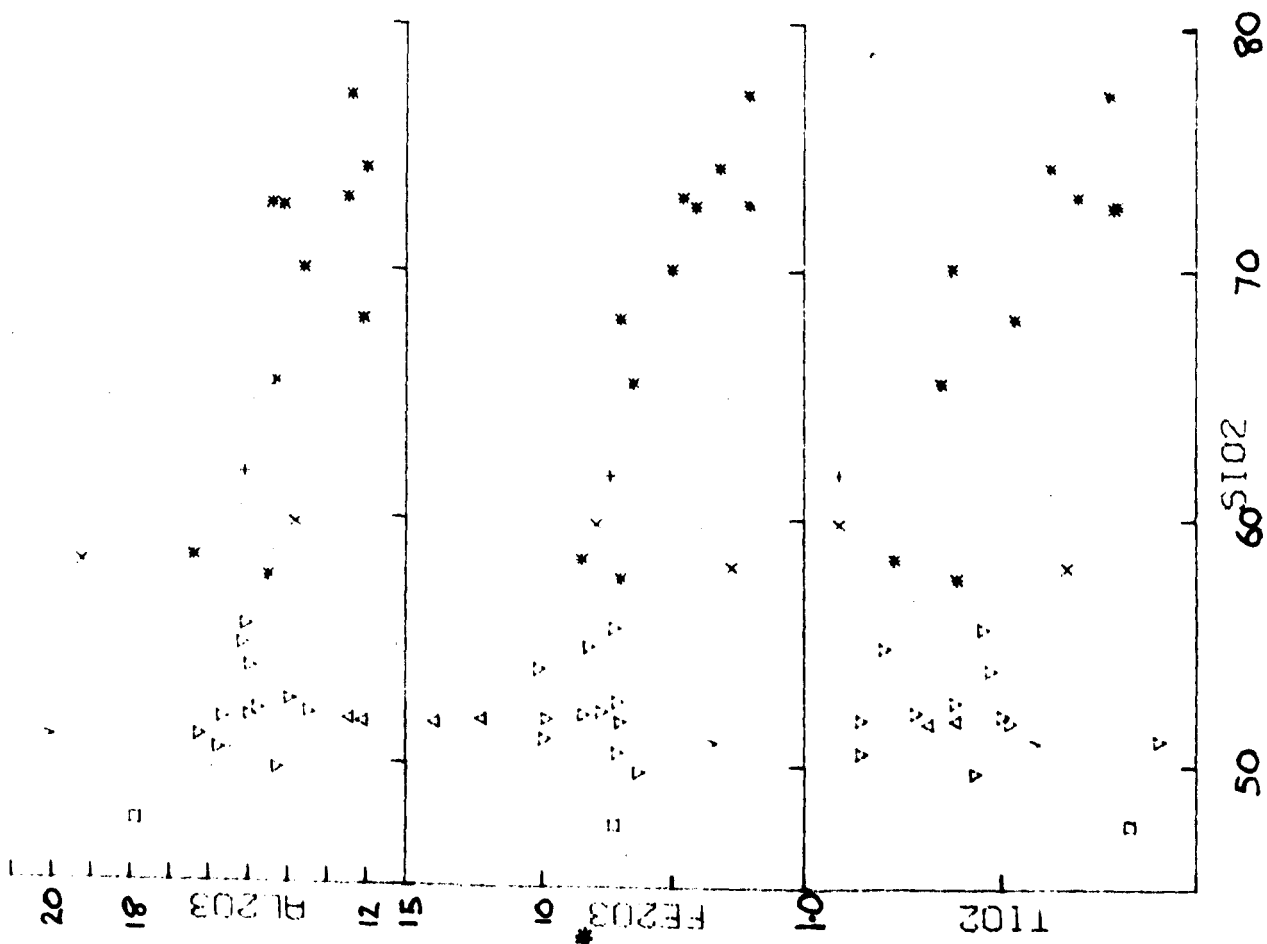
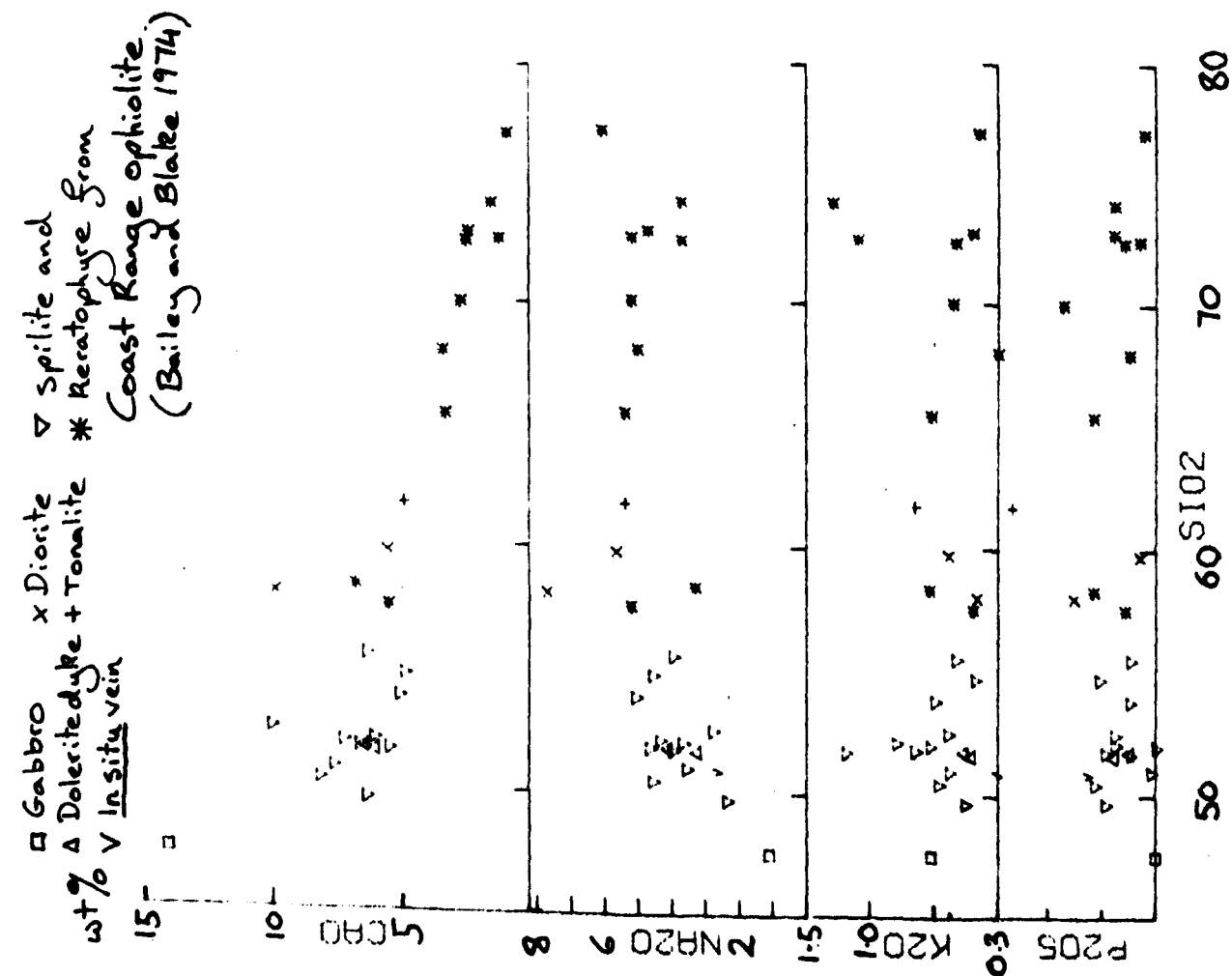
ophiolite, at San Luis Obispo, was described by Page (1972). He interpreted it as a synclinally deformed remnant of Mesozoic ocean crust and overlying sediment which was dragged beneath Upper Cretaceous Great Valley sediments as a tectonic "raft" in the underlying Franciscan melange. The ophiolite consists of a tectonically bounded one kilometre slab of serpentinitised harzburgite, overlain by 1.2 km. of basaltic pillow lavas and breccias. The lower part of the pillow pile is intruded by many dykes and sills of dolerite, gabbro, trondjemite and some quartz albitite. The sheets of quartz-rich rock, up to 10 m thick, are all fine grained and composed of plagioclase with up to 40% quartz, often in interstitial granophyre, and a little hornblende. K-feldspar is absent. Secondary clinozoisite and chlorite are present. Page regarded these plagiogranites as differentiates from the same basaltic magma as the lavas but pointed out they had been emplaced from a separate (unobserved) location.

#### 2.4.3.3 Geochemistry

A limited number of major element analyses are available from Point Sal (Hopson et al., 1975) and the rest of the Coast Range ophiolite (Bailey and Blake 1974). The latter authors compared the compositions of a range of rock-types from the Coast Range ophiolite with specimens from other ophiolites and also from ocean ridges. They concluded that the various suites were fundamentally similar and identified two differentiation trends, often represented in the same area, which gave rise to iron-rich gabbros and amphibolites on one hand and silicic rock types on the other. Bailey and Blake (op. cit.) also found that the basalts from the Coast Range ophiolite were either Ti-rich ( $> 1.8\% \text{TiO}_2$ ) or Ti-poor ( $< 0.9\% \text{TiO}_2$ ). On the basis of Ti and P distribution they decided the Ti-rich basalts are similar to those from ocean islands whereas the Ti-poor variety fall within the same range as ocean ridge basalts.

Seven specimens from Point Sal were analysed for major and trace elements for the present work (Appendix 1 ). The major element data are plotted with the published analyses of Ti-poor splites and keratophyres (Figure 2.4.3). There are insufficient trace element data to define a trend and these are not displayed. The chemistry of two prehnitised veins appears abnormal (very high  $\text{Al}_2\text{O}_3$  and  $\text{CaO}$ ) but this is attributed to high modal plagioclase although there could also have been some Ca-metasomatism. Both veins are also very poor in Sr, Ba, Rb and Zn, probably depleted by hydrothermal activity.

Figure 2.4.3 Variation diagrams :Point Sal ophiolite



The composition of the quartz diorites and dolerites falls within the same range as that of other Coast Range plagiogranites and lavas except for silica. The quartz diorites are less silica-rich than most of the keratophyres, readily explained by differing intensities of silica metasomatism. The geochemistry of the plagiogranites is similar to that described in previous sections (2.1.4, 2.2.3, 2.3.3) and is therefore consistent with the same interpretation.

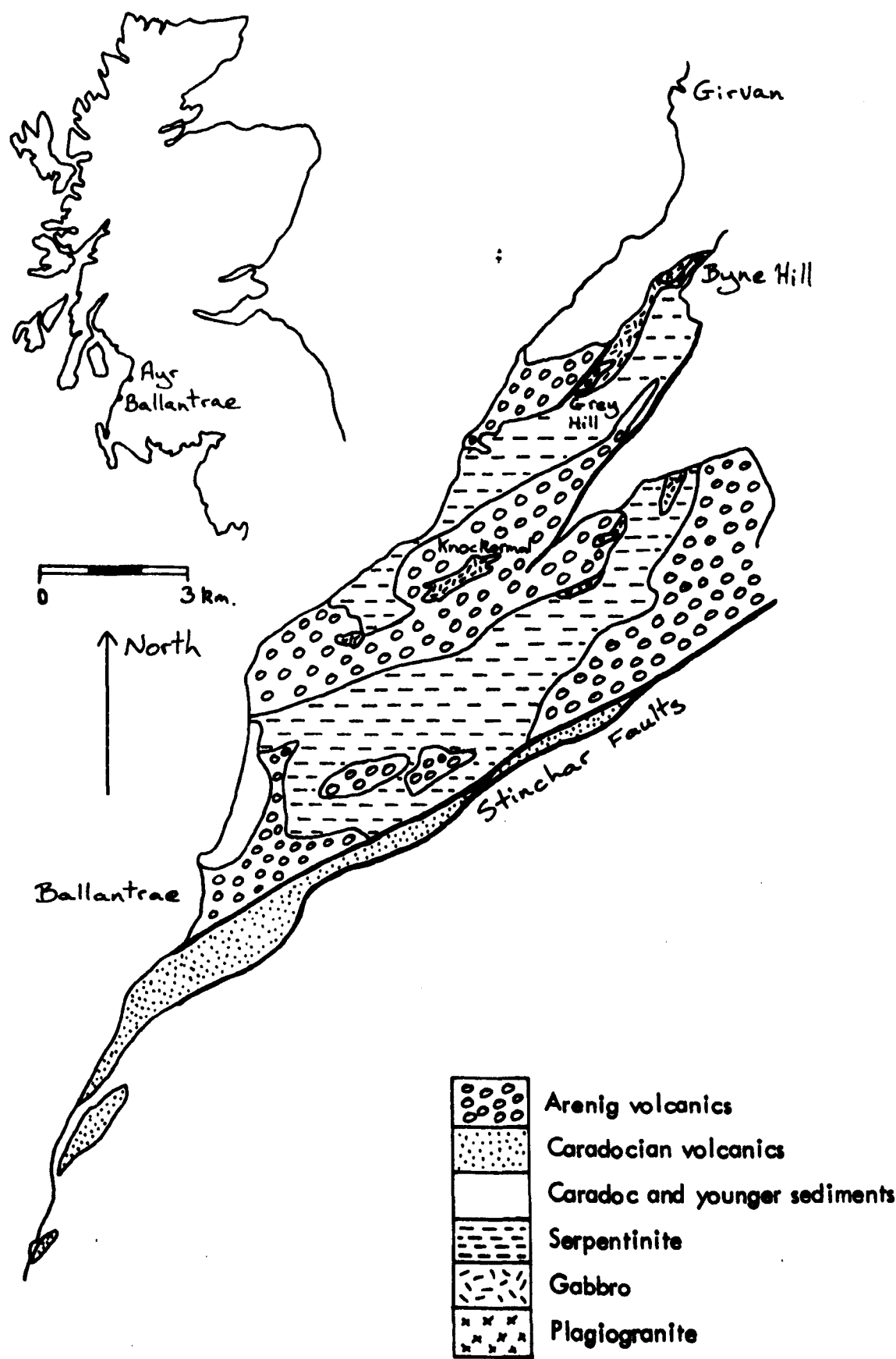
## 2.5 The Ballantrae Complex

### 2.5.1 Introduction and Regional Geology

The Ballantrae Complex lies on the Ayrshire Coast, near the northern edge of the Scottish Southern Uplands. It is a dismembered ophiolite (Church and Gayer 1973); largely serpentinite and pillow lava with associated dolerite, bedded chert, black shale, rare amphibolite, glaucophane schists and eclogite and in the north of the area, at Byne Hill, a gabbro-diorite-trondhjemite complex (Figure 2.5.1).

The Complex was first mentioned by Bonney (1878) and since then a considerable literature has grown around it. (e.g. Bailey and McCallien 1952, who describe the history of research in detail). Interest in the area was rekindled when the significance of ophiolites as possible fragments of ocean crust and their place in palaeogeographic reconstructions in the light of plate tectonics was realised. The concept of a lower Palaeozoic Proto-Atlantic ocean, whose closure resulted in the formation of the Caledonian-Appalachian orogenic belt, was originated by Wilson (1966). Several authors then proposed models in which the Lower Palaeozoic ocean crust of the Proto-Atlantic was consumed in either one (Fitton and Hughes 1970) or more (Dewey 1969, Bird, Dewey and Kidd 1971, Church and Gayer 1973) subduction zones. The approximate position of these zones now marked, it was suggested, by early Ordovician ophiolites in Scotland (Ballantrae Complex and the Highland Border Series), Ireland, Newfoundland and the northeastern U.S.A. (Bird et al., 1971).

Figure 2.5.1 Geological map of the Ballantrae Complex



After Church and Gayer 1973, Bloxham and Lewis 1977

Arenig graptolites have been found in the black shales within the Ballantrae pillows lavas (Walton 1965) and it is presently assumed that the other igneous formations in the main part of the Complex are of approximately the same age. However, Caradocian pillow lavas crop out to the south of the Stinchar Fault. (Walton op. cit.). The Complex is unconformably overlain by the Upper Ordovician (Caradoc) Barr Group, which contains ophiolite debris. (Williams 1962). The Caradocian fossils in the Ballantrae area are more readily correlated with Appalachian rather than Welsh faunas. Moreover, faunal and sedimentary facies indicate that the Girvan area lay close inshore during the Upper Ordovician, to the northwest of a major sedimentary trough, contrasting with Lower Ordovician deep water conditions (Williams op. cit.).

The following interpretations of Caledonian-Appalachian ophiolites have been suggested; (i) Serpentinite intrusions and basalt extrusions into trench sediments (Dewey op. cit., Bird and Dewey 1970) (ii) Layered complexes related to island arc volcanism (Bird and Dewey op. cit.) (iii) Overthrust sheets of oceanic lithosphere (Fitton and Hughes op. cit., Stevens 1970, Church and Stevens 1970, 1971). (iv) Autochthonous remnants of small ocean basins (Dewey, 1971) (v) Oceanic crust formed in small marginal basins and subsequently overthrust onto the continent Bird et al., 1971). Reviewing these alternatives, Church and Gayer (1973) emphasized the similarities between the lithologies found at Ballantrae and in the Newfoundland ophiolites, notably the occurrence of garnet amphibolite beneath peridotite in both areas. They inferred from its presence that the Ballantrae Complex is allochthonous and was emplaced as young, thermally

immature oceanic lithosphere from either a narrow ocean basin or a behind-arc basin.

Three attempts have been made to characterise the genetic environment of the Ballantrae pillow lavas by their immobile trace element content. Bloxham and Lewis (1972) found the lavas had tholeiitic affinities and considered they were probably remnants of ocean crust. However, on the basis of Ti, Zr and Cr content, they could not rule out an origin in an island arc. They reached the same conclusion using the REE. (Lewis and Bloxham 1977). Using Ti, Zr, Y and Nb, Wilkinson and Cann (1974) distinguished two genetic groups amongst the pillow lavas and dolerite; tholeiitic "hot-spot" basalts (i.e. intraplate basalts) and low-potassium island arc tholeiites. The presence of the Byne Hill gabbro-trondhjemite suite and of limited examples of amphibolite and glaucophane schist with trace element content similar to ocean floor basalt suggested to Wilkinson and Cann (op. cit.) that the pillow lavas were erupted onto oceanic, rather than continental crust. They also considered it likely that the intraplate basalts were formed at some distance from an island arc and carried into tectonic contact with the island arc tholeiites. In this context it should be noted that the common clasts of acid extrusive material in the Upper Ordovician and Silurian greywackes of the Southern Uplands indicate that not all volcanicity in the region was basaltic (Walton, 1965).

In summary, it appears that the Ballantrae Complex probably represents ocean crust that was formed in a marginal ocean basin and became the basement to island arc volcanicity.



## 2.5.2 Plagiogranite at Ballantrae

### 2.5.2.1 Introduction

Several outcrops of gabbro are associated with the Ballantrae pillow lavas and serpentinite but plagiogranite only occurs with two of them. As noted by Bloxham (1968) the best exposures are on Byne Hill, one of four hills formed of gabbro in the north of the Complex, although there are also some poor exposures on the nearby Grey Hill. Small amounts of "albite granite" crop out on Knockormal Hill, near the centre of the Complex (Balsillie, 1937).

The large scale geological maps of Byne Hill and environs produced by Bloxham (1968) and Neary (1967) were used during fieldwork.

### 2.5.2.2 Field Relations

The bulk of the Byne Hill-Grey Hill intrusion is composed of gabbro which on two hills is capped by a sub-horizontal sheet of trondhjemite. On Byne Hill the gabbro and trondhjemite are separated by 3 to 5 m. of leucodiorite but this does not occur on Grey Hill. The gabbro is varitextured, coarse to medium grained with leucocractic pods (upto 70 cm. diameter) and masses of fibrous amphibole (up to 10 cm. in diameter). There is no cumulus layering in the gabbro. The amphibole clots are most common close to the gabbro/diorite contact, which is a rapid transition over a metre or so. Diffuse veinlets of coarse feldspar and gabbro pegmatite occur in the lowermost diorite which is also less leucocratic than the rest of the plagiogranite. The contact between gabbro and trondhjemite on

Grey Hill, where the diorite is absent, is a rapid transition, albeit poorly exposed. Although the proportion of quartz in the plagiogranites varies and quartz diorite does exist, the leucodiorite/trondhjemite contact across the south side of Byne Hill is sharp. The shape of the contact surface is sometimes highly irregular and pure feldspar enclosures appear in the trondjemite and quartz-rich patches in the leucodiorite within a few metres of the contact. However, there is always a distinct line to be drawn between a quartz-rich and a quartz-poor rock. There is no chilling at the contact and nothing to suggest that the relationship is that of a liquid intruding a solid. Sparse pegmatitic and aplitic veinlets occur throughout the trondhjemite.

Both gabbro and plagiogranite are intruded by occasional dolerite dykes which are up to 1 m. thick over a maximum observed length of 10 m.. However, the dykes could be either Ordovician or Tertiary in age.

The Byne Hill-Grey Hill gabbro-plagiogranite body intrudes serpentinite, originally a spinel harzburgite, and is faulted against pillow lavas. (Figure 2.5.2). The gabbro is chilled against serpentinite and is partially rodingitized at the contact.

The gabbro-plagiogranite intrusion is unconformably overlain by the Benan Conglomerate (part of the Caradocian Barr Group) which contains a great variety of well-rounded clasts up to 1 m. long in a sandy matrix. Conspicuous pink granite cobbles occur as well as locally derived gabbro, lava and sedimentary

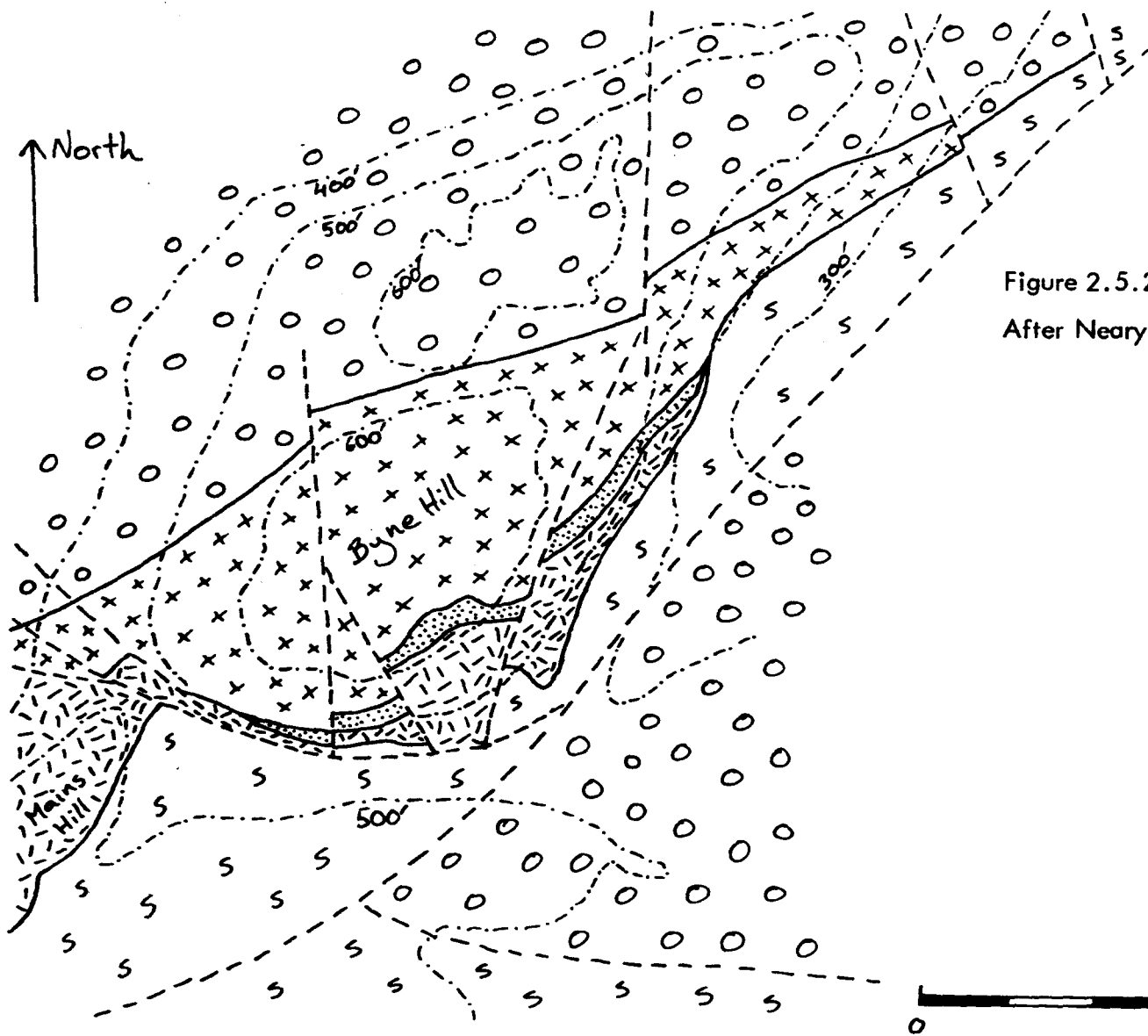
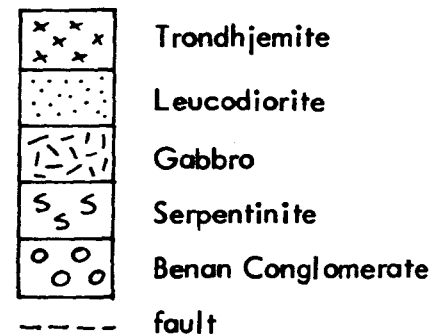


Figure 2.5.2 Geological map of the Byne Hill area  
After Neary 1967, Bloxham 1968 and present work



detritus. The pink granite is rich in K-feldspar (perthite) and is thus quite unlike the Byne Hill plagiogranites. The provenance of such a granite in this area in Caradocian times is problematic (Walton, 1956) although there are a number of pre-Caledonian metamorphism granites in the Scottish Highlands (e.g. Pankhurst and Pidgeon 1976). The absence of high grade gneiss clasts discounts a source in Lewisian-style basement.

### 2.5.2.3 Petrography

Microscopic study reveals several varieties of gabbro and plagiogranite (Table 2.5.1). The gabbro can be dominated by either clinopyroxene or primary hornblende and pyroxene is sometimes completely absent, especially close to the diorite contact. Bloxham (1968) records accessory olivine from the pyroxene gabbro.

The mineralogical alteration of the gabbro is patchy, often on a small scale, except immediately below the leucodiorite where the gabbro is more uniformly and intensely altered than elsewhere. Bloxham (op cit.) called this zone "dioritic hornblende gabbro" but as the rock has more affinity with the gabbro than the diorite the self-contradictory prefix is abandoned.

The most idiomorphic major phase in the Byne Hill suite is always plagioclase and it provides a reference in the sequence of crystallization of the accessory phases (Table 2.5.1). In the gabbros the mafic and accessory phases form in the interstices between plagioclase euhedra. The change from gabbro to diorite,

Table 2.5.1 Summary of petrography of Byne Hill

Rock type	Primary Petrography	Alteration
Gabbro	Pl*, cpx, hnd, <u>Acc</u> Op, ol, biot, ap. Proportions rather variable. Med. to coarse. Fine at contact with serpentinite. Euhedral pl optically enclosed in mafics. Pl weakly zoned, some reverse zones. Hnd is green and/or brown, some fringes and intergrowths with cpx.	Local sauss in pl. Some zones remain pellucid. Fibrous amph with assoc. fine op. after cpx and hnd. Minor chl. Sph after op.
Diorite	Pl*, biot <u>Acc</u> Hnd, ap*, op* Med. grained, subhedral pl, weakly zoned. Euhedral ap very abundant. Op is resorbed.	Pl all turbid except Ab rims. Chl after biot. Sph after op, especially along exsolution lamellae. Cataclastic textures common. Cal infills fractures and interstices. Preh rosettes in voids.
Leucodiorite	Pl.* <u>Acc</u> Biot, qz, ap*, op, zrc. Med grained, subhedral pl, weakly zoned.	
Trondhjemite	Pl*, qz*, <u>Acc</u> Biot, ap*, op, zrc. Subhedral to anhedral pl, interstitial qz, rare granophyre.	2ndy qz nucleates on primary qz. Otherwise as for diorites.

\*Indicates an early formed and/or liquidus phase.

mainly an increase in the proportion of feldspar, is accompanied by a change in the primary mafic phase from hornblende to biotite and also the appearance of apatite on the liquidus. A relatively mafic diorite which crops out immediately above the gabbro has unusual quantities of apatite some of which is enclosed in opaques. The opaques were partly resorbed and then both phases were enclosed in plagioclase. The leucodiorite above has only rare apatite and opaque phases but apatite is again enclosed in euhedral plagioclase, whereas the opaques are interstitial, with biotite and zircon. Trondhjemite which crops out just above (and within) the leucodiorite is only distinguished from it by the presence of quartz and, according to Bloxham, hornblende as interstitial phases. However, trondhjemite near the top of the hill has less idiomorphic plagioclase which encloses apatite and zircon. Here plagioclase/quartz crystal boundaries are of two types; those which indicate plagioclase preceded quartz and those which suggest that the two minerals crystallized simultaneously. Thus only the higher (later) trondhjemite represents a composition which is strictly on the "liquid line of descent", all the other rock types are composed of accumulations of the earlier formed crystals with a certain (unknown) proportion of residual liquid.

Bloxham (1968) suggested two possibilities for the origin of the mafic diorite; fractional crystallization or hybridisation, and pointed out that the two processes cannot be easily distinguished by either mineralogical or chemical criteria. He concluded on the basis of textural criteria that the diorite is a hybrid, "originated from reaction between crystalline gabbro and a silica-sodium-rich liquid". However, I have observed no

textures which cannot be explained by differentiation of a basic magma or subsequent hydrothermal alteration of the differentiates and see no need to invoke an additional hybridization process.

### 2.5.3 Geochemistry

#### 2.5.3.1 Introduction

Major and trace element abundances determined during this study are given in Appendix 1 and Figure 2.5.3. Analyses of the Byne Hill suite from Bloxham (1968) and Neary (1967) are also shown on Figure 2.5.3. These data, determined in different laboratories are, with the exception of Zr abundances, in good agreement. One set of Zr values was consistently higher than the others and was therefore not used. A high proportion of calcite in two of the analysed specimens, both diorites, is part of the cause of their low oxide sums (Appendix 1) and this source of inaccuracy was borne in mind in the interpretation of their geochemistry.

#### 2.5.3.2 Metasomatism

The ubiquitous presence of hydrous secondary minerals suggests that the Byne Hill suite may have been chemically modified during hydrothermal metamorphism. Secondary silica appears in the trondhjemites and so some of the high silica abundances may include a secondary component. However, all the other analysed specimens have a similar proportion of the same kind of secondary minerals and there are too few determinations of

the immobile trace elements to detect differential metasomatism if it has occurred. Very low levels of  $K_2O$ , Ba and Rb, especially in some diorites, is probably due to the chloritization of biotite.

Chemical mobility in and around the peridotite during serpentinization is an additional effect which could have changed the chemistry of the Byne Hill intrusion. Neary (op. cit.) analysed two gabbros which crop out within one metre of the serpentinite. Compared to all the other gabbros, they have very high CaO and low  $SiO_2$ ,  $Al_2O_3$ ,  $Na_2O$ ,  $K_2O$ , Sr and Ba, characteristics due to rodingitization. No other analysed specimens have this pattern of alteration and are therefore assumed to have been unaffected by serpentinization. Specimens which are obviously affected by recent weathering or which are stained red (pre-Benan conglomerate weathering) were not analysed.

#### 2.5.3.3 Major and Trace Element Geochemistry

Excluding the effects of alteration, the sequence of fractional crystallization deduced for the Byne Hill basic parental magma from petrographic evidence can account for the observed geochemical distribution.

Two examples of pyroxene gabbro have very low absolute abundances of  $SiO_2$ ,  $TiO_2$ , Zr, Y, Ba and Zn and low  $Fe_2O_3^*$  and MnO and high  $Al_2O_3$ , CaO and MgO relative to the other gabbros; they are largely composed of calcic plagioclase and iron-poor pyroxene with very little contribution from any residual liquid. Amongst the remaining gabbros, which are regarded as crystal mushes,

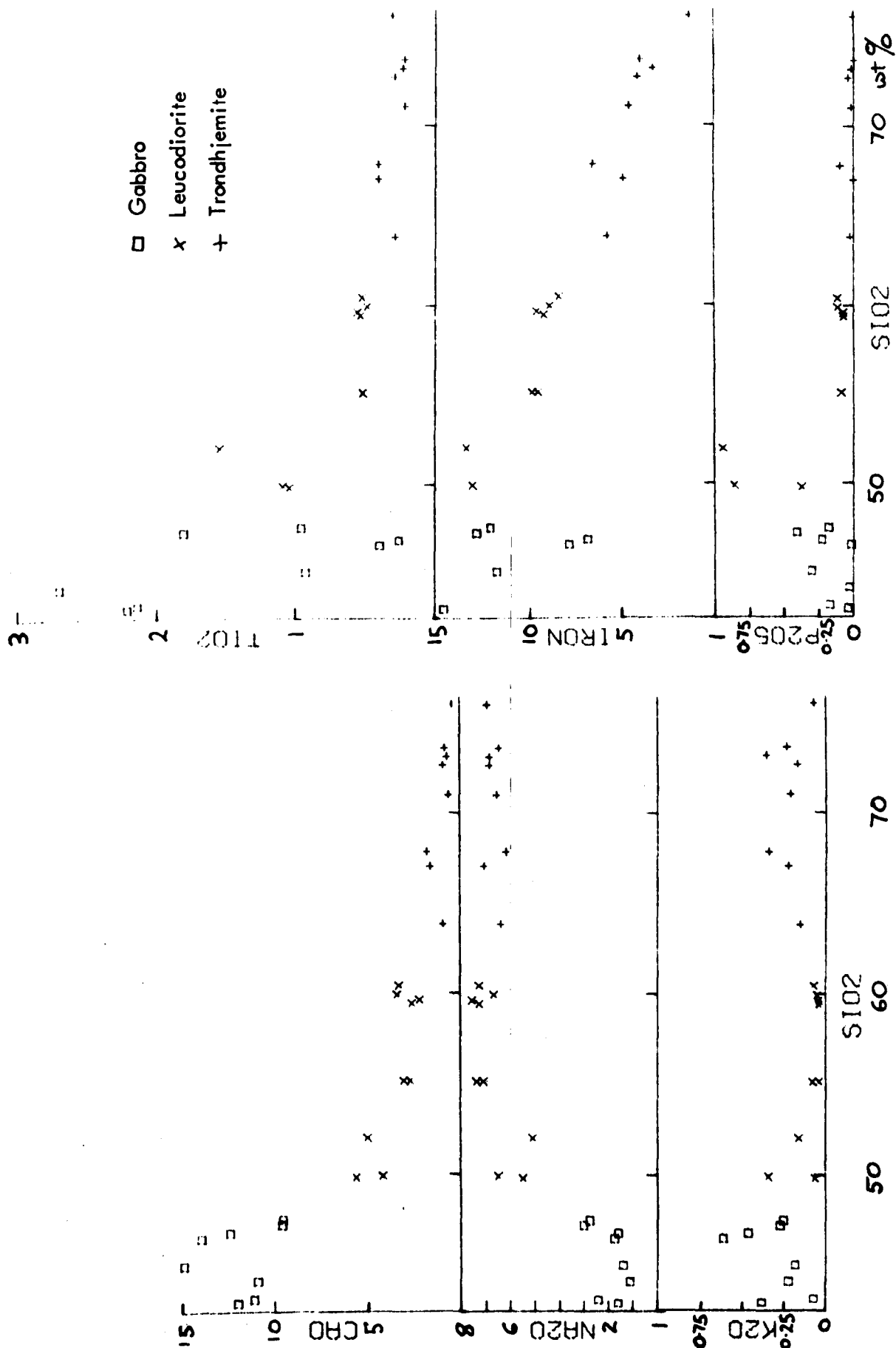


MnO,  $\text{Na}_2\text{O}$ ,  $\text{K}_2\text{O}$ ,  $\text{P}_2\text{O}_5$ , Zr and Y are positively correlated with  $\text{SiO}_2$  whereas MgO and CaO exhibit a negative correlation.  $\text{Fe}_2\text{O}_3^*$  and  $\text{TiO}_2$  tend to increase with  $\text{SiO}_2$  but are also strongly enriched in three silica-poor gabbros with accumulated FeTioxides.

These trends continue towards two  $\text{P}_2\text{O}_5$ -rich diorites which represent the apatite-rich diorite at the base of the plagiogranite sequence. These diorites plot at reversals or inflexions on the binary diagrams. Early precipitation of apatite at this point depletes the liquid in  $\text{P}_2\text{O}_5$ . Apatite also fractionates Y and zircon, Zr and these are subsequently depleted in successive liquids. Abundant  $\text{Al}_2\text{O}_3$  and  $\text{Na}_2\text{O}$  in the leucodiorites relative to the trondhjemites reflects their accumulation of sodic plagioclase.

The relative distribution of  $\text{K}_2\text{O}$  is problematic. The leucodiorites have negligible  $\text{K}_2\text{O}$  but it is present in at least detectable amounts in the trondhjemites. Biotite has been altered to chlorite in both leucodiorite and trondhjemite and if this is the cause of potassium depletion in the diorite it would be expected that the trondhjemite would also be depleted. This can be explained if two plausible conditions are fulfilled; (i) the diorite's potassium was originally contained mostly in interstitial biotite whereas the trondhjemites' was contained in both sodic plagioclase and biotite (ii) chloritization of biotite eliminates potassium from the crystal whereas the hydrothermal alteration of plagioclase does not.

Figure 2.5.3 Variation diagrams : Byne Hill Suite



#### 2.5.3.4 REE Geochemistry

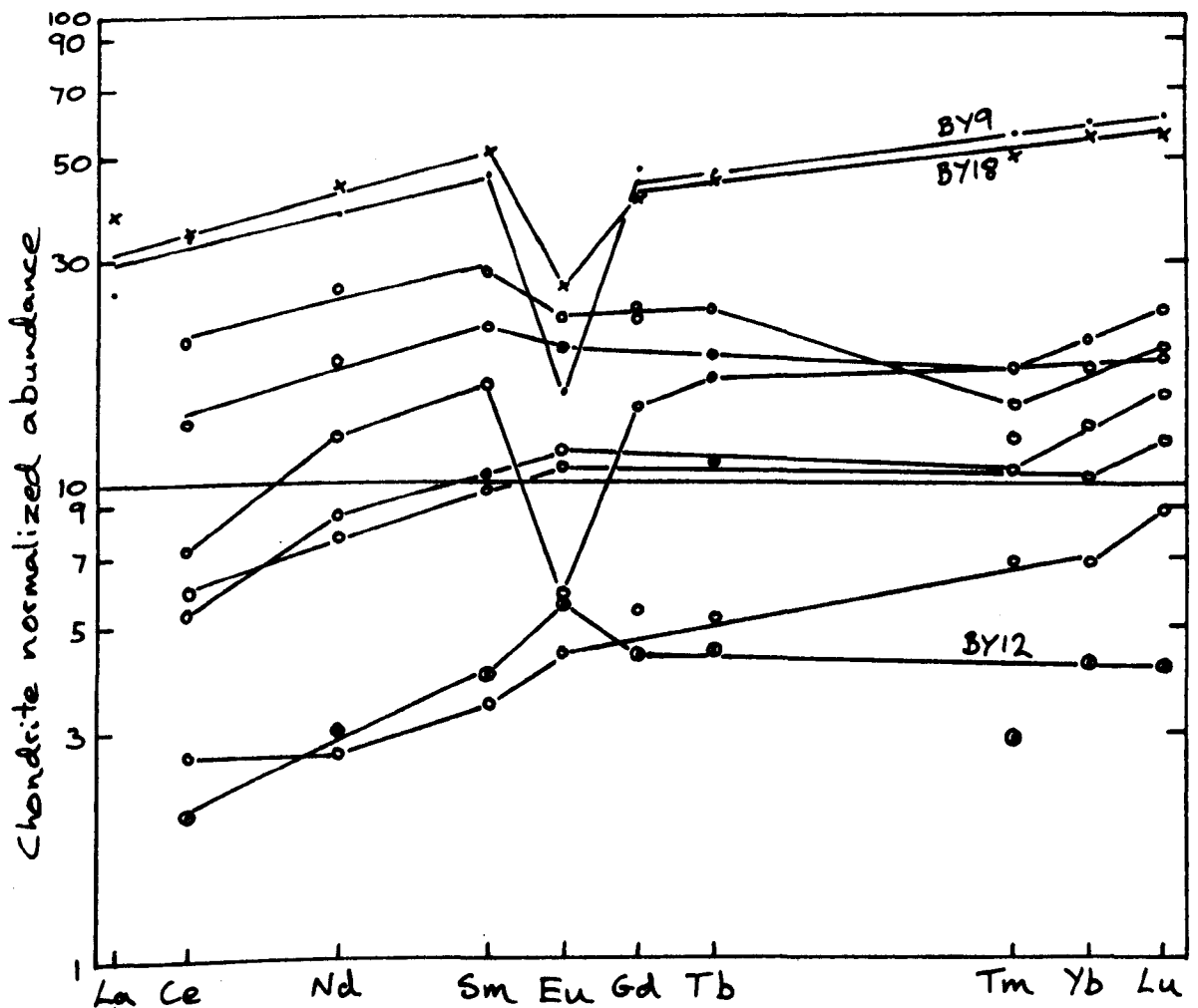
Lewis et al., (1977) found that the Arenig lavas in the main Ballantrae Complex were LRE depleted, whereas the Caradocian lavas to the south were LRE enriched. Three specimens from Byne Hill, a trondhjemite, a leucodiorite and a gabbro, were analysed for the REE (Figure 2.5.4). The Byne Hill suite has similar LRE depleted profiles to the Arenig pillow lavas, suggesting they have a similar origin and therefore supporting the proposal that the Byne Hill intrusion is of Arenig age.

The Byne Hill plutonics have stronger Eu anomalies than the Arenig lavas. Moreover, the gabbro has very low abundances of REE and Hf, somewhat less than the most primitive basalt, supporting the earlier suggestion that its composition is dominated by cumulate plagioclase and pyroxene and not by intercumulus liquid. The positive Eu anomaly is consistent with plagioclase accumulation. The more fractionated nature of the plagiogranites is affirmed by their greater  $\Sigma$ RE content and suggests that, unlike the gabbro, their trace element composition is dominated by interstitial liquid. If the plagiogranites were plagioclase cumulates without trace element rich interstitial phases, for instance, one would expect them to have low  $\Sigma$ RE. Although the leucodiorite seemingly has a high proportion of accumulated feldspar, this does not offset the negative Eu anomaly in the interstitial liquid, inherited from plagioclase fractionation in the gabbros. The difference in the Eu anomaly in the leucodiorite and trondhjemite could be due to the behaviour of Eu in apatite. (Figure 2.1.8). As Eu partition coefficients between apatite and liquid are anomalously low, accumulation of that phase

(expected in the leucodiorite) would tend to increase and fractionation (expected in the trondhjemite) to decrease the size of a negative Eu anomaly.

Figure 2.5.4 RE profiles : Ballantrae Complex

- BY12 Gabbro
- × BY18 Trondhjemite
- BY9 Leucodiorite
- Arenig lavas from Lewis and Bloxham 1977



## 2.6 Other plagiogranites

### 2.6.1 Introduction

So far in Chapter, the granitic rocks found in five ophiolites with three distinct ages and from three orogenic belts have been described. Section 2.6 is a brief listing of other occurrences of plagiogranites from many parts of the world in support of the contention that they are a widespread, if volumetrically minor, component of ophiolites. The descriptions in the previous five sections have indicated that "plagiogranite" encompasses a variety of types but that the same compositions, textures and field associations tend to recur in each ophiolite (Section 3.1). To avoid repetition, only unusual plagiogranite types will be described specially in this section.

### 2.6.2 Ophiolite plagiogranites

Ophiolite assemblages which include plagiogranite are found in the Eocambrian; Jabal al Wask, Saudi Arabia (Bakor et al., 1976) and Bou Azzer, Morocco (Leblanc 1976 ), in the Palaeozoic; The lizard, Cornwall, England (Green 1964), Bay of Islands (Irvine et al., 1972) and Betts Cove, (Mattinson 1975) both in Newfoundland, in the Mesozoic; Montgenevre, Western Alps (Pusztaszeri 1969) Corsica (Beccaluva et al., 1977), Vourinos, Greece (Moore 1969), Guevgueli, Greece/Yugoslavia (Bebien 1977), Baër-Bassit, Syria/Turkey (Parrot 1977), Papua New Guinea, (Davies 1971) Canyon Mountain, Oregon (Thayer and Himmelberg 1968) and South Georgia (Storey et al., 1977) and in the Tertiary; East Taiwan (Liou et al., 1977), New Caledonia (Black et al., 1977), South Alaska (Tysdal et al., 1977), Dun

Mountain Belt (Coombs et al., 1976) and North Cape complex (Bennett, 1976), both in New Zealand. In some areas plagiogranite is found in clastic breccias (e.g. East Taiwan) or only in tectonic melanges. (e.g. New Caledonia).

In addition, there are many ophiolites without any acidic members at all. In most areas this could be due to incompleteness by dismemberment or non-exposure but the following are fairly complete ophiolite assemblages without plagiogranites; Pindos, Greece (Montigny et al., 1973), Antalya, Turkey (Juteau 1975), Southern Chile (Stern et al., 1976), Mings Bight, Newfoundland (Norman et al., 1975). There are two types of granitic rock in the Lizard ophiolite (Green op cit.). The more restricted is leucocratic diorite which intrudes gabbro and dolerite near Porthoustock village. It was described by Brown (1976) as being composed of saussuritized, zoned andesine/oligoclase with some fibrous amphibole and accessory opaque, sphene and zircon. No quartz or K- feldspar is present. The diorite contrasts strongly with the more widely distributed Kennack Gneiss in both mineralogy and field relationship. The misnamed Gneiss includes small bosses of undeformed microgranite and also sheared and/or contaminated dykes and veins in basic migmatite, amphibolite, gabbro and peridotite. (Green op cit.). Typically, it is composed of quartz, oligoclase, orthoclase and biotite. Strong et al., (1975) suggested the Kennack Gneiss formed by partial melting of the amphibolite and this interpretation is accepted here. If this is so, the contrast between the two granitic suites implies the plagiogranites were not formed by partial melting of a basaltic parent.

Highly sodic plagiogranites in Oregon were reported by Thayer (op.cit.). The rocks are a trondjemite with zoned plagioclase of  $An_{15}$  or less and albite granite composed of quartz and albite with minor chlorite and epidote. The albitegranite has replacement and cataclastic textures and is associated with metamorphosed dolerite. However, it seems probable that the oligoclase in the trondhjemite is primary although it is usual for plagiogranite feldspars to be zoned from labradorite or andesine to oligoclase and albite. The Canyon Mountain trondhjemite therefore appears to be evolved acidic liquid from which earlier more calcic plagioclase nuclei have been removed.

The East Papuan ophiolite is a sheet of peridotite, gabbro and basalt thrust over metamorphosed Mesozoic sediments during the early Tertiary (Davies op cit.). It has no dyke complex and the gabbros intrude the base of a 5 km. volcanic sequence which varies from basaltic to dacitic compositions. There are numerous stocks of tonalite up to 5 km. across which intrude both gabbro and basalt, commonly along their mutual contact, and also the peridotite. The tonalite has a typical plagiogranite mineralogy with accessory biotite. Davies (op. cit) suggested that some of the smaller bodies are silicic differentiates. The ophiolite is Upper Cretaceous in age (radiolarian and radiometric ages, Davies op.cit.) whereas K-Ar dates indicate an Eocene age for some of the larger tonalites, which were therefore intruded close to the emplacement date (52 my.) (Coleman 1977, p. 192). However, none of the granitic rocks transgress the basalt thrust or major fault zones within the ophiolite.

### 2.6.3 Island arc plagiogranites

A few examples of plagiogranite from modern island arcs have been described. The Japanese Miocene Tanzawa plutonic complex (20 km. x 5 km.) is composed of tonalite and trondhjemite with associated minor gabbro, intruding a thick submarine sequence of andesitic and basaltic lava, tuff and breccia. (Ishizaka and Yanagi 1977). The tonalites are composed of zoned plagioclase, quartz and amphibole with minor biotite. Pyroxene appears in some melanocratic types. No K-feldspar is found. The analysed specimens were fresh and free from alteration and have low K, Rb,  $K_2O/Na_2O$ , Rb/Sr and  $^{87}Sr/^{86}Sr$  and high K/Rb (Table 2.6.1).

The earliest phase of volcanism on Viti Levu, Fiji, is represented by a submarine series of island arc tholeiite, andesite, rhyolite, spilite and keratophyre (Gill 1970, 1976). This is intruded by penecontemporaneous trondhjemite and olivine gabbro plutons. The trondhjemite consists 60-80% strongly zoned plagioclase with sodic rims intergrown with quartz and less than 10% hornblende and/or biotite with rare hypersthene. Epidote, chlorite, calcite and sericite are common. Both island arc tholeiites and plutons are unconformably overlain by later calc-alkaline extrusives. Low alumina, LIL-depleted dacites, the extrusive equivalent of these trondhjemites, occur on Eua, Tonga (Ewart and Bryan 1972).

Minor intrusions of low-K quartz diorite cut through the lavas of the Izu-Hakone quartz tholeiite province, Japan. (Aoki and



Geochemistry of island arc plagiogranites								
	1	2	3	4	5	6	7	8
	18	1	1	1	1	9	4	43
K <sub>2</sub> O%	0.6	0.31	0.52	0.82	0.24	1.12	0.13-0.85	0.01-0.75
Rb ppm	3.9	4.6	7.9	12.1	1.9	20	<1-8	<1-6
Ba ppm	169	-	-	-	42	-	56-461	<4-140
Sr ppm	187	304	239	209	123	536	89-189	50-230
K/Rb	1282	553	548	561	1068	473		663-1660
K <sub>2</sub> O/ Na <sub>2</sub> O	0.16	0.11	0.13	0.21	0.04	0.17		
<sup>87</sup> Sr/ <sup>86</sup> Sr	-	0.7037	0.7037	0.7037	0.7044	0.7051		
RE	-	LRE enriched La/Yb = 2.0			La/Yb = 4.8	-	-	LRE depleted
Minerals Altered?	No	No	No	No	Yes	-	Yes	Yes

Table 2.6.1

1. Western Sayan, Popolitov et al. (1973), 2, 3, 4. Tanzawa Complex, Ishizaka and Yanagi (1977)
5. Vita Levu, Gill (1970), 6. Dai, Ishizaka and Yanagi (1975) 7. Smartville later plagiogranites
8. Ophiolite plagiogranites

Kuno, 1972). Fragments of similar quartz diorite and also olivine gabbro have been erupted from volcanoes in the region. The quartz diorites are mostly composed of plagioclase and quartz with subordinate pyroxene and accessory iron ore, K feldspar and apatite. Fayalitic olivine is sometimes found as well. Equivalent dacites are mentioned by Yajima et al., (1972). Small dykes and blocks of trondhjemite occur in a serpentinite mass in the Dai area, S.W. Japan (Ishizaka and Yanagi 1975).

Poplitov et al., (1973) mention "several thousand square kilometres" of LIL-depleted plagiogranite in the Western Sayan region of the U.S.S.R.. It is associated with Cambrian mafic and felsic volcanics, chert, shale and "alpine-type" peridotite. Popolitov et al., appear to believe that the plagiogranites formed by partial melting of volatile enriched mantle above a subduction zone.

#### 2.6.4 Comparison of ophiolite and island arc plagiogranites

The most obvious contrast between plagiogranites with these two associations is the occurrence of island arc plagiogranites in large stocks ( $\frac{1}{2}$ -5 km. diameter) which often intrude volcanogenic sedimentary sequences. Some island arc plagiogranites are petrographically unaltered and have anhydrous mafic minerals but the two types have very similar chemistry. The only significant differences are in Rb, Sr and RE content. Although  $K_2O$  is in the same range, Rb tends to be richer in island arc plagiogranites and so K/Rb is lower for some examples (Fig. 3.2). A Rb/Sr distribution diagram (Fig. 3.3) suggests there is a range in island arc plagiogranite compositions which is analogous

to the range from low potassium to calc-alkaline volcanic series. The Rb/Sr diagram must be interpreted with the qualification that whereas ophiolite plagiogranites are invariably hydrothermally altered, those in island arcs are sometimes not. However, the specimens from the Dai area are altered and yet maintain a moderate Rb content. (Figure 3.3). The RE elements are not so sensitive to alteration. Island arc plagiogranites are LRE enriched while most ophiolite plagiogranites are LRE depleted. Assessed by field occurrence and Rb and RE content, the later plagiogranites at Smartville resemble the island arc type more than the ophiolite type (Section 2.3.3.4).

Some island arc plagiogranites could be differentiates of low - potassium tholeiite magmas. However, the large volume of other examples suggests that they formed in the mantle by a small degree of partial melting in analogous fashion to the batholiths of the Andean Cordillera (Brown, 1977).

## 2.7 Plagiogranites from the ocean crust

### 2.7.1 Introduction

Rock types similar to those found in ophiolites have been recovered from the floors of ocean basins. (Section 1.1). Indeed, this is one of the critical pieces of evidence in the interpretation of ophiolites as ancient ocean crust. This similarity includes acidic differentiates; a small number of plagiogranite specimens having been dredged from the ocean floor. The purpose of this section is to review all such discoveries and describe their association, petrography and chemistry. Plagiogranites from present day ocean basins can no longer be collectively referred to as "oceanic plagiogranites", (Coleman, et al., 1975) instead it is proposed that the collective "ocean-crust plagiogranites" should be used to distinguish them from "ophiolite plagiogranites". Acidic rocks from volcanic islands are not considered.

Plagiogranites have been obtained from only eight localities on the ocean floor. This is a very small number when, to date, there have been about 500 DSDP boreholes and in the order of 10,000 dredge hauls. Aumento (1969) reports that 45 dredges were made in an area of the North Atlantic 250 km. by 150 km. before plagiogranites were discovered. The small number of samples is seemingly an indication that plagiogranite forms an even smaller proportion of the ocean crust than of most ophiolites. This is probably due to the fact that, with few exceptions, only the shallow levels of the oceanic crust have been sampled and also, perhaps, that ophiolites are not representative of processes within major oceans but are back-arc in origin.

### 2.7.2 Ocean-crust plagiogranites

The first plagiogranites from the ocean crust to be recognised as such were described from the Mid Atlantic Ridge (MAR) at  $45^{\circ}\text{N}$  (Aumento 1969). Aumento suggested several criteria of wide application by which to distinguish locally derived granitic rocks from ice-rafted continental material. The oceanic specimens are angular and sometimes have fresh broken surfaces. They have outer weathered zones and thick ferromanganese crusts, indicating they have rested on the sea-floor for a long period. By contrast, other granitic fragments are well rounded, sometimes with glacial striae and have no weathering or FeMn crust. Their continental origin has been confirmed in some cases by their radiometric age and isotopic composition.

The plagiogranites from  $45^{\circ}\text{N}$ ; diorite, quartz diorite and trondhjemite, were collected from a scarp-face on an upthrust block and were associated with basalt, basalt breccia and serpentized gabbros and peridotites. They enclose mafic and ultramafic xenoliths and also vary in colour index. Their petrography (Table 2.7.1) is very similar to that of ophiolite plagiogranites but some K-feldspar with sodic plagioclase rims is found in the trondhjemites. Albite rims on the plagioclase sometimes include thin orthoclase lamellae (Aumento op.cit.).

A dredge haul of gabbros from the MAR near  $24^{\circ}\text{N}$  included one specimen of sodic aplite (Miyashiro, Shido and Ewing 1970). Miyashiro et al., suggested the gabbro magma differentiated by low pressure fractionation of olivine and plagioclase to form

Table 2.7.1 Petrography of ocean-crust plagiogranites

---

Locality, rock-type, petrography

---

1. MAR 45<sup>0</sup>N, 70% zoned pl, An 40 - An20, with ab rims, rare  
Diorite K-feldspar cores. 20% primary green hnd, some  
relict cpx cores. Minor red-brown biot. Acc  
qz, mag, ap, zrc, sph, allanite. Ap, op are  
early phases. Alteration generally mild. Some  
saus, chl.

Qz Diorite As diorite, with more Qz.

Trondhjemite As diorite with 30% Qz, no hnd. Zoned pl,  
An 20 - An 5. 5% Biot.

---

2. MAR 0<sup>0</sup>, Romanche Fracture. Quartz Diorite  
Pl, qz, biot. Secondary act, chl, hnd.  
Cataclastic texture.

---

3. MAR 22<sup>0</sup> S Leucodiorite. 87% Pl, An 30, 10% qz,  
2% hnd, 1% op.  
Trondhjemite. 55% Pl, An 35 - An 30, 35% qz,  
5% hnd, 3% op, 1% sph, 1% act.

---

4. Surtsey, Iceland. Xenoliths. Quartz diorite. 85% pl,  
10% qz.  
Trondhjemite, 55% pl, 35% qz. Both with minor  
micropegmatite, K-feldspar, cpx, zrc, glass.

---

5. Argo F.Z. Leucoquartz monzonite. Fine grained, pink  
micropegmatitic. Qz, euhedral/subhedral  
oligoclase, K-feldspar. Acc Biot, hnd, ap, mag,

Table 2.71 continued

sph, zrc. In veinlet which chills on  
"granophyric diabase".

"Granophyric diabase", Med. grained, amphibolitized, with  
granophyric texture. Qz, albitized andesine,  
hnd, or, ep and abundant ap.

Aplite. Fine grained, micropegmatitic, pale green, Qz,  
oligoclase, minor amph, aegirine augite. Acc  
Ap, sph, chl, euhedral zrc.

---

1. Aumento, 1969. 2. Bonatti et al., 1970.

3. Christensen, 1977. 4. Sigurdsson, 1977. 5. Engel  
and Fisher, 1975.

the observed iron-titanium enriched gabbros and the aplite. Transform fault zones often expose sections through the ocean crust. Bonatti et al., (1970) describe harzburgite, lherzolite, dunite and plagioclase peridotite dredged from the base of the north wall of the Romanche Fracture, Equatorial MAR. Gabbros, dolerites and basalts metamorphosed in greenschist and amphibolite facies were sampled from higher up the wall. A vein of quartz diorite was found in one of the unutilized gabbros. A leucodiorite and a trondhjemite were dredged from the MAR at 22°S. (Christensen 1977).

Xenoliths in extrusives on Surtsey, Iceland, include plagiogranites and also a range of refractory materials which are the residue of partly melted plagiogranite (Sigurdsson 1968, 1977). Askja, in the eastern volcanic zone of Iceland, has also ejected partly melted plagiogranites. They are quartz diorites and trondhjemites, with variable amounts of interstitial glass, the product of partial melting. The occurrence of minor clinopyroxene is interesting in comparison to trondhjemites from ophiolites, in which the primary mafic phase is invariably hydrous. To date, only one locality in the Indian Ocean, the Argo Fracture Zone (F.Z.) on the Central Indian Ridge, has yielded plagiogranite. (Engel and Fisher 1975). It is associated with serpentized harzburgite and lherzolite, two-pyroxene gabbro, norite, FeTi gabbro and hornblende gabbro. The plagiogranites are a fine grained quartz monzonite vein cutting a medium grained granophyric quartz diorite and a fine grained aplite. Engel and Fisher (op. cit.) regarded the plagiogranites as differentiates of shallow intrusive stratiform complexes in the Central Indian Ridge.

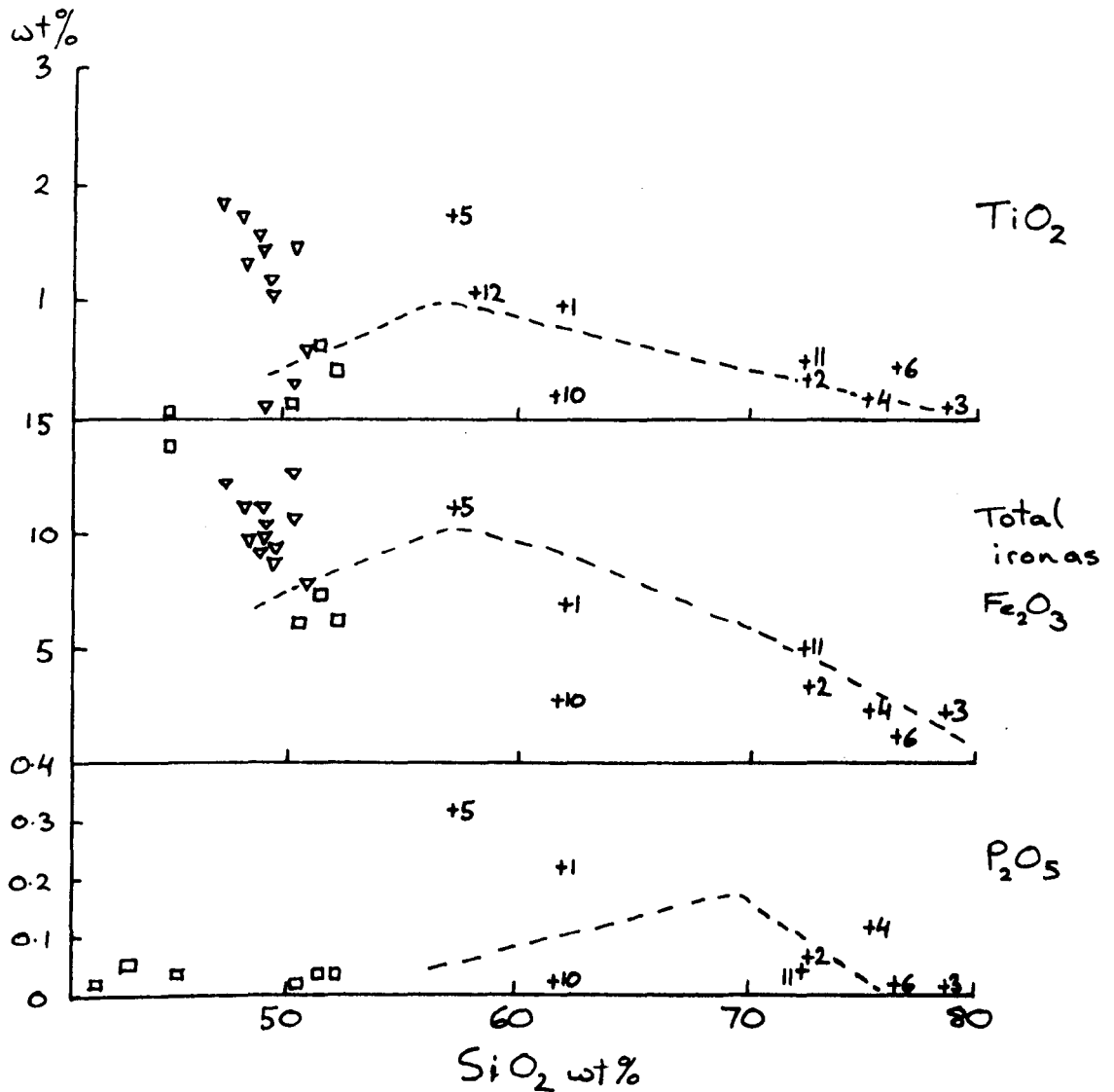


Ishizaka and Yanagi (1975) described plagiogranites from the Pacific, dredged from a seamount on the Kyushu-Palau Ridge, 500 km. south of Japan. The specimens are angular fragments of quartz diorite with a thick ferromanganoan coating. However, Uyeda et al., (1974) believe the Kyushu-Palau Ridge is an island arc. Matsuda et al., (1975) report a single plagiogranite specimen from the nearby Amami Plateau. Potassic granites dredged from the Aves Rise, in the Caribbean, (Walker et al., 1972) are probably related to destructive margin magmatism.

### 2.7.3 Geochemistry of ocean-crust plagiogranites

The published whole rock analyses of deepwater plagiogranites are displayed on chemical variation diagrams with analyses of basalts and pyroxene, hornblende and Fe-Ti rich gabbros i.e. an analogous suite to that displayed in previous sections. These diagrams must be interpreted with some reserve for they represent samples of largely unknown "field" relationships from widely isolated areas. Although the analyses may be representative of certain dredge hauls, they are unlikely to be representative of the oceanic lithosphere as a whole. However, only analyses of gabbros and basalts which are spatially related to the plagiogranites are given (Fig. 2.7.1). As noted elsewhere (Miyashiro et al., 1970, Thompson 1973), the gabbros and basalts fall on a tholeiitic differentiation trend, leading to strong enrichment in iron and titanium. The ocean-crust plagiogranites clearly define the subsequent iron-titanium depletion and alkali enrichment, although some of the more silicic types are potassium depleted. The main exception is the Argo F.Z. quartz monzonite (Engel and Fisher 1975) which

Figure 2.7.1 Variation diagrams : Ocean-crust plagiogranites

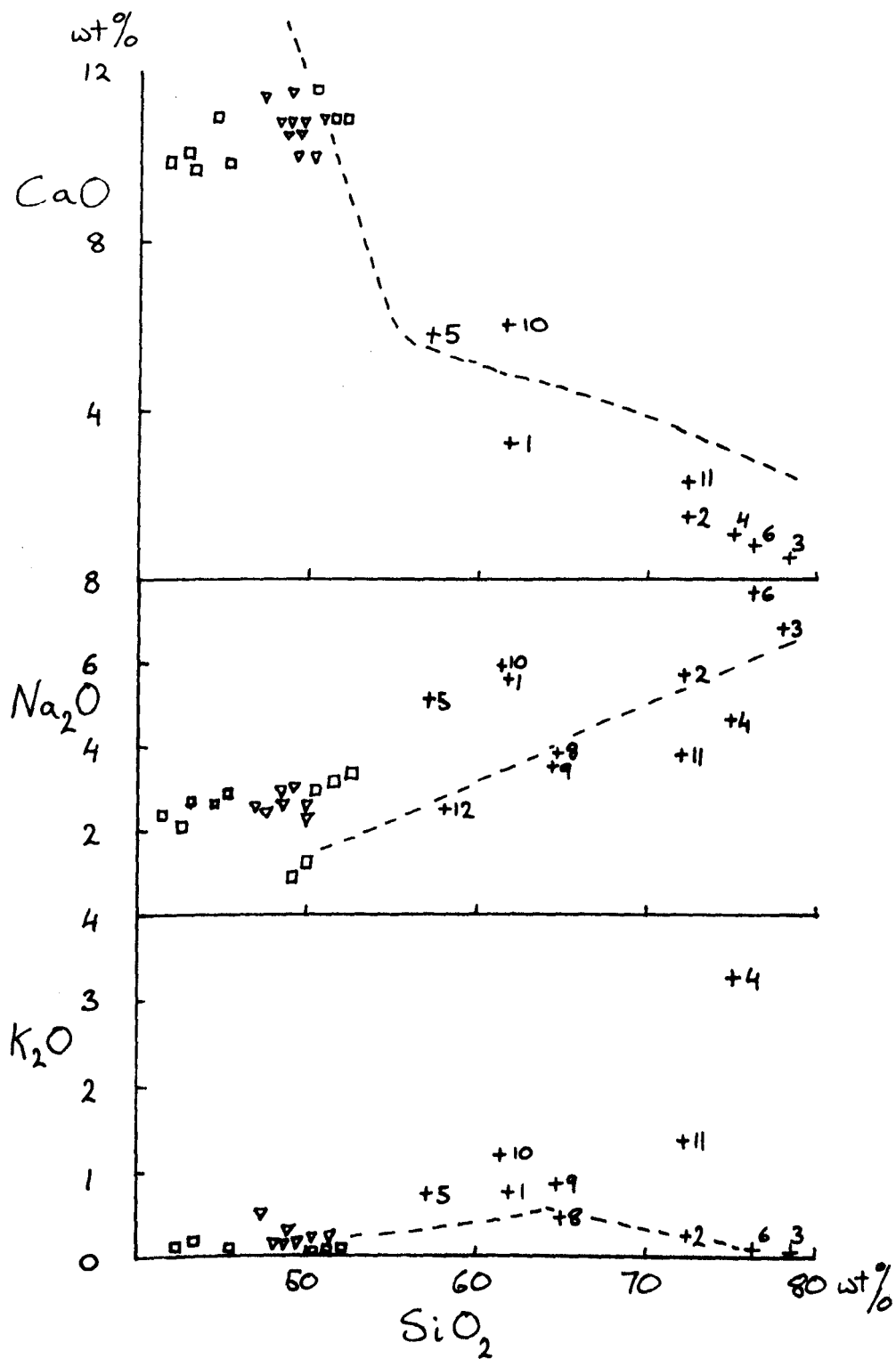


Key to ocean-crust plagiogranites

- + 1. Quartz diorite MAR 45°N Aumento 1969
- + 2. Trondjemite
- + 3. Aplite MAR 24°N Miyashiro et al. 1970
- + 4. Quartz monzonite Argo F.Z. Engel and Fisher 1975
- + 5. Quartz diorite
- + 6., 7. Aplites
- + 8., 9. Quartz diorites Ishisaka et al. 1975
- + 10., 11. Trondjemite xenoliths, Surtsey. Sigurdsson 1977
- + 12. Quartz diorite, xenolith, Izu-Hakone. Aoki and Kuno 1972

- Gabbros from Engel and Fisher 1975, Miyashiro et al. 1970, Thompson, 1973
- ▽ Basalts from Kay et al. 1970

Figure 2.7.1 continued



contains 3.27%  $K_2O$  although it is otherwise very like the rest of the samples.

The Argo F.Z. quartz monzonite and quartz diorite have very high Rb contents, compared with all other plagiogranites. Phosphorus is enriched in certain quartz diorites relative to both basalts and trondhjemites. Differentiation of tholeiitic magmas at oceanic spreading centres has been attributed to shallow level fractionation of plagioclase and olivine (Kay et al., 1970) followed by clinopyroxene, hornblende and titanomagnetite (Thompson 1973). Miyashiro et al., (1970) noted that although primary brown hornblende appeared in M.A.R. gabbros whereas it does not in ocean floor tholeiites or in continental or island arc gabbros. Chemical fractionation by this phase does not change the differentiation products.

Sigurdsson's two xenolithic trondhjemites are both relatively rich in potassium. This coupled with the appearance of clinopyroxene in place of hornblende suggests a rather low magmatic volatile content. (Section 3.2.5).

Strontium isotope ratios have been determined for ocean-crust plagiogranites from only three localities (Table 2.7.2). The close correspondence of the low values for the Argo F.Z. plagiogranites (Engel and Fisher 1975) and basalts from the Mid Indian Ocean ridge (Subbarao and Hedge 1973) indicates that they were both derived from mantle with the same depletion history. The Kyushu-Palau plagiogranites have similar low  $^{87}Sr/^{86}Sr$  values. Ishizaka et al., (1975) pointed out that it is possible that these rocks were derived from the sub-oceanic

Table 2.7.2 Initial Strontium Isotope Ratios  
of ocean-crust plagiogranites

	$^{87}\text{Sr}/^{86}\text{Sr}$	Sr	Rb	K/Rb
1. Quartz Monzonite (Argo F.Z.)	$0.7034 \pm .0003$	26	84	323
2. Quartz Diorite (Argo F.Z.)	$0.7031 \pm .0002$	124	29	206
3. Quartz Diorite (Kyushu-Palau Ridge)	$0.70334 \pm .00021$	261	3.2	1118
4. Quartz Diorite (Kyushu-Palau Ridge)	$0.70329 \pm .00009$	218	13.2	543
5. Plagiogranite (Amami Plateau)	$0.7032 \pm 4$	782	4.9	1110
6. Average basalt (Central Indian Ridge)	0.7034			
7. Basalts and gabbros O <sup>o</sup> , MAR	0.702-0.704			

(1,2) Engel and Fisher, 1975, (3,4,5) Ishizaka et al. 1975

(6) Subbarao and Hedge 1973 (7) Hart 1971

mantle by partial melting. Indeed, their Rb and Sr content is somewhat high, consistent with formation in an island arc. (Figure 3.3).

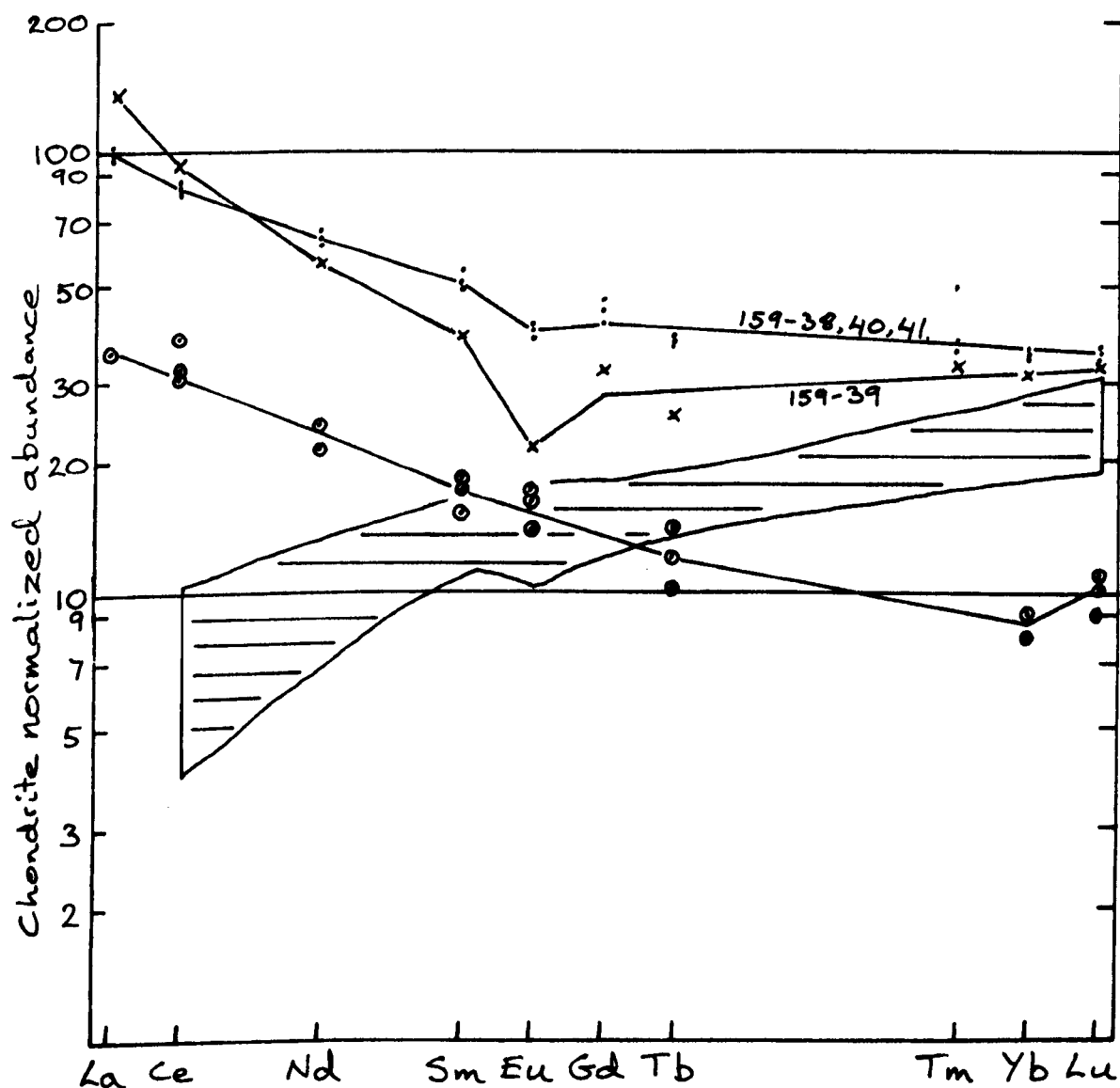
There are, to date, no published analyses of REE in ocean-crust plagiogranites. Four quartz diorites from the MAR at 45°N were analysed at the Open University. They are LRE enriched, with a negative Eu anomaly. (Figure 2.7.2). This area is one of the few sections of the MAR where LRE enriched basalts have been found (Frey et al., 1974), elsewhere they are normally LRE depleted. Basalts at 45°N are similarly enriched in other LIL elements. Schilling (1973a, 1973b) has proposed that LRE enriched basalts in the Iceland area are derived from mantle of a different (less LIL depleted) composition to typical suboceanic mantle. The relationship between the REE content of basalts and plagiogranites is the same as in other comagmatic suites. This implies that plagiogranites associated with LRE depleted basalts will be found to be similarly depleted.

#### 2.7.4 Comparison with ophiolite plagiogranites

Many of the granitic lithologies found in ophiolites have also been dredged from the ocean crust. (Diorite, quartz diorite, trondhjemite, aplite). Plagiogranites of either derivation have the same primary mineralogy, dominated by sodic plagioclase with hornblende as main mafic phase, and the same secondary assemblages and textures. Major element abundance and distribution is similar in both groups of plagiogranite. It is particularly interesting to note a tendency for more silicic ocean-crust plagiogranites to be depleted in potassium.

Figure 2.7.2 RE profiles : Ocean-crust plagiogranites

- , x 4 Quartz diorites from the MAR 45°N (present work)
- 3 Basalts from the MAR 45°N (Frey et al. 1974)
- Troodos plagiogranites (Figure 3.1)



However, the diorites from the MAR at 45°N have more accessory orthoclase and biotite than is usual in ophiolite plagiogranites. They are also somewhat richer in Ba, Zr and Ni. This might be related to the differences in RE geochemistry. (Section 2.7.3).

Neglecting products of destructive margin magmatism, there are only two exceptions to the general similarity of granitic rocks from the ocean-crust with those in ophiolites. These are the two alkalic rocks from the Argo Fracture Zone that have higher  $K_2O$ , Nb, Y and Rb and much lower K/Rb than ophiolite plagiogranites. They are far more alkalic in character than any other rocks from the Central Indian Ridge (Engel and Fisher (op. cit.)). (Table 2.7.2). The only similar rocks in any ophiolite are late Nb-rich alkalic aplites which intruded the ophiolite assemblage of Masirah Island, North Indian Ocean, which are also of unknown origin. (Moseley, 1967, I. Abbotts pers. comm.).

In summary; some ocean-crust plagiogranites cannot be distinguished from some types of ophiolite plagiogranite. This observation supports the hypothesis that ophiolites represent oceanic lithosphere fragments. However, the greater variety in the small sample of granitic rocks from the ocean crust suggests that ophiolites represent the products of only one of the several ensimatic volcanic environments.



## Chapter 3 Integration

### 3.1 Comparison of plagiogranites

#### 3.1.1 Introduction

The ophiolite plagiogranites described in Chapter 2 are here compared with each other and with other types of granitic rock in an attempt to determine (i) whether ophiolite plagiogranites are a uniform, coherent group or whether they vary spatially, temporally or with geotectonic environment and (ii) whether they can be distinguished from other granites with confidence. Even assuming that ophiolites represent oceanic lithosphere of some type (Section 1.1) each one could have been formed in one or more of the four different volcanic environments of modern oceans; (i) mid-oceanic ridges (M.O.R.s) (ii) spreading centres in marginal ocean basins behind or between island arcs (back-arc spreading centres) (iii) island arcs themselves and (iv) ocean islands. Attempts have been made to characterise the geotectonic environment of ophiolites by internal characters such as basalt trace element geochemistry (e.g. Pearce and Cann 1971) and it might seem possible that plagiogranites could be treated in an analogous fashion. However, plagiogranite geochemistry is likely to depend much more on crustal processes and so cannot approach the usefulness of basalts for indicating mantle composition and source of parental magmas.

### 3.1.2 Ophiolite plagiogranites

Comparison of the stratigraphy, lithology and thickness of the five ophiolites (Table 3.1 and 3.2) reveals more similarities than differences. The attenuation of the Point Sal sequence could be due in part to its dismemberment; the quoted thicknesses are the minimum estimates of Hopson et al., (1975). Genetic environment (Table 3.3) is inferred from several criteria discussed in previous sections (e.g. basalt geochemistry, present tectonic situation and lithological association) which do not include plagiogranite character. All the ophiolites studied, except Point Sal, appear to have been formed at back-arc spreading centres. Although there is a considerable variety of plagiogranite field types and lithologies the same types recur in the five different ophiolites. (Table 3.4). Plagiogranites occur discontinuously throughout the larger ophiolites and therefore it is not possible to state whether the non-appearance of certain field types or lithologies in the smaller ophiolites is because they were not formed or merely because of inadequate exposure. Whereas subhorizontal plagiogranite sheets regularly appear in the Upper Plutonic Complex, large, steep-sided stocks are only found in the Semail Nappe, the Smartville Block and the Papuan Ultramafic Complex. Small intrusive plagiogranite veins and dykes in the plutonic complex are ubiquitous but are found at deeper levels in some ophiolites than in others. Many can be interpreted as downward intrusions but load pressure is expected to limit this process and plagiogranite dykes deep in the Semail Plutonic Complex and Mantle Sequence may have a different genesis to those at higher levels. For instance, they could be related to late formed trondhjemitic stocks found in some areas

**Table 3.1 Comparison of ophiolite stratigraphy**

\*1972 GSA definition

Ophiolite * Sequence	Troodos Massif	Semail Nappe	Smartville	Point Sal	Ballantrae Complex
Volcanic Complex	UPL		Upper Volcanic Unit	Upper Volcanic Zone	Pillow lava
	Axis		Lower Volcanic Unit	Lower Volcanic Zone	
Dyke Complex	Sequence		Dyke Complex	Dyke and sill complex	
Gabbro Complex	Upper Plutonic Complex		Upper Plutonic Complex	Upper Plutonic Complex	Gabbro and plagiogranite
	Cumulate Sequence		Cumulate gabbro	Cumulate	
Ultramafic Complex			Serpentinities in bounding faults	Sequence	
	Mantle Sequence			Serpentine in basal fault	
Preservation	Concentrically Uplifted	Undeformed	Faulted	Dismembered by faulting	Dismembered by faulting
Mineralization	Massive and disseminated CuFe sulphide Massive and disseminated chromite		Disseminated Fe Sulphide, Some interbedded CuFeS <sub>2</sub> Sulphide		

Table 3.2 Comparative thicknesses of ophiolites and ocean crust

Vertical scale 1 cm:1 km

From Smewing et al. 1977, Hopson et al. 1975, Lewis and Bloxham 1977 and present work.

Troodos Massif	Semail Nappe	Smartville Block	Point Sal ophiolite	Ballantrae Complex	Ocean crust
volcanic units	volcanic units	volcanic units	volcanic units	volcanic units	Layer One
Dyke Complex	Dyke Complex		<del>sill complex</del>		Layer Two
plagiogranite and gabbro			<del>upper plutonics</del>		
cumulate ubasics			layered complex		
Mantle Sequence	Upper Plutonic Complex	Dyke Complex			Layer Three
	Layered Sequence	plagiogranite and gabbro		plagiogranite and gabbro	
		Mantle Sequence		Nevadan plutons	serpentinite
					Layer Four
	Metamorphic sole				

Table 3.3 Comparison of external characteristics

	Troodos Massif	Semail Nappe	Smartville	Point Sal	Byne Hill
Age of formation	Upper Cretaceous pre-Campanian	Upper Cretaceous pre-Maestrichtian	Mid-late Jurassic	Mid Jurassic (160 MY)	Arenig
"Emplacement"	pre-Maestrichtian	Lower Maestrichtian	pre-end Jurassic	Post upper Jurassic pre oligocene	pre-Caradoc
Suggested Genetic Environment	Ensimatic back-arc spreading centre then immature Bland arc	Probably as Troodos Massif	Ensimatic inter-arc spreading centre then immature island arc then island arc	Midoreanic spreading centre	Back-arc spreading centre or island arc
Geographic location	Most southerly elements in Alpine-Himalayan chain		Westernmost U.S Cordillera		Southern Scottish Caledonides

"Emplacement" refers to the time from which the ophiolite was structurally positioned on a continental margin.

Table 3.4 Distribution of Plagiogranite lithologies and field types

Type	Troodos Massif	Semail Nappe	Smartville	Point Sal	Byrne Hill
(Quartz) Diorite	✓	✓	✓	✓	✓
Leucodiorite	Rare	✓	✓	✓	✓
Tonalite	✓	✓	✓	✓	X
Trondhjemite	✓	✓	✓	X	✓
Aplite	✓	✓	X	X	X
Epidosite	✓	✓	✓	X	X
Albitite/Albite granite	X	X	X	✓	X
Porphyry	Plag and Qz	X	Plag and Or	X	X
In <u>situ</u> vein	✓	✓	✓	✓	✓
Intrusive vein Lowest level in plutonic complex	in Layered pyroxene gabbro	Most common in cumulates, also in Mantle Sequence	in vari- textured gabbro	in cumulate peridotite	-
Massive sheets in upper platonian complex	✓	✓	✓	✓	Not applicable
Intrusions in dyke swarm	✓	✓	✓	X	X
Extrusive	Rhyolites and porphyrys?	Soda-rhyolite	unknown	Quartz Kerotophyre	X
Stocks	X	✓	✓	X	X

of the Semail Nappe. (Section 2.3).

The only major difference in granitic lithology is seen at Smartville where the ophiolite is intruded by orthoclase porphyrys, which are the only rocks with more than accessory amounts of K-feldspar in the studied ophiolites. Granophyric aplites appear to be much more common in the Semail Plutonic Complex than in the others. Magnetite gabbros which are found in the Troodos Massif, the Smartville Block and at Byne Hill do not appear in the Semail Nappe. Varitextured gabbro in the Semail is very thin compared with that of Troodos (J.D. Smewing pers. comm. and present work) and this might be connected with the absence of magnetite gabbros.

The same mineralogies recur so monotonously in each plagiogranite suite that no comparative table is necessary. There are minor differences in the point at which hornblende displaces clinopyroxene as the primary mafic in the plutonic sequence. In Troodos, primary hornblende first appears in varitextured gabbro and some clinopyroxene survives in tonalites whereas at Smartville interstitial primary brown and green hornblende is found in a layered gabbro and pyroxene does not occur in the plagiogranites, even as remnants. This probably reflects differences in magmatic volatile content. Biotite is an accessory phase in several suites but only dominates hornblende as the primary mafic in the Ballantrae plagiogranites. The latter are not especially rich in potassium and so the presence of biotite must be attributed to another factor, perhaps alteration of hornblende by late magmatic fluids.

The only qualitative difference between the plagiogranite suites in secondary mineralogy is the appearance of minor interstitial prehnite in the Semail, Point Sal and Byne Hill plagiogranites. It is a late formed phase associated with, and probably replacing, clinozoisite (Deer et al., 1971 p. 278). Its presence suggests the persistence of hydrothermal activity to slightly lower temperatures than at Troodos and Smartville but does not require a drastic revision of the high geothermal gradient in ophiolites, postulated for the Troodos Axis Sequence metamorphism (Gass and Smewing 1973) as prehnite is potentially stable up to 400°C (although less in the presence of CO<sub>2</sub>). (Liou 1971).

There appear to be quantitative differences in the metasomatic alteration of the Troodos, Smartville and Semail plagiogranites (e.g. silica enrichment is more important on Troodos than elsewhere) but the uniformity in secondary assemblages and textures indicates that overall patterns of metasomatism are essentially similar. (Table 3.5).

The abundances, ranges and distribution patterns of the major elements are similar in each suite. This similarity is also apparent on AFM diagrams. (Bailey and Blake 1974). Each ophiolite suite defines a trend of initial iron enrichment with minor alkali enrichment, followed by strong relative alkali enrichment, typical of tholeiitic suites.

The abundance of immobile trace elements, judged by both range and mean value (Table 3.6) is greatest in the Smartville suite and successively less in the Semail and Troodos suites. The limited data from Point Sal correspond most closely with



Table 3.5

Patterns of Metasomatism

## Mineral

Assemblage	:	<u>Greenschist facies</u>	<u>Epidosite</u>
SiO <sub>2</sub>		+	+
Na <sub>2</sub> O		+	-
K <sub>2</sub> O		±	-
CaO		-	+
Sr		±	+
Rb		±	-
Ba		±	-
Fe <sub>2</sub> O <sub>3</sub> *		-	-
MnO		-	-
Zn		-	-
Fe <sub>2</sub> O <sub>3</sub> /FeO+ Fe <sub>2</sub> O <sub>3</sub>		+	+

+ indicates overall gain during metamorphism

- loss

± gain or loss

Table 3.6 Comparison of plagiogranite Trace element content

Troodos Massif			Semail Nappe			Smartville Block						ppm
$\bar{x}$	Range	n	$\bar{x}$	Range	n	Early			Late			
						$\bar{x}$	Range	n	$\bar{x}$	Range	n	
86	32-188	26	248	122-497	10	323	148-512	4	386	281-628	4	Zr
36	3-80	26	57	41-76	10	68	43-88	5	62	34-95	4	Y
2333	540-5940	26	3834	1620-7800	10	3768	1500-6600	5	2925	1140-6120	4	Ti
<3	<1-9	26	4	3-5	10	9	4-14	4	12	6-18	4	Nb
4.7	3.6-6.0	10	7.1	6.3-7.8	2		11.1	1		8.2	1	Yb
2.5	1.1-3.6	10	6.2	5.6-6.7	2		11.8	1		8.0	1	Hf
	<1-9	26		<1-30	10	15	4-44	4	7	5-7	4	Cr
	<1-5	26		<1-12	10		16	1		-		Ni
124	50-160	26	116	77-190	10	158	74-236	5	123	89-189	4	Sr
54	<4-137	26	93	46-102	10	104	55-155	5	235	56-461	4	Ba
	<1-2	26		<1-1	10	<1	<1-3	5	<4	<1-8	4	Rb
26	6-63	26		<1-36	10	183	7-127	5	22	7-43	4	Zn
0.7	0.2-1.2	10	0.9	0.9-1.0	2		1.3	1		1.2	1	Ge/Yb

Table 3.6 Comparison of plagiogranite Trace element content (2

$\bar{x}$	Point Sal Range	n	$\bar{x}$	Byne Hill Range	n	$\bar{x}$	Overall Range	n	ppm
	116	1		264	1	170	32-628	45	Zr
27	9-44	2		78	1	93	3-95	47	Y
	5460	2		1320	1	2954	540-7800	48	Ti
	5	1		5	1	4	<1-17	45	Nb
2.5	1.6-3.4	3	12.7	12.1-13.2	2	6.1	1.6-13.2	20	Yb
	2.4	1	8.7	8.3-9.1	2	4.9	1.1-11.8	18	Hf
	-			5	1		<1-30		Cr
	-			-			<1-12		Ni
205	182-228	2		37	1	126	50-236	47	Sr
104	68-139	2		99	1	84	<4-461	47	Ba
4	2-6	2		3	1		<1-8	47	Rb
18	17-19	2		15	1		<1-63	47	Zn
0.6	0.4-0.8	3	0.6	0.6	2	0.8	0.2-1.4	20	Ce/Yb

**Table 3.7 Comparison of Axis Sequence Geochemistry**

(1)			(2)			(3)			(4)		
Troodos Massif			Semail Nappe			Smartville Block			Ballantrae Complex		
$\bar{x}$	Range	n	$\bar{x}$	Range	n	$\bar{x}$	Range	n	$\bar{x}$	Range	n
60	5-118	88	75	16-198	38	96	41-162	7	95	64-117	4
5816	1560-9600	88	7498	2100-11340	33	7826	3900-13020	7	9236	6720-11190	4

Data from Smewing et al 1977 (1 and 2), Wilkinson and Cann 1974 (4) and present work (1,2,3)

Samples from (1) and (2) include dolerite dykes. (3) is entirely dykes.

(4) are amphibolites and glaucophane schists with ocean floor basalt characteristic.

the Troodos abundances and those from Byne Hill with Smartville. There are two factors which could affect relative trace element content of plagiogranites; variation in the magmas from which the plagiogranites evolved and variation in the evolution of the plagiogranites. The same contrasts are found in the Ti and Zr content of the Axis Sequence basalts and dolerites in the larger ophiolites suggesting that the variation in plagiogranite trace element content is governed primarily by that of its basic parent. (Table 3.7).

The mobile trace element abundances are similar in each suite, with the exception of the alkali content of the Smartville late plagiogranites and some low Ba values in the Troodos plagiogranites. The latter are attributed to secondary modification (Section 2.1.4.2). The alkali content and field relations of the late plagiogranite stocks and orthoclase porphyrys at Smartville indicate their origin in an immature island arc (Sections 2.3 and 2.6). There are, to date, no analyses of the late stocks in the Semail Nappe and none of trace elements in the Papuan tonalites and so their affinity cannot be tested. Otherwise, none of the differences between the various suites of ophiolite plagiogranites is obviously a function of geotectonic environment or age of the ophiolite, bearing in mind that there is still debate about the genetic environment of most of the areas under consideration.

### 3.1.3 Ophiolite plagiogranites and other granites

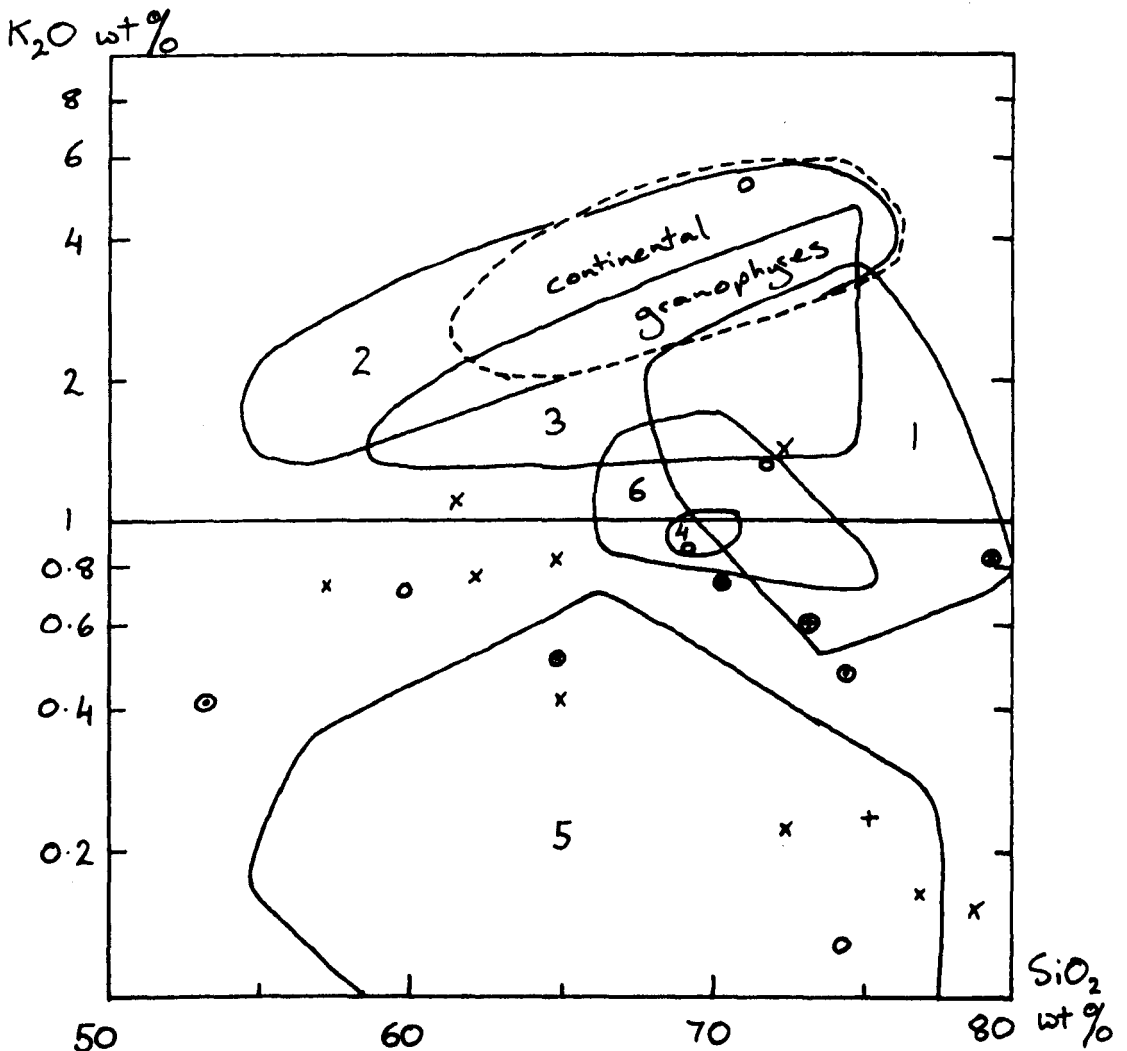
Granitic rocks in ophiolites differ from most other granitic types most simply by their lack of modal K-feldspar but also

by their low  $K_2O$ , Rb and Sr content, high K/Rb and  $Na_2O/K_2O$  ratios. However, one important plagiogranite type, trondhjemite, is also common in Phanerozoic volcanic arcs and in precambrian terrains. Barker and Arth (1976) distinguish two categories of trondhjemite-tonalite magmas; those with greater than 15%  $Al_2O_3$  and those with less. (Section 2.3.3.3). The low-alumina liquids are represented by Phanerozoic plagiogranites in ophiolites, in the ocean crust and in island arcs and also by rare Proterozoic and Archaean gneisses and plutons. They have low Rb and Sr, flat HRE profiles with either moderate LRE enrichment or, in the case of ophiolite plagiogranites only, depletion and a negative Eu anomaly. (Figure 3.1). The high alumina type occurs in precambrian plutonic suites which Barker et al., (op. cit.) believe formed by partial melting of the lower crust and also in differentiated series of all ages. High alumina trondhjemites have higher Sr than the low alumina type and are both enriched in LRE and depleted in HRE, with a small variably Eu anomaly. (Barker et al., (op. cit.)). Ophiolite plagiogranites have less potassium than continental trondhjemites although their ranges almost overlap. (Figure 3.2). Potassium content in island arc plagiogranites overlaps that of both these groups. The Smartville late plagiogranites and two acid extrusives from the Semail Nappe fall within the same range as island arc plagiogranites. Granophyric differentiates of tholeiitic intrusions are perhaps the closest continental analogues of ophiolite plagiogranites but they are much richer in potassium. Exactly the same relationships are observed in the distribution of Rb within the different groups (Figure 3.3) and there is an additional tendency for K/Rb to decrease with increasing Rb. The Rb content and Rb/Sr ratios of island arc plagiogranites fall in the same range as destructive margin



Figure 3.2 Comparative potassium content of granites

1. Low-alumina trondhjemites, New Mexico and Colorado 17 points.
2. American and Arabian calc-alkaline plutons 11 141 points
3. Klamath mountains calc-alkaline suite
4. 4 high-alumina trondhjemites from 3.
5. Plagiogranites from Troodos, Semail and Smartville
6. 7 island-arc plagiogranites, Dai area, Japan.
- ⑦ 7. 3 " , Tanzawa region, Japan.
- 8. 5 tonalites, Smartville Block.
- × 9. Ocean-crust plagiogranites, (Fig.2.7.1)
- 10. Two acid extrusives, Semail Nappe
- ⊕ 11. Average plagiogranite, Sayan, USSR.
- + 12. Low alumina tonalite from Viti Levu, Fiji.

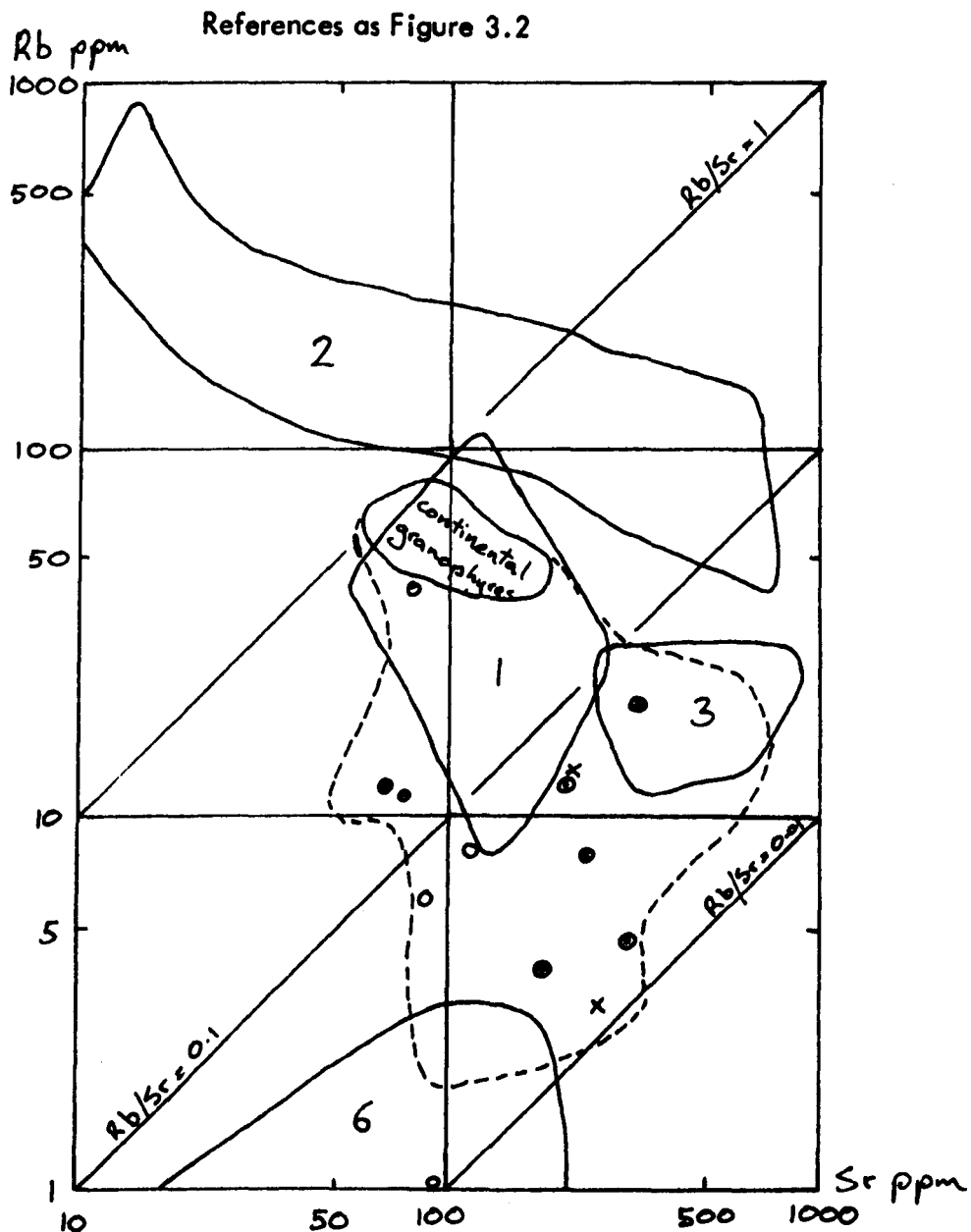


References in text and Coleman et al. 1975, Condie 1978, Barker et al. 1976, Buma 1971, Mackensie et al. 1975, Bateman 1963, Peto 1973, Nasseef et al. 1977, Hotz 1971.



Figure 3.3 Comparative Rb and Sr content of granitic rocks

1. Proterozoic low-alumina trondhjemites 17 points
  2. Calc-alkaline plutonic rocks
  3. 7 island-arc plagiogranites, Dai area, Japan.
  - ⊙ 4. 3 island-arc plagiogranites, Tanzawa region, Japan.
  - ⊕ 5. Average plagiogranite, Sayan region, USSR.
  6. Ophiolite plagiogranites, present work and Coleman et al. 1975
  - x 7. Two ocean-crust plagiogranites, Kyushu-Palao ridge
  - 8. Smartville late plagiogranites
  - 9. Smartville Orthoclase porphyrys
  - ⊗ 10. Two acid extrusives, Semail Nappe.
- Field of destructive margin volcanic rocks (Coleman et al. 1975)



volcanic rocks. Low-K tholeiites overlap the range of ophiolite plagiogranites.

All ophiolite plagiogranites have been hydrothermally altered and it might be thought that this accounts for their low alkali content. However, it has been argued in previous sections that the low abundance of  $K_2O$  is primary and has not been disguised by metasomatism.

In summary, a typical ophiolite plagiogranite can be distinguished with confidence from any other type of granitic rock by (i) very low modal K-feldspar (less than 5%) (ii) low alumina content (less than 15%) (iii) low  $K_2O$  and Rb (less than 0.75% and 4 ppm) (iv) high K/Rb (greater than about 800) and (v) RE profile (usually flat, with LRE depletion and -ve Eu anomaly although extreme differentiates or mushes with high crystal /liquid may not conform).

### 3.2 Petrogenesis of ophiolite plagiogranites

#### 3.2.1. Are ophiolite plagiogranites magmatic differentiates?

A majority of those who have considered the origin of ophiolite plagiogranites have concluded that they arose by differentiation of subalkaline tholeiitic magma (e.g. Coleman et al., 1975) and this has been accepted as the working hypothesis during the present research. The proposition is now considered in retrospect with other possible origins of ophiolite plagiogranites, hereafter referred to as plagiogranites, unless otherwise qualified.

The first of the other possibilities, most difficult to discount in the case of dismembered ophiolites, is that the plagiogranites are younger intrusions or older inclusions unrelated to the rest of the ophiolite. However, plagiogranites never trasgress the margins of the ophiolite and their complex field relations indicate they were contemporary with mafic volcanism. They appear to have been metamorphosed en mass with the Axis Sequence. Geochemical similarities between the plagiogranites, the rest of the Plutonic Sequence and the Axis Sequence, such as their depletion in LIL and LRE elements and low Sr isotope ratios indicate that they are all consanguinous. Therefore, assuming a plagiogranite is reasonably preserved and fulfills these criteria, there can be no doubt that it is cogenetic with the ophiolite.

An ensimatic granitic magma can originate by differentiation of a basic magma or by partial melting of material of basaltic or lherzolithic composition. Plagiogranites are concentrated at the top of the Plutonic Complex and in the lower Axis Sequence,

exactly the horizon at which low density differentiates would be expected to form. However, if the plagiogranites originated by partial melting at this level, there are two potential source rocks; varitextured gabbro and Axis Sequence dolerite. Both are locally recrystallized at contact with a later intrusion but are never observed to have melted. The leucocratic in situ veins in the gabbro are the only feature which could be construed as evidence for partial melting but their host is typically a partially amphibolitized gabbro with remnant igneous textures which shows no indication in hand specimen or thin section of having been reheated to melting point. Moreover, the composition of the in situ veins bears no relation to minima in the Q-Ab-An-Or-H<sub>2</sub>O system (Figure 3.4). The in situ veins have been interpreted as melted acidic xenoliths (Wilson 1959) but there is no gradation of types to unmelted xenoliths towards gabbro/tonalite contacts. The Kennack Gneiss is thought to have originated by partial melting of amphibolite in the Lizard ophiolite (Section 2.6). However, the Kennack Gneiss is unlike any plagiogranite in field association, mineralogy and chemistry.

The third possible source rock for plagiogranites, if they originated by partial melting, is mantle lherzolite. If plagiogranites were primary partial melts of mantle material, they would not be expected to be confined near the top of the Plutonic Complex. Therefore this possibility can be discounted for ophiolite plagiogranites but not, however, for island arc plagiogranites.

### 3.2.2 Constructional Processes

The plagiogranites' "stratigraphic" position overlying mafic

and ultramafic cumulates is the same as that of acidic differentiates in continental layered intrusions - the residue at the top of the magma chamber. The largest ophiolite plagiogranite bodies usually have gradational contacts with varitextured gabbro but intrude the dyke swarm. In situ veins in the gabbro are interpreted as pockets of acidic residual liquid or liquid/crystal mush trapped in the solidifying gabbro. Sharp margined plagiogranite veins and dykes crosscutting gabbro represent material which broke out of such pockets or back-veins from the main accumulation of plagiogranite magma into its host. Back veining occurs when the gabbro underlying the acidic magma is fractured. Material which enters the fracture is either a liquid or a liquid with suspended crystals. When further movement narrows a fracture containing a liquid/crystal mush the liquid is forced out. The retained phenocrysts are often crushed. This mechanism explains the origin of feldspathic veins and why they commonly have cataclastic textures where none occur in the host gabbro and why fewer quartz-rich veins are granulated.

There are two basic models for the structure of the ophiolite magma chamber. One has a single permanent, linear chamber beneath a spreading axis. The chamber is floored by harzburgite and is continually replenished while continuously adding to the plutonic complex and Axis Sequence. (Section 1.2) (Cann 1970, Greenbaum 1972). The alternative model proposes a succession of separate magma "cells" of a few km. diameter which develop at a spreading axis, differentiate and on solidification are in turn intruded by later magma bodies. (Moores and Vine 1971). Lateral breaks and intrusive boundaries in the Layered

Sequence (Allen 1975, Glennie et al., 1974), the intrusion of plagiogranites by dolerite and gabbro and the discontinuity of the plagiogranite horizon at the top of the Plutonic Complex are more difficult to account for by reference to a single magma chamber than by the multiple magma cell model. However, there is geochemical and petrographic evidence for replenishment of the magma cells (Allen 1975). The dolerites which crosscut the Upper Plutonic Complex are neither enriched nor depleted in incompatible trace elements relative to pre-plagiogranite dolerites and therefore include both early and late liquids. They are interpreted as lateral intrusions into a solidified magma cell from an active magma cell further along the spreading axis. The intrusion of plagiogranite by gabbro, which is relatively unusual, occurs when a solidified magma cell is crosscut by a later one. The layered gabbro, deposited on the floor of the magma chamber, is not usually crosscut by dykes which were, therefore, intruded from the top of the magma chamber into its roof. After each dyke is emplaced its base is truncated by the remaining magma. Alternatively the dyke increases grainsize downwards into gabbro but as it appears that relatively little gabbro, even in the Upper Plutonic Complex, represents a liquid composition, relatively few dykes are "rooted" in this way.

The existence of discrete magma chambers below the spreading axis provides two possible explanations for the lateral discontinuity of plagiogranites at the top of the Plutonic Complex. (i) If the roof and upper walls of the magma chamber are lined by massive dolerite, "underplated" as suggested by Allen (1975) for the Troodos Massif, then the residual liquid will be isolated in the middle of the chamber, some distance below the base of the dykeswarm. However, although field

relations indicate underplating in some areas, there is clear evidence that this did not occur everywhere. Where underplated dolerite is not found, the less dense acidic differentiates have pushed upwards into the Axis Sequence by stoping. This will tend to occur in the highest part of the magma chamber roof and so tend to concentrate the plagiogranites towards that point. (ii) The alternative explanation depends on a proposal in the following section; that trends of iron enrichment and alkali enrichment are mutually exclusive in the later stages of magmatic differentiation.

Spooner (1977) considered that the Troodos massive sulphide deposits originated above persistent upward jets of hydrothermal fluid in the centre of stable axially symmetrical convection cells. However, he pointed out that experimental investigations of the geometry of hydrothermal circulation indicate that the convection cells in the Troodos hydrothermal system should have been in constant lateral motion, if the Axis Sequence was heated uniformly from below. He concluded that the existence of stable jets of hydrothermal fluid required thermal highs at the base of the permeable layer which he correlated with discrete magma cells. Moreover, observation of the ocean floor at an active spreading axis during the FAMOUS project showed that lava was extruded in small separate elongate cones, implying the existence of separate magma cells beneath them (Ballard et al., 1977).

### 3.2.3 Magmatic Differentiation

The primary petrography and geochemistry of the plagiogranites, discussed in their separate sections, indicates that they differentiated by the removal of plagioclase, FeTi oxide and apatite from the magma. Zircon fractionation influences the later stages of some plagiogranite series. Hornblende, the primary mafic mineral, is always one of the last phases to crystallize and, with quartz, has little effect on differentiation. Cumulate plagiogranites, leucodiorites and leucotonalites, are direct petrographic evidence of differentiation by crystal settling and segregation of interstitial liquid by filter pressing. It was suggested in Section 3.2.2 that leucodioritic veins represent filter pressed feldspar crystal concentrates. They are most usual crosscutting gabbro, often layered gabbro, whereas intrusions into the dyke swarm were sparsely prophyritic or aphyric liquids. This phenomenon is attributed to concentration of suspended feldspars towards the base of the magma chamber.

The first plagiogranite magma appears after a hiatus in the differentiation sequence indicated by a deficiency of diorite and a change in accumulating phases. There is not a simple progression from a basic to an intermediate to an acid liquid and there is little diorite and quartz diorite relative to the volume of tonalite and trondhjemite. Indeed, many of the diorites are plagioclase cumulates. Other intermediate types which crop out between gabbro and tonalite are inhomogeneous products of incomplete segregation or, possibly, mixing. This diorite gap appears because there is usually very efficient segregation of acidic liquid from its basic parent/host. The process of segregation, suggested by field relations in general



and in situ veins in particular, is supported by the very low Cr and Ni content of the plagiogranites and the gabbros' strong depletion in incompatible elements. Segregation implies a strong contrast in the physical properties of acidic and basic fractions, probably the gabbro was near solid while the acid magma remained a mobile fluid.

The change in accumulating assemblage (from clinopyroxene and plagioclase to FeTioxide and plagioclase) is marked by a reversal or an inflexion on element variation diagrams. There is an overlap in the incompatible trace element content of dolerites and plagiogranites but a divergence in their Fe-Ti contents. This shows that the plagiogranites do not evolve from the most differentiated dolerites. Dolerite evolves to a high FeTi content by precipitating clinopyroxene and plagioclase unless FeTioxide appears on the liquidus. Removal of FeTioxide depletes the liquid in Fe, whereupon the liquid commences a trend of silica-alkali enrichment and pyroxene ceases to be an early formed phase. Therefore the appearance, or not, of a plagiogranite magma depends on the fulfilment, or not, of the particular physico-chemical conditions (probably a particular  $fO_2$ ) which are required for the early precipitation of an FeTioxide. Thus, the iron enrichment trend is "normal", in the sense that if conditions do not change then the magma will evolve to a high FeTibasalt. The existence of alternative differentiation trends strongly implies that the ophiolite magma behaves in discrete batches, at least towards the end of its evolution.

There is evidence that an evolved tholeiitic magma can unmix to two immiscible liquids; one enriched in silica and alkalis, the other in iron and phosphorus. (De 1974). Indeed, certain

magnetite-apatite rocks are the product of an immiscible relationship in a dioritic liquid. (Park et al., 1964 p. 230). However, the two liquids do not correspond to a plagiogranite and a dolerite and so the process could not enable a single batch of magma to follow both iron-enrichment and iron depletion trends. The concept has also been used to explain the origin of the Skaergaard granophyres and ferro-gabbros by McBirney (1975) who proposed that the ferro-gabbros were enriched in iron by retaining or accumulating droplets of the dense iron-rich immiscible phase during separation of the less dense silicic liquid. This has also been suggested for the Troodos plagiogranites and magnetite gabbros (Allen 1975). Magnetite gabbros are also found at Smartville and Byne Hill but not, to date, in the Semail Nappe. This means that the process which concentrates Fe and Ti in the magnetite gabbros is not essential to the generation of the plagiogranite magma.

Plagioclase zoning in the Upper Plutonic Complex follows a characteristic pattern. Crystals in which it is fully developed have an unzoned calcic core of variable size, an intricately zoned inner rim which, although zoned normally overall, often has reverse components and sometimes interzone solution features, and a sodic outer rim. The crystal maintained idiomorphy until the growth of the outer rim which in the plagiogranites is often intergrown with quartz. (Section 2.1.3.2 and 2.1.3.3). The complex inner rim represents a period of rapid disequilibrium growth and its discontinuities are interpreted as sudden depressions of liquidus temperature. As the differentiating magma appears to remain at the same depth these depressions must be due to increases in  $pH_2O$ . In order

for  $\text{pH}_2\text{O}$  to have influenced phase relationships the magma must have been water-saturated. Although Carmichael et al., (1974 p.326) point out that a magma need not be water-saturated to precipitate hydrous phases, the appearance of primary (and secondary) amphibole and variable texture, including pegmatite, at about the same point in the plutonic sequence as complex zoning in the feldspar is also attributed to a marked increase in magmatic water content. Fluid inclusions in quartz phenocrysts are direct evidence for the coexistence of an aqueous phase with the later plagiogranite magmas.

Water saturation could be achieved by concentration of juvenile water during magmatic differentiation but Carmichael et al., (1974 p. 326) consider most magmas do not attain saturation until very late in their evolution unless water enters from the country rock. Taylor (1977) proposed that assimilation of hydrated roof rock is a widespread cause of water saturation in low  $\delta^{18}\text{O}$  magmas and Heaton et al., (1977) made the same suggestion specifically for the Troodos Upper Plutonic Complex. It seems probable that a change in magma chamber conditions from slow equilibrium anhydrous crystallization to relatively rapid disequilibrium hydrated crystallization preceded the formation of the plagiogranite magma.

A change in magmatic volatile content due to indirect, or possibly direct, entry of seawater provides an explanation for the interruption of the iron enrichment trend, if it caused the early precipitation of  $\text{FeTiO}_3$ , presumably by a critical shift in  $f\text{O}_2$ . Moreover, the fall in plagioclase liquidus temperatures associated with rising  $\text{pH}_2\text{O}$  means there is a

pause in crystallization which would enable the efficient segregation of the plagiogranite magma from gabbro host. If the formation of plagiogranites depends on the interruption of one process (differentiation of the basic magma) by another which is not directly related (assimilation of hydrated dolerite xenoliths), variations in both processes might cause changes in the point at which the interruption took place, indeed it might not happen at all. This would explain the lateral discontinuity of plagiogranites in some areas (although not the only possible explanation, Section 3.2.2) and their absence in others. It could also explain the variation in the point at which primary hornblende appears in the Plutonic Complex.

Hydrothermal alteration of the Upper Plutonic complex by seawater means that direct evidence for the entry of seawater into the magma is difficult to obtain. The oxygen and hydrogen isotope content of primary hornblende was probably established during subsolidus reequilibration with hydrothermal fluids. (Heaton et al., 1977). A comparison of the composition of fluid inclusions in primary and secondary quartz could be a conclusive test of the difference in salinity of magmatic and metamorphic fluids.

After segregation of the plagiogranite magma, fractionation by plagioclase continues, the liquid composition moves rapidly towards the plagioclase-quartz cotectic and interstitial granophyres crystallize. The plagiogranites contain so little normative orthoclase (less than 5% of salic phases) that their distribution on a normative Q-Ab-An diagram is a good approximation to that in the salic tetrahedron. (Figure 3.4) Metasoma-

tism will tend to displace points towards the Q-Ab join, except in epidiosites which are shifted towards the Q-An join and so are omitted from the diagram. Even so, bearing in mind the sensitivity of the quartz-plagioclase cotectic to  $\text{pH}_2\text{O}$ , quantitative interpretation of Figure 3.4 must be made with reservation. The quartz feldspar porphyrys represent liquids on the cotectic which have begun to crystallize plagioclase, quartz and, rarely, granophyre phenocrysts and then been cooled rapidly. Their quartz phenocrysts are invariably partly resorbed following a drop in  $\text{pH}_2\text{O}$  which shifts the cotectic toward the Q apex, leaving the liquid in the plagioclase field. The drop in  $\text{pH}_2\text{O}$  also raises the liquidus temperature, whereupon the liquid freezes. Many porphyrys are found in the Axis sequence and the drop in  $\text{pH}_2\text{O}$  could occur during intrusive ascent. The feldspars are not usually zoned and a period of stagnation is suggested while feldspar crystals settle out or requilibrate before the magma is emplaced. At Mosphiloti, on the Troodos Massif, porphyrys are associated with autobrecciated, flowbanded, sparsely vesiculated felsites which could represent the water-rich silicate melt which accumulated at the top of the stagnant chamber and from which volatiles have explosively dissociated from solution during ascent. Granophyric aplite veins represent small quantities of residual magma which intruded the plutonic complex. Two examples from the Semail Nappe lie on the Q-Ab join and like the Troodos porphyrys and felsites they have dishd RE profiles. (Sections 2.1.4.5 and 2.2.3.3).

A fairly small increase in potassium content, as seen in the Smartville later plagiogranites enables the liquid to evolve to a point on the two feldspar cotectic. (above 5 kb).

The Smartville two feldspar porphyrys are equivalent to the Troodos quartz-plagioclase porphyrys.

Figure 3.4 Normative Quartz-Anorthite-Albite

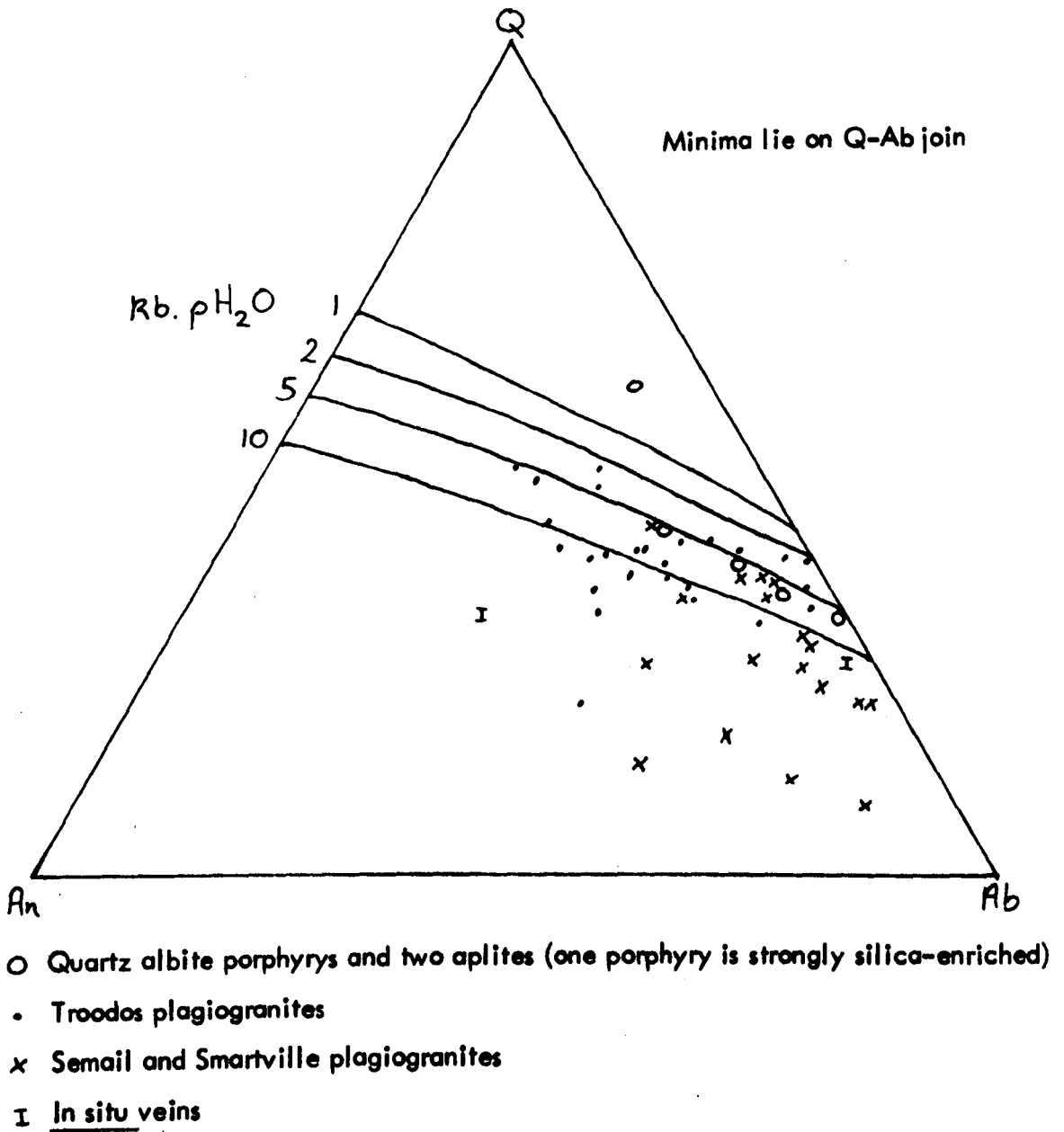


Diagram compiled from Tuttle and Bowen 1958, Luth et al. 1964 and Stewart 1967.

5kb. cotectic from Yoder 1968, other cotectics are extrapolated sub-parallel to this.

#### 3.2.4 Metamorphism

The downward increase in grade of hydrothermal metamorphism in the Axis Sequence (Gass and Smewing 1973) continues with no apparent break into the Upper Plutonic Complex, which has secondary mineral assemblages typical of the upper greenschist and lower amphibolite facies. However, some types of replacement which are found in the Upper Plutonic Complex are usually associated with deuteric alteration (alteration by magmatic volatiles) (saussuritisation of feldspar, uralitisation of cpx. and hnd., silicification) but there is no division between "deuteric" and "greenschist/amphibolite" alteration in this section and they are regarded as successive products of the same cycle of hydrothermal activity. There is also a metasomatic assemblage (epidosite) which can arise in trondhjemite or dolerite but apparently only in rocks previously altered to a greenschist facies assemblage. The same metamorphic assemblages always recur in the upper plutonic complex which always coincides with the stratigraphically lowest limit of hydrothermal activity, regardless of the thickness of the Axis Sequence. Thus, the fairly rapid transition from unaltered gabbro to amphibolitized gabbro approximates the boundary between layered pyroxene gabbro and unlayered or varitextured gabbro (Coleman 1977, and present work). Plagiogranites in the Upper Plutonic Complex are never completely unaltered.

Superimposed on this regional variation in grade is a tendency for more differentiated rock types to be metamorphosed at a lower temperature and also, perhaps consequentially, to have a larger proportion of secondary minerals. The degree of

differentiation of the various rock types can be determined from remnant primary mineralogy and immobile trace element geochemistry despite this metamorphism. There are many exceptions to this general trend which demonstrate that the differences in metamorphic assemblage are not dictated by major element geochemistry. Extreme examples of the phenomenon are altered leucocratic veins (both intrusive and in situ) in unaltered gabbro and epidotised trondhjemite which intrudes unepidotised tonalite (Plate 16) or even gabbro with pellucid feldspar and no trace of epidote. Epidosite derived from dolerite is relatively common in the dykeswarm and so this relationship cannot be due to differences in bulk composition, either. Retrograde metamorphism is also indicated by mineral replacement textures. In every instance the secondary mineral is indicative of a lower temperature. Moreover, secondary minerals are usually fine grained, often fibrous, incoherent clusters and replacement is generally incomplete and inhomogeneously developed through the rock, at hand specimen and outcrop scale. Epidotisation occurs along zones centred on joints in some outcrops, leaving kernels of less altered material but is subsequently concentrated along joints. Indeed, in some localities epidote is only found on joint surfaces or in late quartz-epidote veins.

The retrograde character of the metamorphism of the Upper Plutonic Complex indicates that it is not the result of a widespread influx of hydrothermal fluid after the rocks had formed but is achieved by deuteritic fluids that were progressively concentrated and cooled during differentiation. In contrast, the Axis Sequence metamorphism is prograde, complete and so



homogenous that the zeolite/greenschist facies boundary can be mapped. (Smewing 1975). The differentiated basic magma from which the Upper Plutonic Complex forms includes an aqueous phase in equilibrium with the silicate liquid. As differentiation proceeds, the aqueous phase cools within the silicate liquid, thus moving out of equilibrium with and tending to alter the solid phase. Thus plagioclase cores are often saussuritized by fluid which was in equilibrium with the rim, whereas a postmagmatic fluid would have altered them both. In this way, later differentiates are altered at successively lower temperatures. Ultimately the aqueous phase is discharged into the upward plume of circulating seawater in the Axis Sequence and finally into the ocean.

Spooner (1977) deduced that hydrothermal circulation in the Troodos Axis Sequence took place in persistent individual convection cells with central discharge jets above local thermal anomalies at the base of the dyke swarm associated with specific, discrete magma bodies. Narrow zones of heavily epidotized dolerite in the Troodos dyke swarm are regarded by Smewing (1975) and Heaton et al., (1977) as the heavily leached rock in such high temperature discharge zones. Epidosite is formed in a similar way from plagiogranite; by metasomatic exchange with late concentrations of the magmatic aqueous fluid.

The implications of this model are two fold; (i) that hydrothermal activity depends directly on the presence of magma, not just a geothermal gradient and so (ii) when magma in a particular cell has completely crystallized, hydrothermal activity ceases. This corresponds with previous suggestions

that hydrothermal activity and therefore ore deposition are confined to the spreading axis (Gass and Smewing 1973, Spooner and Fyfe 1973). It seems probable that discharge of deuteritic fluids into the hydrothermal system proceeds for some time before the final solidification of the silicate liquid and so the fluid in equilibrium with the plagiogranite magma is probably physically continuous with that circulating through the Axis Sequence.

### 3.2.5 The Potassium Problem

The low abundance of K, Rb and Ba in plagiogranites, relative to all other granitic rocks, cannot be wholly explained by the fractional crystallization of a subalkaline tholeiitic magma. All ophiolite lithologies are depleted in these elements but the plagiogranites are scarcely enriched with differentiation and, in some cases, later plagiogranites are depleted relative to earlier ones. This lack of enrichment is the "Potassium Problem". There are several indications that this trend is primary and undergoes only slight modification by secondary processes. The evidence for this, discussed separately in each section of Chapter 2 is (i) the general absence of K-rich phases, even their pseudomorphs, (ii) the lack of correlation between potassium depletion and mineralogical alteration. (iii) Relatively K-rich rocks in ophiolites, such as are found at Smartville, retain their alkalis during hydrothermal alteration.

Plagioclase and hornblende are the only primary minerals in plagiogranites which accommodate potassium but both have crystal/liquid partition coefficients of less than one for

potassium in basaltic, dacitic or rhyolitic liquids (Arth 1976, Nagasawa and Schnetzler 1971). Partition coefficients for Ba and Rb into hornblende are generally lower than for K and into plagioclase, about the same. There are few lattice sites in non-potassium minerals which are large enough to accomodate these elements. Therefore any fractionation by these minerals would tend to enrich the liquid in K, Ba and Rb and so an alternative explanation must be sought for a trend of non-enrichment.

If the potassium content of the silicate liquid does not increase with differentiation it must be preferentially partitioned into another coexisting phase and the sole remaining possibility is the volatile phase, probably an aqueous fluid. If the volatile phase escapes from the magma chamber, it will enter the hydrothermal system and so be lost from the Plutonic Complex. The LIL elements will then be absorbed by Axis Sequence rocks or discharged in the ocean.

It is probable that other elements besides K, Rb and Ba are significantly partitioned into the aqueous phase and so it is possible that metalliferous ores in the Axis Sequence are not entirely the product of hydrothermal leaching but include a component which was derived directly from the magma. The occurrence of ferromanganoan garnet in one granophyric aplite is interesting in this context.

Only a small increase in potassium content will enable K-feldspar to crystallize and so retain K, Rb and Ba in the magma. Moreover, if the hydrothermal system was a closed

one, instead of being open to ocean waters, K-rich fluids would be recirculated and, again, potassium would be conserved. Taylor and Coleman (1977) mention potassic granophyres which are associated with the subaerial ophiolite-like assemblage at Jabal al Tif, Saudi Arabia. They suggested that the difference in potassium content is a result of interaction with meteoric ground water instead of NaCl-rich oceanwater. Therefore plagiogranites can be expected in any area of submarine volcanicity in which there are acidic magmas sufficiently subalkaline to precipitate plagioclase followed by quartz instead of a K-feldspar or two feldspars.

### 3.3 Conclusion

Ophiolite plagiogranites, like the rest of the supramoho ophiolite, differentiate from a subalkaline tholeiite magma beneath an oceanic spreading axis, either in a marginal ocean basin or in mid-ocean. The magma evolves on a trend of iron enrichment until FeTioxides appear as fractionating phases, probably as a result of a critical increase in  $fO_2$ , following saturation of the magma by ocean water. The influx of water causes a drop in plagioclase liquidus temperature which enables efficient segregation of the plagiogranite magma from its matrix of varitextured gabbro. Subsequently, the magma follows a trend of strong silica-alkali enrichment, differentiating by the removal of plagioclase, FeTioxides, apatite and, in some suites, zircon. In addition, the alkali elements, and possibly others, are progressively depleted in the magmatic silicate phase as a result of their dissolution by the magmatic aqueous phase in the absence of a K-silicate. If FeTioxide fractionation does not occur, the magma continues on the iron-enrichment trend, evolving to a series of liquids now represented by the Axis Sequence.

The plagiogranites are metamorphosed by reaction with deuteritic fluids. Hydrothermal activity in the vicinity of the magma cell ceases soon after the last of the silicate liquid freezes and there is little repenetration of the Upper Plutonic Complex by hydrothermal fluids.

With the exception of trace element content, there is no variation amongst ophiolite plagiogranites that is related to differences in their age, geographical distribution or original geotectonic environment. Their immobile trace element content is related to that in the basaltic rocks in the same ophiolite and so varies with geotectonic environment in a similar way. Plagiogranites in island arcs are often richer in alkali elements than those in ophiolites and are also LRE enriched but their compositional ranges overlap. Plagiogranites with "island-arc" trace element characteristics occur as late intrusions in some ophiolites.

Some granitic rocks in the modern ocean crust are indistinguishable from ophiolite plagiogranites, others are like island arc plagiogranites and a few more alkalic types have also been sampled. Ophiolite plagiogranites can be distinguished from all other granitic types by their lack of modal K-feldspar, low alumina and alkali content, high K/Rb ratio and characteristic RE profile.

# Appendix 1 Major and trace element

All oxides - wt% All elements ppm

## 1.1 Troodos Massif

### Tonalites and Quartz Diorities

	TM28	TM44	TM58	TM64a	TM64b	TM65	TM81	TM82
SiO <sub>2</sub>	65.66	60.79	69.50	64.32	62.80	75.08	61.96	56.87
TiO <sub>2</sub>	0.68	0.65	0.35	0.35	0.62	0.27	0.96	0.99
Al <sub>2</sub> O <sub>3</sub>	12.93	15.57	12.95	15.27	12.94	13.25	12.65	14.70
Fe <sub>2</sub> O <sub>3</sub>	4.23	0.65	1.56	3.68	3.84	1.89	6.01	4.16
FeO	3.45	2.78	3.30	2.91	5.97	1.49	4.13	6.24
MnO	0.07	0.06	0.06	0.07	0.15	0.03	0.13	0.17
MgO	1.23	3.24	1.25	1.19	1.52	0.60	1.74	3.88
CaO	5.37	11.26	3.72	4.80	5.81	5.48	5.20	6.31
Na <sub>2</sub> O	2.93	2.93	4.69	4.15	3.52	2.74	3.06	3.68
K <sub>2</sub> O	0.58	0.27	0.24	0.51	0.37	0.12	0.32	0.35
P <sub>2</sub> O <sub>5</sub>	<u>0.24</u>	<u>0.07</u>	<u>0.10</u>	<u>0.18</u>	<u>0.06</u>	<u>0.07</u>	<u>0.12</u>	<u>0.13</u>
Total	97.37	98.27	97.72	97.43	97.60	101.02	96.28	97.48
Zr	120	37	82	40	40	107	82	53
Y	53	16	37	17	31	45	37	24
Nb	BL	BL	BL	BL	4	3	3	4
Cr	BL	14	BL	BL	BL	3	BL	3
Ni	3	11	3	3	5	BL	4	6
Sr	144	145	128	148	120	133	141	156
Rb	2	BL	BL	2	BL	BL	BL	3
Ba	70	23	48	60	59	32	53	61
Zn	15	16	30	43	63	15	41	61

- Not analysed, BL : Below detection limit

Detection limit for all trace elements : 2ppm, except Ba : 7ppm

## Appendix 1.1 continued

	TM101	TM108	TM123	TM128	TM144	TM146	TM160
SiO <sub>2</sub>	66.70	68.2	73.07	65.91	65.90	68.2	72.94
TiO <sub>2</sub>	0.47	0.52	0.37	0.55	0.55	0.36	0.23
Al <sub>2</sub> O <sub>3</sub>	11.98	13.52	14.49	13.08	12.93	12.56	14.10
Fe <sub>2</sub> O <sub>3</sub>	5.13	4.91	4.89	3.83	3.19	3.25	2.81
FeO	3.22	3.05	1.85	3.72	4.20	2.98	1.38
MnO	0.17	0.05	0.04	0.09	0.11	0.07	0.03
MgO	1.89	0.75	0.58	1.90	1.52	0.85	0.51
CaO	3.17	4.77	4.07	3.56	5.31	3.83	3.68
Na <sub>2</sub> O	4.51	4.04	4.45	4.00	3.55	4.33	4.78
K <sub>2</sub> O	0.19	0.12	0.08	0.68	0.29	0.22	0.06
P <sub>2</sub> O <sub>5</sub>	<u>0.07</u>	<u>0.24</u>	<u>0.09</u>	<u>0.10</u>	<u>0.10</u>	<u>0.13</u>	<u>0.07</u>
Total	97.5	100.17	103.98	97.42	97.65	96.78	100.59
Zr	34	82	112	94	55	113	84
Y	34	55	49	39	28	44	23
Nb	4	4	4	4	4	3	BL
Cr	BL	BL	4	5	BL	BL	5
Ni	3	6	BL	5	5	4	BL
Sr	69	136	135	143	116	130	152
Rb	BL	BL	BL	2	BL	BL	BL
Ba	38	46	59	48	77	44	88
Zn	62	22	17	14	37	18	13



## Appendix 1.1 continued

	Trondhjemites						
	GA2	GA18	GA19	GA29	GK2	TM33*	TM89
SiO <sub>2</sub>	68.40	73.45	72.54	71.46	65.23	77.02	71.02
TiO <sub>2</sub>	0.47	0.18	0.41	0.39	0.58	0.09	0.38
Al <sub>2</sub> O <sub>3</sub>	12.98	12.28	14.05	12.56	12.24	13.66	12.32
Fe <sub>2</sub> O <sub>3</sub>	2.75	1.27	1.14	4.45	5.28	1.36	4.02
FeO	3.74	2.15	1.45	4.00	3.55	0.88	1.37
MnO	0.08	0.06	0.03	0.09	0.08	0.01	0.07
MgO	0.78	0.51	1.12	0.59	1.56	0.42	0.71
CaO	5.34	2.38	4.79	5.25	2.60	3.10	1.98
Na <sub>2</sub> O	3.81	5.21	4.36	2.85	5.55	3.09	6.40
K <sub>2</sub> O	0.17	0.13	0.09	0.13	0.42	0.68	0.12
P <sub>2</sub> O <sub>5</sub>	<u>0.19</u>	<u>0.03</u>	<u>0.09</u>	<u>0.09</u>	<u>0.05</u>	<u>0.01</u>	<u>0.07</u>
Total	98.71	97.65	100.07	101.86	97.14	100.32	98.46
Zr	82	99	95	36	32	134	188
Y	38	35	25	27	26	80	64
Nb	3	3	BL	4	8	9	5
Cr	3	5	15	6	11	3	BL
Ni	3	BL	BL	BL	BL	2	3
Sr	126	111	150	80	92	118	90
Rb	BL	BL	BL	BL	BL	2	BL
Ba	56	131	76	54	59	54	47
Zn	23	25	12	26	35	30	28

\*Aplite

## Appendix 1.1 continued

	Epidosites						
	TM129	TM156	GA14	GA15	GA17	TM13	TM112
SiO <sub>2</sub>	76.57	76.66	75.73	76.64	75.33	75.69	72.18
TiO <sub>2</sub>	0.32	0.32	0.24	0.16	0.23	0.15	0.37
Al <sub>2</sub> O <sub>3</sub>	12.94	12.77	12.07	12.70	12.92	11.58	12.21
Fe <sub>2</sub> O <sub>3</sub>	0.93	1.93	1.32	2.23	1.85	1.53	2.17
FeO	0.19	0.89	0.72	0.61	1.64	2.42	0.42
MnO	0.02	0.03	0.03	0.01	0.05	0.05	0.02
MgO	0.39	0.70	0.48	0.15	0.37	0.55	2.22
CaO	1.64	4.19	3.29	1.81	2.66	3.58	6.56
Na <sub>2</sub> O	7.26	3.86	5.42	5.98	5.18	3.57	1.88
K <sub>2</sub> O	0.12	0.26	0.08	0.21	0.14	0.22	0.38
P <sub>2</sub> O <sub>5</sub>	<u>0.01</u>	<u>0.06</u>	<u>0.06</u>	<u>0.02</u>	<u>0.04</u>	<u>0.09</u>	<u>0.12</u>
Total	100.39	101.67	99.44	100.52	100.42	99.43	98.53
Zr	128	143	102	122	93	61	114
Y	3	18	35	44	35	42	43
Nb	BL	BL	BL	BL	BL	6	4
Cr	BL	6	BL	BL	8	BL	9
Ni	BL	3	3	3	BL	2	4
Sr	52	126	160	116	130	124	120
Rb	BL	BL	BL	BL	BL	BL	2
Ba	46	48	BL	102	137	56	36
Zn	6	9	10	10	14	17	6

Appendix 1.1 continued

	Rhyolites					Insitu	Varitextured
						Vein	Gabbros
	TM158*	GA11	GA16*	GA25*	QAP*	TM139	TM05
SiO <sub>2</sub>	76.40	76.46	75.60	75.73	80.87	61.71	54.27
TiO <sub>2</sub>	0.18	0.18	0.20	0.16	0.19	0.79	0.25
Al <sub>2</sub> O <sub>3</sub>	13.14	11.77	12.83	12.57	9.84	14.28	14.42
Fe <sub>2</sub> O <sub>3</sub>	2.17	1.08	1.86	2.09	0.10	0.59	2.69
FeO	0.83	0.30	0.91	0.78	1.92	2.93	5.27
MnO	0.04	0.01	0.02	0.02	0.04	0.08	0.13
MgO	0.38	0.42	0.41	0.28	0.61	3.24	10.33
CaO	3.04	0.47	2.80	1.13	1.42	10.16	10.59
Na <sub>2</sub> O	5.01	6.56	5.96	7.68	3.47	2.52	0.70
K <sub>2</sub> O	0.04	0.07	0.21	0.02	0.37	0.26	0.33
P <sub>2</sub> O <sub>5</sub>	<u>0.03</u>	<u>0.02</u>	<u>0.04</u>	<u>0.03</u>	<u>0.03</u>	<u>0.09</u>	<u>0.02</u>
Total	101.26	97.34	100.84	100.49	98.86	96.65	99.00
Zr	90	102	122	81	117	38	14
Y	38	19	43	37	47	84	12
Nb	3	3	3	BL	3	BL	2
Cr	BL	6	7	6	BL	7	72
Ni	3	BL	BL	BL	3	19	33
Sr	139	34	157	42	73	157	56
Rb	BL	BL	BL	BL	4	BL	2
Ba	60	BL	66	54	135	53	33
Zn	25	13	9	8	12	20	24

\*Quartz - plagioclase phyric

## Appendix 1.1 continued

	TM49	TM56	TM79	TM116	TM134	TM140	TM162
SiO <sub>2</sub>				50.48		50.69	54.46
TiO <sub>2</sub>				0.28		0.34	0.23
Al <sub>2</sub> O <sub>3</sub>				13.38		15.71	14.14
Fe <sub>2</sub> O <sub>3</sub>				1.91		1.78	2.54
FeO				6.49		5.67	5.83
MnO				0.16		0.12	0.14
MgO				12.60		10.03	9.02
CaO				12.92		13.98	9.61
Na <sub>2</sub> O				0.94		1.45	2.30
K <sub>2</sub> O				0.11		0.14	0.42
P <sub>2</sub> O <sub>5</sub>				<u>0.02</u>		<u>0.02</u>	<u>0.03</u>
Total				99.29		99.93	98.72

Zr	16	7	11	15	24	20	12
Y	9	2	5	7	8	9	9
Nb	BL	BL	BL	BL	BL	BL	3
Cr	113	351	59	52	114	59	64
Ni	51	80	121	53	42	54	34
Sr	77	26	67	66	98	108	73
Rb	BL	BL	BL	BL	BL	BL	BL
Ba	27	27	24	15	50	31	29
Zn	29	47	64	38	32	37	44

## Appendix 1.1 continued

	GA8	HG	Layered				TM102	TM103	MG
			pyroxene gabbro	Olivine gabbro	Leuco gabbro	Magnetite Gabbros			
			TM59	TM78	TM10				
SiO <sub>2</sub>		51.93	48.23	45.09	47.19	49.00	52.07	48.07	
TiO <sub>2</sub>		0.39	0.20	0.17	1.04	0.89	1.14	1.88	
Al <sub>2</sub> O <sub>3</sub>		15.09	18.15	15.76	28.69	16.24	14.96	12.40	
Fe <sub>2</sub> O <sub>3</sub>		2.38	1.88	2.29	1.83	4.11	3.62	3.69	
FeO		5.51	5.56	9.27	1.05	8.49	9.57	10.64	
MnO		0.15	0.15	0.19	0.02	0.20	0.24	0.19	
MgO		10.13	10.51	15.09	1.38	6.30	4.55	8.55	
CaO		12.93	14.68	10.92	11.77	9.70	6.62	11.55	
Na <sub>2</sub> O		1.35	0.77	0.57	4.24	2.25	2.44	1.10	
K <sub>2</sub> O		0.11	0.02	0.01	0.22	0.46	0.80	0.13	
P <sub>2</sub> O <sub>5</sub>		<u>0.04</u>	<u>0.00</u>	<u>0.00</u>	<u>0.09</u>	<u>0.02</u>	<u>0.03</u>	<u>0.03</u>	
Total		100.01	100.15	99.36	97.52	97.66	96.04	98.23	
Zr	21	22	6	3	70	8	14	18	
Y	9	10	BL	BL	BL	4	12	9	
Nb	BL	BL	BL	BL	3	3	BL	BL	
Cr	275	211	178	165	13	34	8	71	
Ni	77	65	50	226	4	12	5	48	
Sr	85	71	61	60	354	82	84	61	
Rb	BL	BL	BL	BL	BL	2	4	BL	
Ba	43	36	31	7	43	53	63	67	
Zn	34	51	44	68	13	77	99	71	

## Appendix 1.1 continued

Dolerites					
	TM122	TM124*	TM142	TM143**	GA4
SiO <sub>2</sub>	52.86	54.28	58.77	49.48	54.32
TiO <sub>2</sub>	0.43	0.50	0.97	0.79	0.52
Al <sub>2</sub> O <sub>3</sub>	13.38	14.63	12.30	15.41	16.81
Fe <sub>2</sub> O <sub>3</sub>	5.26	3.24	3.61	3.39	2.82
FeO	4.94	6.43	5.61	6.33	5.10
MnO	0.19	0.20	0.15	0.16	0.15
MgO	10.84	8.58	3.22	9.29	5.84
CaO	8.72	10.21	6.46	8.79	9.07
Na <sub>2</sub> O	1.81	1.44	3.91	2.63	3.05
K <sub>2</sub> O	0.27	0.03	0.21	0.11	0.57
P <sub>2</sub> O <sub>5</sub>	<u>0.03</u>	<u>0.03</u>	<u>0.10</u>	<u>0.05</u>	<u>0.03</u>
Total	98.73	99.57	95.31	96.43	98.28
Zr	21	21	70	43	23
Y	9	11	29	17	15
Nb	3	3	BL	BL	BL
Cr	256	167	12	100	17
Ni	66	48	13	49	21
Sr	72	74	144	99	150
Rb	BL	BL	BL	BL	4
Ba	38	33	46	51	77
Zn	37	67	46	61	38

\*Cpx - pl phyric

\*\*Cpx - phyric

# Appendix 1.2

## The Semail Nappe

### Tonalites and Quartz Diorites      Trondhjemites

OM3017   OM3077   OM3107   OM3110   OM3037   OM3119

SiO <sub>2</sub>	58.67	65.57	62.00	62.14	75.57	71.45
TiO <sub>2</sub>	1.30	0.55	0.57	0.89	0.27	0.38
Al <sub>2</sub> O <sub>3</sub>	14.47	13.92	13.25	14.80	12.81	12.78
Fe <sub>2</sub> O <sub>3</sub> *	10.06	5.89	7.28	7.15	2.55	3.17
MnO	0.23	0.10	0.11	0.06	0.01	0.03
MgO	3.89	1.21	1.66	2.28	0.34	1.13
CaO	5.44	3.00	3.66	5.82	1.92	2.04
Na <sub>2</sub> O	5.50	6.93	5.62	4.73	6.66	5.82
K <sub>2</sub> O	0.15	0.18	0.40	0.25	0.06	0.31
P <sub>2</sub> O <sub>5</sub>	<u>0.49</u>	<u>0.22</u>	<u>0.24</u>	<u>0.15</u>	<u>0.03</u>	<u>0.08</u>
Total	100.20	97.57	94.79	98.27	100.22	97.19

Zr	243	122	235	147	497	313
Y	54	68	57	41	46	76
Nb	4	4	4	4	5	3
Cr	2	30	5	9	4	9
Ni	BL	12	BL	10	BL	BL
Sr	181	109	124	190	77	104
Rb	BL	BL	BL	BL	BL	BL
Ba	78	93	51	46	102	65
Zn	36	11	15	3	BL	BL

## Appendix 1.2 continued

	Aplites				Epidosites	
	OM3000	OM3085	OM3090	OM3093	OM3011a	OM3011b
SiO <sub>2</sub>	72.99	77.20	77.44	77.38	66.98	70.13
TiO <sub>2</sub>	0.31	0.08	0.09	0.19	0.87	0.57
Al <sub>2</sub> O <sub>3</sub>	12.98	13.27	12.98	13.31	13.92	13.71
Fe <sub>2</sub> O <sub>3</sub> *	2.44	0.54	0.78	1.22	1.86	1.97
MnO	0.03	0.01	0.03	0.02	0.06	0.04
MgO	1.33	0.13	0.48	0.42	1.58	0.81
CaO	2.35	0.72	0.79	2.99	3.86	3.69
Na <sub>2</sub> O	6.65	8.30	7.98	4.89	8.27	7.76
K <sub>2</sub> O	0.02	0.03	0.03	0.16	0.02	0.01
P <sub>2</sub> O <sub>5</sub>	<u>0.04</u>	<u>0.02</u>	<u>0.01</u>	<u>0.02</u>	<u>0.26</u>	<u>0.12</u>
Total	99.14	100.30	100.61	100.78	97.68	98.81
Zr	140	97	129	40	270	240
Y	5	18	35	9	53	51
Nb	2	3	2	BL	6	3
Cr	35	7	15	7	6	4
Ni	4	BL	BL	BL	BL	BL
Sr	56	31	18	111	66	86
Rb	BL	BL	BL	BL	BL	BL
Ba	24	20	43	75	49	45
Zn	7	BL	BL	3	5	BL



Appendix 1.2 continued

	Rhyolites				<u>Insitu veins</u>	
	OM3024	OM3078	OM3102	OM3104*	OM3071	OM3073
SiO <sub>2</sub>	71.81	67.24	79.08	70.44	72.81	57.55
TiO <sub>2</sub>	0.40	0.59	0.22	0.26	0.31	0.48
Al <sub>2</sub> O <sub>3</sub>	11.63	13.26	9.74	10.91	13.68	17.39
Fe <sub>2</sub> O <sub>3</sub> *	3.50	2.09	3.72	4.85	2.50	5.34
MnO	0.04	0.03	0.14	0.11	0.04	0.07
MgO	1.68	1.19	0.53	0.26	0.61	1.93
CaO	4.33	5.53	1.32	4.73	1.43	8.79
Na <sub>2</sub> O	4.41	6.57	3.61	1.66	7.85	7.82
K <sub>2</sub> O	0.07	0.02	0.83	0.75	0.06	0.01
P <sub>2</sub> O <sub>5</sub>	0.09	0.22	0.03	0.02	0.06	0.13
Total	97.96	97.74	99.22	93.99	99.35	99.51
Zr	180	235	107	138	401	271
Y	63	56	32	40	11	40
Nb	2	4	3	3	2	3
Cr	7	4	3	6	5	4
Ni	2	2	BL	BL	BL	4
Sr	99	218	67	321	54	76
Rb	BL	BL	12	20	BL	BL
Ba	18	43	148	107	21	15
Zn	BL	2	37	60	4	5

\*Glass

## Appendix 1.2 continued

Varitextured  
Gabbros

	OM3088	OM3018*	OM3029	OM3038	OM3074	OM3082
SiO <sub>2</sub>	72.98	54.95	54.19	48.53	47.34	48.47
TiO <sub>2</sub>	0.31	1.50	1.57	0.76	0.40	0.44
Al <sub>2</sub> O <sub>3</sub>	15.19	12.45	13.65	14.55	15.01	15.34
Fe <sub>x</sub> O <sub>3</sub> *	1.49	9.45	11.47	9.16	8.71	8.51
MnO	0.03	0.16	0.14	0.13	0.14	0.14
MgO	0.78	7.03	5.89	8.00	10.74	10.63
CaO	3.87	8.81	7.47	12.43	13.06	12.55
Na <sub>2</sub> O	5.59	4.62	4.30	2.39	1.81	2.01
K <sub>2</sub> O	0.20	0.17	0.21	0.08	0.06	0.20
P <sub>2</sub> O <sub>5</sub>	0.05	0.12	0.12	0.05	0.02	0.04
Total	100.49	99.26	99.01	96.08	97.29	98.33
Zr	114	95	92	39	14	32
Y	10	33	34	21	10	12
Nb	2	4	5	BL	BL	BL
Cr	8	BL	19	47	330	369
Ni	BL	BL	5	39	128	127
Sr	152	213	210	186	103	143
Rb	BL	BL	BL	BL	BL	BL
Ba	77	48	63	28	21	25
Zn	BL	21	22	21	50	24

\*Foliated Qz gabbro

Appendix 1.2 continued

	Dolerites					
	OM3089*	OM3117	OM3010	OM3012	OM3013	OM3039
SiO <sub>2</sub>	49.62	53.39	51.28	50.18	53.95	53.17
TiO <sub>2</sub>	0.14	1.59	0.98	1.89	1.35	1.63
Al <sub>2</sub> O <sub>3</sub>	10.32	13.44	13.53	12.40	13.27	13.77
Fe <sub>2</sub> O <sub>3</sub> *	7.30	12.50	10.35	13.83	10.93	11.84
MnO	0.13	0.12	0.16	0.25	0.11	0.15
MgO	15.53	6.72	8.36	6.49	6.95	5.46
CaO	16.15	7.34	11.60	7.80	10.10	9.81
Na <sub>2</sub> O	0.38	3.94	2.78	2.92	3.20	2.76
K <sub>2</sub> O	0.02	0.16	0.09	0.12	0.12	0.06
P <sub>2</sub> O <sub>5</sub>	0.00	0.11	0.07	0.25	0.11	0.16
Total	99.59	99.31	99.20	96.13	100.09	98.81
Zr	2	67	54	146	83	127
Y	3	29	3	46	35	38
Nb	2	2	BL	5	3	3
Cr	1063	19	136	12	19	36
Ni	144	BL	43	10	5	16
Sr	61	148	61	196	171	170
Rb	BL	BL	BL	BL	BL	BL
Ba	8	53	8	54	42	47
Zn	23	7	23	108	10	8

\*Fresh two-pyroxene gabbro

Appendix 1.2 continued

	OM3063	OM3124	OM3125	OM3126*	OM3127	OM3128
SiO <sub>2</sub>	49.13	55.95	52.43	52.54	50.91	51.41
TiO <sub>2</sub>	0.71	1.16	1.32	1.32	1.26	1.68
Al <sub>2</sub> O <sub>3</sub>	14.94	14.00	11.61	13.14	11.72	12.22
Fe <sub>2</sub> O <sub>3</sub> *	9.56	10.60	12.11	11.88	13.61	13.24
MnO	0.16	0.07	0.10	0.09	0.17	0.10
MgO	8.41	5.95	7.07	5.47	7.95	7.06
CaO	11.78	4.67	5.54	6.12	5.99	6.07
Na <sub>2</sub> O	2.53	3.65	4.46	4.98	3.08	4.02
K <sub>2</sub> O	0.21	0.41	0.09	0.04	0.50	0.19
P <sub>2</sub> O <sub>5</sub>	0.04	0.16	0.13	0.13	0.11	0.11
Total	97.47	96.62	94.86	95.71	95.30	96.10
Zr	42	142	106	120	93	95
Y	21	41	38	41	33	32
Nb	BL	4	BL	2	2	5
Cr	165	7	13	11	16	24
Ni	50	BL	BL	BL	BL	5
Sr	141	526	105	44	236	315
Rb	BL	BL	BL	BL	BL	BL
Ba	25	73	38	30	82	59
Zn	14	7	6	9	18	8

\*Plagioclase phyrlic

Appendix 1.2 continued

	OM3129	OM3130	OM3131	OM3132	Om3133
SiO <sub>2</sub>	57.74	51.70	52.12	50.60	52.38
TiO <sub>2</sub>	1.06	1.42	1.38	1.23	1.64
Al <sub>2</sub> O <sub>3</sub>	13.37	12.27	12.11	12.93	12.12
Fe <sub>2</sub> O <sub>3</sub> *	10.14	12.82	12.46	11.57	13.75
MnO	0.10	0.15	0.09	0.10	0.19
MgO	4.35	7.17	7.32	7.89	6.73
CaO	4.44	6.27	5.67	8.85	6.36
Na <sub>2</sub> O	4.02	3.45	3.61	2.70	3.39
K <sub>2</sub> O	0.15	0.25	0.23	0.24	0.19
P <sub>2</sub> O <sub>5</sub>	0.17	0.11	0.13	0.13	0.10
Total	95.54	95.61	95.12	96.24	96.85
Zr	153	99	114	100	98
Y	44	32	37	32	37
Nb	4	4	3	4	3
Cr	6	15	14	19	18
Ni	BL	BL	BL	2	2
Sr	201	503	567	351	173
Rb	BL	BL	BL	BL	BL
Ba	38	65	56	47	47
Zn	3	18	5	4	23

Appendix 1.2 continued

	OM3134	OM3135
SiO <sub>2</sub>	57.07	57.05
TiO <sub>2</sub>	1.06	1.08
Al <sub>2</sub> O <sub>3</sub>	14.08	13.88
Fe <sub>2</sub> O <sub>3</sub> *	9.95	9.89
MnO	0.13	0.12
MgO	4.37	4.49
CaO	6.27	5.85
Na <sub>2</sub> O	2.77	2.85
K <sub>2</sub> O	0.25	0.24
P <sub>2</sub> O <sub>5</sub>	0.17	0.17
	<hr/>	<hr/>
Total	96.12	95.62
Zr	143	148
Y	44	45
Nb	3	BL
Cr	5	3
Ni	BL	BL
Sr	178	217
Rb	BL	BL
Ba	50	51
Zn	10	9

OM3134 and 3135 are from the same dyke

# Appendix 1.3

## The Smartville Block

	Tonalites and Quartz Diorites				Trondhjemites		
	SM48	SM56	SM64	SM73	SM01	SM11	SM17
SiO <sub>2</sub>	59.73	69.09	61.60	67.24	69.07	74.17	65.75
TiO <sub>2</sub>	1.02	0.31	0.65	0.60	0.51	0.19	0.68
Al <sub>2</sub> O <sub>3</sub>	14.82	13.89	17.30	15.59	14.41	13.41	13.47
Fe <sub>2</sub> O <sub>3</sub> *	8.74	4.56	5.89	4.57	4.82	3.27	6.86
MnO	0.19	0.11	0.08	0.10	0.08	0.08	0.14
MgO	3.92	0.30	0.90	1.04	0.52	0.10	1.19
CaO	2.60	1.82	4.45	5.15	2.65	2.14	2.50
Na <sub>2</sub> O	7.08	6.70	7.41	5.56	8.01	6.61	7.44
K <sub>2</sub> O	0.71	0.85	0.08	0.12	0.04	0.13	0.11
P <sub>2</sub> O <sub>5</sub>	0.31	0.06	0.18	0.27	0.09	0.01	0.16
Total	99.12	97.69	98.54	100.24	99.20	100.11	98.30
Zr	314	322	728	148	512	628	345
Y	57	61	48	43	88	95	69
Nb	13	9	4	4	14	18	9
Cr	7	5	3	4	4	7	9
Ni	BL	BL	BL	BL	BL	BL	BL
Sr	119	89	195	236	105	95	74
Rb	8	6	BL	BL	BL	BL	BL
Ba	276	461	157	155	89	148	55
Zn	43	26	14	13	7	7	28

Appendix 1.3 continued

	Epidosite		<u>Insitu</u>	Orthoclase	Varitextured		
			<u>vein</u>	Porphyrys	Gabbros		
	SM40	SM29	SM28	SM15	SM57	SMO7	SM43
SiO <sub>2</sub>	72.50	76.38	64.09	71.06	71.52	50.30	54.57
TiO <sub>2</sub>	0.25	0.43	0.85	0.22	0.28	0.58	1.44
Al <sub>2</sub> O <sub>3</sub>	13.94	10.52	14.94	14.42	14.12	12.54	14.03
Fe <sub>2</sub> O <sub>3</sub> *	4.04	4.12	2.19	3.03	3.83	8.38	10.75
MnO	0.03	0.06	0.06	0.08	0.15	0.15	0.18
MgO	0.30	0.97	2.80	0.29	0.18	12.07	6.35
CaO	3.42	6.34	8.39	0.94	1.61	13.92	8.25
Na <sub>2</sub> O	5.56	2.59	4.63	4.36	6.63	1.74	3.85
K <sub>2</sub> O	0.08	0.11	0.48	5.32	1.33	0.13	0.19
P <sub>2</sub> O <sub>5</sub>	0.03	0.06	0.02	0.03	0.04	0.03	0.18
Total	100.15	101.58	98.45	99.75	99.69	99.84	99.79
Zr	-	281	237	456	367	28	174
Y	77	34	49	78	66	12	41
Nb	-	6	7	13	9	3	4
Cr	-	7	9	2	5	158	12
Ni	-	1	15	BL	BL	72	11
Sr	207	189	242	81	78	168	173
Rb	BL	2	6	42	11	BL	2
Ba	77	56	151	543	333	25	76
Zn	8	13	5	22	45	56	27



## Appendix 1.3 continued

	Magnetite Gabbro		'Nevadan' Quartz Gabbros		Dolerites		
	SM52	SM74	SM63	SM23	SM91	SMO3	SMO6
SiO <sub>2</sub>	47.68	47.55	44.94	50.44	50.31	49.04	50.57
TiO <sub>2</sub>	0.55	0.27	3.15	0.85	1.03	0.65	1.77
Al <sub>2</sub> O <sub>3</sub>	13.58	20.76	9.69	17.41	17.48	15.20	14.15
Fe <sub>2</sub> O <sub>3</sub> *	7.95	5.79	17.11	10.08	10.38	11.02	10.66
MnO	0.12	0.07	0.21	0.17	0.19	0.22	0.18
MgO	11.64	9.02	8.73	6.08	5.48	7.29	6.04
CaO	14.94	16.71	12.18	11.53	11.03	11.86	11.92
Na <sub>2</sub> O	1.44	0.96	1.86	2.24	2.71	2.63	2.93
K <sub>2</sub> O	0.10	0.05	0.14	0.51	0.59	0.17	0.10
P <sub>2</sub> O <sub>5</sub>	0.04	0.01	0.09	0.23	0.42	0.08	0.24
Total	98.04	101.19	98.10	99.54	99.62	98.16	98.56
Zr	21	19	30	-	46	41	102
Y	10	5	17	17	25	14	33
Nb	BL	BL	2	-	2	BL	5
Cr	295	217	31	-	67	22	41
Ni	94	107	BL	-	18	18	10
Sr	167	173	142	284	295	240	266
Rb	BL	BL	2	10	11	2	BL
Ba	26	12	87	168	218	56	68
Zn	27	15	82	63	69	95	23

## Appendix 1.3 continued

	SM19	SM34	SM39	SM45	SM60	SM61	SM72	SM81
SiO <sub>2</sub>	56.62	54.20	53.85	49.76	46.34	48.28	51.24	53.58
TiO <sub>2</sub>	1.10	1.39	2.30	1.38	1.25	1.13	0.77	2.17
Al <sub>2</sub> O <sub>3</sub>	14.16	13.06	14.10	13.72	14.04	13.38	13.52	14.14
Fe <sub>x</sub> O <sub>3</sub> *	9.80	12.74	11.58	11.18	12.37	9.93	10.05	12.15
MnO	0.29	0.30	0.25	0.22	0.27	0.19	0.27	0.16
MgO	4.61	5.79	4.87	7.59	9.07	10.58	8.55	5.22
CaO	4.36	5.13	8.67	10.44	10.83	12.31	11.55	8.18
Na <sub>2</sub> O	5.83	4.38	4.03	3.58	2.20	1.74	2.20	4.44
K <sub>2</sub> O	0.38	0.38	0.06	0.11	0.10	0.28	0.11	0.08
P <sub>2</sub> O <sub>5</sub>	0.29	0.21	0.78	0.14	0.11	0.12	0.08	0.44
Total	97.44	97.58	100.49	98.12	96.58	97.94	98.34	100.56
Zr	288	132	147	111	81	89	63	162
Y	63	35	55	29	25	24	20	49
Nb	9	5	4	2	3	4	2	7
Cr	44	14	6	78	262	534	284	15
Ni	16	3	BL	36	84	157	79	BL
Sr	166	159	210	311	170	170	173	229
Rb	3	5	BL	BL	BL	2	BL	BL
Ba	142	104	80	63	53	116	79	79
Zn	127	33	40	39	207	77	47	41

## Appendix 1.4

Byne Hill

	Gabbros		Leucodiorites		Trondhjemite
	BY02	BY12	BY9*	BY14*	BY18
SiO <sub>2</sub>	47.57	46.61	55.10	55.11	71.03
TiO <sub>2</sub>	0.96	0.40	0.52	0.52	0.22
Al <sub>2</sub> O <sub>3</sub>	13.65	18.46	15.75	15.43	12.83
Fe <sub>2</sub> O <sub>3</sub> *	12.15	7.90	9.85	9.53	4.58
MnO	0.21	0.11	0.15	0.20	0.09
MgO	7.49	8.13	2.05	1.69	0.35
CaO	9.53	13.94	2.71	3.05	0.59
Na <sub>2</sub> O	2.75	1.75	7.40	7.13	6.57
K <sub>2</sub> O	0.25	0.61	0.08	0.04	0.21
P <sub>2</sub> O <sub>5</sub>	0.18	0.02	0.09	0.09	0.02
Total	94.75	97.89	93.70	92.79	96.67
Zr	36	19	316	300	264
Y	14	8	103	78	78
Nb	BL	2	7	7	5
Cr	136	38	3	BL	5
Ni	60	57	BL	BL	BL
Sr	257	245	50	32	37
Rb	5	8	BL	BL	3
Ba	50	21	48	47	99
Zn	65	28	287	61	15

\*Large proportion of secondary calcite

## Appendix 1.5

Point SalInsitu Pyroxene

	Quartz	diorite	"Albitite"	vein	Gabbro	Dolerites	
	PS01	PS08	PS04	PS02	PS11	PS09	PS13
SiO <sub>2</sub>	61.72	59.72	57.98	50.90	47.55	51.79	51.65
TiO <sub>2</sub>	0.91	0.91	0.33	0.41	0.17	0.61	0.68
Al <sub>2</sub> O <sub>3</sub>	15.09	13.84	19.24	20.05	17.87	12.43	12.06
Fe <sub>2</sub> O <sub>3</sub> *	7.37	7.94	2.77	3.50	7.25	12.25	14.04
MnO	0.13	0.12	0.03	0.04	0.11	0.20	0.25
MgO	1.85	4.37	1.91	2.68	11.02	7.53	6.14
CaO	4.88	5.56	9.97	20.86	14.12	6.47	6.05
Na <sub>2</sub> O	5.40	5.68	7.73	2.64	1.11	4.12	3.23
K <sub>2</sub> O	0.65	0.39	0.17	0.01	0.53	0.27	0.21
P <sub>2</sub> O <sub>5</sub>	<u>0.28</u>	<u>0.03</u>	<u>0.16</u>	<u>0.13</u>	<u>0.00</u>	<u>0.05</u>	<u>0.08</u>
Total	98.28	98.56	100.29	101.22	99.73	95.72	94.39
Zr	116	-	-	-	5	45	56
Y	44	9	14	14	4	15	18
Nb	5	-	-	-	2	2	2
Cr	5	-	-	-	41	71	37
Ni	BL	-	-	-	53	25	10
Sr	228	182	24	11	140	174	143
Rb	6	2	BL	BL	5	2	BL
Ba	139	68	23	13	438	63	49
Zn	19	17	BL	4	21	26	68

## Appendix 2 Rare earths and other elements determined

by INAA

All elements in ppm

### 2.1 The Troodos Massif

	Tonalites			Trondhjeme Epidosite			<u>In situ vein</u>
	TM101	GA2	GK2	GA14	GA17	TM13	TM139
La	-	-	-	-	-	-	-
Ce	3.3	10.2	5.0	20.8	14.9	6.9	3.2
Nd	(3.4)	9.3	3.5	12.9	10.6	6.2	4.7
Sm	2.4	3.5	1.5	4.0	3.6	2.8	1.6
Eu	0.77	1.40	0.54	1.34	1.48	0.78	0.55
Gd	2.9	5.3	0.7	4.8	4.4	4.9	1.6
Tb	0.70	0.95	0.60	0.93	0.94	0.95	0.56
Tm	0.5	0.7	0.4	0.9	0.7	0.9	0.4
Yb	4.19	4.40	3.61	4.50	4.26	5.96	2.57
Lu	0.7	0.8	0.7	0.8	0.7	1.1	0.53
Th	BL	0.7	0.6	1.7	1.1	0.4	BL
Ta	0.5	1.2	1.2	1.3	1.2	1.2	0.5
Hf	1.2	2.7	1.1	3.0	2.7	2.3	1.6
Sc	34.1	-	-	-	-	16.0	40.6

( ) Indicates large peak fitting error

- Not analysed

BL Below detection limit

Appendix 2.1 continued

	Rhyolites				Gabbros		Magnetite Gabbros	
	TM158	GA11	GA16	QAP	TM116	TM140	GA8	TM102
La	-	-	-	-	-	-	-	-
Ce	8.1	15.1	18.9	16.7	1.8	2.4	3.1	(0.9)
Nd	7.9	8.8	14.7	12.1	(2.0)	(3.0)	(2.2)	BL
Sm	3.6	2.5	4.4	3.9	0.8	1.2	1.0	0.5
Eu	0.91	0.69	1.38	0.86	0.31	0.5	0.44	0.27
Gd	4.5	3.3	6.1	5.3	BL	BL	2.6	BL
Tb	0.94	0.62	1.13	1.03	0.23	0.29	0.30	0.18
Tm	0.8	0.7	1.0	0.6	0.2	0.2	0.3	0.2
Yb	5.10	3.85	5.23	5.90	1.06	1.35	1.42	1.25
Lu	0.8	0.7	0.9	1.0	(0.2)	0.3	0.2	(0.2)
Th	0.6	0.9	1.6	1.0	BL	BL	BL	BL
Ta	0.8	0.8	1.3	1.3	0.1	0.2	0.3	0.2
Hf	2.6	2.8	3.6	3.1	0.3	0.4	0.7	0.3
Sc	15.0	-	-	-	52.8	46.0	-	56.0

Appendix 2.1 continued

Appendix 2.2 The Semail Nappe

---

	Leuco gabbro TM10	Dolerites TM142	TM143	Tonalite OM3077	Aplite OM3085	Epidosite OM3011b
La	-	-	-	-	-	-
Ce	(1.7)	6.7	3.5	26.0	13.9	25.0
Nd	BL	7.0	4.3	22.8	8.9	19.0
Sm	0.2	2.8	1.6	7.7	2.7	5.8
Eu	0.42	1.04	0.63	1.81	(0.03)	1.71
Gd	BL	4.1	(2.3)	9.0	3.8	7.3
Tb	0.06	0.71	0.49	1.71	0.74	1.50
Tm	0.2	0.5	0.3	1.3	0.6	1.1
Yb	0.36	3.3	2.04	7.83	4.01	6.27
Lu	(0.1)	0.5	0.4	1.3	0.6	1.1
Th	BL	0.4	BL	0.7	3.3	0.5
Ta	0.4	0.3	0.2	0.8	1.3	1.2
Hf	1.7	1.9	1.1	6.7	5.1	5.6
Sc	27.9	31.3	36.9	16.3	12.9	11.2

## Appendix 2.2 continued

	<u>Insitu</u>					
	Vein	Gabbros	Dolerites			
	OM3073	OM3018	OM3074	OM3082	OM3013	OM3132
La	-	-	-	-	-	-
Ce	13.1	12.9	1.5	3.5	10.5	11.1
Nd	9.6	11.6	1.9	3.0	8.6	8.0
Sm	3.5	4.0	0.9	1.0	3.3	2.8
Eu	1.68	1.33	0.53	0.62	1.27	1.26
Gd	4.7	4.5	0.9	1.7	4.0	3.6
Tb	0.86	0.88	0.23	0.32	0.8	0.76
Tm	0.8	0.6	0.2	0.2	0.5	0.5
Yb	4.97	3.71	1.06	1.32	3.52	3.58
Lu	1.0	0.4	0.2	0.2	0.7	0.5
Th	0.8	0.3	0.1	0.1	BL	BL
Ta	0.4	0.3	0.1	0.2	0.3	BL
Hf	9.1	3.0	0.4	BL	2.3	2.4
Sc	7.0	43.6	-	-	37.0	34.6



## Appendix 2.3

### The Smartville Block

	Tonalite	Trondhjemite	Orthoclase Porphyry	Gabbro	Magnetite Gabbro
	SM56	SM01	SM15	SM52	SM63
La	-	-	-	-	-
Ce	38.5	56.9	52.9	3.3	5.5
Nd	28.8	42.0	31.2	3.0	6.1
Sm	8.3	11.6	8.5	1.3	3.0
Eu	1.87	2.62	1.54	0.53	0.99
Gd	8.4	13.1	9.8	1.4	2.63
Tb	1.8	2.6	2.0	0.3	0.6
Tm	1.2	1.7	1.7	0.2	0.3
Yb	8.22	11.06	9.50	0.97	1.81
Lu	1.3	1.9	1.5	0.2	0.3
Th	2.2	1.8	2.6	0.2	0.3
Ta	1.1	1.4	1.5	0.2	0.2
Hf	8.0	11.8	10.6	0.6	1.2
Sc	-	13.0	6.9	-	-

## Appendix 2.4

### Byne Hill

	Trondhjemite	Diorite	Gabbro
	BY18	BY9	BY12
La	12.4	8.7	-
Ce	29.9	29.7	1.7
Nd	27.3	23.7	1.9
Sm	10.4	9.3	0.8
Eu	2.00	1.19	0.42
Gd	11.1	13.0	1.2
Tb	2.4	2.4	0.2
Tm	1.7	1.9	0.10
Yb	12.12	13.18	0.92
Lu	1.9	2.1	0.14
Th	1.3	1.6	BL
Ta	0.9	0.4	0.2
Hf	8.3	9.1	0.4
Sc	-	-	-

## Appendix 2.5

### Mid-Atlantic Ridge at 45°N

#### Quartz Diorites

##### Prefix 159-

	38	39	40	41
La	35.1	43.8	32.7	33.4
Ce	74.3	81.7	71.6	73.0
Nd	42.2	35.1	39.6	39.3
Sm	11.0	7.7	10.1	10.0
Eu	3.11	1.62	3.05	2.8
Gd	12.6	8.8	12.5	11.3
Tb	2.0	1.3	1.9	1.9
Tm	1.4	1.1	1.3	1.2
Yb	7.7	6.9	7.3	7.4
Lu	1.2	1.1	1.2	1.2
Th	4.5	8.7	3.8	2.3
Ta	3.2	3.2	2.8	3.5
Hf	6.3	7.6	7.4	6.9
Sc	25.9	5.9	21.6	24.8

## Appendix 2.6

	Chondritic Abundance*	Detection Limit	Standard deviation of 20 determinations of BCR-1 as % of abundance
La	0.328	5.0	10.5%
Ce	0.865	1.8	5.2
Nd	0.630	3.6	5.3
Sm	0.203	0.5	8.9
Eu	0.077	0.03	6.5
Gd	0.276	1.6	15.5
Tb	0.052	0.05	4.8
Tm	0.034	0.1	23.5
Yb	0.220	0.06	4.3
Lu	0.034	0.2	16.7
Th		0.3	4.0
Ta		0.1	9.2
Hf		0.22	4.2

\*From Nakumara, 1974, except for Tm and Tb which are extrapolated values

### Appendix 3 Analytical Techniques

Crushing After cleaning, 200 to 300 gm. of each sample was crushed using a steel flypress and then a tungsten carbide TEMA. The only exceptions were four 10-20 gm. specimens of quartz diorite from the MAR at 45°N which were crushed in an agate mortar.

XRF 15 gm. powder pellets were analysed for the major oxides and Zr, Y, Nb, Cr, Ni, Sr, Rb and Ba on a Phillips PW1450 automatic XRF spectrometer at the University of Birmingham by Dr. G.L. Hendry between September 1975 and June 1977. Analytical procedure, operating conditions and standards were those in general use at Birmingham at that time. Inter-element corrections and detection limits were recommended by the analyst.

Wet chemistry FeO was determined by the version of the ammonium metavanadate method (Wilson 1955) in use at the Department of Earth Sciences, Leeds University. An internal standard was included with each batch of digestions.

INAA The REE, Th, Ta, Hf and Sc were determined by instrumental neutron activation analysis at the Department of Earth Sciences, the Open University. Samples of 0.3 gm. rock powder were irradiated in batches of eight, each with an internal and an international standard, usually USGS BCR-1. Details of technique and the analysis of the gamma-ray spectrum are in a departmental publication. (Sarre and Potts 1976). Chondrite RE abundances are taken from Nakamura

1974, except for Tm and Tb which were obtained by extrapolation.

Electron Microprobe Mineral microanalysis was performed on the Cambridge Microscan IX at the Open University. Standards were British Museum standard minerals and BDH pure metals.

#### Appendix 4    Bibliography

---

\* Indicates original reference was not consulted

Alleman, F. and Peters, T. 1972

The Ophiolite-radiolarite belt of the north Oman Mountains.  
Eclogae Geol. Helv. 65 657-697

Allen, C.R. 1975

The Petrology of a portion of the Troodos Plutonic Complex,  
Cyprus. Unpubl. Ph.d. Thesis. Cambridge Univ. 161p

Aoki, K. and Kuno, H. 1972,

Gabbro-Quartz diorite inclusions from Izu-Hakone region,  
Japan. Bull. Volc. 36 164-173

Arth, J.G. 1976

Behaviour of trace elements during magmatic processes.  
A summary of theoretical models and their applications.  
J. Res. USGS 4 p41-47

Arth, J.G. and Barker, F. 1976

Rare Earth Element partitioning between hornblende and  
dacitic liquid and implications for the genesis of  
trondhjemitic-tonalitic liquids.    Geology 4 534-536

Aumento, F. 1969

Diorites from the Mid-Atlantic Ridge at 45°N.  
Science 165 p1112-1113

Aumento, F. Loncarevic, B.D. and Ross, D.I. 1971  
Hudson Geotraverse: Geology of the MAR at 45°N  
Phil. Trans. Ry. Soc. A268 p623-650

\*Bailey, E.B. and McCallien, W.J. 1952  
Ballantrae Igneous Problems: Historical Review. Trans.  
Edinb. Geol. Soc. 15 14-18

\*Bailey, E.H. Irwin, W.P. and Jones, D.L. 1964.  
Franciscan and related rocks and their significance  
in the geology of western California: Calif. Div.  
Mines and Geology Bull. 183 177p

Bailey, E.H. Blake, M.C. and James, D.L. 1970  
On-land Mesozoic Oceanic Crust in California Coast Ranges  
USGS Prof. Paper 700c C70-c81

and Blake, M.C. 1974  
Major chemical characteristics of Mesozoic Coast Range  
Ophiolite in California Jour. Res. USGS. 2 637-656

Bakor, A.R. Gass, I.G. and Neary, C.R. 1976  
Jabal al Wask, N.W. Saudi Arabia - An Eocambrian Back-Arc  
Ophiolite. Earth Planet. Sci. Letts. 30 1-9

Ballard, R.D. and van Andel, T.H. 1977  
Morphology and tectonics of the inner rift valley at lat.  
36° 50'N on the M.A.R. Geol. Soc. Am. Bull. 88 507-530

\*Balsillie, D. 1937

Further observations on the Ballantrae Complex, South  
Ayrshire Geol. Mag. 74 20-33

Barker, F. and Arth, J.G. 1976

Generation of trondhjemitic-tonalitic liquids and  
Archean bimodal trondhjemite-basalt suites.

Geology 4 596-600

Bateman, P.C. Clark, L.D. Huber, N.K. Moore, J.G. and  
Rinehart, C.D. 1963.

The Sierra Nevada Batholith, A Synthesis of recent work  
across the central part. Geol. Soc. Am. Spec. Publ.  
414D. 46p

Bebien, J. 1977

Mafic and Ultramafic rocks associated with granites in  
the Vardar Zone. Nature 270 232-234

Beccaluva, L. Ohnenstetler, D. and M., Venturelli, G. 1977

Trace Element Geochemistry of Corsican Ophiolites

Contrib. Min. and Pet. 64 11-31

Bennett, M.C. 1976,

Ultramafic-Mafic Complex at North Cape, Northernmost  
New Zealand. Geol. Mag. 113 61-76



\*Bird, J.M. Dewey, J.F. and Kidd, W.S.F. 1971  
Proto-Atlantic Oceanic Crust and Mantle: Appalachian/  
Caledonian Ophiolites. Nat. Phys. Sci. 231 28-31

Black, P.M. and Brothers, R.N. 1977  
Blueschist ophiolites in the Mélange Zone, Northern  
New Caledonia. Contrib. Min. Pet. 65 69-78

Bloxham, T.W. 1968  
The Petrology of Byne Hill, Ayrshire. Trans. Roy. Soc.  
Edinb. 68 105-122

and Lewis, A.D. 1972  
Ti, Zr and Cr in some British pillow lavas and their  
petrogenetic affinities. Nat. Phys. Sci. 237 134-136

Bonatti, E. Honnorez, J. and Ferrara G. 1970  
Equatorial Mid-Atlantic ridge: Petrologic and Sr.  
isotopic evidence for an Alpine-type rock assemblage.  
Earth Planet. Sci. Letts. 9 247-256

\*Bonney, T.G. 1878  
On the serpentinites and associated igneous rocks of the  
Ayrshire Coast. Quart. J. Geol. Soc. Lond. 34 769-85

\*Brongniart, A. 1827  
Classification et caractères minéralogiques des roches  
homogènes et hétérogènes. Paris: F.G. Levrault

Brown, G.C. 1977

Mantle Origin of Cordilleran Granites Nature 265 21-24

Brown, M.A. 1976

The Petrography and geochemistry of gabbros, dolerites and leuco-diorites from Porthoustock quarry, Lizard, Cornwall. Unpubl. B.Sc. thesis, Southampton Univ. 41p

Burchfiel, B.C. and Davis, G.A. 1972

Structural framework and evolution of the southern part of the Cordilleran Orogen, Western U.S.A.

Am. J. Sci. 272 97-118

Buma, G. Frey, F.A. Wones, D.R. 1971

New England granites: trace element evidence regarding their origin and differentiation. Contrib. Min. Pet. 31 300-320

\*Cady, J.W. 1975

Magnetic and gravity anomalies in the California Great Valley and western Sierra Nevada metamorphic belt  
Geol. Soc. Am. Spec. Paper 168

Cann, J.R. 1970a

Rb, Sr, Y, Zr and Nb in some ocean floor basaltic rocks.  
Earth Planet Sci. Letts. 10 7-11

Cann, J.R. 1970b

New Model for the Structure of the Ocean Crust.

Nature 226 928-930

1971

Petrology of basement rocks from Palms Ridge, N.E.

Atlantic. Phil. Trans. Ry. Soc. A268 605-617

1974

A model for oceanic crustal structure developed.

Geophys. J.R. Astr. Soc. 39 169-187

Carmichael, I.S.E. Turner, F.J. and Verhoogen, J. 1974

Igneous Petrology. McGraw-Hill 739p

Christensen, N.I. 1970

Composition and Evolution of the Oceanic Crust.

Mar. Geol. 8 139-154

1977

Geophysical Significance of Oceanic Plagiogranite.

Earth Planet. Sci. Letts. 36 297-300

\*Church, W.R. and Stevens, R.K., 1970

Mantle Peridotite and Early Ophiolite Complexes of the  
Newfoundland Appalachians. Prog. Int. Symp. Mech.

Properties and Processes of the Mantle, Flagstaff,

Arizona, 38-39

\* Church, W.R. and Stevens, R.K., 1971

Early Palaeozoic Ophiolite Complexes of the Newfoundland  
Appalachians as Mantle-Oceanic Crust Sequences.

JGR 76 1460-1466

Church, W.R. and Gayer, R.A. 1973

The Ballantrae Ophiolite. Geol. Mag. 110 497-510

Coleman, R.G. 1971

Plate Tectonic Emplacement of Upper Mantle Peridotite  
along Continental Edges JGR. 76 1212-1222

1977

Ophiolites. Springer-Verlag. 229p

and Peterman, Z.E. 1975

Oceanic Plagiogranite JGR 80 1099-1108

Condie, K.C. 1978

Geochemistry of proterozoic granitic plutons from  
New Mexico, U.S.A. Chem. Geol. 21 131-149

Coombs, D.S. Landis, C.A. Norris, R.J. Sinton, J.M.

Borns, D.J. and Craw, D. 1976

The Dun Mountain Ophiolite Belt, with special reference  
to the southern portion. Am. J. Sci. 276 561-603

\*Davis, G.A. 1969

Tectonic Correlations, Klamath Mountains and western  
Sierra Nevada, California, Geol. Am. Bull. 80 1095-1108

Davies, H.L. 1971

Peridotite-Gabbro-Basalt Complex in Eastern Papua:  
an overthrust plate of oceanic mantle and crust.  
Aust. Bur. Mineral. Resources Bull. 128 1-48

De A. 1974

Silicate liquid immiscibility in the Deccan Traps and  
its petrogenetic significance. Geol. Soc. Am. Bull.  
85 471-474

Deer, W.A. Howie R.A. and Zussman, J. 1971

An introduction to the Rock Forming Minerals Longmans 528p

Degens, E.T. and Ross, D.A. 1969

Hot brines and Recent heavy metal deposits in the Red Sea.  
Springer-Verlag 600p

Dewey, J.F. 1969

Evolution of the Appalachian/Caledonian Orogen. Nature  
222 124-129

\*Dewey, J.F. 1971

A model for the Lower Palaeozoic evolution of the southern  
margin of the Early Caledonides of Scotland and Ireland.  
Scott. J. Geol. 7 220-40

\*Dewey, J.F. and Bird, J.M. 1970

The evolution of the Scottish Caledonides in relation to  
their isotopic age pattern. Trans. Ry. Soc. Edin.  
68 51-55

Dewey, J.F. and Bird, J.M. 1975

Origin and emplacement of the ophiolite suite:

Appalachian ophiolites in Newfoundland. JGR 76 3179-3206

Dietz, R.S., 1963

Alpine serpentinites as oceanic rind fragments.

Geol. Soc. Am. Bull. 74 947-952

Engel, C.G. and Fisher, R.L. 1971

Granitic to Ultramafic rock complexes of the Indian Ocean ridge system,

Western Indian Ocean. Geol. Soc. Am. Bull. 86 1553-1578

\*Ernst. W.G. 1965

Mineral parageneses in Franciscan metamorphic rocks,

Panoche Pass, Calif. Geol. Soc. Am. Bull. 76 879-914

Ernst, W.G. 1970

Tectonic contact between the Franciscan Mélange and the Great Valley Sequence - Crustal expression of a late

Mesozoic Benioff Zone. JGR 75 886-901

Ewart, A. and Bryan, W.B. 1972

Petrology and geochemistry of the igneous rocks from Eua, Tonga. Geol. Soc. Am. Bull. 83 3281-3298

\*Fairbanks, H.W. 1896.

The geology of Point Sal: Calif. Univ. Dept. Geology Bull. 2 1-92

Fitton, J.G. and Hughes, D.J. 1970

Volcanism and Plate Tectonics in the British Caledonides  
Earth Plan. Sci. Letts. 8 223-228

Frey, F.A. Haskin, M.A. Poetz, J.A. and Haskin, L.A. 1968

Rare earth abundances in some basic rocks. JGR 73 6085-6098

Frey, F.A. Bryan, W.B. and Thompson, G. 1974

Atlantic Ocean Floor: Geochemistry and Petrology of  
basalts from Legs 2 and 3 of the Deep-Sea Drilling Project.  
JGR 79 5507-5527

Gass, I.G. 1968

Is the Troodos Massif a fragment of Mesozoic ocean floor?  
Nature 220 39-42

1977

Origin and emplacement of ophiolites: in Volcanic Processes  
in Ore Genesis p72-76. Spec. publ. No.7, Geol. Soc. Lond.

and Masson-Smith, D. 1963

The geology and gravity anomalies of the Troodos Massif.  
Phil. Trans: Ry. Soc. 255A 417-467

and Smewing, J.D. 1973

Intrusion, extrusion and metamorphism at constructive  
margins: Evidence from the Troodos Massif. Nature 242 26-29

Gass, I. G. , Neary, C.R. Plant, J. Robertson A.H.F.  
Simonian, K.O. Smewing, J.D. Spooner, E.T.C. and  
Wilson, R.A.M. 1975

Comments on 'The Troodos Ophiolitic Complex was probably  
formed in an island arc' by A. Miyashiro and subsequent  
correspondence by A. Hynes and A. Miyashiro,  
Earth Planet. Sci. Letts. 25 236-238

Geol. Map of California, 1965  
California Div. Mines and Geology

Geotimes 1972

Penrose Field Conference-Ophiolites 17 No. 12 24-25

Gill, J.B. 1970

Geochemistry of viti Levu, Fiji, and its evolution as an  
island arc. Contrib. Min. Pet. 27 179-203

1976

From island arc to oceanic islands: Fiji, Southwestern  
Pacific. Geology 4 123-126

Glennie, K.W. Boeuf, M.G.A. Hughes-Clarke, M.W. Moody-Stuart, M.  
Pilaar, W.F.H. Reinhardt, B.M. 1973

Late Cretaceous nappes in the Oman Mountains and their  
geologic evolution AAPG Bull. 57 5-27

1974

Geology of the Oman Mountains (Three parts) Kon.  
Nederlands Geol. Mijb. Gen. Ver. Verh. 31, 423p



Grapes, R.H. 1975

Actinolite-Hornblende pairs in metamorphosed gabbros,  
Hidaka Mountains, Hokkaido, Contrib. Min. Pet. 49 125-140

Green, D. 1971

Evolution in meaning of certain geologic terms  
Geol. Mag. 108 177-179

\*Green, D.H. 1964

A restudy and reinterpretation of the geology of the  
Lizard Peninsula, Cornwall in Hosking K.F.G.  
and Shrimpton, G.J. (eds.) Present views of some aspects  
of the geology of Cornwall. Ry. Geol. Soc. Cornwall,  
Truro, Cornwall.

Greenbaum, D. 1972

Magmatic processes at ocean ridges: Evidence from the  
Troodos Massif, Cyprus, Nat. Phys. Sci. 238 18-21

Griffiths, J.R. and Varne, R. 1972

Evolution of the Tasman Sea, Macquarie Ridge and  
Alpine Fault, Nat. Phys. Sci. 235 83-86

Hart, S.R. 1971

K, Rb, Cs, Sr and Ba contents and Sr isotope ratios of  
ocean floor basalts. Phil. Trans. Ry. Soc. Lond.

A268 573-587

Hart, S.R. 1974

Sea floor basalt alteration: Some chemical and  
Strontium isotope effects. Contrib. Min. Pet. 44 219-230

Heaton, T.H.E. and Sheppard, S.M.F. 1977

Hydrogen and oxygen isotope evidence for seawater-  
hydrothermal alteration and ore deposition, Troodos  
Complex, Cyprus; in Volcanic Processes in Ore Genesis.  
Spec. Publ. No. 7, Geol. Soc. Lond.

Hellman, P.L. and Henderson, P. 1977

Are REE mobile during spilitization? Nature 267 38-40

Hietanen, A. 1973

Origin of andesitic and granitic magmas in the northern  
Sierra Nevada, Calif. Geol. Soc. Am. Bull. 84 2111-2118

1974

Amphibole pairs, epidote minerals, chlorite and plagioclase  
in metamorphic rocks, northern Sierra Nevada, Calif.

Am. Min. 59 22-40

Hopson, C.A. and Frano, C.J. 1973

Jurassic oceanic crustal sequence at Point Sal, Calif.

Eos 54 1220

Hopson, C.A. Pessagno, E.A. and Mattinson, J.M. 1975  
Preliminary Report and Geologic Guide to the Jurassic  
Ophiolite near Point Sal. Prepared for the 71st  
Ann. Meeting of the Cordilleran Section of the GSA.

Hotz, P.E. 1971

Plutonic Rocks of the Klamath Mountains, California and  
Oregon, USGS Prof. Paper 684B B1-B20

\*Hsu, K.J. 1968

Principles of mélanges and their bearing on the  
Franciscan-Knoxville paradox. Geol. Soc. Am. Bull.  
79 1063-1074

Hsu, L.C. 1968

Selected phase relationships in the system Al-Mn-Fe-Si-O-H  
A model for garnet equilibria J. Pet. 9 40-83

\*Hudson, R.G.S. McGugan, A. and Morton, D.M. 1954  
The structure of the Jebel Hagab area, Trucial Oman:  
Geol. Soc. London Quart. Jour. 110 p121-152

\*Irvine, T.N. and Findlay, T.C. 1972

Alpine-type peridotite with particular reference to the  
Bay of Islands complex. Pub. Earth Physics Branch,  
Dept. Energy, Mines Res. Can. 42 97-128

\*Irwin, W.P. 1964

Late Mesozoic orogenies in the ultramafic belts of  
northwestern California and southwestern Oregon. USGS  
Prof. Paper 501C, C1-C9

Ishizaka, K. and Yanagi, T 1975

Occurrence of oceanic plagiogranites in the Older  
Tectonic Zone, S.W. Japan. Earth Planet, Sci. Lett.  
27 371-377

1977

K, Rb and Sr abundance and Sr isotope composition  
of the Tanzawa granitic and associated gabbroic rocks,  
Japan: Low-K island arc plutonic complex.  
Earth Planet. Sci. Lett. 33 345-352

Juteau, T. 1975

Les ophiolites des nappes d'Antalya. (Taurides occidentales,  
Turquie) Sci. de la Terre, Mem. 32 692p

Kay, R.W. Hubbard, N.J. and Gast, P.W. 1970

Chemical Characteristics and Origin of oceanic ridge  
volcanic rocks. JGR 75 1585-1613

Kay, R.W. and Senechal, R.G. 1976

The rare earth chemistry of the Troodos ophiolite complex.  
JGR 81 964-970

Khan, M.A. Summers, C. Bamford, S.A.D. Chroston, P.N.

Poster, C.K., and Vine, F.J. 1972.

Reversed seismic refraction line on the Troodos Massif,  
Cyprus. Nat. Phys. Sci. 238 134-136

Kidd, R.G.W. and Cann. J.R. 1964

Chilling statistics indicate an ocean-floor spreading origin for the Troodos Complex, Cyprus. Earth Planet. Sci. Lett. 24 151-155

Lambert, R.S. + J. and Holland, J.G. 1974

Yttrium geochemistry applied to petrogenesis utilizing Ca-Y relationships in minerals rocks Geochem. et Cosmos. Act. 37 1393-1414

Lanphere, M.A. 1971

Age of the Mesozoic oceanic crust in the California Coast Ranges. Geol. Soc. Am. Bull 82 3209-3211

\*Lapierre, H. 1975

Les formations sédimentaires et éruptives des nappes de Mamonia et leur relations avec le massif due Troodos. Mem. Soc. Géol. Fr. 123 132pp.

Leblanc, M. 1976

Proterozoic ocean crust at Bou Azzer Nature 261 34-35

\*Lees, G.M. 1928

The geology and tectonics of Oman and parts of southeastern Arabia. Geol. Soc. Lond. Quart. Jour. 84 585-670

Lewis, A.D. and Bloxham, T.W. 1977

Petrotectonic environments of the Girvan-Ballantrae

lavas from rare-earth element distributions Scott.J.Geol. 13 211-222

\*Lindgren, W. and Turner, H.W. 1895

Smartsville, Calif. USGS Geol. Atlans, folio 18.

Liou, J.G. 1971

Synthesis and stability relations of prehnite,

$\text{Ca}_3 \text{Al}_2 \text{Si}_3 \text{O}_{10} (\text{OH})_2$  Am. Miner. 56 507-31

Liou, J.G. Lan, C.Y., Suppe, J. and Ernst, W.G. 1977

The East Taiwan Ophiolite. MRSO Spec. Report No.1

Luth, W.C. Johns, R.H. and Tuttle, O.F. 1964

The granite system at 4 to 10 kbs. JGR 69 759-773

Mackensie, C.B. and Clarke, D.B. 1975

Petrology of the South Mountain Batholith, Nova Scotia.

Can. J. Eth. Sci. 12 1209-1218

\*Mantis, M. 1971

Palaeontological evidence defining the age of the

Troodos Pillow Lava Series in Cyprus. Kypriakos Logos

3 202-208

\*Matsuda, J. Saito, K. and Zashu, S, 1975.

K-Ar ages and Sr isotopic study of the igneous rock

fragments in the manganese nodules dredged from the

Western Philippine Sea and the Amami Plateau, Preprint

Symp. Geological Problems in the Phillipine Sea, Ann.

Meeting Geol. Soc. Jap. 99-101

Mattinson, J.M. 1975

Early Palaeozoic ophiolite Complexes of Newfoundland:

Isotopic ages of zircons. *Geology* 3 181-183

Maxwell, J.C. 1974

Anatomy of an Orogen. *Geol. Soc. Am. Bull.* 85 1195-1204

McBirney, A.R. 1975

Differentiation of the Skaergaard Intrusion *Nature* 253 691

Menzies, M. Moores, E.M. Buer, K. Day, D. and Kemp, W. 1975

The Smartville Ophiolite, Sierra Nevada foothills,  
California. Field guide prepared for Int. Conf. on the  
Nature of Oceanic Crust, La Jolla, California

Menzies, M. and Blanchard, D. 1977

The Smartville Arc-Ophiolite, Sierra Nevada, California:  
Geochemical evidence. *EOS* 58 1245

Miyashiro, A. 1973

The Troodos ophiolitic complex was probably formed in  
an island arc. *Earth Planet. Sci. Lett.* 19 218-224

1975

Origin of the Troodos and other ophiolites: a reply to  
Moores. *Earth Planet. Sci. Lett.* 25 227-235

Shido, F. and Ewing, M. 1969

Diversity and Origin of Abyssal tholeiites from the  
Mid-Atlantic Ridge at 24°N and 30°N. Contrib. Min. Pet.  
23 38-52

1970

Crystallization and differentiation in abyssal  
tholeiite and gabbro from mid-oceanic ridges.  
Earth Planet. Sci. Lett. 7 361-365

Montigny, R. Bougault, H. Bottinga, Y and Allegre C.J. 1973  
Trace element geochemistry and genesis of the Pindos  
ophiolite suite. Geochim. Cosmochim. Acta 37 2135-2147

Moore, E.M. 1969

Petrology and structure of the Vourinos ophiolite complex  
of northern Greece. Spec. Paper Geol. Soc. Am. 118

and Jackson, E.D. 1974

Ophiolites and oceanic crust. Nature 250 136-139

and Vine, F.J. 1971

The Troodos Massif and other ophiolites as oceanic  
crust-evaluation and implications. Phil.Trans. Ry. Soc.  
268A 443-466

Moseley, F. 1969

The Upper Cretaceous ophiolite complex, Masirah Island,  
Oman. Geol. J. 6 293-306



Nagasawa, H. and Schnetzler, C.C. 1971

Partitioning of RE, alkali and alkaline earth elements between phenocrysts and acidic igneous magma. Geochim. Cosmochim. Acta. 35 953-968

Nakamura, N. 1974

Determination of REE, Ba, Fe, Mg, Na and K in carbonaceous and ordinary chondrites. Geochim. Cosmochim. Acta. 38 757-775

Nasseef, A.O. and Gass, I.G. 1977

Granitic and metamorphic rocks of the Taif area, western Saudi Arabia. Geol. Soc. Am. Bull 88 1721-1730

Neary, C.R. 1967

Igneous rocks of the Girvan District. Unpubl. B.Sc. thesis. Dept. Earth Sciences, Leeds University 111p

Norman, R.E. and Strong, D.F. 1975

Geology and geochemistry of ophiolitic rocks exposed at Ming's Bight, Newfoundland. Can. J. Eth. Sci. 12 777-797

Oxburgh, E.R. and Turcotte, D.L. 1968

Mid-oceanic ridges and geotherm distribution during mantle convection. JGR 73 2643-2661

Page, B.M. 1972

Oceanic Crust and Mantle fragments in subduction  
complex near San Luis Obispo, California. Geol. Soc.  
Am. Bull. 83 957-972

Pankhurst, R.J. and Pidgeon, R.T. 1976

Inherited isotope systems and the source region pre-history  
of early Caledonian granites in the Dalradian series of  
Scotland. Earth Planet. Sci. Lett. 31 55-68

Pantazis, T.M. 1967

The geology and mineral resources of the Pharmakas-  
Kalavassos area. Geol. Surv. Cyprus Mem., 8

Park, C.F. and McDiarmid, R.A. 1964

Ore Deposits. W. H. Freeman and Co. 475p

Parrot, J.P. 1974,

L'assemblage ophiolitique du Baer Bassit. Cah. Orstom.  
ser. Geol. 6 97-126

Pearce, J.A. 1973

Some relationships between the geochemistry and tectonic  
setting of basic volcanic rocks. Unpubl. Ph. D. Thesis,  
Univ. East Anglia

1975 Basalt geochemistry used to investigate  
past tectonic environments on Cyprus. Tectonophysics  
25 41-67

Pearce, J.A. and Cann, J.R. 1971

Ophiolite origin investigated by discriminant analysis  
using Ti, Zr and Y. Earth Planet. Sci. Lett. 12 339-349

1973

Tectonic setting of basic volcanic rocks using trace  
element analyses. Earth Planet. Sci. Lett. 19 290-300

Pessagno, E.A. 1973

Age and geologic significance of radiolarian cherts  
in the California Coast Ranges. Geology 1 153-156

Peterman, Z.E. Coleman, R.G. and Hildreth, R.A. 1971

$^{87}\text{Sr}/^{86}\text{Sr}$  in mafic rocks of the Troodos Massif.

USGS Prof. Paper 750D D157-D161

Peto, P. 1973

Petrochemical Study of the Similkameen Batholith,  
British Columbia. Geol. Soc. Am. Bull. 84 3977-2984

\*Pilgrim, G. 1908

Geology of the Persian Gulf and adjoining portions of  
Persia and Arabia. India Geol. Surv. Mem. 34 No.4 1-177

Popolitov, E.I., Filosofova, T.M. and Selivanova, G.I. 1973

Geochemical characteristics and genesis of plagiogranite  
intrusives in the Western Sayan orogenic zone.

Geochem. Int. 10 1209-1214

\*Pusztaszeri, L. 1969

Étude pétrographique due Massif du Chenaillet.

Sch. Min. Pet. Mitt. 49 426-466

Reinhardt, B.M. 1969

On the genesis and emplacement of ophiolites in the

Oman Mountains Geosyncline. Sch. Min. Pet. Mitt. 49 1-30

\*Ricou, L.E. 1971

Le croissant ophiolitiques péri-arabe, une ceinture  
de nappes mises en place au Crétacé supérieur.

Rev. Géogr. Phys. Geol. Dyn. 13 327-349

Robertson A.H.F. 1977

The Moni Mélangé, Cyprus. An olistostrome formed at a  
destructive plate margin. Jl. Geol. Soc. Lond.

133 447-466

Robertson A.H.F. and Hudson, J.D. 1973

Cyprus Umbers: Chemical precipitates on a Tethyan ocean  
ridge. Earth Planet. Sci. Lett. 18 93-101

and Fleet, A.J. 1976

Origins of REE in metalliferous sediments, Troodos Massif.  
Earth Planet. Sci. Lett. 28 385-394

Sarre, M. and Potts, P.J. 1976

The use of 'Sampo' in determination of REE by Instrumental  
neutron activation analysis. Departmental Handbook,  
Dept. Earth Sciences, The Open University

Schilling, J-G., 1971

Sea-floor Evolution: rare earth evidence. Phil. Trans.  
Roy. Soc. A268 663-706

1973a. Iceland mantle plume: Geochemical  
evidence along Reykjanes Ridge Nature 242 565-571

1973b. Iceland mantle plume. Nature 246 141-143

\*Schnetzer, C.C. and Philpotts, J.A. 1968

Partition coefficients of rare earth elements and barium  
between igneous matrix materials and rock forming mineral  
phenocrysts. I. in Origin and Distribution of the Elements  
ed. L.H. Ahrens. p.929-938., Pergamon Press.

1970

Partition coefficients of rare earth elements between  
igneous matrix material and rock forming mineral phenocrysts.  
II Geochim. Cosmochim. Act. 34 331-340

Schweickert, R.A. and Cowan, D.S. 1975

Early Mesozoic tectonic evolution of the western  
Sierra Nevada, California. Geol. Soc. Am. Bull.  
86 1329-1336

Sigurdsson H. 1968

Petrology of acid xenoliths from Surtsey. Geol. Mag. 105  
440-453

1977

Generation of Icelandic rhyolites by melting of  
plagiogranites in the oceanic layer. Nature 269 25-28

Simonian, K.O. 1975

The geology of the Arakapas Fault Belt Area, Troodos Massif,  
Cyprus. Unpubl. Ph.D. Thesis, Open University

Smewing, J.D., 1975

Metamorphism of the Troodos Massif, Cyprus. Unpubl.  
Ph.D. thesis, Open University

Simonian, K.O. and Gass, I.G. 1975

Metabasalts from the Troodos Massif, Cyprus: Genetic  
Implication deduced from petrography and trace element  
geochemistry. Contrib. Min. Pet. 51 49-64

and Potts, P.J. 1976

REE abundances in basalts and metabasalts from Troodos.  
Contrib. Min. Pet. 57 245-258

Simonian, K.O. Elboushi, I. Gass, I.G. 1977

Mineralized fault zone parallel to the Oman Ophiolite  
Spreading axis

Smith, A.G. and Woodcock, N.H. 1976

Emplacement model for some Tethyan ophiolites. Geology 4  
653-656

Spooner, E.T.C. 1977

Hydrothermal model for the origin of the ophiolitic  
cupriferous pyrite ore deposits of Cyprus.

p58-71 in Volcanic Processes in Ore Genesis.

Spec. Publ. No.7 Geol. Soc. Lond.

and Fyfe, W.S. 1973

Subseafloor metamorphism, heat and mass transfer.

Contrib. Min. Pet. 42 287-304

Beckinsale, R.D., Fyfe, W.S. and Smewing, J.D. 1974

$^{18}\text{O}$  enriched ophiolitic metabasic rocks from E. Liguria  
(Italy), Pindos (Greece) and Troodos (Cyprus)

Contrib. Min. Pet. 47 41-62

Chapman, H.J. and Smewing, J.D. 1977

Strontium isotopic contamination and oxidation during  
ocean floor hydrothermal metamorphism of the ophiolitic  
rocks of the Troodos Massif, Cyprus. Geochim.

Cosmochim. Act. 41 873-890

\*Steinmann, G. 1906

Geologische Beobachtungen in den Alpen (II). Die  
Schardtsche Überfaltungstheorie und die geologische  
Bedeutung der Tiefseeabsätze und der ophiolithischen  
Massengesteine. Ber. Natf. Ges. Freiburg 16 1-49

1927 Die ophiolithischen Zonen in  
dem mediterranen Kettengebirge. 14th int. Geol. Congr.  
Madrid. 2 638-667

Stern, C. de Wit, M.J. and Lawrence, J.R. 1976  
Igneous and metamorphic processes associated with the  
formation of Chilean ophiolites and their implication  
for ocean floor metamorphism, Seismic layering and  
magnetism. JGR 81 4370-4379

\*Stevens, R.K. 1970  
Cambro-Ordovician flysch sedimentation and tectonics  
in Western Newfoundland, and their possible bearing on a  
proto-Atlantic Ocean pl65-77 in Flysch Sedimentology in  
North America. Spec. Pap. Geol. Ass. Canada 7.

Stewart D.B. 1967  
Four phase curve in the system  $\text{CaAl}_2\text{Si}_2\text{O}_8\text{-SiO}_2\text{-H}_2\text{O}$   
between 1 and 10kb. Sch. Min. Pet. Mitt. 47 35-59

Storey, B.C. Mair, B.F. and Bell, C.M. 1977  
Occurrence of Mesozoic Oceanic floor and ancient continental  
crust on South Georgia. Geol. Mag. 114 203-208

Streckeisen, A. 1976  
To each plutonic rock its proper name. Eth. Sci. Reviews  
12 1-33



Strong, D.F. Stevens, R.K. Malpas, J. and Badham, J.P.N. 1975

A new tale for the Lizard. Proc. Ussher, Soc. 3 252

Subbarao, K.V. and Hedge, C.E. 1973

K, Rb, Sr and  $^{87}\text{Sr}/^{86}\text{Sr}$  in rocks from the Mid-Indian ocean ridge. Earth Planet. Sci. Lett. 18 223-228

Taylor, H.P. 1977

Water/rock relations and the origin of water in granite batholiths. Jl. Geol. Soc. Lond. 133 509-558

And Coleman, R.G. 1977

Oxygen isotopic evidence for meteoric-hydrothermal alteration of the Jabal at Tirf igneous complex, Saudi Arabia. EOS 58 516

Taylor, S.R. 1966

Applications of trace element data to problems in petrology. Phys. and Chem. of the Earth 6 133-213

Thayer, T.P. and Himmelberg, G.R. 1968

Rock succession in the Alpine-Type mafic complex at Canyon Mountain, Oregon, 23rd Int. Geol. Cong. 1 175-186

Thompson, G. 1973

Trace element distributions in fractionated oceanic rocks. 2. Gabbros and related rocks. Chem. Geol. 12 99-111

\*Tshopp, R.H. 1967

The general geology of Oman; 7th World Petroleum Cong.  
Proc. Mexico 2 231-242

Tuttle, O.F. and Bowen, N.L. 1958

Origin of granite in the light of experimental studies  
in the system  $\text{NaAl Si}_3 \text{O}_8$ - $\text{K Al Si}_3 \text{O}_8$ - $\text{SiO}_2$ - $\text{H}_2\text{O}$ .  
Geol. Soc. Am. Mem. 74 153p

Tysdal, R.G. Case, J.E. Winkler, G.R. and Clark, S.H.B. 1977  
Sheeted dikes, gabbro and pillow basalt in flysch of  
coastal souther Alaska, Geology 5 377-383

Uyeda S and Miyashiro A. 1974

Plate tectonics and the Japanese Islands - A synthesis.  
Geol. Soc. Am. Bull. 85 1159-1170

Varne, R. Gee, R.D. and Quilty, P.G.J. 1969

Macquarie Island and the cause of oceanic linear  
magnetic anomalies. Science 166 230-232

Vine, F.J. Poster, C.K. and Gass, I.G. 1973

Aeromagnetic survey of the Troodos Igneous Massif.  
Nat. Phys. Sci. 244 34

\*Wager, L.R. and Mitchell, R.L. 1951

The distribution of trace elements during strong  
fractionation of basic magma: A further study of the  
Skaergaard intrusion, East Greenland. Geochim.  
Cosmochim. Act. 1 129-208

Walker, B.M. Vogel, T.A. and Ehrlich, R. 1972

Petrogenesis of oceanic granites from the Aves Ridge  
in the Caribbean Basin. Earth Planet. Sci. Lett. 15  
133-139

Walker, G.P.L. and Skelhorn, R.R. 1966

Some associations of acid and basic igneous rocks.  
Eth. Sci. Review 2 93-109

Walton, E.K. 1956

Two ordovician conglomerates in South Ayrshire.  
Trans. Geol. Soc. Glas. 22 133-156

1965

p161-227 in The Geology of Scotland G.Y. Craig (ed.)  
Oliver and Boyd 556p

Wilkinson, J.M. and Cann, J.R. 1974

Trace elements and tectonic relationships of basaltic  
rocks in the Ballantrae Complex. Geol. Mag. 111 35-41

\*Williams, A. 1962

The Barr and Lower Armillan Series (Caradoc) of the  
Girvan district, south-west Ayrshire, with descriptions  
of the Brachiopoda. Mem. Geol. Soc. Lond. 3 1-267

Williams, S. and Murthy, B.R. 1977

Sr-isotopic and trace element geochemistry of the  
Macquarie ridge ophiolite complex. EOS 58 536

\*Wilson, A.D. 1955

A new method for the determination of ferrous iron in  
rocks and minerals. Bull. Geol. Surv. G.B. No.9 56-58

\*Wilson, H.H. 1969

Late Cretaceous eugeosynclinal sedimentation, gravity  
tectonics and ophiolite emplacement in Oman mountains,  
Southeast Arabia: AAPG Bull. 53 p.626-671

Wilson, J.T. 1966

Did the Atlantic close and then reopen? Nature 211 676-681

Wilson, R.A.M. 1959:

The Geology of the Xeros-Troodos area  
Cyprus Geol. Survey Dept. Mem. 1, 184p

Wood, D.A. Gibson, I.L. and Thompson, R.N. 1976

Elemental mobility during zeolite facies metamorphism  
of tertiary basalts - Eastern Iceland. Contrib. Min.  
Pet. 55 241-254

\*Woodring, W.P. and Bramlette, M.N. 1950

Geology and palaeontology of the Santa Maria district,  
California, USGS Prof. Paper 222 185p

Yajima, T. Higuchi, H and Nagasawa, H. 1972

Vavriation of rare earth concentrations in pigeonitic  
and hypersthenic rock series from Izu-Hakone region,  
Japan. Contrib. Min. Pet. 35 235

Yoder, H.S. 1968

Albite-Anorthite-Quartz-water at 5kb: Carnegie Inst.  
Washington, Year Book 66 477-478